The role of endocytic sorting and ESCRT machinery in regulation of cellular migration and receptor signalling

by

Dmitri Kharitidi

A final thesis submitted to McGill University in full fulfillment of the requirements

Of the degree of Doctor of Philosophy

Department of Biochemistry

McGill University

Montreal, QC, Canada

December 2015

ABSTRACT

The endocytic sorting of cell surface receptors is a crucial process for maintaining eukaryotic cell homeostasis and for organism's development and physiology. Several decades of research in this field have yielded the understanding of molecular processes governing endocytosis and postendocytic sorting of receptors. However the emergence of additional regulatory mechanisms for the individual receptors and discovery of new players of endocytic machinery provide new areas for investigation and research. This work provides understanding of the regulation of integrin α5β1 and Tumor Necrosis Factor Receptor (TNFR) by endocytic sorting and ubiquitination, as well as the characterization of a novel endosomal sorting machinery.

Our study of integrin α5β1 trafficking has identified a dynamic mechanism for α5β1 partitioning between the degradative and the recycling pathways, with a profound implication in cellular migration and invasion. The work presented here outlines the timecourse of integrin α5β1 ubiquitination following ligand engagement, its deubiquitination by USP9x upon ligand dissociation in acidic endosomes, promoting the receptor resensitization and its cell surface return. The smaller fraction of integrins, that maintain their ubiquitination status, are targeted to the lysosomal degradation via the action of the ESCRT components (HD-PTP and UBAP1). Overall, this dynamic sorting of integrin receptors represents a novel mechanism of cell migration regulation by integrin recycling.

Moreover, we have identified a key function for HD-PTP in the regulation of TNFR1 downstream signalling, affecting both NF-κB pathway and the induction of apoptosis following TNFα stimulation. TNFR1 endocytic sorting is poorly understood, and little is known about the role of ESCRT machinery in the sorting of TNFR1 or its downstream signalling. Our findings provide the first evidence for the negative regulation of TNFR1 signalling by ESCRT component HD-PTP, since its depletion leads to increased scaffolding of the TNFR1 signalling complex, accelerated NF-κB signalling and target gene expression. The impact of the endosomal sorting machinery of TNFR1 has potential implications in inflammation, apoptotic signalling, and cell survival.

Finally, we identify and characterize novel binding partners of HD-PTP by mass spectrometry. Among these, we focus on Endofin, an endosomal protein capable of ubiquitin

recognition, and essential for lysosomal sorting of polyubiquitinated cargo molecules. Endofin was proposed to act as an alternative ESCRT module, and we provide the evidence for its role in sorting of ubiquitinated receptors. Overall, these studies outline the key function of endocytic sorting mechanisms of cell surface receptors during cell migration and inflammation and propose a new ESCRT complex as a module involved in sorting of ubiquitinated molecules. Future studies are needed to examine the control of inflammatory response by ESCRT machinery and the function of ESCRTs in carcinogenesis.

ABRÉGÉ

Le trafic endosomal et triage des récepteurs sont des processus essentiels dans une cellule eucaryote et sont responsables pour le développement des organismes multicellulaires et maintien de leur physiologie. Les recherches dans ce domaine ont permis d'identifier des mécanismes moléculaires et la complexes protéiques responsables pour la régulation du triage endosomal. Néanmoins, il est nécessaire d'identifier des nouveaux mécanismes de triage de récepteurs et les molécules impliquées dans ces processus, afin de mieux comprendre le rôle physiologique du trafic endosomal. Cette thèse décrit les nouveaux mécanismes de triage d'intégrine α5β1 et de TNFR1 par ubiquitination, et introduit les molécules émergentes responsables pour la dégradation des récepteurs polyubiquitinés.

Nos études de trafic endosomal de l'integrin α5β1 soulignent une régulation importante pour son ségrégation entre le recyclage à la surface de la cellule et son dégradation aux lysosomes, affectant la migration et invasion cellulaire. Nous démontrons l'ubiquitination de l'intégrine α5β1 suite à son activation par fibronectine et son deubiquitination par USP9x, suite à la dissociation de ligand dans les conditions acides de l'endosome. Ce dernier est responsable pour le recyclage de l'intégrine α5β1 à la surface. Une partie des intégrines maintient leur statut ubiquitiné et sont targetés pour dégradation lysosomal par machinerie ESCRT (HD-PTP et UBAP1). Alors ce mécanisme est important pour la régulation de la migration cellulaire orchestrée par trafic des intégrines.

En plus, nous avons évalué le rôle de HD-PTP dans la régulation de la signalisation de TNFR1, en affectant NF-κB et apoptose suite à la stimulation avec TNFα. La régulation de TNFR1 par trafic endosomal est peu étudié, et l'impact de ESCRT dans ce processus. Nos résultats démontrent pour la première fois le rôle négatif de HD-PTP dans la signalisation par TNFR1. Déplétion cellulaire de HD-PTP augmente la présence de TNFR1 à la surface cellulaire, la formation du complexe TNFR1 et la voie de signalisation NF-κB. La régulation de ces processus par trafic endosomal a une implication importante dans la survie des cellules, l'inflammation et l'apoptose.

Finalement, nous avons identifié et caractérisé les nouveaux partenaires d'interaction de HD-PTP par spectrométrie de masse. Parmi ceux-là, nous avons identifié Endofin, une protéine endosomale, responsable pour tri des récepteurs polyubiquitinés vers dégradation lysosomale.

Endofin a été hypothétisé d'agir comme une module d'ESCRT alternative, et nous démontrons son implication dans cette voie et son action en recognition de molécules polyubiquitinées et leur dégradation. Dans l'ensemble, ces études soulignent l'importance de trafic endosomal des récepteurs ubiquitinés durant la migration cellulaire et inflammation et l'identification d'une nouveau module d'ESCRT. Des études futures sont nécessaires afin d'élucider la fonction des ESCRT dans le carcinogenèse et la régulation de l'inflammation et réponse immunitaire.

ACKNOWLEDGEMENTS

I would like to thank many colleagues, who have helped me during Ph.D. studies:

- Dr. Arnim Pause and Dr. Gergely Lukacs, for having enough patience to work with me during the last few years and their invaluable input on the project.
- Dr. Pirjo Apaja and Sanaz Manteghi, for being amazing colleagues and collaborators in several projects that we undertook together.
- Members of my Research Advisory Committee, Dr. Morag Park, Dr. Peter Siegel, Dr. John Silvius, Dr. Nathalie Lamarche, for their relevant input and productive discussions.
- Members of Pause and Lukacs labs for helping out on the projects, their names are listed in every chapter.
- Dr. Junichi Takagi and his lab members for their great work on integrin-fibronectin interaction.

On a personal side, I would like to thank my friends who have supported me throughout my studies:

- At McGill: Dmitry Rodionov, Anders Dydensborg, Charles Meunier, Gordana Maric, Colin Ratcliffe, Fanny Dupuy, Vlad Grouza, Sebastien Latapie, Jae Park, Jonathan Blanchet, Takla Griss, Nathaniel Robichaud, Charles Rajadurai, Said Izreig, Eric Ma.
- Members of ProVivoX team: Shawn McGuirk, Vincent Menard, Etienne Audet-Walsh, Edwin Ferrer, Lucas Collecchia.
- Dragonboat teams and their honorary members: MFM, Shockwave and Arsenal. Specifically: Yohan Thierry, Dominic Mai, Dave Garant, Alex “Thor”, Alex Lehouiller, Haig “Scottish”, JP Le Justicier Masque, Joey Angers, Dominic Tremblay, Jason Manning, Willy Chen, Toulouse “T-Bone” Roy, Anthony Malouf, Kifunda Manika, and many others.
- Last but not least, my mom and dad.

Funding:

Supported by Fonds de la Recherche en Sante Quebecois Doctoral Award, McGill Integrated Cancer Research Training studentship, Canderel studentship, Max. E. Binz Award, Maysie McSporran Studentship, Graduate Excellence Fellowship for Merit.

PREFACE

The following thesis is written in manuscript format. It contains one published manuscript and two in preparation, outlined in Chapters 2-4.

1. Dmitri Kharitidi*, Pirjo M. Apaja*, Sanaz Manteghi, Kei Suzuki, Elena Malitskaya, Ariel Roldan, Marie-Claude Gingras, M, Junichi Takagi, Gergely L. Lukacs and Arnim Pause, *Ligand occupancy and endosomal pH regulate integrin a5b1 ubiquitination, endocytic sorting and cell migration*, Cell Reports, 2015.
2. Sanaz Manteghi*, Dmitri Kharitidi*, Maya Poffenberger, and Arnim Pause, *HD-PTP is required for both NF-κB pathway activation and apoptosis signaling by the TNF receptor.*
3. Dmitri Kharitidi, Pirjo Apaja, Sanaz Manteghi, Elena Malitskaya, Marie-Claude Gingras, Gergely Lukacs and Arnim Pause, *Identification of novel ESCRT component and its role in endocytic sorting.*

Authors contributions:

1. I have designed and performed experiments and contributed to manuscript writing. P.A. has designed and performed stability measurements, FRIA experiments, and in vivo dissociation experiments. S.M has performed some initial migration experiments. K.S. performed BLI measurements. E.M. performed ubiquitin pulldowns. A.R. performed HPLC. D.K, P.A., A.P. and G.L. have written the manuscript and performed the necessary revisions.
2. I designed and performed of the experiments and wrote the manuscript draft. S.M. has designed and performed the experiments in Figures: 3.1B, C, E; 3.2A, B, C; 3.3A, B; and equally contributed to conceptualization and design of this chapter. M.P. and E.M. performed cytokine analysis by ELISA in 3.2E, F, G.
3. I have designed and performed the experiments and wrote the manuscript draft. P.A. performed FRIA experiments in 4.4B-C. M-C. G. performed preliminary MS analysis. A-C. G. performed the MS-SAINT analysis presented in the chapter.

Additional publications:

1. **Dmitri Kharitidi**, Sanaz Manteghi and Arnim Pause, *Pseudophosphatases: identification methods and physiological significance,* Methods, S1046-2023(13)00378-2, (2013) IF: 4.6 http://www.ncbi.nlm.nih.gov/pubmed/24064037
2. Gingras Marie-Claude, Zhang Yu-Ling, **Kharitidi Dmitri**, Barr Alastair, Knapp Stephen, Michel Tremblay and Arnim Pause. *HD-PTP Is a Catalytically Inactive Tyrosine Phosphatase Due to a Conserved Divergence in Its Phosphatase Domain.* PLoS ONE 4(4): e5105. (2009) IF: 3.7 http://www.ncbi.nlm.nih.gov/pubmed/19340315
3. Marie-Claude Gingras, **Dmitri Kharitidi**, Valérie Chénard, Noriko Uetani, Maxime Bouchard, Michel L. Tremblay and Arnim Pause, *Expression analysis and essential role of the putative tyrosine phosphatase His-domain-containing protein tyrosine phosphatase (HD-PTP)*, Int. J. Dev. Biol. 53: 1069 - 1074 (2009) IF: 2.6 http://www.ncbi.nlm.nih.gov/pubmed/19378249

Table of Contents

Table of Figures:

CHAPTER 1:

Literature review on cell surface receptor endosomal sorting, cellular machinery involved and its impact in disease

1.1 General introduction on endosomal sorting

Endocytosis of cell surface molecules and their subsequent endosomal sorting is a key eukaryotic process that governs a plethora of cellular and physiological events. Several decades of research in the field of endocytosis demonstrated that endosomal system is a dynamic trafficking pathway connecting multiple cellular compartments, including the plasma membrane, endocytic vesicles, endosomes, trans-Golgi network and lysosomes. Not surprisingly, the implication of endosomal sorting is well described in several human pathologies, including cancer, immune disorders, lysosomal storage diseases, neurodegeneration and others. Here, we describe the general concepts of the endocytic sorting of cell surface receptors starting from their internalization at the plasma membrane until their degradation inside the lysosomal compartment.

1.1.2. Overview of endolysosomal system

Receptor-mediated endocytosis and the consequent cargo sorting in endolysosomal system is a crucial process for regulation of steady-state components of plasma membrane (Figure 1.1). Endocytosis is initiated upon receptor internalization via clathrin-dependent or independent mechanisms. Afterwards, the internalized cargo is delivered to the early (sorting) endosome. In early endosomal compartment, receptors can undergo sorting either towards recycling (cell surface return) or lysosomal delivery and degradation. The sorting process is complex and relies on a panel of sorting signals, post-translational modifications, ligand interaction, sorting adaptor molecules and the endosomal pH. The recycling cargo can return to the plasma membrane via Rab4 (quick recycling) or Rab11 (slow recycling) pathways. On the other hand, the ubiquitinated receptors are incorporated within the endosomal lumen during the formation of Multivesicular Body. The fusion of the latter with the lysosome results in a proteolytic degradation of its content. Thus, the endocytic sorting serves as a control mechanism for regulation of cell surface components, their localization, their levels and downstream signalling.

Figure 1.1: General overview of endosomal trafficking pathways

Typically, cell surface receptor endocytosis is initiated upon ligand activation of the receptor followed by the receptor recruitment into clathrin coated pit (CME). Other endocytic pathways exist (i.e. caveolae, pinocytosis, phagocytosis, etc), but are not depicted here. The cargo containing clathrin vesicle undergoes uncoating and fuses with the early endosome, a central sorting station for endocytosed cargo. Receptors may be sported to the rapid (Rab4-mediated) or slow (Rab11-mediated) cell surface recycling. Alternatively, ubiquitinated receptors are captured by the ESCRT machinery and are internalised within intraluminal vesicles, forming Multivesicular body (MVB). Fusion of MVB with lysosome (not shown) leads to the degradation of receptors. Details in text.

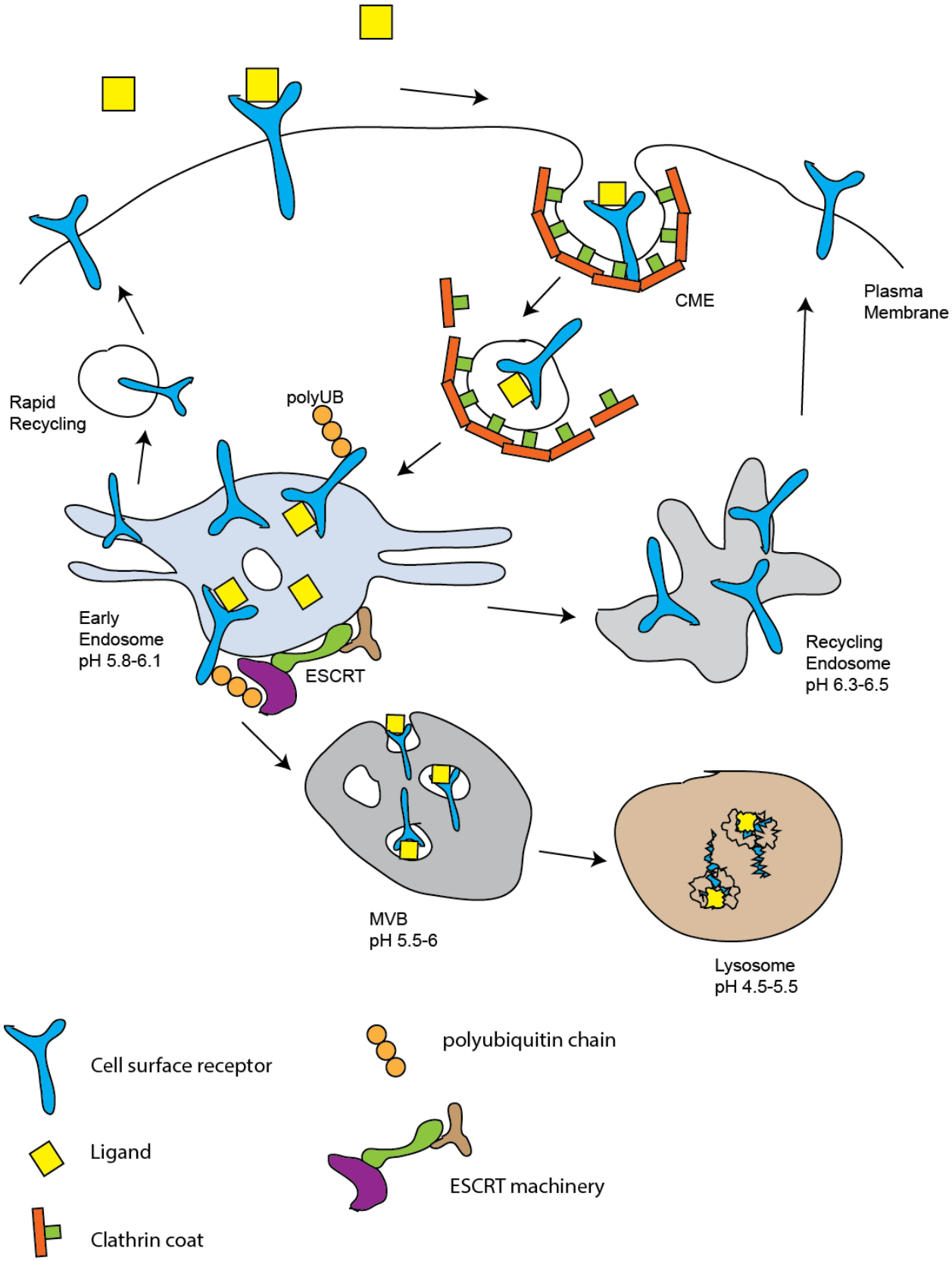
CME
Plasma
Membrane
Rapid
Recycling
polyUB
Early
Endosome
pH 5.8-6.1
ESCRT
Recycling
Endosome
pH 6.3-6.5
MVB
pH 5.5-6
Lysosome
pH 4.5-5.5
Cell surface receptor
Ligand
Clathrin coat
polyubiquitin chain
ESCRT machinery

1.1.3. Mechanisms of cell surface receptor internalization

Receptor-mediated endocytosis is initiated by the clustering and internalization of cell surface receptors at the plasma membrane. Internalization of cargo can be facilitated by specific coat proteins, such as clathrin, leading to clathrin-mediated endocytosis (CME) (Figure 1.1). In other instances, the receptor internalization occurs via "caveolae", which are orchestrated by the lipid binding protein caveolin, or by other clathrin-independent endocytic mechanisms.

CME is initiated by an assembly of clathrin-coated pit on the plasma membrane (reviewed in (Kirchhausen et al., 2014)). Clathrin is recruited to the plasma membrane via AP2 adaptor molecule, which recognises PIP2 on the inner leaf of the plasma membrane (Cocucci et al., 2012). Clathrin molecule exists as a triskelion and has the capacity to interact with other clathrin triskelia to form the coat of a clathrin pit (Kirchhausen and Harrison, 1981). The recruitment of two clathrins by four AP2 molecules is sufficient to nucleate the clathrin pit and promote its stable assembly (Cocucci et al., 2012). As the clathrin pit matures, it recruits accessory adaptor molecules, such as Eps15, Epsin and FCHo1/2 (Cocucci et al., 2012; Umasankar et al., 2012). The growing clathrin coat drives membrane deformation, thus initiating the invagination of plasma membrane inside the cytosol (Stachowiak et al., 2013; Stachowiak et al., 2012). The membrane curvature is further exacerbated upon cargo loading into the forming pit by clathrin adaptor molecules. Notable examples include AP2, which serves as an adaptor for tyrosine based endocytic motifs and transferrin receptor endocytosis (Ohno et al., 1995), and ARH and Dab2 in the case of LDL receptor (McMahon and Boucrot, 2011). The ubiquitinated cargo is incorporated in the clathrin pit following its recognition by Eps15 and Epsin (Barriere et al., 2007a). Upon the completion of clathrin assembly, the pit becomes a deeply invaginated cargo containing bud with a thin neck, ready to pinch off from the plasma membrane. The action of dynamin GTPase is required to drive the scission of the neck and the consequent release of the clathrin coated vesicle into the cytosol (Dannhauser and Ungewickell, 2012; Macia et al., 2006). Shortly after pinching off from the plasma membrane, the clathrin coated vesicle undergoes uncoating, driven by Hsc70 and auxilin activity (Bocking et al., 2011; Merrifield et al., 2005), leading to the dissociation of clathrin and adaptor molecules from the vesicle and their reuse in the next rounds of CME.

Several clathrin-independents endocytosis pathways exist, including the small scale endocytic carriers like caveolae, and RhoA, Cdc42 and Arf6 mediated endocytosis, and processes for a larger volume engulfment of extracellular molecules, such as phagocytosis and pinocytosis (Mayor et al., 2014). Caveolin-mediated endocytosis is the second best studied endocytic process after CME. Caveolae are assembled as multimeric complexes composed of caveolin-1, 2 and the associated peripheral membrane proteins, cavins (Hansen and Nichols, 2010; Parton and del Pozo, 2013). These are important for the stabilization of caveolae and the curvature of the plasma membrane trough the recruitment of Pacsin2 (Hansen et al., 2011). The packaging of cargo in caveolae and recruitment of dynamin leads to caveolae pinching off from the plasma membrane and their delivery to the early endosome (Henley et al., 1998).

Larger-volume endocytic processes include phagocytosis and pinocytosis. Phagocytosis mediates internalization of large particles (i.e. pathogens, cell debris) which are recognized by the defined phagocytic receptors through actin-mediated membrane deformation and engulfment of the extracellular material (Flannagan et al., 2012). Pinocytosis originates through actin-mediated membrane ruffling, where PM extensions close-in on each other and create fluid-filled vesicles that can pinch off from PM (Swanson, 2008).

1.1.4. Post-endocytic sorting of cargo at early endosome

Internalized cargo-containing vesicles are destined to fuse with the early endosomal compartment of the cell (Figure 1.1). The early endosome is a highly complex pleomorphic organelle composed of a vesicular body and tubular extensions (Gruenberg et al., 1989). The tubular compartments give rise to the recycling endosomes and are involved in the sorting of receptors towards plasma membrane (recycling) (Maxfield and McGraw, 2004), while the large vesicle undergoes maturation and transitions into Multivesicular body (MVB) by incorporating small parts of its membrane inside its lumen (Piper and Katzmann, 2007). MVBs act as a degradative compartment for ubiquitinated molecules present at the endosomal membrane (Felder et al., 1990; Hicke and Dunn, 2003). Moreover, early endosomes have an acidic luminal pH, which is essential for the dissociation of ligands from their receptors and the consequent sorting of both (Clague et al., 1994; Marshansky and Futai, 2008).

Cargo destined to recycle is rapidly sorted to the tubular compartments of early endosomes (Maxfield and McGraw, 2004). The activity of Arf GTPase leads to the separation of tubular

compartment from early endosome. Thus produced small recycling vesicles are rapidly returned to the cell surface via a Rab4 small GTPase positive compartment (Sheff et al., 1999; van der Sluijs et al., 1992). Alternatively, receptors can be routed to the slow recycling compartment and recycle via Rab11-positive endosomes (Sheff et al., 1999; Sonnichsen et al., 2000). The activity of Rab11's and its isoforms' (Rab11b and c) is essential for the cell surface recycling of several receptors, including transferrin and integrins (Caswell et al., 2007; Sonnichsen et al., 2000). The sorting of receptors to recycling compartment is dependent on the specific sorting signals and the presence of adaptor proteins, such as GGA3 or sorting nexin family proteins (SNX). GGA3 is required for efficient selection of Met receptor into the recycling tubules and its consequent recycling via Rab4 pathway (Parachoniak et al., 2011). SNX27 mediates selection of beta2 adrenergic receptor (B2AR) into the recycling tubules (Temkin et al., 2011), while SNX1 is responsible for E-cadherin recycling (Bryant et al., 2007). Importantly, the mechanism of recruitment of these recycling sorting molecules may be highly dynamic and may depend on cytoplasmic tails motifs, such as suring integrin β1 NPxY-motif-dependent recycling by SNX17 (Bottcher et al., 2012; Steinberg et al., 2012). The specificity of the cargo recycling is further exemplified by a differential requirement of Rabs for the cell surface return of individual cargoes. While Rab4 and Rab11 mediate fast and slow recycling, respectively, other Rabs can act as specific mediators of the select cargo recycling, as in the case of direct Rab25- and indirect Rab35-mediated integrin recycling (Allaire et al., 2013; Caswell et al., 2007).

Alternatively, the ubiquitinated cargo is incorporated within the early endosomal lumen by the mechanism of action of Endosomal Sorting Complex Required for Transport (ESCRT) (Henne et al., 2011; Luzio et al., 2009). This protein complex can recognize the polyubiquitinated receptors and subsequently incorporate them within the intraluminal vesicles (ILVs) during the formation of MVB (Henne et al., 2013; Katzmann et al., 2001; Rodahl et al., 2009). Upon fusion with the lysosome, the contents of MVB are degraded by the proteolytic activity of lysosomal proteases (Luzio et al., 2009). These events lead to an efficient downregulation of the ubiquitinated cell surface receptors and attenuation of their signalling (Rodahl et al., 2009).

1.1.4. Endolysosomal pH and its impact of cargo sorting

As mentioned above, the key feature of endosomes and lysosomes is their low luminal pH. The acidification of endosomes is initiated rapidly at the early endosome stage, reaching pH values of

6.8-6.1. Upon endosome maturation and MVB formation, the pH drops further, reaching 6.0-4.8 range in the late endosomal compartment and ~4.5 in the lysosome (Maxfield and Yamashiro, 1987; Yamashiro and Maxfield, 1987). The progressive acidification is due to presence and activity of endosomal V-ATPases (Marshansky and Futai, 2008). These enzymes act as proton pumps at the endosomal membrane and are the subjects of tight regulation by their complex composition and subunits concentration (Marshansky and Futai, 2008).

Within the endosomal compartment, the acidic pH plays a central role in dissociation of certain ligands from their receptors, such as LDL, transferrin and others (Davis et al., 1987; Harford et al., 1983; Rajan and Menon, 1985). This event allows for the efficient recycling of the receptor via the tubular endosomal network and concentration of luminal cargo (i.e. dissociated ligands) within vesicular portion of endosomes (Maxfield and McGraw, 2004). The luminal contents of endosome are degraded by lysosomal enzymes following the fusion of the two compartments (Luzio et al., 2007). The mechanism of acid-induced ligand dissociation allows for rapid resensitization of the receptor and its return to the cell surface for additional rounds of ligand engagement and downstream signalling (Maxfield and McGraw, 2004).

1.1.5. Ubiquitin and its role in endocytic sorting to degradation

The process of endocytic sorting relies on a number of cargo sorting signals and numerous adaptor molecules responsible for specific signal recognition. The sorting signals include well-defined amino acid motifs (Kelly et al., 2008; Kelly and Owen, 2011) and post-translational modifications such as phosphorylation (Goodman et al., 1997; Krupnick et al., 1997; Wolfe and Trejo, 2007) and ubiquitination (Barriere et al., 2007a; Barriere et al., 2006b; Erpapazoglou et al., 2014; Lauwers et al., 2009). The latter is especially important, since ubiquitination has been demonstrated as a targeting endocytic signal for some cell surface receptors, and their subsequent degradation through the MVB pathway (Lauwers et al., 2009).

Lysine ubiquitination of proteins is a common covalent modification, which orchestrates many signalling cascades. The ubiquitin molecules are capable of forming polyubiquitin chains of various configurations, since every ubiquitin molecule in itself contains seven lysines suitable for addition of another ubiquitin molecule (reviewed in (Trempe, 2011)). Therefore, polyubiquitin chains can form several scaffolding signals, depending on the polyubiquitin chain conformation (i.e. K11, K29, K48, or K63 polyubiquitin chains) (Trempe, 2011). These polyubiquitin chains

variants confer the extreme plasticity of ubiquitin signalling and the specificity of different polyubiquitin chains to a particular signalling pathway (Chen and Sun, 2009; Fushman and Walker, 2010; Lauwers et al., 2009; Matsumoto et al., 2010).

The substrate of ubiquitination is modified by the action of ubiquitin conjugation system, composed of E1-ubiquitin activating enzyme, E2-ubiquitin conjugation enzyme and E3-ubiquitin ligase (reviewed in (Varshavsky, 2012)). These enzymes act in concert to covalently attach a ubiquitin moiety to a lysine residue of the target protein. E3-ligases dictate substrate specificity and are responsible for the type of polyubiquitin chain formed (Budhidarmo et al., 2012; Schulman, 2011). Therefore, E3-ligases are a diverse family of enzymes and they can participate in the regulation of several signalling cascades. However, ubiquitination is not a permanent posttranslational modification, since the action of ubiquitin ligases can be counteracted by the activity of deubiquitinating enzymes (DUBs) (Clague et al., 2013). These enzymes act as ubiquitin proteases capable of removing polyubiquitin chains from the substrate molecules in a substrate specific manner, providing an additional layer of regulation to the ubiquitin signalling (Figure 1.2). Therefore, just like E3-ligases, DUBs play a pivotal role in the ubiquitin-dependent cellular events, including ubiquitin-dependent endocytic sorting.

1.1.6. Ubiquitin function in endocytic sorting of plasma membrane receptors

Cell surface receptor endocytosis is typically initiated following receptor activation by ligand binding. In several cases (i.e. RTKs, GPCRs), the activated receptor is ubiquitinated at the plasma membrane by an E3-ligase such as Cbl (Levkowitz et al., 1999; Waterman et al., 1999). The modification of the receptor with multiple mono and/or polyubiquitin chains leads to its recognition by the endocytic adaptor proteins, such as Epsin and Eps15, that are capable of binding to ubiquitin (Sen et al., 2012; Sigismund et al., 2005), leading to arapid internalization of the receptor complex (Barriere and Lukacs, 2008a; Barriere et al., 2007a; Hawryluk et al., 2006).

The degradative endocytic sorting of cargo molecules requires its polyubiquitination with K63-polyubiquitin chains (Lauwers et al., 2009). This specific chain conformation enables recognition of cargo by the ESCRT machinery upon cargo arrival to the early endosomal compartment (Randles and Walters, 2012; Ren and Hurley, 2010). The ESCRT pathway is responsible for the polyubiquitinated cargo sequestration within the MVB lumen, leading to the termination of

receptor signalling and eventual proteolysis of cargo upon lysosome fusion with the MVB (Rodahl et al., 2009).

Figure 1.2: Interplay of E3-ligases and DUBs in endosomal sorting

Ubiquitination of the cell surface receptors is under tight control by the coordinated activity of E3-ligases and deubiquitinating enzymes (DUBs). E3-ligases are largely responsible for the ubiquitination of cell surface receptors, thus mediating their internalization and their ESCRT-dependent degradation. DUBs counteract the E3-ligases activity by deubiquitinating their targets and promoting the cell surface return of receptors via recycling pathways.

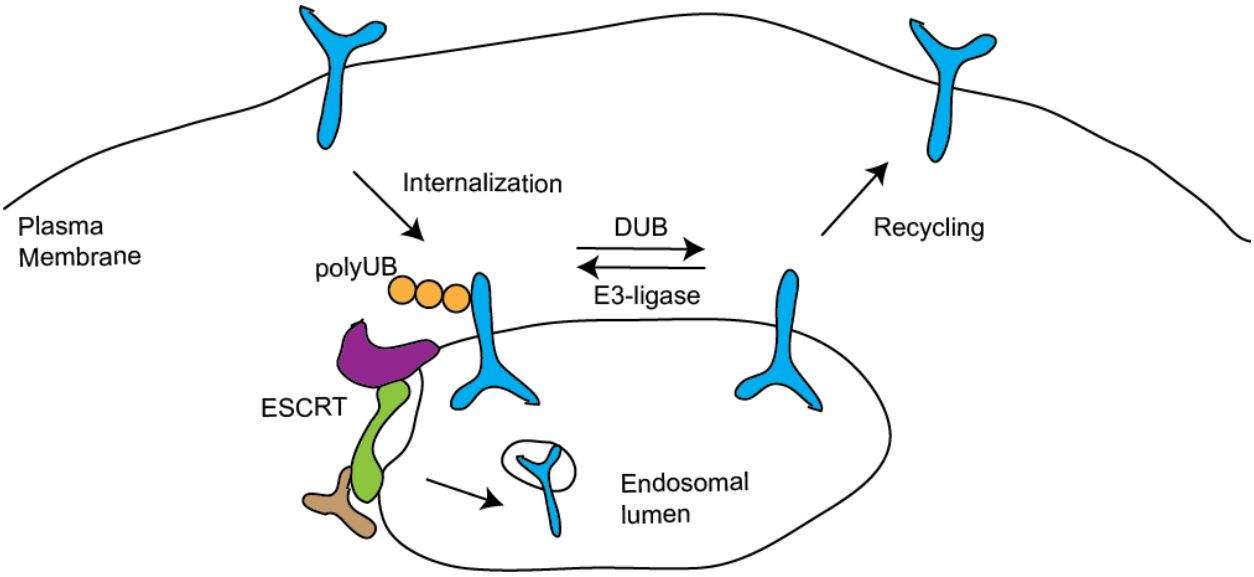

1.1.7. E3-ligases role ubiquitin-dependent endosomal sorting

Ubiquitin conjugation to cell surface molecules is a necessary step for cargo internalization and its subsequent sorting. While several E3-ligases were described to be responsible for this step of endocytosis, the most remarkable examples are Cbl, Itch and MARCH family E3-ligases.

Cbl was described as a E3-ligase required for the internalization of the activated EGFR (Levkowitz et al., 1999). During EGFR endocytosis, Cbl cooperates with GRB2 to heavily modify the receptor with numerous mono- and poly-ubiquitin chains, routing EGFR to degradation (Huang et al., 2006; Stang et al., 2004). A similar mechanism of Cbl activity was proposed in endocytosis of many other cell surface receptors, including VEGFR, PDGFR and integrins (Duval et al., 2003; Haglund et al., 2003; Kaabeche et al., 2005; Miyake et al., 1998; Peschard et al., 2001).

Itch ligase (member of Nedd4 family of E3-ligases) is recruited to its substrate via its WW-domain (Courbard et al., 2002). The recruitment of Itch to Erbb4, CXCR-4 and Notch receptors catalyses their ubiquitination and their consequent targeting to the lysosomal degradation (Bhandari et al., 2007; Qiu et al., 2000; Sundvall et al., 2008). In addition, Itch is able to ubiquitinate the endocytic sorting machinery, including endophilin and PI4-kinase (Angers et al., 2004; Bhandari et al., 2007), suggesting that Itch ubiquitin-conjugation activity can play a dual role in endocytic sorting: via the regulation of cargo ubiquitination and the modulation of stability of trafficking molecules.

1.1.8. Deubiquitinating enzymes and their role in endocytic sorting

Ubiquitination is not a permanent modification, and a special family of deubiquitinating enzymes (DUBs) are responsible for cleaving the ubiquitin chains off the substrate molecules (reviewed in (Clague et al., 2013)). DUBs are diverse in nature and play key roles in processes governed by the ubiquitin-dependent signalling, such as endocytic sorting, NF-κB and Wnt signalling cascades, and transcription regulation (Clague et al., 2013; Clague et al., 2012).

The function of DUBs is primordial in the endocytic sorting of ubiquitinated cell surface receptors, since the targeted DUB activity allows for an additional control step in the fate of ubiquitinated receptors (Clague et al., 2012). One of the DUBs' functions at endosomes is the deubiquitination of cargo, which allows for receptors' escape from the degradative pathway and their return to the plasma membrane for additional rounds of ligand engagement (Wright et al.,

2011). This DUB function was originally demonstrated in the context of the regulation of Wnt signalling pathway, which is initialised by activation and ubiquitination of Frizzled receptor (Fz) leading inducing its internalization (Koo et al., 2012; Rives et al., 2006). Upon Fz targeting to endosomes, the ubiquitin moieties are cleaved off by USP8, allowing the escape of Fz from ubiquitin-dependent degradative MVB targeting in favor of receptor recycling (Mukai et al., 2010). In the absence of USP8, the ubiquitinated Fz is targeted to degradation and Wnt signalling is attenuated (Mukai et al., 2010).

A similar regulatory mechanism of DUB-dependent receptor stabilization was proposed for TGFβ receptor I-II. The lysosomal targeting and the degradation of TGFβR are promoted by the activity of E3-ligases SMURF1/2 and Nedd4-2 (Ebisawa et al., 2001; Kavsak et al., 2000; Kuratomi et al., 2005). However, the receptor can be stabilized by the deubiquitinating step, which occurs following the recruitment of USP4 and USP15 by the receptor signalling scaffold (Eichhorn et al., 2012; Zhang et al., 2012). Strikingly, USP15 recruitment to TGFβR is inversely correlated with TGFβ ligand availability, therefore providing a limit to receptor resensitization and preventing excessive downstream signalling (Eichhorn et al., 2012).

A number of other DUBs regulate the sorting of receptors via similar mechanisms or by acting on the degradative sorting machinery. For instance, AMSH DUB cleaves off K63 polyubiquitin chains specifically (McCullough et al., 2004) and its activity is required for stabilization and cell surface return of EGFR (Bowers et al., 2006). In addition, AMSH deubiquitinates some of the ESCRT components, a mechanism which is essential for the ESCRT-0 complex remodeling and for the efficient recognition of the ubiquitinated cargo at endosome by ESCRT (Sierra et al., 2010). Similarly, USP9x is an endosomal DUB responsible for the deubiquitination of ErbB2 receptor since the deficiency in USP9x expression leads to a destabilization of ErbB2 via the lysosomal degradation (Marx et al., 2010). Moreover, USP9x regulates endocytic trafficking by association with Itch E3-ligase and counteracting Itch auto-ubiquitination (Mouchantaf et al., 2006). Therefore, USP9x is essential for Itch stabilization and activity (Azakir and Angers, 2009), a notion that is indicative of USP9x implication in the endocytic sorting at several levels.

1.1.9. The physiological impact of the deubiquitinases

Due to their central role in regulation of the ubiquitin signalling, DUBs are involved in several disease-relevant cellular pathways. For instance, DUBs regulate stability and function of many

cancer related molecules, such as PTEN and p53 tumor suppressors (Li et al., 2002; Song et al., 2008), as well as MDM2, MYC and MCL1 oncogenes (Popov et al., 2007; Schwickart et al., 2010; Stevenson et al., 2007). The regulation of these factors critical in tumor development suggests a key role for DUBs in cancer and the emergence of certain DUBs as therapeutic targets (reviewed in (Heideker and Wertz, 2015)).

Cylindromatosis tumor suppressor gene (CYLD) is a well-characterized DUB responsible for NF-κB pathway regulation (Brummelkamp et al., 2003; Trompouki et al., 2003; Yoshida et al., 2005). NF-κB signalling heavily relies on ubiquitination of many components of the signalling scaffold (including TRAF2, TRAF6, NEMO and RIP1), which allows for the complex formation and activation of several kinases. CYLD negatively regulates NF-κB signalling pathway by deubiquitinating the central signalling molecules and promoting signalling scaffold disassembly (Brummelkamp et al., 2003; Kovalenko et al., 2003; Trompouki et al., 2003; Yoshida et al., 2005). CYLD tumor suppressive function is likely due to its role in NF-κB signalling and the downstream inflammatory response.

The implication of USP9x in tumor development is more complex. USP9x has been reported to be either an oncogene or a tumor suppressor, since both overexpression and downregulation of USP9x in tumors has been observed (Peng et al., 2013; Perez-Mancera et al., 2012; Wang et al., 2014). The oncogenic property of USP9x comes from its role in stabilization of MCL1 antiapoptotic protein (Glaser et al., 2012), the overexpression of which may block some apoptosis inducing therapies (Peddaboina et al., 2012). Indeed, inhibition of USP9x activity leads to destabilization of MCL1 and resensitization of lung carcinoma cells to apoptosis inducing chemotherapy and radiotherapy (Peddaboina et al., 2012; Trivigno et al., 2012).

On the other hand, USP9x can exert a tumor suppressive function through its interplay with mutant K-Ras G12D. Genetic deficiency of USP9x promotes tumor growth and progression in K-Ras G12D expression context (Perez-Mancera et al., 2012). Although the exact molecular interplay between USP9x and K-Ras G12D is not known, it is possible that it is mediated by Itch ligase, since overexpression of Itch could rescue USP9x deficiency phenotype (Perez-Mancera et al., 2012). The endocytic function of USP9x is likely to influence its role in tumorigenesis, especially via cell surface receptor stabilization (discussed in further detail in Chapter 2).

1.2 The ESCRT machinery and lysosomal degradation

The ESCRT is evolutionary conserved endosomal protein machinery responsible for degradation of the ubiquitinated cargo (Babst, 2005; Katzmann et al., 2001). The key function of the ESCRT pathway is to sequester ubiquitinated receptors within Multivesicular Bodies, thus confining them to degradation and attenuating their signalling (Henne et al., 2011; Katzmann et al., 2001). ESCRT machinery acts as a series of endosomal protein complexes (ESCRT-0, I, -II and –III) able to of recognize the K63-polyubiquitinated molecules (i.e. cell surface receptors, etc.), cluster the cargo on endosomal membrane and subsequently form MVBs and containing the incorporated receptors inside (Katzmann et al., 2001; Luzio et al., 2009). In the absence of ESCRT machinery, formation of MVBs is severely compromised, resulting in the "class E" compartments, incapable of cargo degradation {Raymond, 1992 #134}. While the nature of ESCRTs is well conserved, some ESCRT components participate in multiple cellular functions in addition to their role in endocytic sorting, including viral budding, cytokinesis and autophagy (Filimonenko et al., 2007; Lee et al., 2007; Martin-Serrano et al., 2001; Morita et al., 2007). For the purpose of this thesis, we solely focus on the description of ESCRT endocytic sorting function in the MVB pathway (Figure 1.3).

Figure 1.3: ESCRT machinery mechanism

The ubiquitinated cargo at endosomal surface is recognized and packaged within endosomal lumen by the complex action of the ESCRT machinery. ESCRT-0 components Hrs/STAM1 are capable of polyubiquitinated cargo recognition via their UIM and VHS domains. The polyubiquitinated cargo is then transferred to ESCRT-I complex, which recruits ESCRT-II. HD-PTP acts as an exchange factor mediating ESCRT-0 and ESCRT-III sequential recruitment, and the recruitment of DUB USP8, which is responsible for cargo deubiquitination prior to its incorporation within intraluminal vesicles. The coordinated function of Vps20 and HD-PTP initiates polymerization of CHMP4b filaments driving the ILV neck constriction and scission. The activity of VATPase complex is driving depolymerisation of CHMP4 filaments promoting the pinching off of the ILV and CHMP4 monomer recycling.

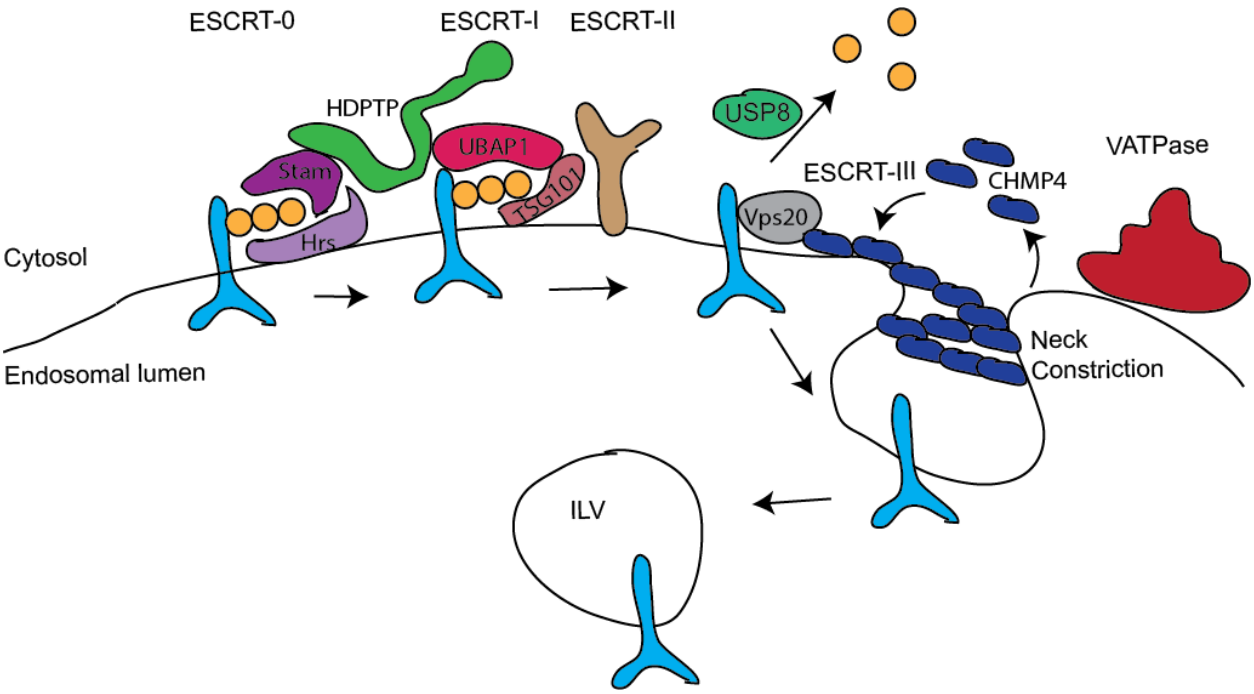

1.2.1 ESCRT complexes

ESCRT-0

ESCRT-0 is the first complex in the ESCRT pathway and it is composed of Hrs (Hepatocyte Growth Factor-regulated tyrosine kinase substrate) and STAM1/2 (Signal Transducing Adaptor Molecule ½) (Asao et al., 1997). Hrs acts as the endosomal recruiting factor for ESCRT-0 complex via its FYVE-domain, a phosphatidylinositol 3-phopshate (PI3P) binding domain (Mao et al., 2000). In addition, Hrs is able to bind to the endosomal clathrin, a key feature of the ESCRT-0 component (Raiborg et al., 2002; Raiborg et al., 2001b). Both Hrs and STAM1 contain ubiquitin binding domains (UIM and VHS) (Hirano et al., 2006), which are essential during the polyubiquitinated cargo recognition by ESCRT-0 complex (Ren and Hurley, 2010). The assembly of Hrs and STAM1 into a heterotetrameric complex increases its UB-binding domains avidity to polyubiquitinated cargo, increasing efficiency of cargo engagement into ESCRT pathway (Ren and Hurley, 2010). Hrs interaction with clathrin assists in the first step of cargo clustering at endosomal membrane, creating ESCRT enriched microdomains that serve as the origin for ILV formation during the later steps of the ESCRT pathway (Raiborg et al., 2002; Raiborg et al., 2001a). On top of its function in the polyubiquitin recognition, ESCRT-0 acts as a recruitment module of the subsequent ESCRT-I complex via its direct interaction with TSG101 and HD-PTP (Bache et al., 2003; Katzmann et al., 2003; Lu et al., 2003).

ESCRT-I

The core of ESCRT-I complex consists of TSG101, Vps28, Vps37 and Mvb12 (Katzmann et al., 2001). Later studies have identified additional components of ESCRT-I complex, namely Ubiquitin Associated Protein 1 (UBAP1)(Stefani et al., 2011) and isoforms of Vps37 (Bache et al., 2004) and Mvb12 (Curtiss et al., 2007). The recruitment of UBAP1 and Mvb12 by ESCRT-I confers a stronger ubiquitin binding ability to ESCRT-I, which is essential for the polyubiquitinated cargo transfer from ESCRT-0 to ESCRT-I (Stefani et al., 2011; Wunderley et al., 2014). In addition, there is a number of ESCRT-I associated proteins that interact with ESCRT-I and are essential for its function. These include two Bro-domain containing proteins, HD-PTP and Alix, which are required for ESCRT-I sorting function and MVB morphogenesis (Ali et al., 2013; Doyotte et al., 2008; Luhtala and Odorizzi, 2004; Odorizzi et al., 2003). The complex nature of ESCRT-I interactions involves the bidding to both ESCRT-0 and ESCRT-II, an event responsible for cargo transfer and ESCRT-II recruitment (Gill et al., 2007).

ESCRT-II

The third complex in the ESCRT pathway is ESCRT-II. This Y-shaped module is composed of Vps22, Vps36 and two subunits of Vps25. ESCRT-II bears a PI3P binding GLUE-domain within Vps36 (Gill et al., 2007; Teo et al., 2006), which is responsible for the endosomal targeting of the complex. ESCRT-II is essential for the recruitment of the last complex in ESCRT pathway, ESCRT-III, via the interaction of Vps25 with Vps20 (Teo et al., 2004). This event is indispensable for the nucleation of ESCRT-III scaffold and for the formation of intraluminal vesicles (ILV) within MVBs (Teo et al., 2004).

ESCRT-III

ESCRT-III is a highly dynamic protein complex that forms on the endosomal membrane following the binding of Vps20 by ESCRT-II subunit. This interaction initiates the recruitment of CHMP4b monomers to the endosomal membrane (Saksena et al., 2009; Teis et al., 2010). In steady state, CHMP4b monomers exist in an autoinhibited conformation in cytosol due to electrostatic intramolecular interaction (Shim et al., 2007), yet CMHP4b can be activated by the ESCRT-III nucleating event induced by Vps20 (Teo et al., 2004). Active CHMP4b assembles in homo-oligomeric structures, driving endosomal membrane deformation and shaping the first step of ILV formation (Hanson et al., 2008; Saksena et al., 2009; Wollert et al., 2009). The recruitment of Vps24 to CHMP4b filaments' cap terminates oligomerization and leads to the recruitment of Vps2, completing the ESCRT-III assembly (Babst et al., 2002a).

The key function of ESCRT-III is the abscission of cargo-containing ILVs inside MVB lumen. This event, and the consequent disassembly of ESCRT-III polymers, is driven by the recruitment of the class I AAA ATPase Vps4 (Davies et al., 2010; Shestakova et al., 2010). In complex with Vta1, Vps4 forms a dodecamer of two hexameric rings (Scott et al., 2005a; Scott et al., 2005b), catalyzing the scission of ILV neck and disassembly of CHMP4 filaments (Wemmer et al., 2011). The ILV scission event is the last step in ESCRT pathway and is crucial for the ESCRT functionality.

1.2.2. The ESCRT dependent sorting mechanism

The complex structure of the individual modules of the ESCRT machinery described above ultimately serves to sort the polyubiquitinated cargo inside MVB for lysosomal degradation. The first step in cargo sorting process by ESCRT is ESCRT-0 mediated recognition of the

polyubiquitinated receptors after their endocytosis and arrival to the early endosomes. Both ESCRT-0 components, Hrs and STAM1, contain ubiquitin binding domains, UIM and VHS (Bilodeau et al., 2002; Hirano et al., 2006). These domains act in concert to recognize polyubiquitinated cargo modified with K63 ubiquitin chains (Ren and Hurley, 2010), a specific signal targeting molecules to the ESCRT pathway and consequently MVB/lysosomal degradation (Erpapazoglou et al., 2012; Lauwers et al., 2009). Once the polyubiquitinated cargo has been engaged by the ESCRT-0 complex, the ESCRT-I complex is recruited and the cargo is transferred from ESCRT-0 to ESCRT-I. The subsequent interactions of ESCRT-I with ESCRT-II and ESCRT-accessory proteins HD-PTP and UBAP1 are responsible for the retention of polyubiquitinated cargo by ESCRT-I (Pashkova et al., 2013; Stefani et al., 2011) and for the initiation the nucleation of ESCRT-III (Babst et al., 2002b). At this stage, the ubiquitinated cargo is clustered at the origin of ILV formation and the initial membrane deformation is initiated. A key requirement for the efficient cargo packaging within a nascent ILV is the deubiquitination of cargo (Luhtala and Odorizzi, 2004; Odorizzi et al., 2003). Once the cargo was commited to ILV incorporation through ESCRT-0,-I,-II action, HD-PTP recruits a deubiquitinating enzyme UBPY/USP8 to cleave off the ubiquitin moieties from cargo (Ali et al., 2013). This process allows for both recycling of ubiquitin molecules and efficient cargo packaging within ILVs.

The final step in the ESCRT pathway is the scission of the ILV inside MVB lumen driven by ESCRT-III oligomerization (Wollert et al., 2009). There are several models proposed for the mechanism of ILV formation and scission by ESCRT-III machinery. The general consensus is that the formation of CHMP4b oligomers drives the inverted tube deformation of the membrane, leading to the nascent ILV formation (Lenz et al., 2009a). The accumulation of spiral-like CHMP4b-Vps24-Vps2 oligomers constricts the neck of the forming ILV (Lata et al., 2008), eventually driving the vesicle scission and its budding inside the MVB lumen (Lenz et al., 2009a; Lenz et al., 2009b). Following this step, the ESCRT-III complex filaments disassemble via the activity of Vps4 ATPase complex (Lata et al., 2008). While hypothetical, it is likely that the ATPase also provides the energy required for ILV scission. This is possibly due to the destabilizing activity of depolymerisisng CHMP4b filaments, which constricts the ILV neck (Saksena et al., 2009), in manner similar to a “purse string”. Another hypothesis suggests that the drastic depolymerisation of ESCRT-III by Vps4 activity simply leads to an energetic collapse of

highly curved membrane at the neck of the ILV and the consequent scission of the vesicle (Bashkirov et al., 2008).

Pinching off of the cargo containing ILV into MVB is the culmination of ESCRT pathway. The isolation of the receptor cargoes from the cytosol results in their signalling termination and the subsequent fusion of MVB with lysosome results in cargo degradation (Miaczynska, 2013). This process is responsible for the attenuation of receptor signalling and for the regulation of the total receptor cellular levels.

1.2.3. ESCRT function in receptor sorting and downstream signalling

The crucial function of ESCRT machinery in the cell surface receptor sorting to degradation attenuates receptor signalling (Rodahl et al., 2009). Thus, the ESCRT-mediated negative regulation of receptor signalling can be manifested either by a reduction in concentration of the receptor at the cell surface or decreased duration of receptor signalling due to its incorporation within the MVBs (Rodahl et al., 2009; Sorkin and von Zastrow, 2009). Moreover, several receptors use distinct signalling complexes at the plasma membrane and the endosomes (i.e. EGFR, TNFR1, TGFR, some GPCRs), resulting in a spatiotemporal regulation of their downstream signalling, which can also be affected by ESCRT activity (Chen et al., 2007; Lu et al., 2009; Mullershausen et al., 2009; Schutze et al., 2008; Shi et al., 2007; Sigismund et al., 2013; Sigismund et al., 2008).

As expected, ESCRT function is required for the appropriate regulation of several receptors' signalling cascades. The signalling downstream of EGFR is one of the earliest described examples of receptor signalling cascades negatively regulated by ESCRT. Upon depletion of ESCRT-0 and –I components, EGFR degradation is compromised, leading to an increased recycling of the receptor to cell surface and a sustained signalling through MAPK cascade (Malerod et al., 2007; Raiborg et al., 2008). Interestingly, the downregulation of ESCRT-II or –III constituents does not result in this phenotype, suggesting that the EGFR signalling complex is disassembled prior to the ESCRT-II recruitment (Bache et al., 2006; Malerod et al., 2007). A similar role of the ESCRT machinery is likely to regulate several other receptor tyrosine kinases, since many RTKs' signalling is attenuated by the ubiquitination dependent receptor downregulation.

Similarly, ESCRT-0 and -I depletion results is a sustained activation of the Notch pathway. Notch receptor was described to be ubiquitinated and sorted within MVBs, an event that leads to a reduction of the receptor cleavage and signalling (Vaccari et al., 2008). However, in the absence of the ESCRT machinery, Notch receptor cleavage is exacerbated, presumably due to its prolonged presence on the endosomal membrane (Vaccari et al., 2008; Windler and Bilder, 2010). In mosaic Drosophila ESCRT mutants, Notch signalling acts in a non-autonomous manner due to a paracrine signalling mechanism of the mutant cells to the surrounding WT cells, driving the Notch pathway activation and its persistent signalling (Moberg et al., 2005).

ESCRTs also play a key role in the regulation of cellular migration and cell polarity. For instance, integrin receptors are degraded via the ESCRT pathway, thus impacting cell migration and invasion (Lobert et al., 2010; Lobert and Stenmark, 2011, 2012). A similar degradative route is required for the downregulation of E-cadherins during Epithelial-Mesenchymal Transition (EMT) in polarized cells (Fujita et al., 2002; Palacios et al., 2005). EMT is characterised by the loss of adherent junction proteins, an abrogation of cell-cell contacts and the acquisition of promigratory qualities. E-cadherins are key constituents of the adherent junctions and are ubiquitinated by E3-ligase Hakai upon EMT induction. The consequent degradation of E-cadherin is mediated by the ESCRT machinery, ultimately resulting in an efficient EMT (Palacios et al., 2005).

1.2.4. Physiological relevance of ESCRTs

The profound effect of the ESCRT sorting function on several cell surface receptors implies a key role of the ESCRT function in physiology and pathology. Previously, the ESCRT machinery was proposed to have a tumor suppressive function, due to its role in attenuation of cell surface receptor signalling.

ESCRT-0 component Hrs was identified as tumor suppressive gene in *Drosophila* and mammalian models, due to its negative role in EGFR signalling (Lloyd et al., 2002). However, cancer cells deficient of Hrs displayed reduced colony formation and metastatic potential (Toyoshima et al., 2007). The ESCRT-I constituent, TSG101, is the most studied ESCRT member in the context of tumorigenesis. Cellular depletion of TSG101 results in an anchorage independent growth and a higher metastasis rate of xenograft models (Li and Cohen, 1996). However, the function of TSG101 mediates several cellular processes, including cytokinesis,

making some of the findings about TSG101 tumor suppressive potential ambiguous. Another ESCRT-I component, Vps37a, displayed similar tumor suppressive function, as its deficiency conferred potentiated growth and invasive properties (Wittinger et al., 2011). Similar phenotypes were observed upon knockdown of ESCRT-III proteins, Chmp3 and Chmp1a (Dukes et al., 2008; Li et al., 2008).

The tumor suppressive role of ESCRT proteins is further supported by the studies of their expression status in human tumors. The mRNA levels of TSG101, Vps37a, Chmp1a and Vps4 were found to be downregulated in lung carcinomas, hepatocellular carcinomas, melanomas/pancreatic tumors and aggressive breast cancer, respectively (Cai et al., 2008; Li et al., 2008; Lin et al., 2012; Lu et al., 2003; Wittinger et al., 2011). In addition, the ESCRT component HD-PTP is localised to 3p21.3 chromosomal region, frequently deleted in human cancers (Yamakawa et al., 1993; Yau et al., 2006), while UBAP1 was reported to be lost via chromosomal deletion in nasopharyngeal carcinomas (Xiao et al., 2006). These findings are indicative that ESCRT machinery function can have a broad impact in tumorigenesis and disease progression. Additional studies of the ESCRT machinery's role in tumorigenesis are needed, since the *in vivo* evidence for their tumor suppressive potential is lacking due to the limitations of ESCRT animal models (reviewed in (Michelet et al., 2010)).

1.2.5. Emerging players in the ESCRT pathway

Although the initial discovery of the ESCRT machinery is over a decade old, the extensive studies of the endolysosomal pathway have resulted in a recent identification of several new ESCRT components and various associated proteins. Some of these findings pinpoint that the ESCRT pathway is more diverse in its nature than previously thought, and some of the current ESCRT components arose later in the evolution than others.

Two of the key novel ESCRT components, HD-PTP (described in details below) and UBAP1, were described by Phillip Woodman group. Both proteins participate in ESCRT-0 and –I function, have ubiquitin binding capacity and are required for the efficient degradation of the polyubiquitinated cargo. UBAP1 contains two ubiquitin binding motifs (N-terminal UIM and c-terminal UBDs). It forms a complex together with HD-PTP and the core ESCRT-I constituents, namely TSG101, Vps37a and Mvb12. Depletion of UBAP1 compromises the ESCRT's endosomal function, while the other ESCRT functions remain unaffected. Therefore, UBAP1

containing ESCRT-I complex is specifically involved in the polyubiquitinated cargo sorting and thus represents a useful model to study ESCRT-I sorting mechanism.

The ESCRT-0 complex is well established to be composed of Hrs and STAM1. The Hrs/STAM1 complex carries out the essential role of polyubiquitinated cargo recognition and engagement into the ESCRT pathway. However, Hrs/STAM1 complex has appeared relatively late in the evolution (Herman et al., 2011; Leung et al., 2008), suggesting that the ancient organisms must rely on an alternative ESCRT-0 complex, hypothetically represented by TOM1 (Target of Myb1) protein (Blanc et al., 2009; Herman et al., 2011). TOM1 contains ubiquitin binding VHS and GAT domains and is necessary for cargo sorting in the MVB pathway in lower organisms (Blanc et al., 2009; Herman et al., 2011; Misra et al., 2000; Shiba et al., 2004; Yamakami et al., 2003). Notably, TOM1 is evolutionary conserved in mammals, and is seemingly involved in the ESCRT function (Wang et al., 2010). In human cells, TOM1 is targeted to endosome via its interaction with Endofin (Endosomal FYVE domain protein) (Seet and Hong, 2005; Seet et al., 2004), that also mediates clathrin recruitment to the complex. Altogether, TOM1/Endofin complex displays the key properties of an ESCRT-0 and therefore was proposed to act as an alternative ESCRT-0 complex in mammalian cells (Katoh et al., 2004; Wang et al., 2010). It is likely that TOM1/Endofin complex can act in parallel with Hrs/STAM1 complex during the early steps of endosomal sorting of ubiquitinated cargo.

1.3. Histidine Domain containing Protein Tyrosine Phosphatase, HD-PTP

1.3.1. HD-PTP is an inactive phosphatase

HD-PTP is an evolutionary conserved molecule with a complex domain architecture. It contains N-terminal Bro1-domain, followed by a V-domain, a proline rich region (PRR) and Protein Tyrosine Phosphatase domain. The Bro1-domain of HD-PTP is homologous to the yeast Bro1 protein, reported to play a role in the vacuolar sorting, ESCRT pathway and MVB biogenesis (Odorizzi et al., 2003). The V-domain of HD-PTP is is able to bind ubiquitin and and mediates the interaction with UBAP1 (Pashkova et al., 2013; Stefani et al., 2011). The PTP domain of HD-PTP does not bear phosphatase activity, thus HD-PTP is classified as a pseudophosphatase (Gingras et al., 2009b).

HD-PTP is an inactive protein tyrosine phosphatase due to an evolutionary conserved mutation in its PTP domain (Gingras et al., 2009a). Classical PTPs' catalytic domains are defined by series of catalytic residues within the domain organized in a highly conserved signature motifs within the phosphatase domain, among which motif 9 (H/V)C(X_5)R(S/T) is responsible for the PTP enzymatic activity. The cysteine residue in the motif 9 is required for the catalytic activity, while several others promote the dephosphorylation reaction. For instance, the arginine residue is essential for the phosphatase activity as a stabilizer of the transition state intermediate. These residues, together with the WPD loop (motif 8) and the Q-loop (motif 10) define a minimal catalytic core of a protein tyrosine phosphatase (Tonks, 2006, 2013).

While HD-PTP maintains the critical catalytic cysteine residue (C1392), its PTP domain contains an evolutionary conserved mutation (motif 9 consensus alanine residue mutated to a serine, S1394). Previous analysis of similar mutations in PTP IA-2 and IA-2β suggests that the consensus alanine is essential for PTP activity (Gross et al., 2002). Indeed, the backmutation of HD-PTP to consensus motif (S1394A) restores its phosphatase activity (Gingras et al., 2009b). However, while HD-PTP does not have a phosphatase enzyme function, it remains a key molecule in cell biology due to its emerging role as a scaffolding protein in endocytic sorting and the ESCRT pathway.

1.3.2. HD-PTP – an ESCRT associated protein required for efficient cargo sorting

Recently, HD-PTP has been classified as part of the Endosomal Sorting Complex Required for Transport (ESCRT) machinery. HD-PTP was shown to interact with several core ESCRT-0, I and -III proteins, including TSG101, UBAP1, Hrs, Stam1 and CHMP4b (Ali et al., 2013; Doyotte et al., 2008; Stefani et al., 2011).

Originally the role of HD-PTP in ubiquitinated sorting was proposed based on the observation of the impaired EGFR trafficking and the MVB biogenesis upon HD-PTP depletion (Doyotte et al., 2008). Recently, HD-PTP was shown to mediate the exchange between ESCRT-0 and ESCRT-III during EGFR sorting and the recruitment of USP8 to deubiquitinate the receptor prior to its incorporation into ILVs (Ali et al., 2013). The interaction between HD-PTP, Stam1 and CHMP4b occurs in a sequential manner, since Stam1 and CHMP4b recognize the same binding site in HD-PTP Bro1 domain. The exchange of Stam1 for CHMP4b and recruitment of USP8 by HD-PTP drives the release of cargo from ESCRT-0, its deubiquitination

by USP8 and its consequent incorporation into ILVs. While HD-PTP is not required for ILVs formation per se, it is necessary for the efficient ubiquitinated cargo targeting into ILVs.

Importantly, the pseudophosphatase domain of HD-PTP is dispensable for its function in endocytic sorting (Doyotte et al., 2008; Pradhan-Sundd and Verheyen, 2014). The trafficking defects resulting from HD-PTP depletion can be rescued by Bro1-V domain deletion construct, which is responsible for the interaction with ESCRT machinery and ESCRT-0,-III exchange (Ali et al., 2013; Doyotte et al., 2008).

1.3.3. Recognition of polyubiquitin chains by HD-PTP

Capacity for K63 polyubiquitin chains recognition is a hallmark property of the ESCRT components and is an essential first step in the degradative MVB sorting pathway. The structure of HD-PTP does not contain classical ubiquitin binding domains, such as UBD or UIM. Nevertheless, the V-domain of HD-PTP has been reported to recognize K63 polyubiquitin chains *in vitro* (Pashkova et al., 2013). This feature of the V-domain is preserved in several Bro1-family V-domain containing proteins, including ALIX (Dowlatshahi et al., 2012). While the exact interaction interface between polyubiquitin and HD-PTP V-domain is not known, it is likely that the ability of HD-PTP to interact with polyubiquitin assists the cooperative cargo recognition function of ESCRT complex and facilitates the cargo transfer from ESCRT-0 complex. In addition, the V-domain of HD-PTP contributes to the polyubiquitin binding via its interaction with UBAP1, which bears UIM and UBA domains and is involved in ESCRT-I function (Stefani et al., 2011).

1.3.4. HD-PTP cellular and physiological functions

The function of HD-PTP within the ESCRT pathway suggests its broad role in endosomal sorting of receptors and in the regulation of cell signalling. Importantly, this function of HD-PTP is conserved across species. Drosophila orthologue of HD-PTP, *Myopic (Mop),* was described to play a role in trafficking of EGFR, Toll-like receptor and integrins. *Mop* is responsible for EGFR downregulation via the endosomal pathway following receptor internalization and ubiquitination (Miura et al., 2008). Similarly, *mop* is responsible for the proper trafficking and activation of Toll-receptor, since deletion of *mop* results in lack of Toll downstream signalling (Huang et al., 2010). Furthermore, *mop* is responsible for integrin β1 receptor trafficking and cellular distribution (Chen et al., 2012); as well as Wnt signalling, by

affecting both Wingless receptors sorting to lysosomes and the ligand Wg resecretion in basal surface of polarized cells (Pradhan-Sundd and Verheyen, 2014). In addition, endosomal function of *mop* is required for the regulation of the oncogene Yorkie, as *mop* controls Yorkie endosomal localization and transcriptional activity (Gilbert et al., 2011). Collectively, these studies suggest that Drosophila *Myopic* can affect the sorting and signalling of several cell surface receptors.

HD-PTP plays a key cellular function in receptor sorting in mammalian systems and is essential for several developmental processes in vertebrates. HD-PTP is indispensable in mouse development, as the homozygous deletion of HD-PTP leads to embryonic lethality (Gingras et al., 2009b). This developmental defect may be attributed to several processes affected by HD-PTP function. In addition to regulation of the endocytic sorting and cell surface receptor signalling, HD-PTP functions in neuronal pruning and Survival Motor Neuron complex (SMN), essential for mRNA splicing process (Husedzinovic et al., 2015; Loncle et al., 2015). Moreover, HD-PTP was also demonstrated to act as an inhibitor of cellular migration and invasion (Castiglioni et al., 2007; Lin et al., 2011; Mariotti et al., 2009), a phenotype that can potentially be due to its role in sorting of cell adhesion receptors.

1.4. Integrin adhesion receptors

1.4.1. Integrin family of adhesive molecules

Integrins are a family of transmembrane adhesion receptors that play a key role in cellular adhesion, migration, mechanotransduction, proliferation and cell survival (Barczyk et al., 2010; Hynes, 2002). Integrins act as heterodimeric type I receptors, composed of α and β subunits (Luo et al., 2004; Vinogradova et al., 2002). The human integrin family consists of 18 α-subunits and 8 β-subunits. These subunits can form 24 heterodimers, each serving as a receptor for a specific extracellular matrix (ECM) component (Hynes, 2002). Integrin heterodimers can be classified into RGD-receptors (i.e. α5β1, αvβ3, αvβ5; binding to fibronectin and vitronectin), collagen-receptors (i.e. α1β1, α2β1), laminin-receptors (i.e. α3β1, α6β4) and leukocyte-specific receptors (i.e. αLβ2, αMβ2, α1β1, α4β7) (Margadant et al., 2011).

The structure of integrin receptors is rather complex and is very dynamic. The structural shifts in integrin heterodimers are responsible for the activation mechanism of the receptor upon ligand engagement. The α-subunit is composed of seven β-propeller domains, followed by the Thigh-domain, Calf-1 and Calf-2 domains, a transmembrane region and a short cytoplasmic tail (Larson

et al., 1989) (Figure 1.4A). The β-propeller region bears Ca^{++} binding capacity, which is essential for the ligand interaction (Humphries et al., 2003). Nine α subunits also contain a αI-domain with a site responsible for the ligand recognition in a Mg^{++} -dependent manner (Kamata and Takada, 1994; Michishita et al., 1993). Therefore the metal-ion-dependent adhesion site (MIDAS) acts as a key ECM engagement module within αI-domain containing integrins (Lee et al., 1995).

The β integrin subunit is composed of a PSI-domain, a hybrid domain, a βI-domain, four EGF-repeats, followed by a transmembrane region and a short cytoplasmic tail, responsible for interaction with a number of signalling molecules (Xiong et al., 2001; Xiong et al., 2004) (Figure 1.4A). The heterodimerization of α and β subunits occurs through an interaction between the α-subunit propeller and the hybrid domain of β-integrin. Similarly to the α-subunits, the βI-domain of β-subunit also contains a MIDAS site (Lee et al., 1995), which coordinates metal-ion dependent ligand binding in integrins devoid of αI-domain (i.e. integrin α5β1). In the case of αI-domain containing heterodimers, the βI-domain of β-subunit plays a regulatory role (Xie et al., 2010). Importantly, the cytoplasmic tail of β-integrins contains several binding sites (NPxY-motifs) for its interacting proteins (talin, kindlin and others) (Moser et al., 2008; Wegener and Campbell, 2008), linking integrins with the actin cytoskeleton and providing motifs that regulate integrin endocytic sorting (Wegener and Campbell, 2008).

1.4.2. Mechanism of integrin activation

Integrin α5β1 heterodimers are structurally complex molecules and have an elaborate mechanism of activation. Typically, integrin α5β1 can exist in three ligand-affinity states: low, intermediate and high affinity (Beglova et al., 2002; Shimaoka et al., 2002; Takagi et al., 2002; Takagi and Springer, 2002) (Figure 1.4B). The cell surface population of integrin receptors is in a dynamic equilibrium between the three states. The three affinity states of integrin are defined by major conformational shifts in their structure. The "inactive" (low ligand affinity state) is characterized by a bent conformation, where the head of integrin heterodimer extracellular domains is folded back onto the receptor stalk and the cytoplasmic tails of α and β subunits are in an inhibitory (unable to bind the cytoplasmic components) state (Beglova et al., 2002; Takagi and Springer, 2002; Vinogradova et al., 2002). The intermediate state is characterized by the extended form of integrin extracellular domain, yet the integrin head preserves its low ligand affinity state. The fully activated α5β1 integrin receptors has a high ligand affinity, an upright shape and α and β

cytoplasmic tails are separated leading to the recruitment of cellular factors to the beta 1 cytoplasmic tail and adhesion initiation (Luo and Springer, 2006; Luo et al., 2004; Nishida et al., 2006).

Integrin α5β1 activation can occur via its interaction with the respective ligand (outside-in signalling) or following the binding of activating proteins, such as talin and kindlin, to the integrin cytoplasmic tail (inside-out signalling) (Luo and Springer, 2006; Takagi and Springer, 2002). The outside-in signalling is essential for the formation of early adhesion complexes, their function and the cell migratory properties (Giancotti and Ruoslahti, 1999). The inside-out signalling is responsible for the translation of intracellular changes into cellular adhesive state and dictates the cellular interaction with ECM from within the cell (Luo and Springer, 2006). In both cases, the active form of integrin α5β1 promotes the focal adhesion formation, acts as a link between the cytoskeleton and ECM, and serves as a signalling scaffold to drive the pro-migratory signalling (Byron et al., 2010).

Figure 1.4: Mechanism of integrin activation

(A) Structural organization of integrin α5β1 domains.

(B) Inactive integrins exist in a bent conformation, in low ligand affinity state and close cytoplasmic tails positioning, which does not allow signalling complex formation. The biding of Talin to integrin β1 cytoplasmic tail induced intermediate activation state of integrins, leading to the upright conformation and a high-ligand affinity. The binding of a ligand (here: fibronectin in case of α5β1 integrin) induces the full activation of integrin and scaffolding of signalling complex. The recruitment of Vinculin, Paxilin, FAK and Src promotes formation of nascent adhesions, which mature into focal complexes upon actin linkage. Details in text.

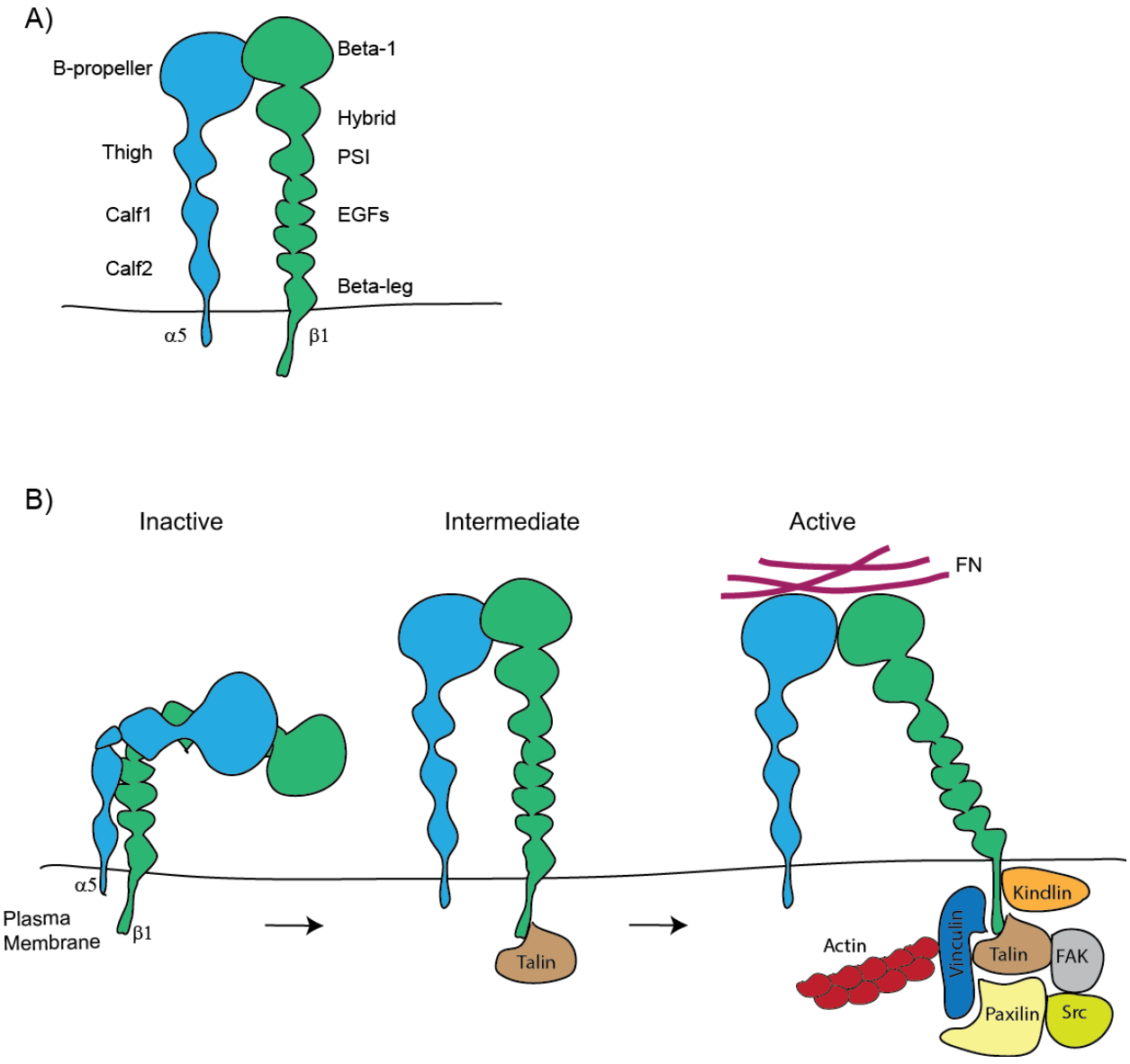

1.4.3. Extracellular matrix and fibronectin as integrin substratum

Extracellular matrix (ECM) is an indispensable structural constituent in multicellular organisms. While ECM serves as support for cells and tissues, it is also involved in organ homeostasis, development and cell signalling. The ECM composition includes several fibrous molecules, such as collagens and elastin, and glycoproteins, such as fibronectin, proteoglycans and laminin. The fibrous ECM is formed by a complex assembly of collagens into higher order fibrillary structures through an extensive crosslinking between the individual molecules. This type of ECM forms the basis of ligaments and tendons in mammals. Basal lamina is the other type of ECM meshwork

involved in cell layers support, segregation, tissue homeostasis/signalling and providing sites for cell adherence.

Fibronectin is an essential ECM component that mediates connection between cells and ECM via integrin receptors (α5β1 and others). Fibronectin is secreted as a large dimeric glycoprotein, composed of three modules repeats (type-I, II, III). Every fibronectin molecule is stabilized by the intramolecular disulfide bonds within type-I, II modules repeats. The type-III modules are responsible for integrin α5β1 interaction via module III_{10} RGD-motif. The assembly of the individual fibronectin dimers is catalysed by their interaction with cell surface integrins, a process which induces clustering of fibronectin dimers and promotes their self-assembly. The mechanotransduction force resulting from integrin interaction deforms fibronectin molecules, exposing additional self-assembling sites, ultimately driving formation of the mature fibronectin fibrils. Fibronectin fibrils become the essential component of ECM via their interactions with other ECM molecules, such as collagens and proteoglycans. Therefore, fibronectin serves as a key connection molecule between cells and their substratum, regulating a number of processes including cell migration, differentiation and growth factor signalling.

1.4.4. Regulation of adhesion formation by integrins

Integrins play a key role in cellular adhesion to the extracellular matrix and the migration of cells. During cellular migration, integrins assemble in focal adhesion complexes at the plasma membrane, which mediate the interaction of ECM with cytoskeleton (Byron et al., 2010; Zaidel-Bar et al., 2007a; Zaidel-Bar et al., 2007b). The formation of focal adhesions is initiated at the leading edge of migrating cells (lamellipodium), where integrins assemble into clusters and engage ECM (Parsons et al., 2010). These initial points of cell contact with the matrix are termed nascent adhesions, small protein complexes, mainly composed of integrins and associated activating proteins, such as talin and paxilin (Parsons et al., 2010; Zaidel-Bar et al., 2007a; Zaidel-Bar et al., 2007b). Upon their maturation, nascent adhesions are linked to the actin cytoskeleton via the recruitment of vinculin to talin, thus reinforcing the adhesive structure and providing a solid integrin-actin link (del Rio et al., 2009; Grashoff et al., 2010).

Further maturation of adhesion complexes occurs as the lamellipodium advances forward. Integrin-containing adhesion complexes become larger and recruit additional components to link it with actin stress fibers, an interaction that is essential for the mechanical transduction of the

cytoskeletal pulling force on matrix translating into the cell movement forward (Choi et al., 2008).

Eventually, a migrating cell must disassemble the focal adhesions in order to detach its trailing edge and move further (Broussard et al., 2008). Alongside with the depolymerisation of the focal adhesions, this process requires a rapid turnover of adhesion components back tto the migrating edge of the cell for further rounds of matrix engagement (Digman et al., 2008; Palecek et al., 1998). Largely, the mechanism of focal adhesion turnover is regulated by endocytic trafficking of integrin receptors and their recycling at the leading edge of the cell.

1.4.5. Endocytic sorting of integrins

The endocytic sorting of integrins has recently emerged as a key regulatory mechanism of several signalling pathways and physiological processes (reviewed in (Caswell and Norman, 2006; Rainero and Norman, 2013; Valdembri and Serini, 2012)). Typically, integrins can be internalized by the clathrin-dependent and clathrin-independent routes, leading to the delivery of integrins to the early endosomes. The sorting process of integrins occurs at this cellular compartment, and the degradative or the recycling fate of integrins is determined by a number of factors, including sorting signals, ubiquitination status, and the interactions with the sorting machinery. Importantly, the rates ofrecycling and degradation of integrin receptors have a key implication in cell migration, invasion and metastasis formation. These endocytic events and their impact on cellular signalling and physiology are described here (Figure 1.5).

1.4.6. Routes of integrin internalization

Canonically, integrin α5β1 was described to be internalised via the clathrin-dependent mechanism (Ezratty et al., 2009). Remarkably, the clathrin-mediated endocytosis (CME) of integrins is closely linked with the disassembly of focal adhesions (Chao and Kunz, 2009; Ezratty et al., 2009). The CME adaptors Dab2 and ARH are required for this process, as their depletion results in an impaired endocytosis of β1 integrins (Chao and Kunz, 2009; Teckchandani et al., 2009). In addition, Eps15, an endocytic adaptor for ubiquitinated receptors, plays a role in Dab2-mediated integrin internalization (Teckchandani et al., 2012).

The cytoplasmic tail of integrin β1-subunits contains a proximal and a distal NPxY-motif. These amino acid sequences are necessary for the efficient internalization of integrin receptors (Margadant et al., 2012; Pellinen et al., 2008). While neither of these motifs mediates the

interaction with clathrin adaptors, they are important for recruitment of talin and kindlin, mediating the assembly of integrins cluster in focal adhesions. Therefore, it is likely that NPxY-motifs are responsible for the localization of integrins to the adhesive structures from which their clathrin-mediated endocytosis occurs (Ezratty et al., 2009).

Recently, other routes of integrin endocytosis have been described. These include: caveolin-dependent endocytosis, clathrin-independent carriers, and macropinocytosis. Caveolin-dependent pathway is responsible for the internalization of the active (ligand-bound) integrins (Shi and Sottile, 2008; Sottile and Chandler, 2005). The clathrin-independent carriers were found to contain β1 integrins and to mediate endocytosis at the leading edge of the cell (Doherty et al., 2011; Howes et al., 2010), where the rapid integrin plasma membrane turnover is crucial for migration. Furthermore, integrin internalization can be stimulated by various growth factors that promote the assembly of dorsal ruffles and the initiation of macropinocytosis (Gu et al., 2011).

The activation state of integrins is an important factor during their endocytosis. The active integrins are endocytosed at a significantly higher rate than their inactive counterparts (Arjonen et al., 2012). During active integrin endocytosis, the ECM ligand (i.e. fibronectin or collagen) is internalized together with the receptor (Shi and Sottile, 2011; Sottile and Chandler, 2005). Given the dimensions and rigidity of the mature fibronectin structures, the internalization of ECM requires the activity of matrix metalloproteases, such as MT1-MMP (Shi and Sottile, 2011). The proteolytic cleavage of the fibronectin fibrils at the site of integrin endocytosis allows for the internalization of integrin-ECM complexes (Shi and Sottile, 2011). Therefore, the integrin activation by ECM engagement and its internalization are tightly linked and constitute the first step in integrin endocytic sorting.

Figure 1.5: Integrin α5β1 endosomal sorting

Integrin α5β1 internalization is promoted by the FN-activation and can occur through clathrin-mediated endocytosis (shown here) or other mechanisms. The inactive integrins are also internalized, but at a slower rate. The active and ubiquitinated integrin is targeted to lysosomal degradation via ESCRT pathway. A pool of inactive receptors is rapidly recycled to cell surface

via Rab4 recycling pathway. A subset of active integrins is delivered to recycling endosome, from which their return to cell surface by the action via Rab11 and Arf6 recycling pathways. Details in text.

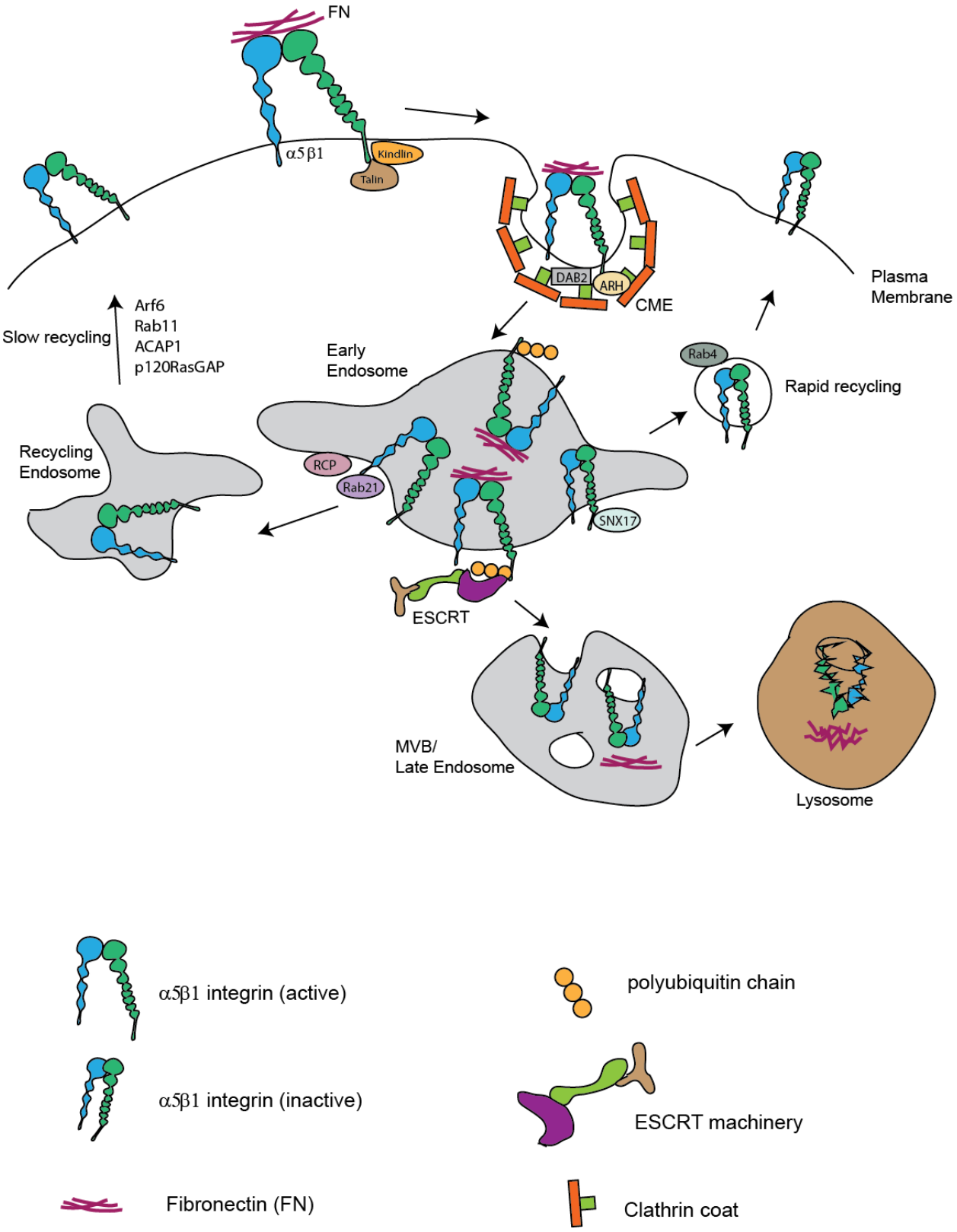
FN
α5β1
Kindlin
Talin
DAB2
ARH
CME
Plasma
Membrane
Slow recycling
Arf6
Rab11
ACAP1
p120RasGAP
Early
Endosome
Rab4
Rapid recycling
Recycling
Endosome
RCP
Rab21
SNX17
ESCRT
MVB/
Late Endosome
Lysosome
α5β1 integrin (active)
α5β1 integrin (inactive)
Fibronectin (FN)
polyubiquitin chain
ESCRT machinery
Clathrin coat

1.4.7. Post-endocytic sorting of integrins towards recycling

Following their endocytosis, integrins arrive to the early endosome, where they are sorted either towards cell surface recycling or lysosomal degradation. Importantly, integrins can recycle via several recycling routes and the selection of the recycling path is dependent on the activity state of receptor, sorting motifs and signals, as well as the endosomal sorting machinery (Caswell and Norman, 2006; Jones et al., 2006; Rainero and Norman, 2013).

Integrin β1 cytoplasmic tail contains two sorting NPxY motifs that regulate association with the endocytic sorting machinery and integrin recycling. At the cell surface, the distal NPxY motif is required for β1 integrin association with Kindlin-2 and for the regulation of ECM affinity (Harburger et al., 2009; Ma et al., 2008). However, upon integrin internalization and endosomal delivery, Kindlin-2 is displaced from the distal NPxY motif by sorting nexin 17 (SNX17) (Bottcher et al., 2012). The association with SNX17 drives the sorting of α5β1 integrin receptors into a Rab4 recycling pathway and protects integrins from the lysosomal degradation (Bottcher et al., 2012; Steinberg et al., 2012).

Moreover, integrin α5β1 recycling is regulated by several signalling pathways. For instance, Akt/GSK3β signalling promotes the delivery of α5β1 integrins to the plasma membrane via Rab11 recycling compartment (Cohen and Frame, 2001). This occurs via the phosphorylation of microtubule associated proteins, such as tau or APC (Cohen and Frame, 2001), or by phosphorylation of an Arf6 GAP, ACAP1 (Dai et al., 2004). The phosphorylated ACAP1 acts as a recruiting adaptor for β1 integrins into Arf6 recycling pathway (Li et al., 2005). Similarly, Rab21 associates with α5 subunit cytoplasmic tail and promotes its delivery to the recycling compartment (Mai et al., 2011), where Rab21 is displaced from α5 by p120RasGap (Mai et al., 2011). The latter drives integrin α5β1 recycling to the cell surface and thus promotes cell migration. Alternatively, Rab-coupling protein (RCP) is recruited to α5β1 in the presence of αvβ3 inhibition (i.e. Cilengitide treatment) and promotes integrin α5β1 recycling to the cell surface (Caswell et al., 2008). Importantly, RCP interaction with α5β1 allows for a concomitant recycling of EGFR and Met (Muller et al., 2009; Muller et al., 2013), indicating that the recycling of integrin α5β1 is in a tight crosstalk with other receptors (Ivaska and Heino, 2011).

Similarly to the integrin endocytosis, the dynamics of integrins' recycling significantly depend on their activations state. Ligand-bound α5β1 integrins in active conformation progress towards the late endosomal and lysosomal compartments, and recycle at a slower rate than their inactive counterparts (Arjonen et al., 2012). A possible explanation for this observation is that the increasingly acidic environment of late endosomes/lysosomes may induce ligand displacement from integrins, and the consequent recycling of the active integrins via Rab25/CLIC3 pathway (Dozynkiewicz et al., 2012; Rainero and Norman, 2013). The inactive integrins undergo a rapid cell surface return via Rab4 pathway, following their efficient sorting into Arf6 tubules at early endosomal level (Arjonen et al., 2012).

Overall, the recycling of integrin receptors is a key mechanism protecting integrins from the lysosomal degradation and promoting integrin cell surface return for the additional rounds of matrix engagement and adhesion contacts formation.

1.4.8. Integrin ubiquitination and degradative sorting

Cell surface receptor ubiquitination is a well-known sorting signal for the lysosomal degradation. Recently, integrin α5β1 was demonstrated to be ubiquitinated, potentially via the action of cCbl E3-ligase (Kaabeche et al., 2005; Lobert et al., 2010). The ubiquitination of integrin α5β1 is a key signal for its targeting to degradation and its ESCRT-dependent incorporation within MVBs (Lobert et al., 2010). Depletion of the ESCRT machinery subunits, Hrs and TSG101, results in the stabilization of integrin α5β1 levels. Similarly, an extensive lysine mutagenesis (K/R) of α5β1 cytoplasmic tails leads to the stabilization of the receptor and its cell surface recycling, likely due to an inefficient lysosomal delivery of non-ubiquitinatable integrins (Bottcher et al., 2012; Steinberg et al., 2012). Importantly, the active, ligand-bound, integrins are ubiquitinated and are sorted to the late endosomal/lysosomal compartment while maintaining their ligand interaction and the activation state, suggesting that only the activated integrins are ubiquitinated.

However, the ubiquitination of integrin α5β1 and its impact on integrin sorting remains poorly understood. For instance, the persistent ubiquitination of integrins is in controversy with their long half-life, the dynamics of integrin ubiquitination are poorly defined, and the effect of ligand engagement on integrin ubiquitination state is not clear (Rainero and Norman, 2013). Also, it is inknown how the ubiquitination and the degradation of integrins act in concert with the other sorting motifs and integrin sorting pathways and how, altogether, these mechanisms affect the

cellular functions of integrins. Some of these topics are addressed and explained in the Chapter 2 of this thesis.

1.4.9. The impact of integrin sorting on cell migration

Since integrins play a pivotal role in the ECM binding and the formation of adhesion complexes in migrating cells, it is not surprising that their cell surface dynamics considerably influence cell migration and invasion.

The very first studies of integrin recycling showed that integrin cell surface return is a key requirement during cell movement (Powelka et al., 2004). The recycling of the integrin α5β1 via Rab25 action occurs at the leading edge of the 3D invading cell, thus promoting cellular invasion (Caswell et al., 2007). In this case, the active integrin receptors are internalized and are maintained at the tip of an invasive pseudopod, constantly circulating between the cell surface and Rab25 vesicles. This pool of receptors is responsible for the formation of the necessary adhesions at the pseudopod tip to move the cell protrusion forward. A portion of the active integrin receptors proceeds to the CLIC3 positive lysosomal compartments and recycles from these to the trailing edge of the invading cell (Dozynkiewicz et al., 2012). The rear recycling of integrins is likely to be accompanied with a release of lysosomal proteases, contributing to the matrix digestion and cell rear release.

Accelerated recycling of integrin α5β1 is also driven by the activity of RCP and promotes invasion in fibronectin rich matrices (Caswell et al., 2008). The association of RCP with α5β1 is induced by the inhibition of αvβ3 integrin with Cilengitide treatment and by p53 mutations in certain cancer cells types (Caswell et al., 2008; Muller et al., 2009). While inducing integrin α5β1 recycling, RCP promotes the recycling of EGFR in association with integrins (Caswell et al., 2008). Together, these receptors activate Akt-signalling and RhoA activation, driving pseudopod formation and rapid migration. Therefore, RCP acts as a molecular switch in α5β1 vs. αvβ3 dependent migration in a fibronectin rich environment.

While most studies suggest that the integrin recycling machinery is a requirement for the cell migration and invasion, the degradative pathways and ESCRT machinery were proposed to carry a similar function in cell migration (Lobert et al., 2010; Lobert and Stenmark, 2012). These studies have brought a significant amount of controversy in the field, since the cell surface

receptor recycling and degradation are fundamentally opposing sorting processes. The degradative pathway may contribute to the integrin-dependent migration by eliminating ligand-occupied integrins from focal adhesions, thus allowing for the formation of new adhesions.

1.4.10. Endocytic sorting of integrins in cancer

Due to the severe implication of the endocytic sorting and recycling in integrin-dependent cell invasion, the molecular players mediating integrin recycling may be key factors underlying cancer invasion and metastasis. Indeed, the deregulated endocytosis of β1 and β3 integrins contributes to the progression of several cancers. Such, endocytic adaptors Dab2, Numb and HAX1 were reported to be involved in integrin internalization and their downregulation was correlated with an increased metastasis formation and poor patients' prognosis (Maiorano et al., 2007; Tong et al., 2010; Trebinska et al., 2010; Westhoff et al., 2009; Xu et al., 2014).

Key evidence for the integrin recycling implication in metastasis came from the study of integrin α5β1 dependent migration in the context of p53 mutant expression. The presence of p53 mutations induces the RCP-driven integrin α5β1 recycling and the downstream promigratory signalling (Muller et al., 2009). In mouse models, the mutant p53 promotes metastasis formation, in line with the aggressive tumor behavior in the patient population bearing mutant p53 tumors (Muller et al., 2009). High expression of RCP in the luminal B-subtype breast cancer was correlated with a low survival rate and cancer aggressiveness, suggesting that the RCP role in integrin recycling can be a key factor favoring breast cancer progression (Dai et al., 2012; Mills et al., 2009; Zhang et al., 2009). In addition, the expression of CLIC3, which is responsible for the integrin recycling from the lysosomal compartment, significantly correlates with a poor prognosis of ovarian, breast and pancreatic cancer (Dozynkiewicz et al., 2012; Macpherson et al., 2014). These and other examples of the overexpression of mediators of integrin recycling in cancers suggest that the mechanism of integrin recycling is often hijacked by cancer cells in order to acquire invasive properties and metastasise (Figure 1.6).

Moreover, the recycling of integrin receptors impact on cancer progression is not limited to the integrin-mediated cell invasion. The extensive crosstalk of integrins with other receptors affects processes such as angiogenesis and cellular proliferation. For instance, inhibition of αvβ3 integrin with Cilengitide induces rapid recycling of VEGFR2 (Reynolds et al., 2009). The increase of VEGFR2 on the cell surface increases the extent of its downstream signalling,

leading to the endothelial cell migration and tumor vascularization (Reynolds et al., 2009; Weller et al., 2009). These effects of Cilengitide are the likely explanation of the enhanced angiogenesis observed in tumors treated with low concentrations of Cilengitide (Weller et al., 2009). Similar pro-angiogenic phenotype is observed upon knockout of β3 *in vivo* (Reynolds et al., 2002). The crosstalk between integrin α5β1 and several RTKs, such as EGFR and MET, is initiated by RCP recruitment to α5β1 (Caswell et al., 2008; Muller et al., 2013). The enhanced recycling of integrins and RTKs drives the downstream MAPK signalling cascade, promoting cancer cells survival, scattering and migration.

Collectively, these studies indicate a crucial role of the integrin postendocytic sorting in cancer progression. The complex interplay between several signalling cascades initiated by the integrin recycling machinery is responsible for the metastasis formation and increased cancer aggressiveness.

Figure 1.6: Integrin sorting during cell migration

Integrin sorting plays a pivotal role during cell migration. Ligand-engaged integrins are internalized at the leading edge of the cell and are recycled back to the lamellopodium edge to allow the new rounds of matrix engagement and the nascent adhesion formation driving cell protrusion forward. The rear end integrins are endocytosed and are delivered to the lysosomes for degradation, thus promoting cell detachment. A portion of integrins can be recycled from late endosomal/lysosomal compartments via CLIC3 pathway further promoting cell migration. ESCRT pathway promotes degradation of ubiquitinated active integrin receptors. Details in text.

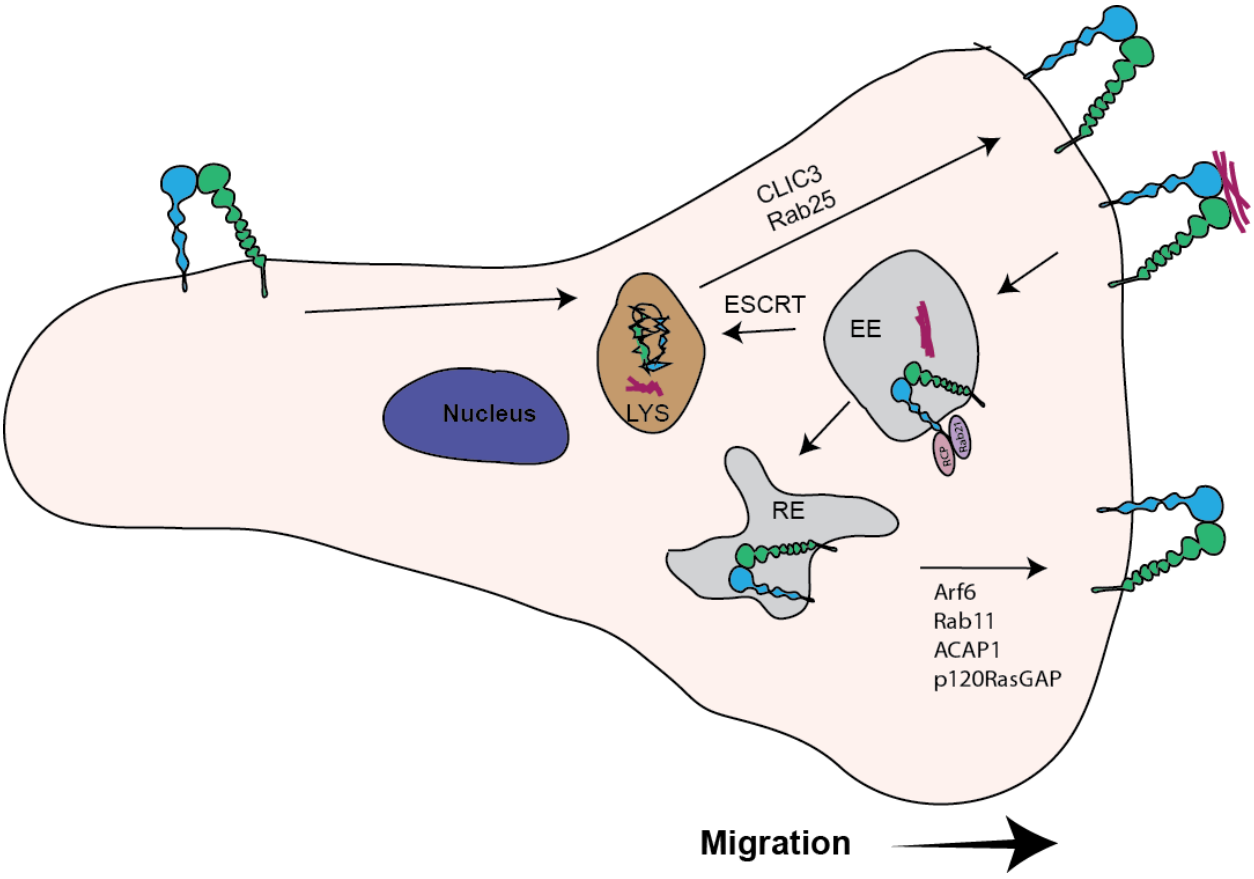

1.5. Tumor Necrosis Factor receptor and its downstream signalling

The endocytic sorting affects several cell surface receptors' downstream signalling. While the effect of the sorting machinery on receptors is well studied for the families of receptor tyrosine kinases, adhesion receptors and GPCRs, sorting of other crucial cell surface molecules has not been investigated in such details yet. For instance, the death receptor family trafficking dynamics and impact on their signalling just begins to emerge. Death receptors play a complex role in cell biology and regulate a variety of cellular processes, including apoptosis, cell survival and inflammation. Here, we discuss the key signalling events downstream of a classic death receptor (TNFR1) and the spatiotemporal regulation of its downstream signalling.

1.5.1. Tumor Necrosis Factor Receptor 1 (TNFR1) and its activation

Tumor Necrosis Factor Receptor 1 (TNFR1) belongs to a large family of type I transmembrane death receptors (Idriss and Naismith, 2000). These receptors share similarities in their extracellular domain, but differ in their intracellular domains. Indeed, a key distinctive element of TNFR1 and other similar receptors is the presence of Death Domain (DD) in their cytoplasmic domain (Peter and Krammer, 2003; Tartaglia et al., 1993a; Tartaglia et al., 1993b). Upon activation, the scaffolding events at the intracellular domain of these receptors lead to the activation of a pro-inflammatory response, regulation of the innate immunity and induction of apoptosis (reviewed in (Israel, 2000, 2010; Landskron et al., 2014; Micheau and Tschopp, 2003; Ofengeim and Yuan, 2013) (Figure 1.7).

The activation of TNFR1 is initiated by its engagement with the ligand TNFα. The ligand binding induces trimerization of the receptor at the plasma membrane and the recruitment of TRADD and RIP1 to the DD of the receptor (Locksley et al., 2001; Tartaglia et al., 1993a). Consequently, TRADD recruits TRAF2 and E3-ligases cIAP1/2, which polyubiquitinates RIP1 (Chen et al., 2008; Lee et al., 2004; Li et al., 2006; Micheau and Tschopp, 2003). These events result in the formation of the TNFR1 signalling complex I (TNFR1-SCI) that is responsible for the pro-inflammatory and the pro-survival signalling downstream of TNFR1 (Hsu et al., 1996b; Micheau and Tschopp, 2003). The K63-polyubiquitinated RIP1 acts as a scaffold for LUBAC complex, which adds linear polyubiquitin chains on RIP1 (Rahighi et al., 2009). The different polyubiquitin chains on RIP1 are responsible for the recruitment of TAB-TAK1 and IKK complexes onto TNFR1-SCI (Emmerich et al., 2011; Gerlach et al., 2011; Ofengeim and Yuan, 2013). The kinase activity of IKK complex leads to the phosphorylation and the degradation of

inhibitor of κB (IκB), releasing the NF-κB from inhibition and activating the NF-κB transcription program (Ea et al., 2006; Emmerich et al., 2013; Hoffmann et al., 2002).

TNFR1 signalling complex 1 is not a permanent molecular entity and undergoes disassembly via the activity of DUBs, such as CYLD, Cezanne and A20, which are recruited to the complex after signalling initiation (Enesa et al., 2008; Kovalenko et al., 2003; Wertz et al., 2004). Therefore, these deubiquitinating enzymes act as negative regulators of the TNFR1-SCI and prevent excessive NF-κB signalling (Harhaj and Dixit, 2011).

The downstream signalling of TNFR1 is not terminated after the disassembly of TNFR1-SCI. TNFR1 preserves its interaction with several components of the complex, notably deubiquitinated RIP1 (Christofferson et al., 2012; Degterev et al., 2008). In addition, it recruits FADD and caspases-8/10, thus forming a pro-apoptotic complex (TNFR1-SCII) (Micheau and Tschopp, 2003; Ramakrishnan and Baltimore, 2011). Alternatively, TNFR1 may recruit RIP3 kinase promoting cellular necrosis. Therefore, TNFR1 Complex II can induce cell lethality via both apoptosis and necrosis (Cho et al., 2009). However, the NF-κB transcriptional activity downstream of TNFR1-SCI produces cFLIP, which counteracts the pro-apoptotic and the pro-necrotic signalling of TNFR1-SCII (Dillon et al., 2012; Oberst et al., 2011; Pop et al., 2011). cFLIP can exist as two isoforms, $cFLIP_L$ and $cFLIP_S$ that prevent necrosis and apoptosis respectively, thus TNFR1 signalling is controlled by the scaffolding of receptor complexes and a complex feedback regulation of its own downstream signalling (Oberst et al., 2011).

1.5.2. Endocytic dynamics of TNFR1

Similarly to other cell surface receptors, TNFR1 is internalized after ligand binding and initial scaffolding of the signalling complex I at plasma membrane (Schneider-Brachert et al., 2004). The internalization of TNFR1 is clathrin-dependent and it requires YQRW-motif in the TNFR1 cytoplasmic domain (Schneider-Brachert et al., 2004). In addition, TNFR1 is modified with K63 polyubiquitin chains by RNF8 E3-ligase (Fritsch et al., 2014). The ubiquitination of the receptor is also required for its internalization, since cells deficient of RNF8 display slower dynamics of TNFR1 endocytosis (Fritsch et al., 2014).

Following TNFR1 endocytosis, the receptor is localized to receptosomes, an early endosome type organelle where TNFR1-SCI is disassembled and the TNFR1-SCII is formed (Micheau and

Tschopp, 2003). Interestingly, the NF-κB signalling downstream of TNFR1-SCI is not affected by the receptor internalization inhibition, rather the efficient assembly and pro-apoptotic signalling of the TNFR1-SCII is reduced (Fritsch et al., 2014). Moreover, the K63-ubiqutination of TNFR1 is required for the assembly of FADD/caspase-8 complex on TNFR1 and its pro-apoptotic signalling (Fritsch et al., 2014). This implies that TNFR1 compartmentalization is responsible for the segregation of its inflammatory/survival and its apoptotic/necrotic signalling.

Despite recent advances in understanding of the TNFR1 spatiotemporal regulation, little is known about the endocytic machinery responsible for its sorting, its dynamics of degradation and the effect of ESCRT pathway on TNF-induced NF-κB activation and apoptosis.

1.6. The rationale and significance of the present study

In the light of primordial importance of the endocytic sorting processes in cellular biology and signalling, we have turned our attention to the regulation of this process at multiple levels. In the first instance, we investigated the regulation of integrin receptor sorting during cell migration. More specifically, we investigated the dynamics of integrin α5β1 complex ubiquitination and activation state during the sorting stages of the receptor. A deeper understanding of these events is necessary to reconcile some of the important controversies in the field of integrin trafficking and define the new framework of integrin-dependent cell migration regulation. Similarly, we took advantage of the function of HD-PTP in the degradative sorting of cargo receptors and use it to investigate the role of ESCRT machinery in TNFR1 downstream signalling. These studies can demonstrate for the first time the implication of endosomal sorting machinery in NF-κB pathway regulation, inflammation and TNFα-induced apoptosis. Moreover, our preliminary mass-spectrometry analysis has identified an interesting endosomal protein, Endofin, as a binding partner of HD-PTP. Given the previous unproven hypothesis that Endofin may act as an ESCRT component, we studied the biochemical and functional characteristic of this complex, and we demonstrated for the first time the role of Endofin in ubiquitinated cargo sorting. Altogether, our work underscores the new paradigms in integrin sorting, receptor signalling and repositions ESCRT machinery as a unique sorting complex.

Figure 1.7: Spatiotemporal regulation of TNFR1 signalling

TNFR1 activation is induced by TNFα binding and the trimerization of the receptor. The trimeric receptor recruits the signalling scaffold complex that constitutes of TRADD, TRAF2, RIP1 and cIAP1/2 (TNFR1 Complex I). RIP1 is heavily modified by polyubiquitin chains, which serves as docking sites for kinase complexes TAB1/2-TAK1 and NEMO-IKKα/β. The activity of IKKα/β leads to phosphorylation of IκB and its proteasomal degradation, releasing the NF-κB p50/p65 dimer from inhibition. Translocation of NF-κB to the nucleus induces a transcription program promoting inflammation and cell survival. Following TNFR1 ubiquitination, the signalling complex partially dissociates and the receptor is internalized via CME. The recruitment of FADD and Caspase-8 underlines the formation of a new signalling complex localised at endosomes (TNFR1 Complex II). This signalling complex promotes apoptosis by activating the caspase cascade. Therefore, the two spatiotemporally segregated TNFR1 signalling scaffolds regulate several cellular pathways.

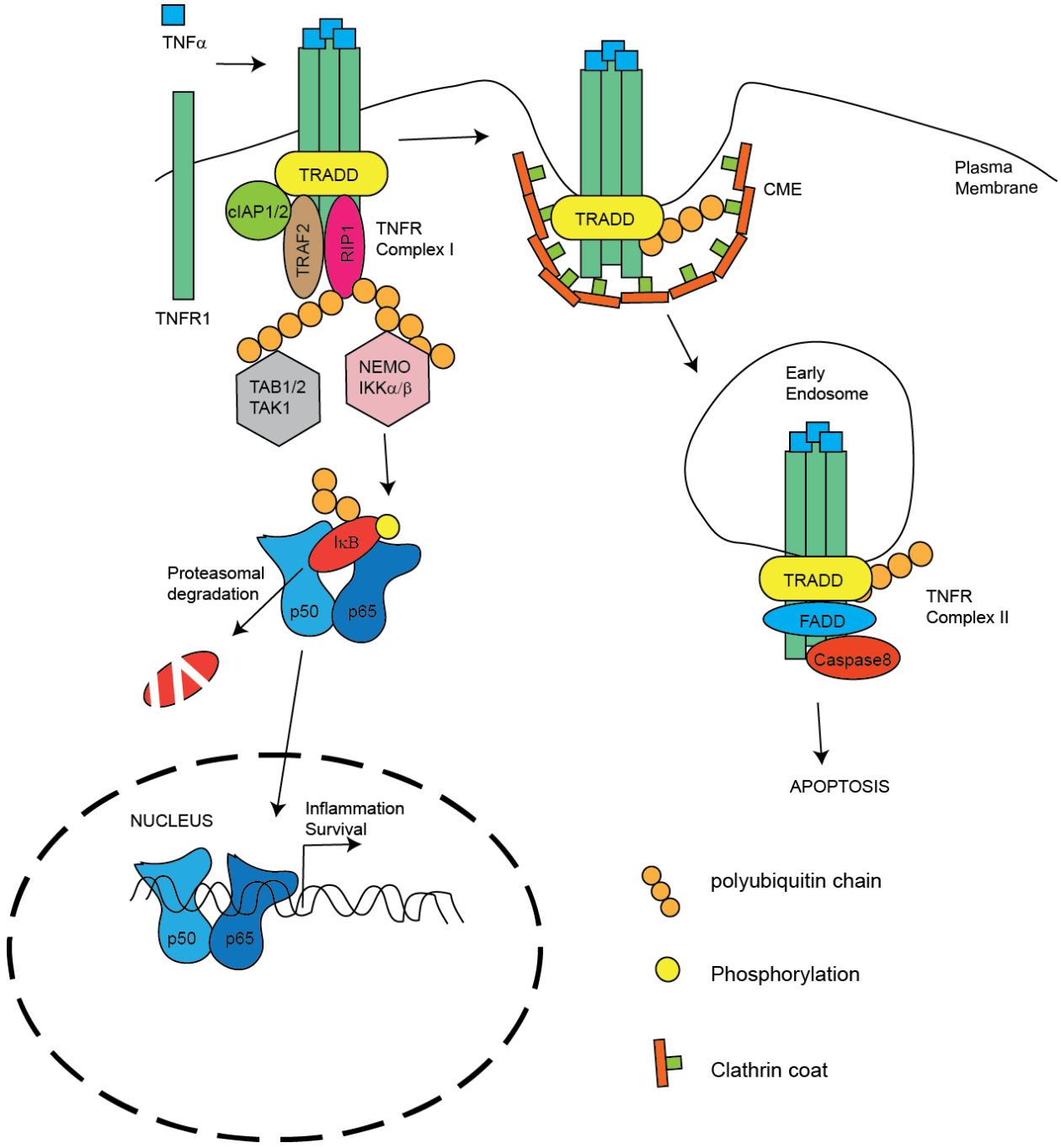
TNFα
TRADD
cIAP1/2
TRAF2
RIP1
TNFR
Complex I
TNFR1
TAB1/2
TAK1
NEMO
IKKα/β
IκB
p50
p65
Proteasomal
degradation
NUCLEUS
Inflammation
Survival
p50
p65
TRADD
CME
Plasma
Membrane
Early
Endosome
TRADD
FADD
Caspase8
TNFR
Complex II
APOPTOSIS
polyubiquitin chain
Phosphorylation
Clathrin coat

CHAPTER 2:

2. Interplay of endosomal pH and ligand occupancy in integrin α5β1 ubiquitination, endocytic sorting and cell migration

Dmitri Kharitidi*, Pirjo M. Apaja*, Sanaz Manteghi, Kei Suzuki, Elena Malitskaya, Ariel Roldan, Marie-Claude Gingras, Junichi Takagi, Gergely L. Lukacs and Arnim Pause

*equal contribution

2.1 Preface

As outlined in the literature review chapter of the thesis, endocytic sorting of the cell surface receptors is key for regulation of several cellular processes including cell migration and invasion. Adhesion receptors, such as integrin α5β1, are required for cellular movement. In the recent years it became evident that the endocytic sorting of integrin receptors is a key regulatory mechanism of cell migration. However, the molecular mechanism of integrin α5β1 sorting is not fully understood and it remains unclear whether cell migration relies on integrin degradation or cell surface recycling of the receptor. In this chapter, we demonstrate that ligand binding and dynamic ubiquitination of integrin α5β1 is a key sorting mechanism of the receptor. Moreover, we identify the deubiquitinase USP9x and ESCRT machinery components HD-PTP and UBAP1 as key regulators of integrin α5β1 sorting during the process of cells migration. This work clarifies the previously conflicting hypothesises on integrin receptor sorting and showcases endosomal pH and as crucial regulator of integrin turnover.

2.2. Abstract

Membrane trafficking of integrins plays a pivotal role in cell proliferation, migration and invasion. How endocytosed integrins are targeted either for recycling or lysosomal delivery is not fully understood. Here we show that fibronectin (FN) binding to α5β1 integrin triggers ubiquitination and internalization of the receptor complex. Acidification facilitates FN dissociation from integrin α5β1 *in vitro* and in early endosomes, promoting receptor complex deubiquitination by the USP9x and recycling to the cell surface. Depending on residual ligand occupancy of receptors, a fraction of internalized α5β1 integrins remains ubiquitinated and is captured by ESCRT-0/I, containing Histidine Domain containing Protein Tyrosine Phosphatase (HD-PTP) and Ubiquitin-Associated Protein 1 (UBAP1) and directed for lysosomal proteolysis, which limits receptor downstream signalling and cell migration. In accord, HD-PTP or UBAP1 depletion is associated with a pro-invasive phenotype. Thus, pH-dependent FN-integrin dissociation and deubiquitination of the activated α5β1 are required for receptor resensitization and cell migration, representing potential targets to modulate tumor invasiveness.

2.3. Introduction

Cell migration is central in development, wound healing and metastasis (Ridley et al., 2003). Migration is tightly regulated by cytoskeletal proteins, Rho-family GTPases and adhesion receptors, such as integrins, which are constitutively internalized and recycled at the leading edge to form new adhesion contacts with extracellular matrix (ECM) molecules (Caswell et al., 2007). Upon ECM binding, integrins undergo conformational changes leading to activation of downstream signalling (Hynes, 2002). Signalling intensity is partly defined by the plasma membrane (PM) density of integrins, regulated by the rate of receptor secretion, internalization, recycling and degradation (reviewed in (Rainero and Norman, 2013)).

Integrin α5β1, a fibronectin (FN) receptor, can be ubiquitinated (Lobert et al., 2010). Ubiquitination, a reversible posttranslational modification, can serve as an endocytic and Multivesicular Body (MVB)/lysosomal targeting signal for PM proteins (Barriere et al., 2007b; Piper et al., 2014). Ubiquitinated PM proteins are recognized by a subset of endocytic adaptors containing ubiquitin binding domains (UBD) and internalized via clathrin-dependent or independent pathways (Piper et al., 2014). Internalized cargoes may recycle back to the PM following the removal of Ub moieties by deubiquitinating enzymes (DUB) at early endosomes (McCullough et al., 2004). Alternatively, ubiquitinated cargoes can be captured by the UBDs of the Endosomal Sorting Complex Required for Transport (ESCRT) and sequestered into MVB/lysosomes (Henne et al., 2013; Katzmann et al., 2001). The Histidine-Domain containing Protein Tyrosine Phosphatase (HD-PTP) is an endosomal pseudophosphatase that acts as a scaffold for the ESCRT-0 and -I complexes via binding to Stam11-Hrs and UBAP1 (Ali et al., 2013; Gingras et al., 2009b). In concert with HD-PTP and ESCRT-0, UBAP1, a Ub-binding ESCRT-I subunit, and a DUB (UBPY/USP8) have been shown to orchestrate the lysosomal delivery of EGFR (Ali et al., 2013; Stefani et al., 2011).

Upon depletion of ESCRT-0 and -I subunits Hrs and TSG101 the lysosomal degradation of α5β1 integrin was inhibited similarly to replacement of the cytosolic tail Lys residues in α5β1 (Bottcher et al., 2012; Lobert et al., 2010). Both modifications impeded cell migration, suggesting that lysosomal proteolysis of ubiquitinated FN-α5β1 integrin complex is required for cell migration and invasion (Bottcher et al., 2012; Lobert et al., 2010; Lobert and Stenmark, 2012). Other reports, however, indicated that interfering with Rab11- or Rab4-dependent integrin recycling, which is facilitated by SNX17, Rab25 and Syntaxin6, compromised cellular

migration/invasion (Bottcher et al., 2012; Caswell et al., 2008; Tiwari et al., 2011). Rab25 directs activated α5β1 integrin to late endosomes, however, α5β1 integrin is rerouted toward recycling in the presence of chloride intracellular channel protein 3 (CLIC3) (Dozynkiewicz et al., 2012). To elucidate the molecular mechanism of α5β1 integrin segregation between recycling and lysosomal targeting and its influence on cell migration, we determined the role of ligand-occupancy and receptor ubiquitination in postendocytic sorting and signalling of α5β1 integrin.

Here, we show that FN-binding induces rapid ubiquitination and accelerated internalization of α5β1 receptors from the PM. Most of endocytosed α5β1 receptors are deubiquitinated by USP9x and recycled upon FN dissociation due to endosomal acidification, while the residual amount of ubiquitinated receptors is targeted for lysosomal proteolysis. The latter requires HD-PTP and UBAP1, depletion of which leads to enhanced α5β1 resensitization and cell migration/invasion.

2.4. Results

2.4.1. FN binding stimulates the ubiquitination of α5β1 integrin complexes

While the ligand-induced ubiquitination of α5β1 integrin has been shown (Lobert et al., 2010), neither the time course of ubiquitination nor its role in the α5β1 sorting has been fully elucidated. The time course of α5β1 integrin ubiquitination was measured by immunoprecipitation (IP) of anti-α5 Ab prelabelled PM receptor after 0-15 min FN-stimulation at 37°C followed by Ub detection by immunoblot (WB). The ubiquitination of integrin α5β1 complexes was increased by ~5-fold upon FN stimulation (Figure 2.1A), and a similar ubiquitination kinetics were observed upon β1 integrin IP (Figure S2.1A). α5β1 ubiquitination was abolished by JBS5 α5β1 blocking Ab, which prevented integrin activation (Figure 2.1B). Internalization is not a required for ubiquitination of the receptor complex, since inhibition of clathrin- and caveolin-mediated endocytosis of α5β1 (Barriere et al., 2006a) (Figure 2.1C) did not prevent its ubiquitination (Figure 2.1D). Thus ligand-binding acutely stimulates the α5β1 receptor complex ubiquitination at the PM and/or in endosomes.

2.4.2. FN-induced ubiquitination accelerates α5β1 integrin internalization

To determine the role of ubiquitination in α5β1 integrin trafficking, its endocytic sorting was analysed at three levels of activation. Integrin α5β1 was either fully activated with exogenous FN, or inactivated with the JBS5 blocking Ab, or studied in the presence of endogenous FN (steady state). The internalization rate of the inactive receptor (3.3±2%/5min) was stimulated by >3-fold (11±3%/5min) and >10-fold (30±3%/5min) in the presence of endogenous and exogenous FN, respectively, shown by cell surface ELISA (cs-ELISA) (Figure 2.2A). As a corollary, the PM density of α5β1 decreased by 47±5% or increased by 72±19%, upon activation with exogenous FN or inactivation with the JBS5 Ab, respectively, relative to steady state conditions (Figure 2.2B). A similar effect on α5β1 ubiquitination and α5β1 internalization kinetics was observed upon stimulation with RGD peptide agonist (Figure S2.1B, C and F). The FN-induced intracellular retrieval of α5β1 integrin was transient, since after 15 min of FN treatment, the α5β1 integrin PM pool was gradually replenished (Figure 2.2C), probably through the recycling PM delivery of the receptor. Inhibition of other FN receptors

(integrin αvβ3 and αvβ5) by Cilengitide accelerated the α5β1 PM recovery (Figure 2.2C), due to accelerated recycling of the α5β1 (Caswell et al., 2008).

To assess the contribution of ubiquitination to the activated α5β1 internalization, α5β1 endocytosis was measured in ts20 CHO cells, harboring a temperature-sensitive E1 Ub-activating enzyme. Following heat inactivation of E1 (Apaja et al., 2010; Kulka et al., 1988), FN-receptor internalization was inhibited by 50% (Figure 2.2D). After minimizing the αv integrin contribution to FN-uptake by Cilengitide treatment, E1 inactivation delayed the uptake of integrin α5β1 by 76%, (Figure 2.2D), suggesting that FN-induced ubiquitination largely accounts for the accelerated internalization of activated α5β1 integrins.

2.4.3. FN-induced transient ubiquitination promotes α5β1 integrin lysosomal targeting

To assess whether the postendocytic fate of α5β1 integrins is influenced by their activation, the α5β1 lysosomal transport kinetics were determined by monitoring the pH of α5β1 containing vesicles (pH_v) by fluorescent ratiometric image analysis (FRIA, Figure S2.2A) (Barriere and Lukacs, 2008b). The PM α5β1-receptors were prelabelled with anti-α5 Ab on ice and the pH-sensitive FITC-Fab was monitored after synchronized internalization by pH_v measurement during 1-7h chase. While the inactive receptors were largely confined to recycling endosomes at pH_v~6.4±0.1 even after 7h, most of the FN-activated receptors reached late endosomes (pH_v<5.58±0.02) and lysosomes (pH_v~5.0±0.2) after 4h and 7h chase (Figure 2.2E and Figure S2.2B). The integrity of receptor-Ab complex and FITC fluorescence was preserved at pH7.4-5.5 (Figure S2.2C and D). These observations and the FN-induced accelerated α5β1 internalization suggest that the activation state plays a determining role in the turnover rate of the PM integrin α5β1 pool.

Consistent with the α5β1 endolysosomal transfer rate, the PM half-life ($T_{1/2}$) of integrin α5β1 is longer for the inactive ($T_{1/2}$ >9 h) than the activated ($T_{1/2}$~2 h) state, measured by cs-ELISA (Figure 2F and S1C). A similar relationship was observed between the turnover and activation state of the internalized receptor pool (Figure 2.2G, S2.1D and E). Remarkably, the observed PM turnover of integrin α5β1 was ~10-fold slower ($T_{1/2}$ ~2 h, Figure 2.2F) than the value ($T_{1/2}$ ~0.2h) calculated based on the receptor internalization rate (6%/min, Figure 2.2A).

Similarly, the slow lysosomal transfer kinetics of activated α5β1 was in contrast with the fast lysosomal delivery of ubiquitinated model cargoes, CD4t-Ub_n or the CD4tcc-UbRΔG_4 chimeras (Figure 2.2E-F) (Apaja et al., 2010; Barriere et al., 2007b), and other PM receptors undergoing Ub-dependent downregulation (Hicke, 1999).

A possible explanation for the slow PM turnover and lysosomal delivery of activated α5β1 could be receptor deubiquitination at endosomes. Indeed, the ubiquitination of the FN-activated α5β1 complex was decreased by 45% after 30 min of FN exposure (Figure 2.2H). The incomplete deubiquitination of α5β1 integrin complex may explain the slower recycling rate of the FN-activated α5β1 (38%/10min) as compared to its inactive receptor (54%/10 min; Figure 2.2I). The Ub-dependent internalization rate was indeed decreased to the steady state level after 30 min of exogenous FN wash-out (Figure 2.2J). Thus, endosomal deubiquitination of a significant fraction of activated α5β1 receptor complexes may contribute to slow PM turnover and inefficient lysosomal degradation of the activated α5β1 receptor, facilitating its resensitization.

2.4.4. FN dissociates from integrins in early endosomes

Lysosomal degradation has been suggested to counteract the recycling of the FN-integrin α5β1 complexes (Lobert et al., 2010). Alternatively, dissociation of FN-integrin α5β1 has been proposed in early endosomes (Arjonen et al., 2012; Rainero and Norman, 2013). Since endosomal acidification-induced conformational change of receptors can cause ligand dissociation (e.g. LDL, asialoglycoprotein and mannose-6P receptors (Davis et al., 1987; Harford et al., 1983; Rajan and Menon, 1985), we tested whether a similar paradigm prevails for the α5β1 integrin. First, α5β1 integrin and FN were visualised after endocytosis. While α5β1 and FN colocalized after 5-15min of uptake, they were confined to distinct compartments at 30min of chase (Figure 2.3A). Their divergent sorting was confirmed by FRIA, as the mean pH_v of FN or α5 integrin containing vesicles was similar at 15min (pH_v ~6.0 and ~6.1, respectively), but became different after 20min chase (pH_v ~5.7 and ~6.2, respectively) (Figure 2.3B-C). Eventually, FN was confined to lysosomes (pH_v~5.4), while α5 remained in early endosomes (pH_v~6.3, Figure 2.3B-C). The temporospatial segregation of the ligand-receptor complex was in line with the 8-fold longer half-lives of the receptor ($T_{1/2}$ ~4 h) and internalized biotin-FN ($T_{1/2}$

~0.5 h) (Figure 2.2G vs. Figure 2.3D) and suggested that endosomal acidification promotes FN dissociation.

2.4.5. pH-dependent FN binding to α5β1 integrin at the cell surface

The pH-sensitivity of FN-integrin binding was monitored following saturation of the PM receptors with biotin-FN and measuring the pH-dependent FN dissociation kinetics. Nearly 70% of prebound FN was lost at pH~6.1 after 10min incubation (Figure S2.3A and B). Comparable dissociation kinetics were observed upon αv integrins block by Cilengitide or αv blocking Ab (Figure S2.3C) and were confirmed by monitoring the steady-state FN-binding with cs-ELISA and IF (Figure 2.3E and Figure S2.3C-D). Cilengitide treatment and Ca^{2+} concentration did not affect FN dissociation, yet the FN binding to integrin showed negative cooperativity with increasing acidity (Hill-coefficient: -2±0.2), whereas inhibition of αvβ3 and αvβ5 integrins resulted in a loss of cooperativity (Hill-coefficient: -1±0.23; (Figure S2.3C and E).

2.4.6. pH-sensitive FN dissociation from the recombinant α5β1 integrin ectodomain

We used immobilized biotin-FN and recombinant ectodomain of the α5β1 integrin (containing 1-954aa and 1-708aa of α5 and β1, respectively), to assess the intrinsic pH-sensitivity of FN and α5β1 integrin dissociation by biolayer interferometry (BLI) (Nagae et al., 2012). The dissociation rate constant (k_{off}) of the α5β1 ectodomain was increased by two- and six-fold at pH 6.0 and pH 5.0, respectively, relative to k_{off} at pH 7.5 (Figure 2.3F-G and S2.3H). The full ectodomain is required for pH-sensitive ligand binding, since the truncated α5β1 head domain (1-623aa and 1-445aa) lost its pH-sensitivity (Figure 2.3G and S2.3G-H).

Based on the pH-dependent FN-binding, endosomal alkalinisation may inhibit FN-dissociation from and consequent deubiquitination of α5β1 integrins. Dissipation of endo-lysosomal pH-gradient by chloroquine (CQ) or NH_4Cl (see Figure 2.3B) maintained the ubiquitination of FN-α5β1 integrin complex (Figure 2.3H-I), consistent with persistent ligand binding to and activation of the receptor. Jointly, our *in vitro* and *in vivo* results strongly suggest that the FN-α5β1 ligand-dissociation is pH-dependent, which plays a pivotal role in the endosomal α5β1 integrin complex inactivation and deubiquitination.

2.4.7. Integrin α5β1 complex is deubiquitinated by USP9x

To identify the deubiquitinating enzyme (DUB) responsible for the endosomal deubiquitination of the activated α5β1 integrin complex, we performed a phenotypic DUB siRNA screen, based on the assumption that sustained ubiquitination would result in accelerated downregulation of α5β1 complex from the PM. The extent of FN-induced receptor downregulation was determined in HeLa cells, treated with a siRNA library of 110 DUBs, by cs-ELISA after 60min of FN exposure (Figure S2.4A).

USP9x was identified and validated as the most effective DUB that increased the α5β1 FN-stimulated removal to 82 % relative to control 60% (NT) (Figure 2.4A-B). USP9x depletion did not affect the internalization of α5β1, the recycling of the transferrin receptor (Tf) and the lysosomal targeting of CD4-Lamp1 chimera (Figure S2.4B-C), ruling out non-specific effects. Importantly, USP9x depletion augmented and maintained the FN-induced integrin α5β1 complex ubiquitination (Figure 2.4C-D) and led to slower migration rate (Figure 2.4E), suggesting that USP9x contributes to deubiquitination of FN activated integrin α5β1 complex, a prerequisite for the receptor resensitization and PM recycling.

2.4.8. Lysosomal targeting of ubiquitinated α5β1 integrin requires HD-PTP and UBAP1

Despite the majority of integrin α5β1 being deubiquitinated and recycled, a small, but significant fraction of integrin receptor maintains its ubiquitination and is targeted to ESCRT-dependent lysosomal degradation (Lobert et al., 2010). Depletion of ESCRT components HD-PTP and UBAP1 by shRNAs increased the α5β1 cellular and PM levels (Figure 2.5A-C), without affecting its transcript levels (Figure S2.5A).

This could be attributed to impeded lysosomal delivery of α5β1 integrin as indicated by the receptor accumulation in early and recycling endosomes and exclusion from lysosomes (Figure 2.5D-E). FRIA confirmed the inhibition of α5β1 lysosomal delivery by shHD-PTP or shUBAP1 as internalized receptors were retained in early endosomes (pH_v ~5.9-6.3) as compared to CTL shRNA (pH_v ~4.7-5.6) cells (Figure 2.5F and Figure S2.5B). Importantly, HD-PTP and UBAP1 depletion had little effect on α5β1 internalization, transferrin recycling or the lysosomal targeting of CD63/Lamp and FITC-dextran (Figure S2.5C, D). HD-PTP and UBAP1 depletion,

however, potentiated α5β1 recycling by 2-3 fold (Figure 2.5G). The accelerated α5β1 recycling could be explained by enhanced deubiquitination (>30%) (Figure 2.5H-I) and decreased degradation of α5β1 integrin (Figure 2.5J). Thus, both HD-PTP and UBAP1 are involved in the MVB/lysosomal targeting of ubiquitinated α5β1 integrins and their loss-of-function stabilizes α5β1 integrin at PM and early endosome.

2.4.9. UBAP1 and HD-PTP contribution to ubiquitinated cargo sorting in endosomes

HD-PTP and UBAP1 are part of ESCRT as demonstrated by co-IP with TSG101, Hrs, Stam11, and are responsible for MVB biogenesis (Figure S2.6A and (Ali et al., 2013; Doyotte et al., 2008)). To confirm the role of HD-PTP and UBAP1 in ubiquitinated cargo sorting, the endo-lysosomal transfer kinetics of two model proteins (polyubiquitinated CD4t-Ub_n and tetra mono-Ub exposing CD4cc-UbRΔG_4) were measured by FRIA. Both shHD-PTP and shUBAP1 abrogated the MVB/lysosomal delivery of CD4t-Ub_n (Figure 2.6A, S2.5E). In contrast, shUBAP1 and shHD-PTP failed to prevent the MVB/lysosomal delivery of CD4cc-UbRΔG_4, implying that these ESCRT constituents, in contrast to Hrs, Stam11 and TSG101, are dispensable for the recognition of tetra-mono-Ub sorting signal (Figure 2.6A, lower panel) and supporting the hypothesis of their Ub-chain-specific sorting function (Wunderley et al., 2014).

While the V-domain of HD-PTP has K63-linked poly-Ub binding capacity (Pashkova et al., 2013), the Ub-chain specificity of UBAP1 is unknown. We determined the Ub-chain binding specificity of UBAP1 by GST-UBAP1 pulldown, demonstrating its preference to K63-linked rather than K48-linked polyUb chains or mono-Ub (Figure 2.6B). Accordingly, α5 integrin could be isolated with GST-UBAP1 from FN-stimulated cell lysates (Figure 2.6C). While these observations suggest that both HD-PTP and UBAP1 may participate in the polyubiquitinated α5β1 integrin recognition and lysosomal delivery, they may also be integral to the functionality of other ESCRT constituents, since HD-PTP depletion reduces the expression level of TSG101, Stam11 and Hrs (Figure S2.6C-D). The loss-of-expression phenotype conceivably contributes to enhanced capacity of ESCRT to recognize and sort ubiquitinated cargoes.

2.4.10. Integrin α5β1 dependent cell migration is suppressed by HD-PTP and UBAP1

α5β1 integrin stabilization, as a consequence of HD-PTP or UBAP1 depletion, increased integrin signalling via phosphorylation of Akt, Erk1/2, FAK and Src, as well as 2-3 fold increase in trans-well cell migration and matrigel invasion of HeLa cells (Figure 2.7A-B, S2.7A). In a wound-healing assay, HD-PTP- or UBAP1-depletion also stimulated cell movement, but decreased motion persistence (Figures 2.7B-D), a phenotype associated with increased α5β1 recycling (White et al., 2007). Accelerated migration of HD-PTP knockdown cells can be partly attributed to altered sorting and signalling of integrin α5β1, since the JBS5 blocking Ab significantly reduced migration (Figure 2.7C) and FN substrate preference for migration and spreading (Figure S2.7E-G).

Migration of HD-PTP- or UBAP1-depleted cells was impeded by chloroquine treatment (Figure 2.7D), consistent with sustained ubiquitination of integrin α5β1 and inhibited receptor recycling (Figure 2.3B and H), similarly to USP9x depletion (Figure 2.4D and E). Thus, the deubiquitination-induced recycling of integrin α5β1 mediated by USP9x promotes cell migration, while the degradative HD-PTP/UBAP1 pathway is required for ESCRT-dependent lysosomal degradation of α5β1 integrin to impede cell migration and invasion. Importantly, the promigratory phenotype of HD-PTP depleted cells cannot be attributed only to EGFR signalling (Ali et al., 2013; Doyotte et al., 2008), since HD-PTP depletion-induced accelerated migration was preserved upon EGFR inhibition by Gefitinib (Figure 2.7E), and HD-PTP depletion alone or with FN stimulation failed to activate EGFR signalling (Figure S2.7H).

2.5. Discussion

Here we have demonstrated the pH-regulated ligand binding to integrin α5β1 and coupled ubiquitination-dependent sorting and signalling mechanism of integrin α5β1 receptor complex. We propose that ligand-induced rapid ubiquitination of integrin receptor drives its internalization, but is counteracted by the acidification induced ligand dissociation and USP9x-mediated deubiquitination of the receptor complex, which ensures that most receptors escape from ESCRT-dependent lysosomal degradation in favor of recycling to the cell surface. The remaining ubiquitinated integrin α5β1 is targeted for lysosomal degradation via ESCRT pathway. We highlight novel regulatory targets for the postendocytic fate of the activated α5β1 receptor and help to reconcile the propositions that PM recycling or ubiquitin-driven lysosomal degradation are requirements for integrin dependent cell migration (Caswell et al., 2008; Lobert et al., 2010). It is likely a similar sorting mechanism is applicable to other adhesion receptors, e.g. neuronal adhesion molecule NCAM or DN-GRASP, since their deubiquitination is essential for their recycling (Thelen et al., 2008; Wobst et al., 2012). Transient integrin α5β1 complex ubiquitination promotes its internalization, as well as PM and intracellular turnover. This is in contrast with the unaltered internalization of non-ubiquitinatable integrin α5β1 (α5-4K/R and β1-7K/R) (Bottcher et al., 2012; Lobert and Stenmark, 2010). Such extensive mutagenesis may induce conformational changes that influence the α5β1 association with activation complex components (e.g. Talin, Vinculin, FAK, Src). The activation induced ubiquitination of integrin α5β1 complex (Arjonen et al., 2012), will modulate the partitioning between endocytic recycling of inactive receptors and lysosomal degradation of activated receptors.

We provide evidence of the endosomal acidification induced FN-α5β1 dissociation, with temporal coupling to the receptor inactivation and subsequent deubiquitination, allowing receptor resensitization and cell surface return. Endosomal FN-receptor dissociation and subsequent deubiquitination do not only allow integrin recycling for further rounds of ECM engagement during migration, but also provide an efficient degradation pathway for the internalized ECM. The pH-dependent ligand dissociation may be common to other RGD-receptors, since extracellular acidification can remove the majority of prebound FN from the PM, expressing various integrins. In accordance with CLIC3 mediated recycling of integrin α5β1 from lysosomes (Dozynkiewicz et al., 2012), the proposed α5β1 integrin regulation reconciles a

recent model, invoking that all of the internalized FN-α5β1 complexes are degraded in migrating cells to prevent the recycling of ligand occupied adhesion contacts (Lobert et al., 2010).

The deubiquitination event of integrin α5β1 complex is, at least partly, mediated by USP9x, a DUB with demonstrated role in cancer, development (reviewed in (Murtaza et al., 2015)), cell polarity, adhesion (Theard et al., 2010) and neuronal migration (Homan et al.). The spatiotemporal regulation of the USP9x and its recruitment to the α5β1 integrin complex remains to be elucidated. USP9X was reported to be associated with components of vesicular trafficking in polarized epithelia (Murray et al., 2004; Theard et al., 2010) and in endosomes USP9X can form a complex with Itch E3 ubiquitin ligase (Mouchantaf et al., 2006). In addition to acting on integrin α5β1 complex, USP9x may modulate other E3 ligases (e.g. Cbl and SMURF1) (Magnifico et al., 2003; Xie et al., 2013), and influence endosomal sorting of other ubiquitinated receptors (Marx et al., 2010).

Despite the recycling of the majority of integrin α5β1, a small fraction of α5β1 maintains ubiquitination and is targeted to lysosomal degradation via ESCRT pathway, in competition with the recycling and deubiquitination machinery (Lobert et al., 2010). Our study shows the role of ESCRT-0 and -1 components (HD-PTP and UBAP1) with K63 poly-Ub chain recognition capacity, to deliver cargoes to MVB/lysosomes (Agromayor et al., 2012; Pashkova et al., 2013). The depletion of either HD-PTP or UBAP1 delayed integrin α5β1 degradation, in favour of receptor recycling. This phenotype is the reverse of USP9x depletion, which promoted the α5β1 complex ubiquitination, destabilisation at the PM, and diminished cell migration, in accord with USP9x loss-of-function phenotypes (Homan et al., 2014). Overall, the competitive nature of integrin α5β1 recycling/degradation is likely dependent on an interplay between dynamic ubiquitination and the effect of other sorting motifs in the integrin β1 cytoplasmic tail mediating recycling via the SNX17 pathway (Bottcher et al., 2012; Steinberg et al., 2012). The latter is likely to require USP9x, since the ubiquitination status may be the key factor in integrin endosomal sorting. In addition, receptor cross talks may influence the ligand-receptor dissociation kinetic since Cilengitide decreases FN cooperative binding to α5β1 and enhances its recycling (Caswell et al., 2008).

The phenotypic difference between individual ESCRT components is illustrated by their effect on cell migration. Depletion of core components of the ESCRT0-I (Hrs/TSG101) resulted in

abrogation (Lobert and Stenmark, 2012), while the depletion of HD-PTP or UBAP1 led to potentiation of cell migration. TSG101 depletion resulted in mislocalization of activated Src and decreased myosin light chain phosphorylation, attenuating the promigratory signalling, contractility, and inhibiting turnover of focal adhesions, all process being required for cell migration (Lobert and Stenmark, 2012; Tu et al., 2010). Because TSG101 plays a broad role in other cellular functions (Elia et al., 2011; Martin-Serrano et al., 2001), thus its depletion might have non-specific effects, masking its direct endocytic sorting function in integrin-dependent migration. Possibly, different ESCRT subcomplexes exist with distinct cargo specificity. Thus, the essential components of ESCRT-1 such as TSG101, Vps25, Vps28, and Vps37 act as the core machinery, whereas BRO-domain proteins, such as ALIX or HD-PTP, may confer substrate specificity (Wunderley et al., 2014).

In conclusion, we provide a novel framework for future studies of α5β1 endocytic trafficking by identification of previously unrecognized factors, including the receptor ligand-dependent reversible ubiquitination, the role of endosomal acidification that triggers FN-α5β1 dissociation and the coupled USP9x mediated deubiquitination, as well as the role of HD-PTP/UBAP1 in integrin α5β1 postendocytic trafficking, with far reaching implications in cell migration/invasion.

2.6. Experimental Procedures

Plasmid constructs, reagents and cell culture

UBAP1 was cloned into pGEX2 vector. Ubiquitin GST-Ub/2Ub/3Ub/4Ub were in pGEX-4T1, and pcDNA3 -CD4 c-tail was replaced either with WT Ub (CD4t-Ub_n) or CC tetramerization domain with mutant Ub (all K to R and deletion of 76GG (CD4cc-UbRΔG_4) as described (Barriere et al., 2007b). Complete list of antibodies, reagents and primers is included in Table S1 and S2.

HeLa cells were cultured in DMEM, 10% FBS (Wisent), and serum depleted 1h to overnight. FN negative HeLa has been described before (Kurban et al., 2008; Kurban et al., 2006). E36 and ts20 cells were cultured in DMEM/F12, 10% FBS. Constitutive Mission shRNA TRC2 Lentiviral plasmids pLKO1-puro for human HDPTP (clone ID: NM_015466.x-1004s1c1; NM_015466.x-167s1c1), UBAP1 (clone ID: NM_016525.x-1086s1c1; NM_016525.x-2226s1c1) and scramble control (clone ID: SHC002) were purchased from Sigma. The siRNA DUB sublibrary was from Qiagen Human Whole-genome siRNA library. Individual USP9x siRNAs were from Qiagen (SI00066584, SI00066598) and Dharmacon SMARTpool.

Cell surface density, internalization, metabolic stability and recycling measurements for integrin α5β1 using cs-ELISA

Cell surface ELISA based assays were performed as described earlier (Apaja et al., 2013; Apaja et al., 2010) in live cells. Briefly, cells were serum depleted, labelled with integrin Abs on ice and detected with HRP-conjugated secondary Ab (Amersham Biosciences or Jackson Immunoresearch) revealed with Amplex®Red (Life Technologies Inc.). Biotin-FN was bound on ice and detected with HRP-Neutravidin (Pierce). Thermolabile E1 mutant CHO cells *ts20* and control E36 cells were preincubated at 40°C for 3h to inactivate E1 (Apaja et al., 2010; Kulka et al., 1988). Cilengitide (Selleckchem) was used to isolate specific α5β1 signal. Internalization was measured for the 5min at 37°C both in HeLa and CHO cells, pretreated with 0.3M sucrose and/or 25ug/ml nystatin (Sigma) where indicated. In recycling assay, serum starved cells were labelled with anti-α5 (CD49e) Ab, stimulated with FN (10ug/ml) for 10min at 37°C to induce

integrin uptake. Remaining Ab-complexes were blocked with mouse monovalent $F(ab')_2$ fragments (Jackson Immunoresearch), recycling was activated and PM signal was measured.

Cell surface-ubiquitination assay by IP

The cs-IP, FN and RGD-peptide stimulation was done as described above with anti-α5 or α5β1-blocking Ab. Cells were lysed in buffer A (+20mM N-ethylmaleimide; 1mM MG-132, 1mM WP1130), and Ub signal was probed with P4D1 Ab. Chloroquine (100μM) and NH_4Cl (4mM) pre-treatment was done for 20min, and maintained during FN stimulation. Ub signal was normalized to the amount of integrin α5 in IP.

FN dissociation analysis *in vitro* using biolayer interferometry

Soluble human integrin α5β1 ectodomain fragments, either the full-length (1–954aa of α5 and 1-708aa of β1) or the head-piece (1–623aa of α5 and 1-445aa of β1), were expressed and purified as described before (Nagae et al., 2012). Ligand dissociation kinetics of integrin at different pH were analyzed by BLI using Octet RED system (Pall ForteBio) at 30 °C with orbital sensor agitation at 1,000 rpm, running buffer (20 mM MES, 150 mM NaCl, 1 mM $MnCl_2$, 0.005% Tween20, pH range 5.0~7.5) . First, streptavidin sensors were loaded with 1 μg/ml biotinylated Fn7-10 fragment (Takagi et al., 2003). The sensors were then transferred to 25 nM integrin solution (full-length or head-piece) at pH 7.5 for 2min. Dissociation was initiated by transferring the sensor tips to wells containing running buffers with varying pH, and monitored for additional 5 min. Dissociation rate constants were derived using BIA evaluation software (GE Healthcare).

FN dissociation analysis *in vivo* and vesicular cargo tracking using FRIA

Methodology for cargo labelled vesicular pH determination in live cells by using FRIA has been described in detail before (Apaja et al., 2013; Apaja et al., 2010; Barriere and Lukacs, 2008b). Integrin α5β1 receptor was labelled with anti-α5 (CD49e) or α5β1-blocking Ab and fluorescein isothiocyanate (FITC)-conjugated goat anti-mouse secondary Fab (Jackson ImmunoResearch, USA) on ice and chased for indicated times. Transiently expressed CD4-Ub or CD4tCCUb were used as before (Apaja et al., 2010). Concentrated ascites fluid against CD63/LAMP2 1:1 mixture and the fluid phase marker, FITC-dextran (10 kDa, 50 μg/ml, Molecular Probes) were used as controls for lysosomal delivery. Dextran was endocytosed for

1h and chased for 2 h at 37 °C. For determining FN kinetics, cells were labelled on ice with biotin-FN and FITC-Neutravidin, and internalized for 5min at 37°C. The remaining FN was washed out with pH 5.0 MES buffer (see above). Zeiss Observer Z1 (Carl Zeiss MicroImaging) equipped with X-Cite 120Q system (Lumen Dynamics Group Inc.) and MetaFluor software (Molecular Devices) were used to measure fluorescence intensities.

Size-Exclusion Chromatography fractionation:

Cells were lysed in buffer (150mM NaCl, 0.1% NP40, 6.25mM TrisHCl ph8, 2mM EDTA, 0.1mM MgCl2, 1mM EGTA, +Protease inhibitor cocktail) on ice. The lysate was centrifuged first at 16000g for 10min, and then the resulting supernatant was centrifuged at 100,000g for 1h. The supernatant was loaded on Superdex200 HPLC column and 0.3ml fractions were collected. Protein analysis was performed on collected fraction by SDS-PAGE followed by western blot.

Cell surface (cs) biotinylation and recycling assay

The biotinylation based recycling assay has been described before (Caswell et al., 2008; Caswell et al., 2007). Serum depleted HeLa cells were cs-labelled with NHS-SS-biotin (Pierce). Internalization was stimulated with FN (10ug/ml) for 10min at 37°C, the remaining biotin was stripped with 100 mM sodium 2-mercaptoethanesulfonate (Sigma) for 10 min on ice, repeat twice. Recycling was initiated with FBS 10% and stripping repeated after every time point. Cell lysates were incubated with streptavidin agarose beads (Pierce) and the amount of remaining intracellular integrin α5 was quantified.

Cell surface immunoprecipitation (Cs-IP) of integrin α5β1 and fibronectin

The isolation of the α5β1 cell surface pool was done by IP, HeLa cells were incubated on ice with anti-α5 Ab for 1h and stimulated or not with FN (10μg/ml) or RGD peptide (20μM) at 37°C. Cells were lysed in buffer A (50mM Hepes pH 7.5; 150mM NaCl; 1mM EDTA; 0.5% Triton; 5% Glycerol; 4mM DTT; protease inhibitors) and Ab-α5 complexes were bound to protein G beads (Millipore) and quantified by SDS-PAGE/immunoblot. In FN degradation assay, biotin-FN (Cytoskeleton) was bound to cell surface on ice, chased at 37°C, and the remaining biotin-FN was quantified by immunoblotting using HRP-Neutravidin (Pierce).

FN dissociation at the cell surface and competitive binding assay

Cs-ELISA was done as described above. Biotinylated-FN (4µg/ml, Cytoskeleton Inc.) was incubated on ice for 1h, cells were washed (PBS, 0.1mM $CaCl_2$, 1mM $MgCl_2$) and washed again for 10min with buffers adjusted to pH <6.5, containing 140mM NaCl, 5mM KCl, 10mM MES or pH>6.5 containing 10mM Hepes, 10mM glucose, 1mM CaCl2, 0.1mM $MgCl_2$). Cilengitide or α_v-blocking Ab (Calbiochem) pretreatment (30min at 37°C) was applied to eliminate ligand-induced binding and activation of other FN specific integrins, except α5β1. Decreased Ca^{2+} concentration (10-100 µM) had no effect on FN pH dependent dissociation at pH 6.0 (see also Figure S3C). The remaining biotin-FN signal on the PM was detected with HRP-Neutravidin (Pierce). For analysing the binding at different proton concentrations [H^+], the data from Figure 3F was plotted using GraphPad Prism equation for specific binding with Hill slope function. Non-specific biotin-FN binding was determined using competition binding assay, in the presence of 100-fold excess of label-free FN and of increasing concentration of biotin-FN (0-10 µg/ml). The non-specific biotin-FN binding was 23-27±11% and 24.7 ±4.7% in E36/ts20 and HeLa cells, respectively, and was subtracted from the total signal to calculate the specific signal.

siRNA DUB sublibrary screen

Qiagen siRNA sublibrary for human DUBs and SUMO proteases was transfected into HeLa cells as triplicate 96-well plates. Like in cs-ELISA experiments, integrin α5 antibody was bound on cells, the excess antibody was washed out and cells were stimulated with FN for 60min at 37°C to activate receptor complex. After stimulation, the remaining PM integrins were detected with HRP-conjugated secondary antibody and luminescence measurement. The PM integrin α5β1 amount after chase was expressed at percentage of initial integrin remaining on plasma membrane.

Immunofluorescence

HeLa cells were serum deprived, pre-labelled with anti-α5 (CD49e) and/or biotin-FN on ice and the excess ligand washed off. Labelled complexes were internalized; cells were fixed with 4% paraformaldehyde and permeabilized for secondary Ab labelling. Colocalization of integrin-α5 with EEA1, LAMP1 and Tf was done similarly, and Mandels coefficient was calculated by Zeiss

ZEN software. Sequential image acquisition was done on LSM710 microscope (Carl Zeiss MicroImaging, Inc), using the Plan-Apochromat 63x/NA 1.4 objective. To visualize FN dissociation from the HeLa cell surface, the cells were pretreated with 0.3M sucrose and 25 μg/ml nystatin to inhibit integrin internalization and labelled with biotin-FN and a5-Ab on ice for 1h. Cell surface was washed with buffers of increasing acidity, prepared as described above, for 10min and remaining biotin-FN and integrin α5β1 was visualised with FITC-streptavidin or Alexa 594 conjugated secondary Ab respectively. Fluorescence was visualized by a Zeiss Observer Z1 inverted fluorescence microscope (Carl Zeiss MicroImaging).

Integrin α5β1 signalling and expression analysis

HeLa cells were serum starved and stimulated with FN (10μg/ml) for 8h. Cells were collected and analysed by SDS-PAGE followed by immunoblot. For mRNA analysis, cells were lysed in Trizol (Bioshop), RNA was isolated by phenol chloroform extraction followed by DNAse treatment and cDNA was produced with RT (BioRad). qPCR was performed using SYBR-green reagent (BioRad) and expressed as relative to control cells, normalized to RPL0 housekeeping gene.

Recombinant protein production and pull-down assay

Full-length GST-UBAP1 expression in *E. Coli* BL21 was induced with 0.1mM IPTG for 4 h at 22 °C and bacteria was lysed in (100mM Tris HCl pH 7.5; 150mM NaCl; 5mM EDTA; 0.75% Triton; 5% Glycerol; 4mM DTT; protease inhibitors, 1mM PMSF), and affinity purified on glutathione-Sepharose beads (Pierce). The recombinant Ub-constructs expression, purification and GST pull-down were done as described (Barriere et al., 2006a). Hela cell lysate (2mg) was used to detect protein interactions. To determine Ub chain specificity of UBAP1, glutathione-Sepharose bound GST-UBAP1 was incubated with purified mono-Ub, K48- or K63-linked Ub-chains (Boston Biochem) for 2h at 4°C.

HeLa cell migration/invasion and spreading assays

Migration/invasion assays were performed using xCELLingence system (Roche). 60,000 HeLa cells in serum free media were allowed to migrate for 6h towards 10% FBS medium. In invasion assays, the chamber separating membrane was coated with Matrigel, FN (20μg/ml) or Collagen I

(Calbiochem). Invasion was scored after 18h. Pre-treatment with α5β1-blocking Ab or chloroquine (100μM) was done for 20min and maintained during the experiment. In wound-healing, cells were plated on FN-coated wound-healing chambers. After removing the insert, 10% FBS was added, time-lapse images (18h) were acquired using Zeiss Axiovert200 microscope with 20x objective. Cell displacements were quantified using Metamorph (Molecular Devices).

Cell spreading: 250,000 cells were plated on FN (20μg/ml) or collagen I for 15min, non-attached cells were removed. The attached cells spread for 45min at 37°C, were fixed, stained with Alexa 549 Phalloidin (Life Technologies inc.), and visualized on a Zeiss Axiovert200 microscope. The relative cell surface area was quantified using ImageJ software (NIH).

Statistical analysis:

Data were analysed by Student's unpaired t-test or one-way Anova (where applicable). P-values at $p<0.05$ were considered significant and are described in the figure legends.

2.7. Acknowledgements:

The authors thank Colin Ratcliffe, Yaakov Stern and Dr. Christine Parachoniak for critical reading of the manuscript. D.K. holds Fonds de la recherche en santé du Quebec doctoral award. S.M. holds McGill Biochemistry Merit Fellowship. A.P. was a recipient of the Canada Research Chair in Molecular Oncology. This work was supported by Canadian Cancer Society Research Institute grant 2010-700525 and Cancer Research Society grant (to A.P.). G.L. is the holder of a Canada Research Chair. J.T. holds Grants-in-Aid for Scientific Research (A) and by the Grants-in-Aid for Scientific Research on Innovative Areas (transient macromolecular complexes), both from the Ministry of Education, Culture, Sports, Science, and Technology of Japan.

2.8. Figures and Figure Legends

Figure 2.1 : FN binding induces integrin α5β1 ubiquitination:

(A) Cells surface integrins were labelled with α5 Ab on ice, immunoprecipitated (IP) after FN (10μg/ml) exposure for 0-15 min at 37ºC and the IP was probed by immunoblotting (IB) with the P4D1 anti-Ub Ab. The ubiquitination signal, indicated by vertical bracket, was normalized for the precipitated amount of integrin α5 (right panel). Means ±SEM; n=3; *p< 0.02.

(B) α5β1 blocking Ab prevents the FN-induced ubiquitination of the α5β1 complex. Cell surface IP (cs-IP) and ubiquitination detection of α5β1 was performed by using α5 or blocking α5 Ab, followed by FN stimulation at 37ºC as in (A). (n=3; *p< 0.02).

(C) Inhibition of α5β1 internalization. Internalization of α5 was measured by cell surface ELISA (cs-ELISA) in HeLa cells exposed to 0.3M sucrose and/or 25μg/ml nystatin to inhibit clathrin and caveolin mediated endocytosis, respectively. Means ± SEM; n=3; *p<0.02.

(D) Cs-IP and ubiquitination measurements of the α5β1 complex was performed as in (A) in presence or absence of clathrin and caveolin endocytosis inhibitors. Means ±SEM; n=3; *p<0.02.

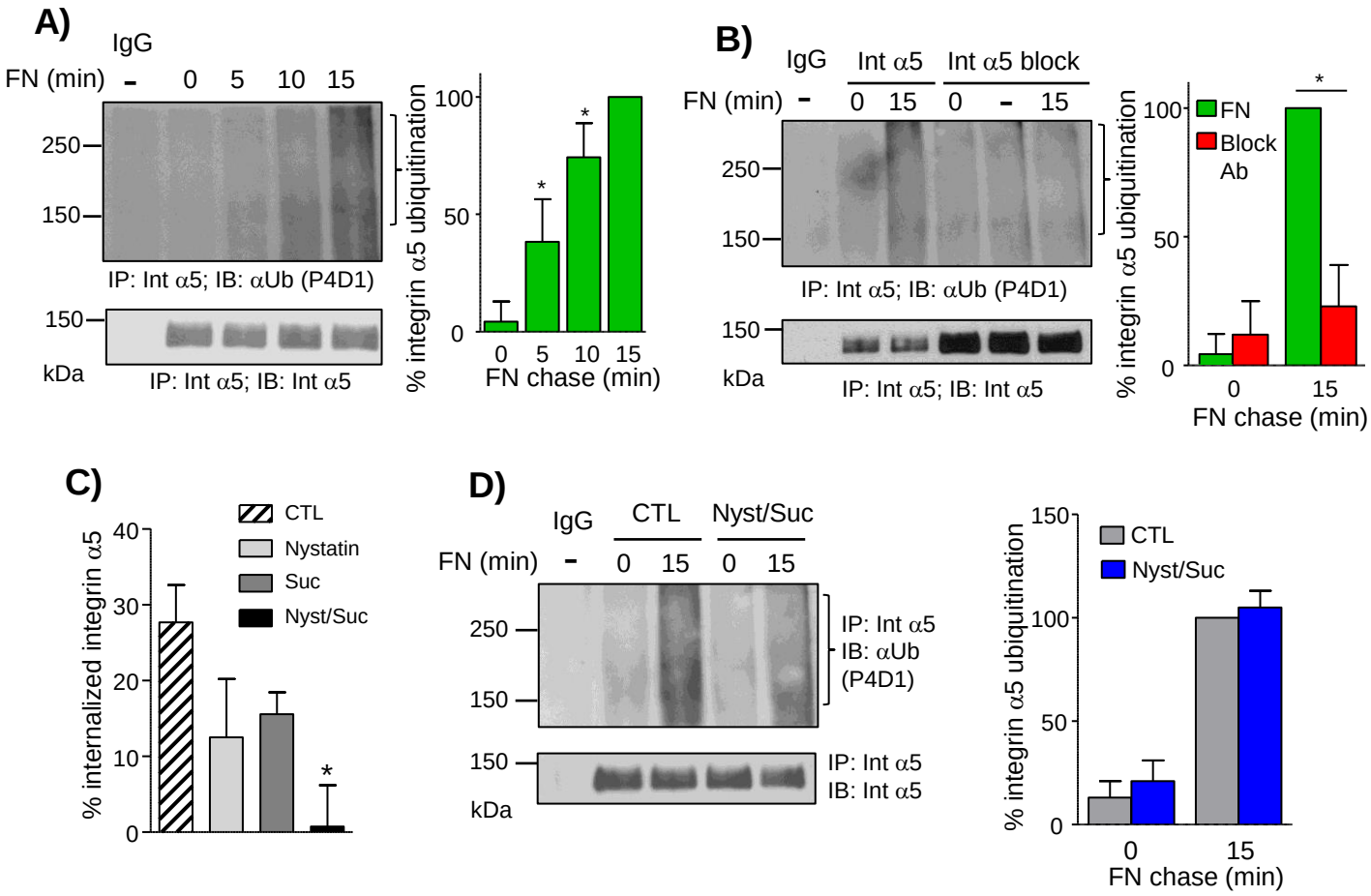
A)
IgG
FN (min) - 0 5 10 15
250
150
IP: Int α5; IB: αUb (P4D1)
150
kDa
IP: Int α5; IB: Int α5
% integrin α5 ubiquitination
100
50
0
0 5 10 15
FN chase (min)
B)
IgG
Int α5
Int α5 block
FN (min) - 0 15 0 - 15
250
150
IP: Int α5; IB: αUb (P4D1)
150
kDa
IP: Int α5; IB: Int α5
% integrin α5 ubiquitination
FN
Block Ab
100
50
0
0 15
FN chase (min)
C)
% internalized integrin α5
40
30
20
10
0
CTL
Nystatin
Suc
Nyst/Suc
D)
IgG
CTL
Nyst/Suc
FN (min) - 0 15 0 15
250
150
IP: Int α5
IB: αUb
(P4D1)
150
kDa
IP: Int α5
IB: Int α5
% integrin α5 ubiquitination
150
100
50
0
CTL
Nyst/Suc
0 15
FN chase (min)

Figure 2.1

Figure 2.2 : FN induces integrin α5β1 receptor targeting to lysosomal degradation from the plasma membrane

(A-B) Internalization (A) and steady state density (B) of the inactive, constitutively and exogenously activated α5β1 were determined using cs-ELISA. 5min FN stimulation was performed at 37ºC where indicated. FN caused 3-fold acceleration in integrin internalization. The effect of inactivation of α5β1 by blocking Ab was measured by pretreating cells with blocking Ab (block Ab), followed by cs-ELISA detection with biotin-anti-α5 Ab (B). Means ±SEM; n=5; *p<0.05.

(C) FN activation transiently reduces the α5β1 PM density, determined by cs-ELISA. After FN exposure of HeLa cells for 15 min, the receptor PM reappearance was measured in presence or absence (CTL) of Cilengitide (1μM).

(D) Ubiquitination is required for FN-receptor internalization, since the depletion of the E1 Ub-activating enzyme abrogated the FN induced internalization. E1 enzyme was inactivated at 40ºC for 3h in ts20 cells and α_v integrins were inhibited with Cilengitide (1μM) for 30min prior to biotin-FN stimulation. FN receptors at the PM were detected by biotin-FN labelling and cs-ELISA. Means ±SEM; n=3; *p< 0.02; ***p< 0.0002.

(E) Endo-lysosomal transfer kinetics of α5 integrin and CD4-Ub chimeras. Mean vesicular pH (pH_v) of indicated cargo containing endocytic vesicles was determined by FRIA in HeLa cells (see diagram in Figure S2A). Anti-α5 integrin Ab, α5β1 blocking Ab or anti-CD4 Ab and FITC-Fab were bound on ice and FRIA was performed during 7h chase in the presence or absence of FN at 37ºC. The graph shows the mean pH_v at each chase point. The transfer kinetics of CD4-chimeras bearing a poly-Ub (CD4t-Ub_n), tetra-Ub chain (CD4t-UbRΔG_1) or tetrameric mono-Ub (CD4cc-UbRΔG_4) are indicated. Means ±SEM; n=5.

(F-G) Activation-dependent PM turnover of the integrin α5β1. The PM stability of α5 integrin was measured either by cs-ELISA (F) or by cs-IP and immunoblotting (G) with or without FN stimulation or in presence of α5 blocking Ab. The CD4 chimeras turnover are also indicated for reference in (F).

(H) Ubiquitination detection of cell surface integrin α5 during long FN stimulation was measured as described in Figure 2.1A. Means ±SEM; n=5; ***p<0.001.

(I) Recycling of α5 integrin in FN stimulated or α5β1 blocking Ab treated cells measured by cs-ELISA. Integrins were cell surface labelled with Ab on ice, internalized by FN stimulation, and the remaining PM Ab was blocked with Fab on ice. The recycling of internalized integrins was induced at 37ºC and the PM returned pool of Ab-labelled integrins was quantified. Means ± SEM; n=3; *$p<0.05$.

(J) Internalization rate of α5 is FN activation dependent. Internalization was determined as in (C) at the indicated time after FN stimulation and wash-out. Means ±SEM; n≥3; NS: non-stimulated, CTL: control.

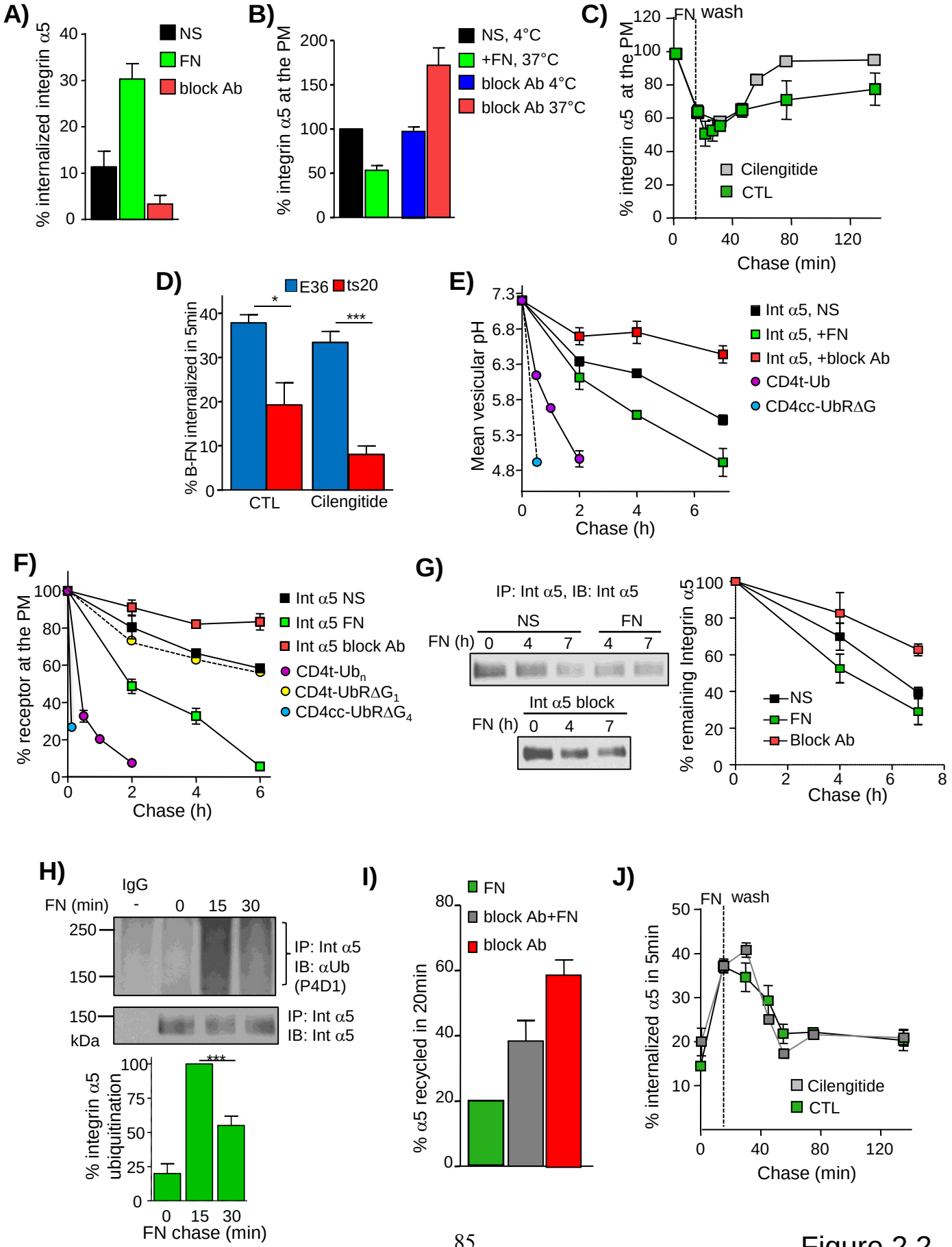
A)
% internalized integrin α5
NS
FN
block Ab
B)
% integrin α5 at the PM
NS, 4°C
+FN, 37°C
block Ab 4°C
block Ab 37°C
C)
FN wash
% integrin α5 at the PM
Cilengitide
CTL
Chase (min)
D)
E36
ts20
% B-FN internalized in 5min
CTL
Cilengitide
E)
Mean vesicular pH
Int α5, NS
Int α5, +FN
Int α5, +block Ab
CD4t-Ub
CD4cc-UbRΔG
Chase (h)
F)
% receptor at the PM
Int α5 NS
Int α5 FN
Int α5 block Ab
CD4t-Ub$_n$
CD4t-UbRΔG$_1$
CD4cc-UbRΔG$_4$
Chase (h)
G)
IP: Int α5, IB: Int α5
NS
FN
FN (h)
Int α5 block
% remaining Integrin α5
NS
FN
Block Ab
Chase (h)
H)
IgG
FN (min)
IP: Int α5
IB: αUb
(P4D1)
IP: Int α5
IB: Int α5
kDa
% integrin α5 ubiquitination
FN chase (min)
I)
FN
block Ab+FN
block Ab
% α5 recycled in 20min
J)
FN wash
% internalized α5 in 5min
Cilengitide
CTL
Chase (min)

Figure 2.2

Figure 2.3: FN binding to integrin α5β1 is regulated by endocytic pH and FN dissociation is required for integrin α5β1 deubiquitination

(A) Immunocolocalization dynamics of internalized FN-α5 integrin complex in HeLa cells. FN-α5 complexes were labelled with anti-α5 Ab and biotin-FN on ice, chased at 37ºC for indicated times and visualized by Alexa-594 conjugated secondary Ab and FITC-streptavidin, respectively, using laser confocal fluorescence microscopy. Colocalization was measured by the Mander's coefficient (right panel). Means ±SEM; n=110 cells.

(B-C) FRIA analysis of FITC-labelled biotin-FN or integrin α5 endocytosis kinetics. (B) Representative pH_v distribution of internalized biotin-FN and integrin α5 after 15 and 20min internalization. The mean pH_v of the distinct peaks and the number of vesicles are indicated. The FN and integrin α5 are largely segregated into late endosome/lysosome (pH ~5.3-5.7) and recycling endosomes (pH ~6.5), respectively. Means ± SEM; n=3.

(D) Degradation kinetics of FN analyzed by Western blotting in HeLa cells. Biotin-FN was prebound on ice, chased at 37ºC and quantified by immunoblotting, using Neutravidin-HRP and the ImageJ software.

(E) The pH-dependent dissociation of FN from HeLa cells. The PM dissociation of biotin-FN was measured by cs-ELISA after 10 min of incubation at the indicated pH.

(F) Biolayer Interferometry (BLI) sensorgrams of full-length (FL) recombinant α5β1 ectodomain binding to FN. For each measurement, association rate was monitored for 2 min at pH 7.5, followed by measurement of dissociation rate in indicated pH buffer.

(G) Dissociation rate constants for FN and full-length or headpiece of α5β1 integrin at various pH, obtained by BLI measurements as in (F). Means ±M.S.D.; n=3.

(H-I) Inhibition of α5 deubiquitination by weak bases. α5 integrin ubiquitination was measured as in Figure 2H after pre-incubation of cells with lysosomotropic agents chloroquine (CQ, 100μM, 20min) or NH_4Cl (4mM, 5min). Integrin deubiquitination was inhibited at 30min of FN stimulation. Means ±SEM. n=3; *$p<0.03$.

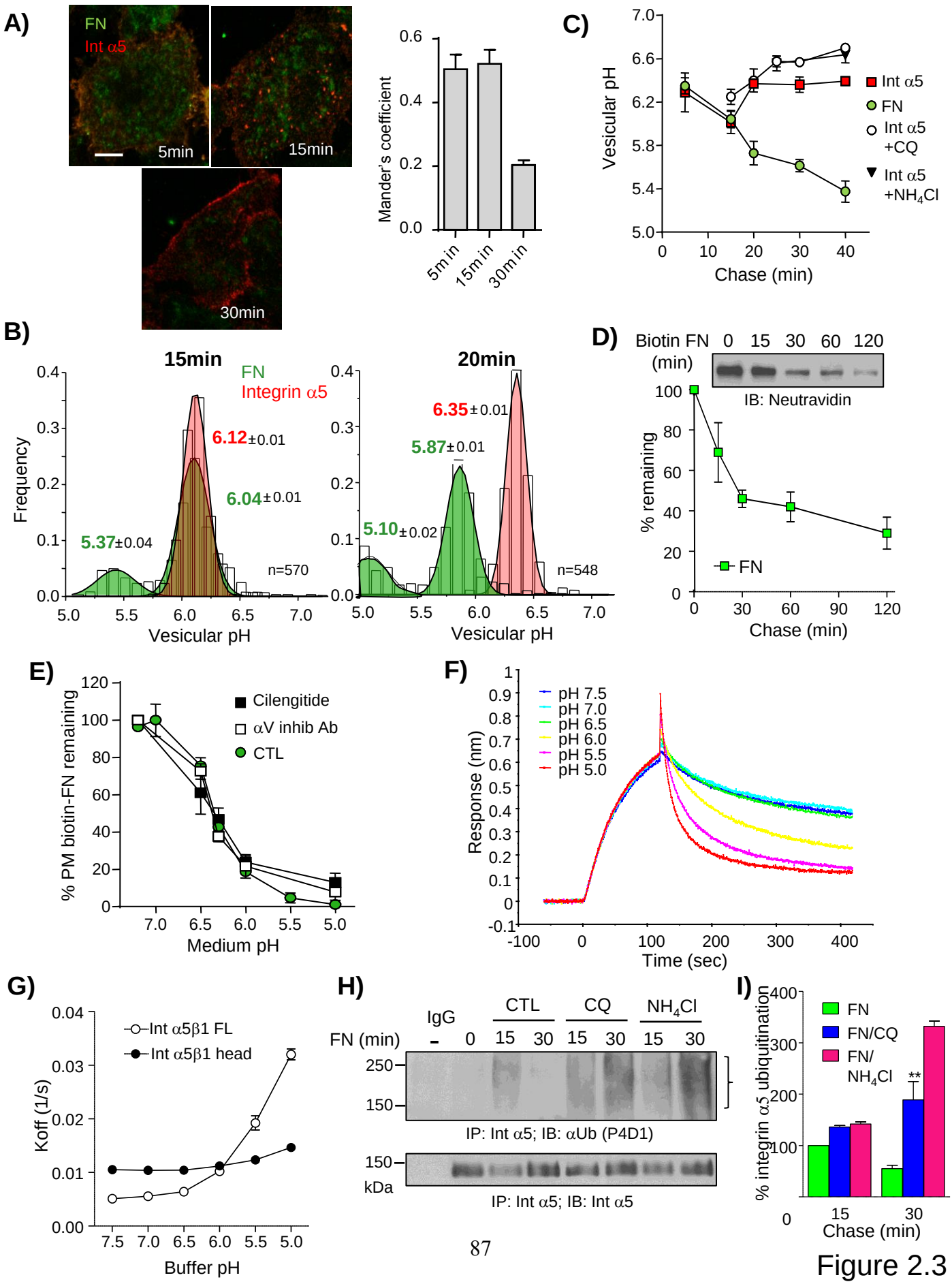
A)
FN
Int α5
5min
15min
30min
Mander's coefficient
5min
15min
30min
C)
Vesicular pH
Chase (min)
Int α5
FN
Int α5 +CQ
Int α5 +NH4Cl
B)
15min
20min
FN
Integrin α5
Frequency
6.12±0.01
6.04±0.01
5.37±0.04
n=570
6.35±0.01
5.87±0.01
5.10±0.02
n=548
Vesicular pH
D)
Biotin FN (min)
0 15 30 60 120
IB: Neutravidin
% remaining
FN
Chase (min)
E)
% PM biotin-FN remaining
Cilengitide
αV inhib Ab
CTL
Medium pH
F)
Response (nm)
pH 7.5
pH 7.0
pH 6.5
pH 6.0
pH 5.5
pH 5.0
Time (sec)
G)
Koff (1/s)
Int α5β1 FL
Int α5β1 head
Buffer pH
H)
IgG
CTL
CQ
NH4Cl
FN (min)
- 0 15 30 15 30 15 30
250
150
IP: Int α5; IB: αUb (P4D1)
150
kDa
IP: Int α5; IB: Int α5
I)
% integrin α5 ubiquitination
FN
FN/CQ
FN/ NH4Cl
**
Chase (min)

Figure 2.3

Figure 2.4: USP9x mediates integrin α5β1 deubiquitination

(A-B) USP9x siRNA efficiency was validated by Western blot analysis and actin as a loading control. USP9x ablation decreases the α5β1 PM density, measured by cs-ELISA after treating the cells with individual (siUSP9x-1 and -2) and smartpool siRNA (siUSP9x pool). Integrin α5 was labelled with α5 Ab at the PM, followed by 60min chase with FN at 37ºC. Mean ±SEM; n=3 **p<0.01.

(C-D) FN-induced ubiquitination of α5 complexes is augmented in USP9X depleted HeLa cells. Ubiquitination level of α5 complexes was monitored as described in Figure 2.2H in USP9X siRNA treated cells as a function of FN (10μg/ml) exposure time. IgG was used as non-specific Ab control. Densitometric quantification of ubiquitination was normalized for the α5 amount in the IP. Means ± SEM; n≥3; *p<0.05.

(E) HeLa cells were transfected with siUSP9x smartpool and subjected to xCELLigence RTCA (real-time cell analysis) system migration assay. Depletion of USP9x leads to slower cell migration. Means ±SEM; n>3; *p<0.05.

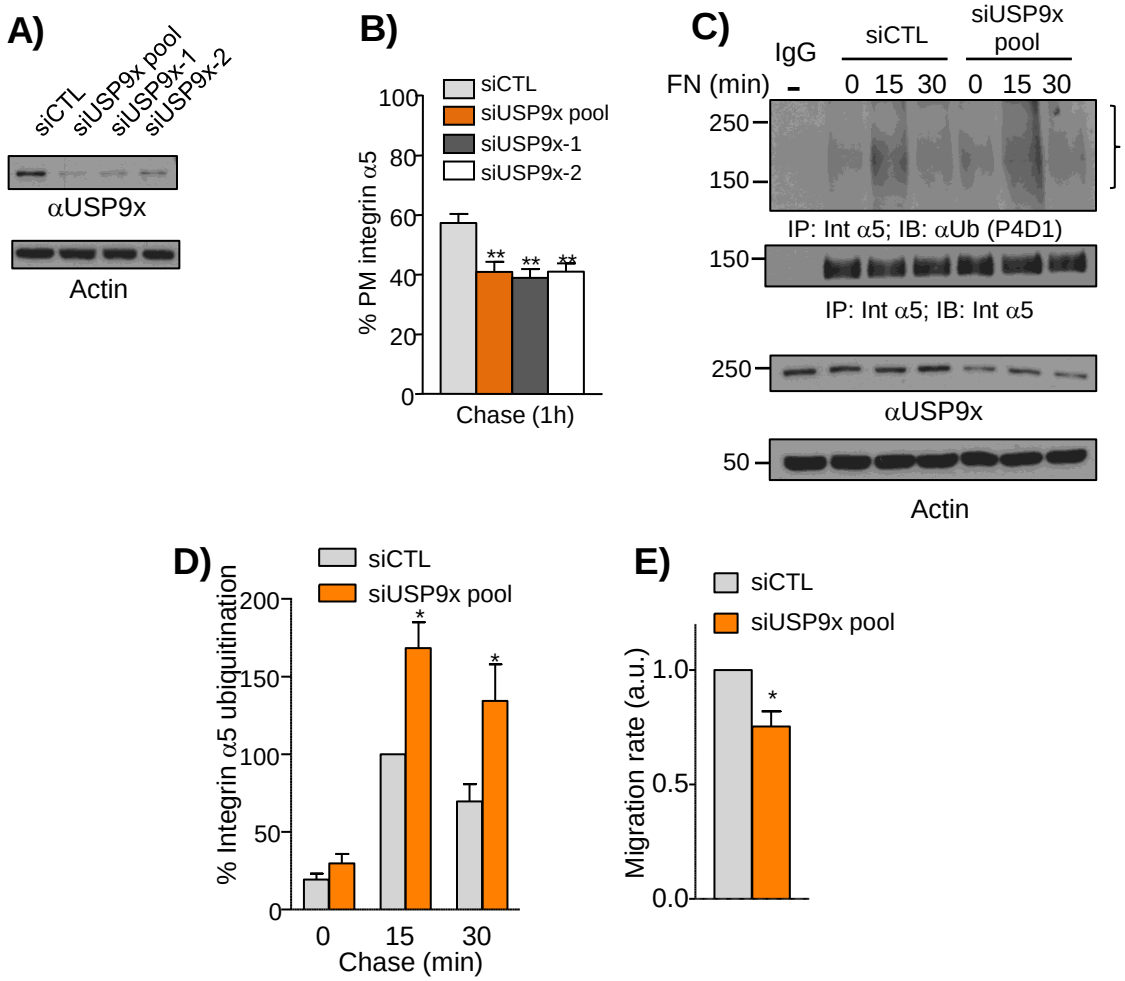
A)
siCTL
siUSP9x pool
siUSP9x-1
siUSP9x-2
αUSP9x
Actin
B)
siCTL
siUSP9x pool
siUSP9x-1
siUSP9x-2
% PM integrin α5
100
80
60
40
20
0
**
**
**
Chase (1h)
C)
IgG
siCTL
siUSP9x pool
FN (min) -
0 15 30 0 15 30
250
150
IP: Int α5; IB: αUb (P4D1)
150
IP: Int α5; IB: Int α5
250
αUSP9x
50
Actin
D)
siCTL
siUSP9x pool
% Integrin α5 ubiquitination
200
150
100
50
0
*
*
0 15 30
Chase (min)
E)
siCTL
siUSP9x pool
Migration rate (a.u.)
1.0
0.5
0.0
*

Figure 2.4

Figure 2.5: ESCRT-0/I components HD-PTP and UBAP1 are required for integrin α5β1 lysosomal delivery

(A) Integrin α5β1 abundance is increased upon HD-PTP or UBAP1 depletion by two independent shRNAs, detected by immunoblotting in HeLa cells. The shRNA giving the more pronounced phenotype was used in the consequent experiments.

(B) Steady state level of α5β1 was monitored by Western blotting of in HD-PTP or UBAP1 depleted cells after serum starvation and FN stimulation for 7h.

(C) The PM density of α5β1 integrin was increased in HD-PTP or UBAP1 depleted HeLa cells, determined by cs-ELISA. Means ± SEM; n=3; ***p<0.001.

(D-E) Immunofluorescence colocalization of internalized α5 with organelle markers. α5 Ab labelled receptors were chased for 7h at 37°C in the presence of FN (10μg/ml) and visualized with the EEA1 or LAMP1, early endosomal and lysosomal marker respectively. Recycling compartment was labelled with Alexa-594 transferrin. Integrin α5 was observed primarily in early/recycling compartments in HD-PTP or UBAP1 depleted HeLa cells, in contrast to control cells, where a significant fraction was localized to late endosomal/lysosomal compartments. Bar: 10μm. (E) Quantification of integrin α5 colocalization with EEA1, LAMP1 or transferrin from experiments shown in (D) and using Mander's coefficient. Means ±SEM; n=3; *p<0.05; **p<0.01; n=30-40 cells/condition.

(F) The lysosomal delivery of integrin α5β1 was significantly compromised in shHD-PTP and shUBAP1 depleted cells. Mean pH_v of integrin α5β1 containing endocytic vesicles in shHD-PTP and shUBAP1 depleted cells was determined by FRIA after 2-7 h chase as in Figure 2.2E. Means ±SEM; n=5; *p<0.05; **p<0.01.

(G) Integrin α5 recycling is activated by HD-PTP or UBAP1 depletion. Biotin-based integrin recycling was determined as described (Caswell et al., 2008; Caswell et al., 2007). Cell surface proteins were biotinylated with NHS-SS-Biotin on ice and stimulated with FN (10μg/ml) for 10min at 37°C. The remaining PM biotin was stripped with MesNA on ice, and recycling of integrins was allowed at 37ºC. At indicated timepoints cells were stripped again with MesNA, lysed and the biotinylated proteins were bound to Neutravidin resins. The remaining pool of

biotinylated integrins was quantified by Western blot analysis. Integrin α5 is recycled faster in cells depleted for HD-PTP or UBAP1 (**$p<0.01$). Data are means ±SEM; $n\geq3$.

(H-I) Deubiquitination of integrin α5 receptor complex is accelerated in HeLa cells depleted for HD-PTP or UBAP1. Ubiquitination of cells were surface labelled α5 was measured at the indicated time after 10μg/ml FN stimulation in HD-PTP or UBAP1 depleted cells as in Figure 2H Data are means ± SEM; n=3; *$p<0.05$.

(J) α5 degradation from the PM is inhibited by HD-PTP or UBAP1 depletion. The remaining PM labeled α5 was measured by cs-IP and immunoblotting after FN stimulation after the indicated chase (as in Figure 2G). Data are means ± SEM; n=3; * $p<0.05$.

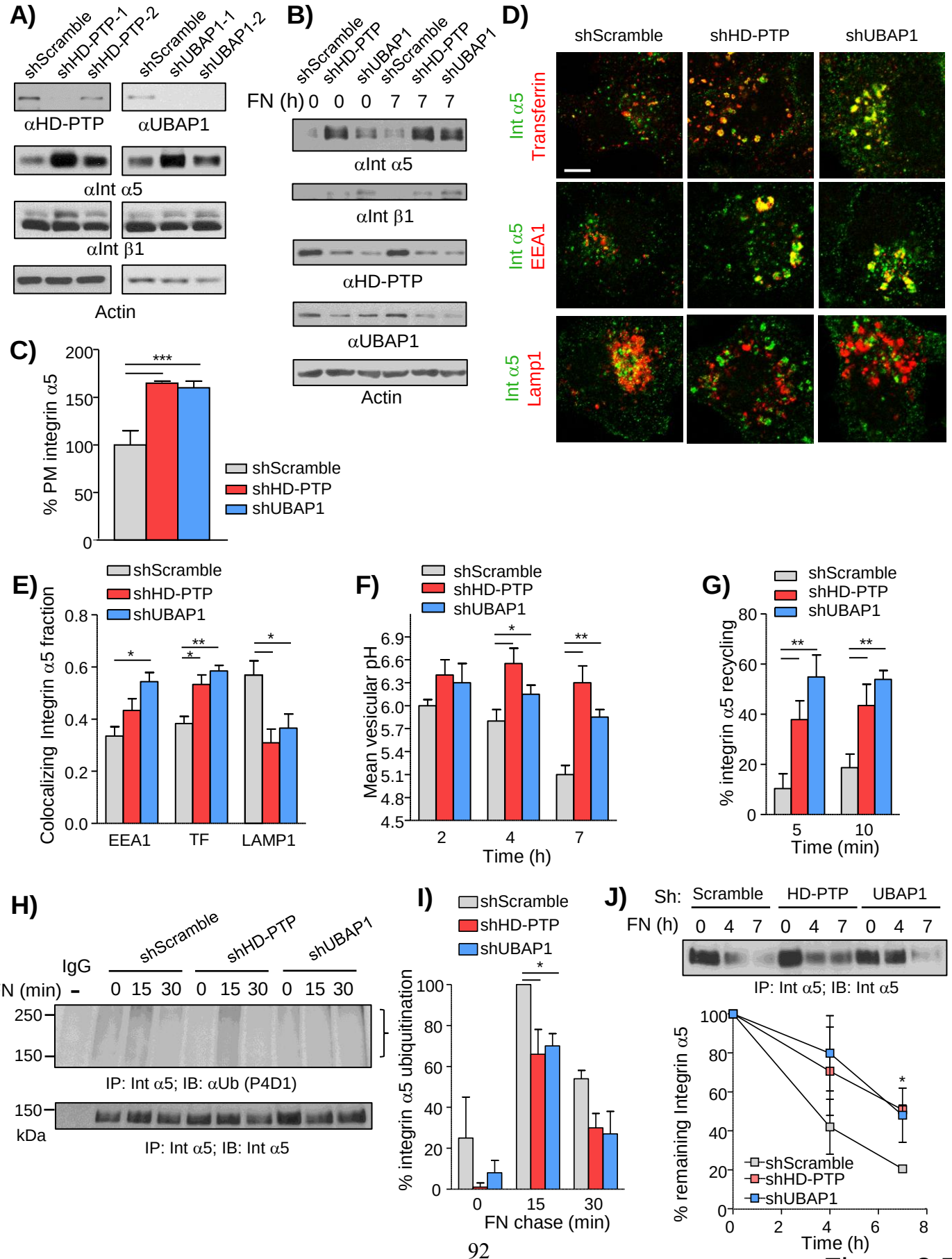
A)
shScramble
shHD-PTP-1
shHD-PTP-2
shScramble
shUBAP1-1
shUBAP1-2
αHD-PTP
αUBAP1
αInt α5
αInt β1
Actin
B)
shScramble
shHD-PTP
shUBAP1
shScramble
shHD-PTP
shUBAP1
FN (h) 0 0 0 7 7 7
αInt α5
αInt β1
αHD-PTP
αUBAP1
Actin
C)
% PM integrin α5
200
150
100
50
0
***
shScramble
shHD-PTP
shUBAP1
D)
shScramble
shHD-PTP
shUBAP1
Int α5 Transferrin
Int α5 EEA1
Int α5 Lamp1
E)
shScramble
shHD-PTP
shUBAP1
Colocalizing Integrin α5 fraction
0.8
0.6
0.4
0.2
0.0
EEA1
TF
LAMP1
F)
shScramble
shHD-PTP
shUBAP1
Mean vesicular pH
6.9
6.6
6.3
6.0
5.7
5.4
5.1
4.8
4.5
2
4
7
Time (h)
G)
shScramble
shHD-PTP
shUBAP1
% integrin α5 recycling
80
60
40
20
0
5
10
Time (min)
H)
IgG
shScramble
shHD-PTP
shUBAP1
FN (min) – 0 15 30 0 15 30 0 15 30
250
150
IP: Int α5; IB: αUb (P4D1)
150
kDa
IP: Int α5; IB: Int α5
I)
shScramble
shHD-PTP
shUBAP1
% integrin α5 ubiquitination
100
80
60
40
20
0
0
15
30
FN chase (min)
J)
Sh: Scramble HD-PTP UBAP1
FN (h) 0 4 7 0 4 7 0 4 7
IP: Int α5; IB: Int α5
% remaining Integrin α5
100
80
60
40
20
0
0
2
4
6
8
Time (h)
shScramble
shHD-PTP
shUBAP1

Figure 2.5

Figure 2.6: HD-PTP and UBAP1 are required for poly-Ub recognition and ubiquitinated cargo lysosomal delivery

(A) The mean pH_v of the indicated CD4-Ub chimeras was measured in HD-PTP or UBAP1 depleted HeLa cells at the indicated chase as in Figure 2E. Both HD-PTP and UBAP1 were required for poly-Ub CD4t-Ub_n, but not for the tetrameric CD4cc-UbRΔG_4 lysosomal delivery. Means ±SEM; n≥3.

(B) UBAP poly-Ub chain binding selectivity. Pulldown assay was performed with GST-UBAP1 or GST and mono-, poly-K48 or poly-K63 Ub. Bound Ub moieties were probed with P4D1 anti-Ub Ab as described in Methods. GST-UBAP1 interacts specifically with poly-K63 Ub chain, n=3.

(C) Integrin α5 and K63-linked polyubiquitinated proteins associate with GST-UBAP1. Western blot analysis of GST pull-downs using recombinant GST-UBAP1 incubated with serum starved and FN stimulated (15min) HeLa cell lysates, n=3.

.

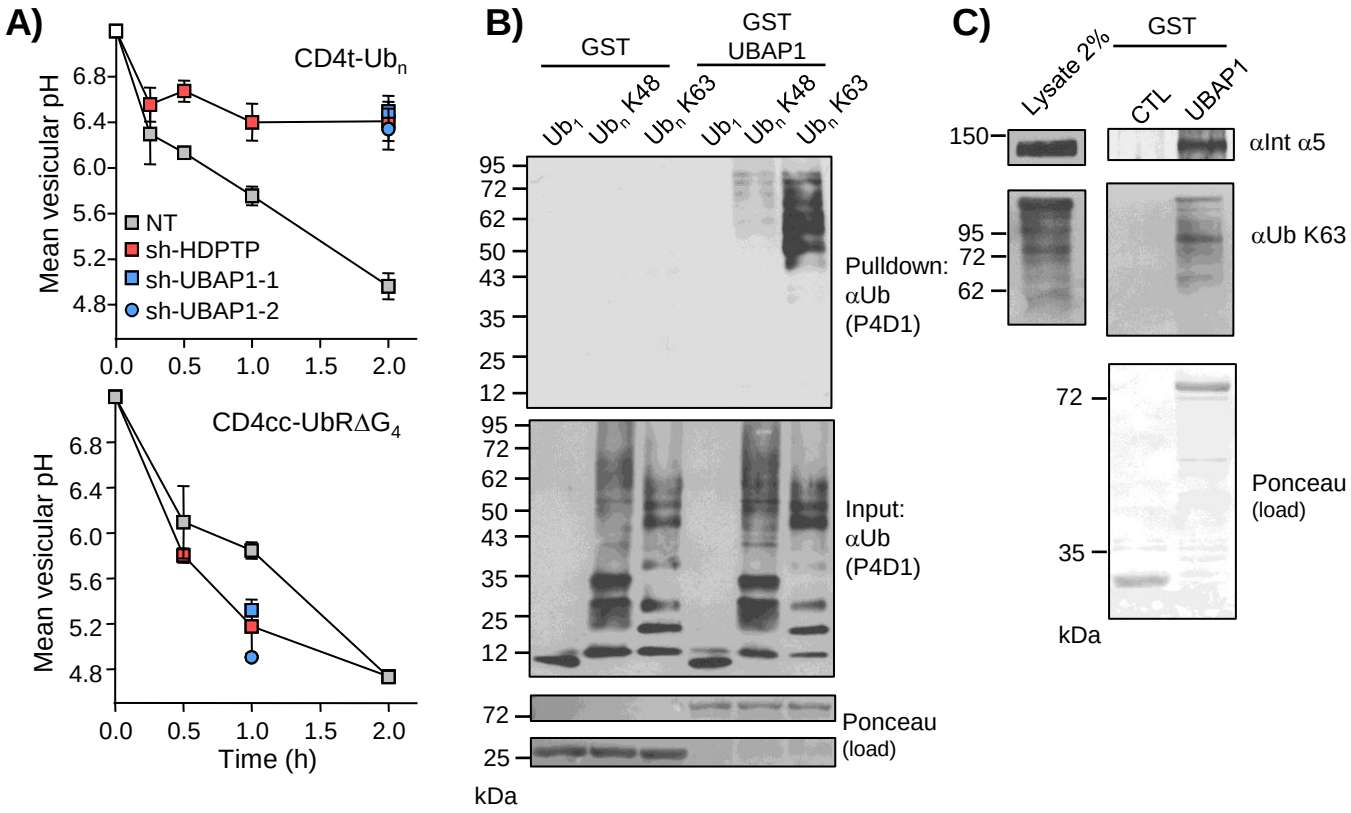
A)
CD4t-Ubn
Mean vesicular pH
6.8
6.4
6.0
5.6
5.2
4.8
NT
sh-HDPTP
sh-UBAP1-1
sh-UBAP1-2
0.0
0.5
1.0
1.5
2.0
CD4cc-UbRΔG4
Time (h)
B)
GST
GST
UBAP1
Ub1
Ubn K48
Ubn K63
95
72
62
50
43
35
25
12
Pulldown:
αUb
(P4D1)
Input:
αUb
(P4D1)
Ponceau
(load)
kDa
C)
Lysate 2%
GST
CTL
UBAP1
150
αInt α5
95
72
62
αUb K63
72
35
Ponceau
(load)
kDa

Figure 2.6

Figure 2.7: Regulation of α5β1 signalling and cell migration by HD-PTP and UBAP1.

(A) Phosphorylation state of pro-migratory (pFAK, pSrc) and pro-survival (pAkt, pErk1/2) signalling molecules in FN stimulated (7h) in HeLa cells.

(B) HeLa cells were subjected to migration or matrigel invasion assays using xCELLigence RTCA (real-time cell analysis) system. HD-PTP and UBAP1 depletion potentiated pro-migratory and pro-invasive phenotype (*$p<0.05$; **$p<0.01$). Means ± SEM; $n\geq3$.

(C) Inhibition of integrin α5β1 function by blocking Ab has severely compromised migration in shHD-PTP cells (*$p<0.05$) as performed in (B). Cells were incubated for half-hour with CTL mouse IgG or α5β1 blocking Ab. Means ±SEM; $n\geq3$.

(D) Disruption of integrin sorting by chloroquine (100μM CQ) leads to abrogation of cell migration as performed in (B). Means ±SEM; $n\geq3$.

(E) Inhibition of EGFR does not eliminate the stimulatory effect of shHD-PTP on cell migration. HeLa cells were treated with EGFR inhibitor Gefitinib (2μM) for 30min prior to the migration assay that was conducted as in (B). Means ±SEM; $n\geq3$, *$p<0.05$.

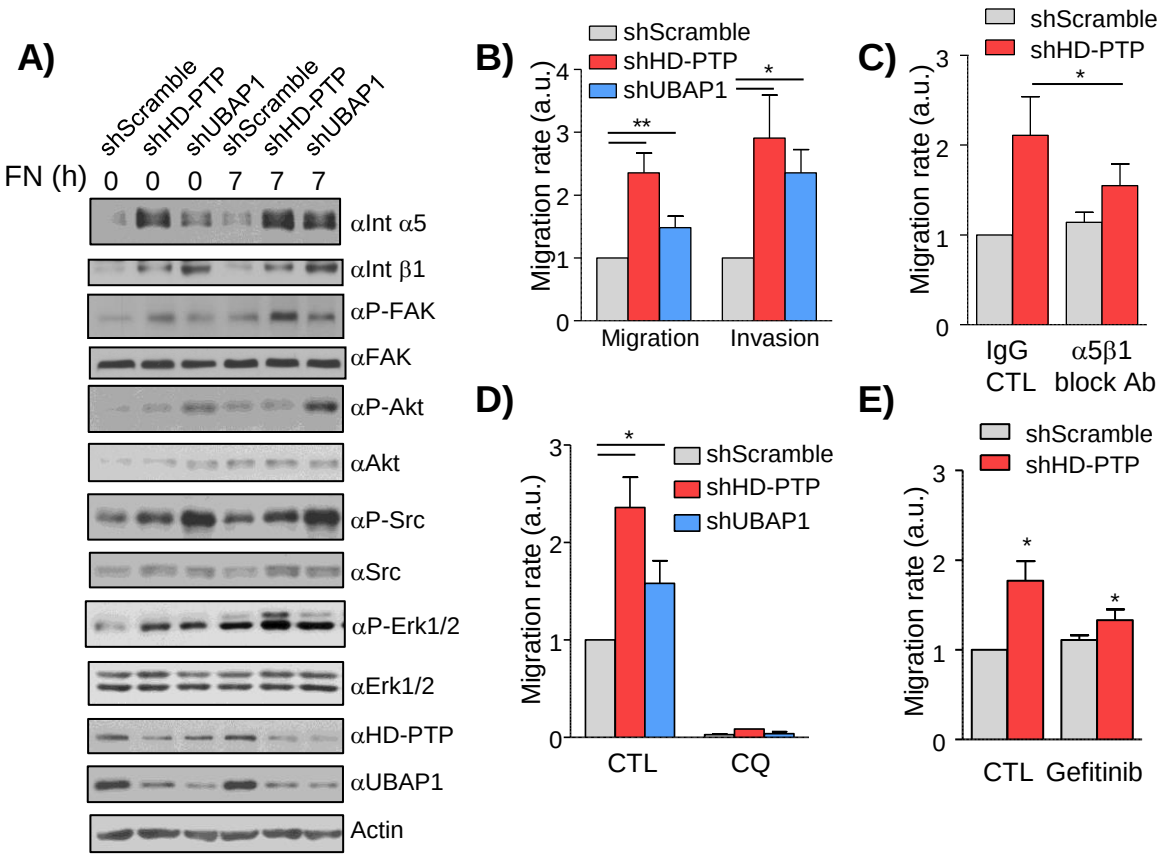
A)
shScramble
shHD-PTP
shUBAP1
shScramble
shHD-PTP
shUBAP1
FN (h) 0 0 0 7 7 7
αInt α5
αInt β1
αP-FAK
αFAK
αP-Akt
αAkt
αP-Src
αSrc
αP-Erk1/2
αErk1/2
αHD-PTP
αUBAP1
Actin
B)
shScramble
shHD-PTP
shUBAP1
Migration rate (a.u.)
Migration
Invasion
C)
shScramble
shHD-PTP
Migration rate (a.u.)
IgG CTL
α5β1 block Ab
D)
shScramble
shHD-PTP
shUBAP1
Migration rate (a.u.)
CTL
CQ
E)
shScramble
shHD-PTP
Migration rate (a.u.)
CTL
Gefitinib

Figure 2.7

2.9. Supplemental Figures:

Figure S2.1: RGD-peptides recapitulate the effect of FN on integrin α5β1 receptor stability, turnover and ubiquitination.

(A) Ubiquitination of the integrin β1 complex following FN (10μg/ml) treatment for the indicated time, measured as in Figure 2.1A, but the cs-IP was carried out using anti-β1 integrin Ab (clone TS2/16).

(B) RGD peptides (10μM) accelerate integrin internalization and its internalization can be prevented by α5β1 blocking Ab. α5b1 internalization was monitored by cs-ELISA as described in Figure 2.2A. Means ±SEM, n≥3; *p<0.05.

(C) RGD peptide (10μM) treatment accelerates the PM turnover of α5b1 integrin, which was counteracted by the α5b1 blocking Ab. Integrin α5b1 cell surface stability measurement was performed by cs-ELISA as in Figure 2.2F.

(D) The turnover of the α5b1 cellular pool. HeLa cells were serum starved, pretreated with cycloheximide for 2hrs (10μM) and chased in the presence (FN) or absence (NS) of FN (10μg/ml). At the indicated timepoints the remaining amount of integrin α5b1 expression was measured by SDS-PAGE and immunoblotting.

(E) RGD peptide (10μM) accelerates integrin α5b1 removal from the cell surface similar to FN stimulation. Integrin α5b1 cell surface elimination was determined by cs-IP as in Figure 2G.

(F) Integrin α5β1 complex is ubiquitinated following RGD (10μM) treatment. RGD-peptide induces a biphasic change in the ubiquitination of integrin α5b1 complex similar to the one observed upon FN stimulation as performed in Figure 2H.

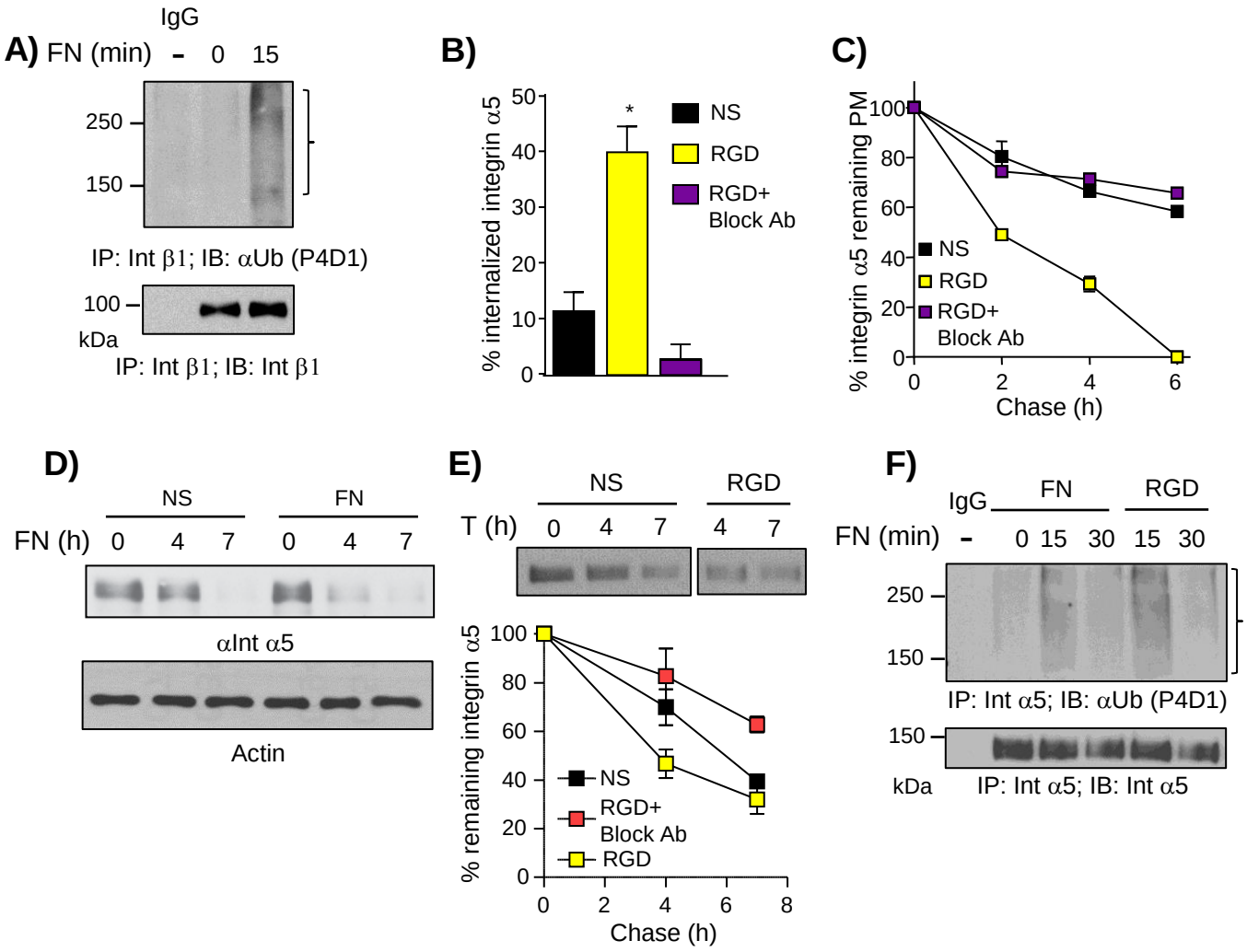
A)
IgG
FN (min) - 0 15
250
150
IP: Int β1; IB: αUb (P4D1)
100
kDa
IP: Int β1; IB: Int β1
B)
% internalized integrin α5
NS
RGD
RGD+ Block Ab
C)
% integrin α5 remaining PM
Chase (h)
D)
NS
FN
FN (h) 0 4 7 0 4 7
αInt α5
Actin
E)
NS
RGD
T (h) 0 4 7 4 7
% remaining integrin α5
Chase (h)
F)
IgG
FN
RGD
FN (min) - 0 15 30 15 30
IP: Int α5; IB: αUb (P4D1)
IP: Int α5; IB: Int α5

Figure S2.1

Figure S2.2: FRIA methodology and experimental controls.

(A) Schematic representation of the FRIA methodology. Receptors are labelled with primary and FITC-conjugated secondary Fab on ice. Upon transfer to 37°C, the receptor-Ab complexes are endocytosed and the FITC fluorescence is visualised by FRIA. The fluorescence excitation ratio value of FITC is determined by pH, allowing measurement of the luminal pH of receptor-Ab containing vesicles. The characteristic pH_v of the endo-lysosomal compartments are indicated.

(B) The pH distribution frequency of individual vesicles, containing integrin α5 after 2h or 7h FN chase from FRIA experiments as depicted in Figure 2.2E (condition: anti- α5 +FN). The mean pH_v of the integrin α5 vesicular population is indicated. After 2h chase integrin α5 is predominantly confined to early endosomes and endocytic vesicles (pH_v ~6-6.93), in contrast to the late-endosomal/lysosomal distribution after 7 h chase (pH_v ~4.54-5.38).

(C) pH-dependent Ab dissociation from the integrin α5-Ab or anti-α5 and secondary Ab complex (α5 +biotin-mouse Ab) at the indicated pH. Incubations with the indicated acidic buffer was done as in FN dissociation experiment (Figure 2.3E) and the remaining Ab was detected by cs-ELISA. Acidity similar to late endosomal/lysosomal pH conditions (pH 5.5) did not affect anti- α5 /secondary Abs complex integrity, suggesting that the complex was preserved in late-endosomal/lysosomal compartments during vesicular pH measurements by FRIA.

(D) Detection of the total fluorescence intensity of FITC during 4-7h chase using primary and FITC-conjugated secondary Fab labelled integrin α5 (right panel) and 4-32 min chase for FITC-Neutravidin biotin-FN (left panel). The acidification is not accounted by the degradation of the Abs, since the total amount of internalized FITC-conjugated Fab, inferred from the fluorescence intensities determined by dissipating the vesicular pH gradient with 4mM NH_4Cl, remained largely the same during the chase.

.

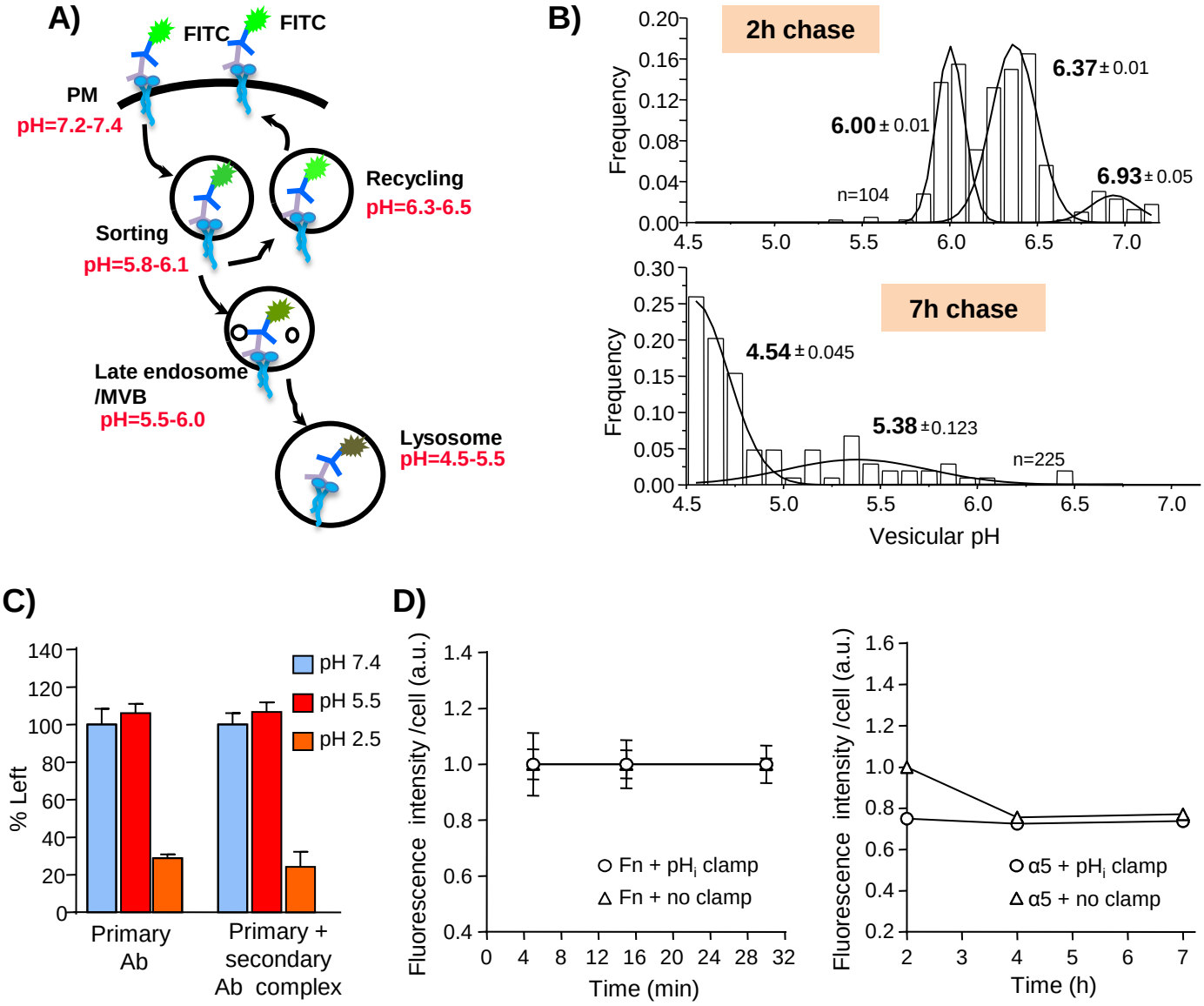
A)
FITC
FITC
PM
pH=7.2-7.4
Recycling
pH=6.3-6.5
Sorting
pH=5.8-6.1
Late endosome
/MVB
pH=5.5-6.0
Lysosome
pH=4.5-5.5
B)
2h chase
Frequency
6.37 ± 0.01
6.00 ± 0.01
6.93 ± 0.05
n=104
7h chase
4.54 ± 0.045
5.38 ±0.123
n=225
Vesicular pH
C)
% Left
pH 7.4
pH 5.5
pH 2.5
Primary
Ab
Primary +
secondary
Ab complex
D)
Fluorescence intensity /cell (a.u.)
Fn + pH$_i$ clamp
Fn + no clamp
Time (min)
α5 + pH$_i$ clamp
α5 + no clamp
Time (h)

Figure S2.2

Figure S2.3: pH-dependent binding of FN to integrinα5β1 receptor

(A) Saturation binding biotin-FN binding to HeLa cells. Biotin-FN binding to integrin receptors was determined using cs-ELISA in the absence (control) and presence of 100-fold excess label-free FN (+FN) as a function of biotin-FN concentration (0-10 μg/ml). Biotin-FN detection by cs-ELISA was carried out as described in experimental procedures for biotin-FN dissociation analysis.

(B) Biotin-FN dissociation kinetics from HeLa cells (as in Figure 2.3E) at pH 6.1. The majority of prebound biotin-FN dissociates within 10min of acidic washout. Means ±SEM, n≥3.

(C) Specific cell surface biotin-FN binding was plotted as the function of buffer proton concentration in cells pretreated with DMSO, Cilengitide, blocking Ab of αvβ3 and αvβ5. The calculated Hill coefficients for $[H^+]$ of FN dissociation cooperativity are indicated. The decreased binding cooperativity upon integrin αv inhibition suggests that α5β1 and αv integrins display allosteric FN binding cooperatively.

(D) Effect of acid washes on biotin-FN and Ab- α5β1 complexes integrity on cell surface. HeLa cells were pretreated with 0.3M sucrose and 25 μg/ml nystatin to inhibit integrin internalization and labelled with biotin-FN and α5-Ab on ice for 1h. Cells were washed with 37°C buffers of increasing acidity for 10min and the remaining biotin-FN and integrin α5β1 was visualised with FITC-streptavidin or Alexa 594 conjugated secondary Ab, respectively. Cell surface pH-buffer wash was done as described in supplemental experimental procedures. Bound FN and integrin α5 were visualized by a Zeiss Observer Z1 inverted fluorescence microscope. Acid wash effectively removes biotin-FN from cell surface, but does not dissociate the integrin-Ab complexes.

(E) $[Ca^{2+}]$ effect on the biotin-FN pH-dependent dissociation from the cell surface. Cell surface binding assay was performed as in Figure 2.3E at the indicated $[Ca^{2+}]$ concentration. Decreased $[Ca^{2+}]$ (10-100 μM mimicking endosomal $[Ca^{2+}]$) had no effect on FN pH-dependent dissociation at pH 6.0. Means ±SEM, n≥3.

(F) BLI sensorgrams of α5β1 headpiece fragment binding dynamics with fibronectin. Experiments were performed as in Figure 3F. The α5β1 headpiece fragment lost the pH-sensitive FN dissociation.

(G) Table summarizing the dissociation constants of FN from the full-length or headpiece of the integrin α5β1ectodomain, measured by BLI. Experiments are described in Figure 2.3F and S2.3F.

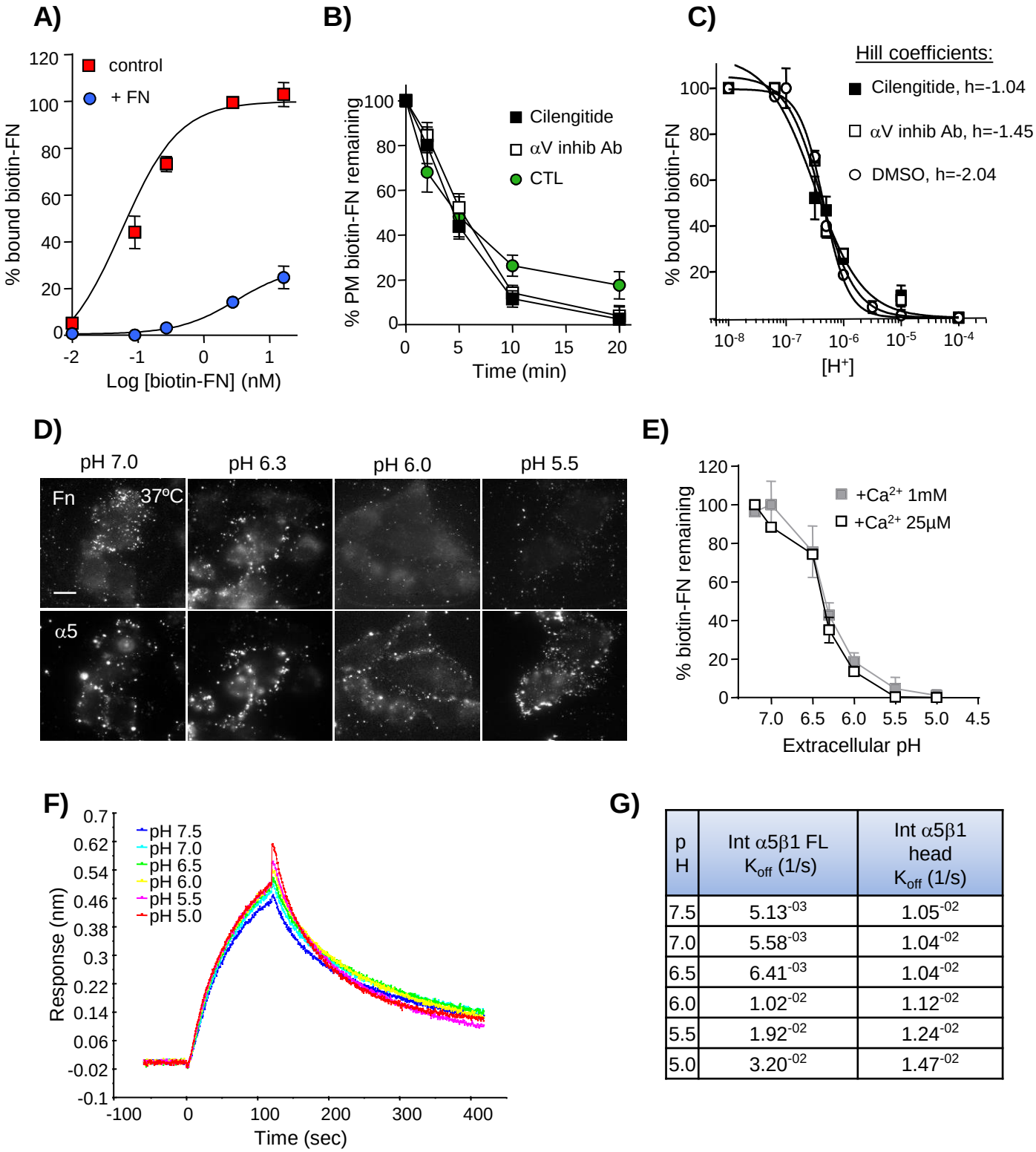

G)

pH	Int α5β1 FL K_{off} (1/s)	Int α5β1 head K_{off} (1/s)
7.5	5.13^{-03}	1.05^{-02}
7.0	5.58^{-03}	1.04^{-02}
6.5	6.41^{-03}	1.04^{-02}
6.0	1.02^{-02}	1.12^{-02}
5.5	1.92^{-02}	1.24^{-02}
5.0	3.20^{-02}	1.47^{-02}

Figure S2.3

Figure S2.4: Integrin α5β1 DUB siRNA screen and USP9x validation

(A) DUB siRNA targeted library screen was performed as described in Supplemental Materials. The steady state integrin α5 density and the remaining integrin α5 after 60min FN chase were measured by cs-ELISA. DUB candidates were considered at FN density lower than 3xM.S.D. of the non-target siRNA (siCTL) value. ESCRT siRNA (siTsg101, siHD-PTP) were included as positive controls.

(B) USP9x depletion does not affect integrin α5β1 internalization dynamics, determined by cs-ELISA after 5min FN stimulation at 37ºC as in Figure 2.2A. Means ±SEM, n=3.

(C) Effect of USP9x depletion on the cell surface density of control cargoes. The PM level of Transferrin receptor (Tf) and lysosomal cargo (CD4-Lamp1) was measured by cs-ELISA upon USP9x depletion. Means ±SEM, n≥3.

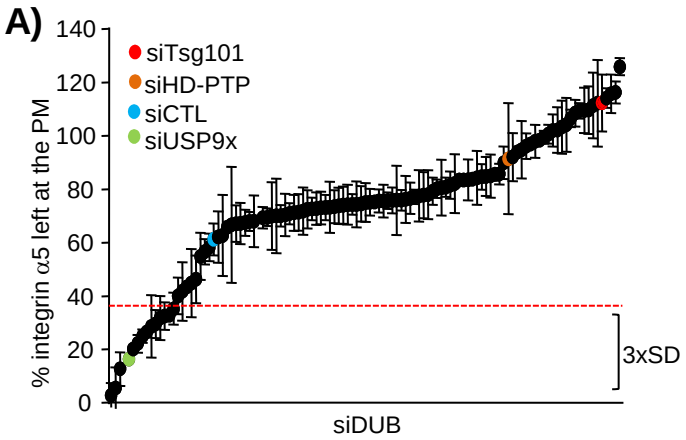
A)
siTsg101
siHD-PTP
siCTL
siUSP9x
% integrin α5 left at the PM
140
120
100
80
60
40
20
0
3xSD
siDUB

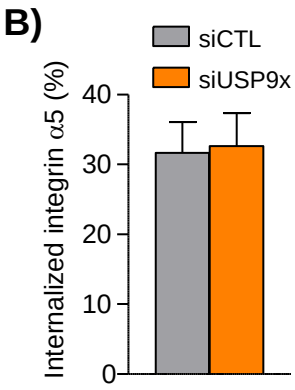
B)
siCTL
siUSP9x
Internalized integrin α5 (%)
40
30
20
10
0

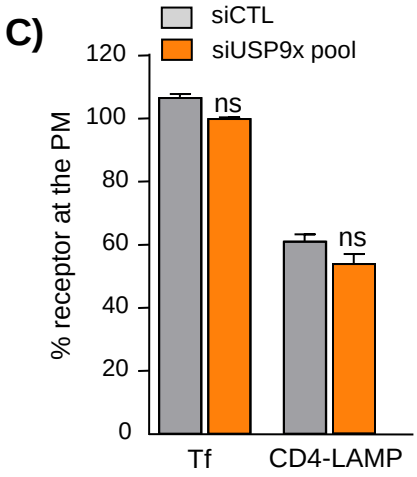
C)
siCTL
siUSP9x pool
% receptor at the PM
120
100
80
60
40
20
0
ns
ns
Tf
CD4-LAMP

Figure S2.4

Figure S2.5: Integrin and cargo trafficking in HD-PTP and UBAP1 depleted cells

(A) Depletion of HD-PTP or UBAP1 does not alter the transcript level of integrin α5. Integrin α5 mRNA levels were measured by qRT-PCR.

(B) pH_v distribution of integrin α5 containing vesicles at 7h chase timepoint measured by FRIA from Figure 2.5F (n=1024). The mean pH_v of the integrin α5 population is shown in bold. Depletion of HD-PTP or UBAP1 resulted in sorting/recycling endosomal distribution of integrin α5 (pH 6.2-6.4), while the control (shScramble) cells contained a significant fraction of integrins in the late endosomal/lysosomal compartments (pH ~5.4).

(C) HD-PTP depletion had only a mild effect on integrin internalization. Internalization rate of integrin α5β1 was measures by cs-ELISA as in Figure 2.2A in shHD-PTP or shUBAP1 cells. Means ±SEM, n≥3; *p<0.01.

(D) Targeting of transferrin to recycling endosomes, the lysosomal cargo Lamp1, and dextran to lysosomes was not affected by depletion of HD-PTP. FRIA analysis of the FITC-labeled respective cargo (transferrin, LAMP1 and the fluid-phase marker, dextran) sorting in cells depleted of HD-PTP or UBAP1.

(E) Acidification rate of cargo molecules (integrin α5β1, CD4t-Ub_n or CD4tCC-UbRΔG_4) containing compartments was measured by FRIA. HD-PTP depletion decreased the transfer rate of poly-ubiquitinated model cargo to acidic compartments. Means ±SEM, n≥3; ***p<0.001.

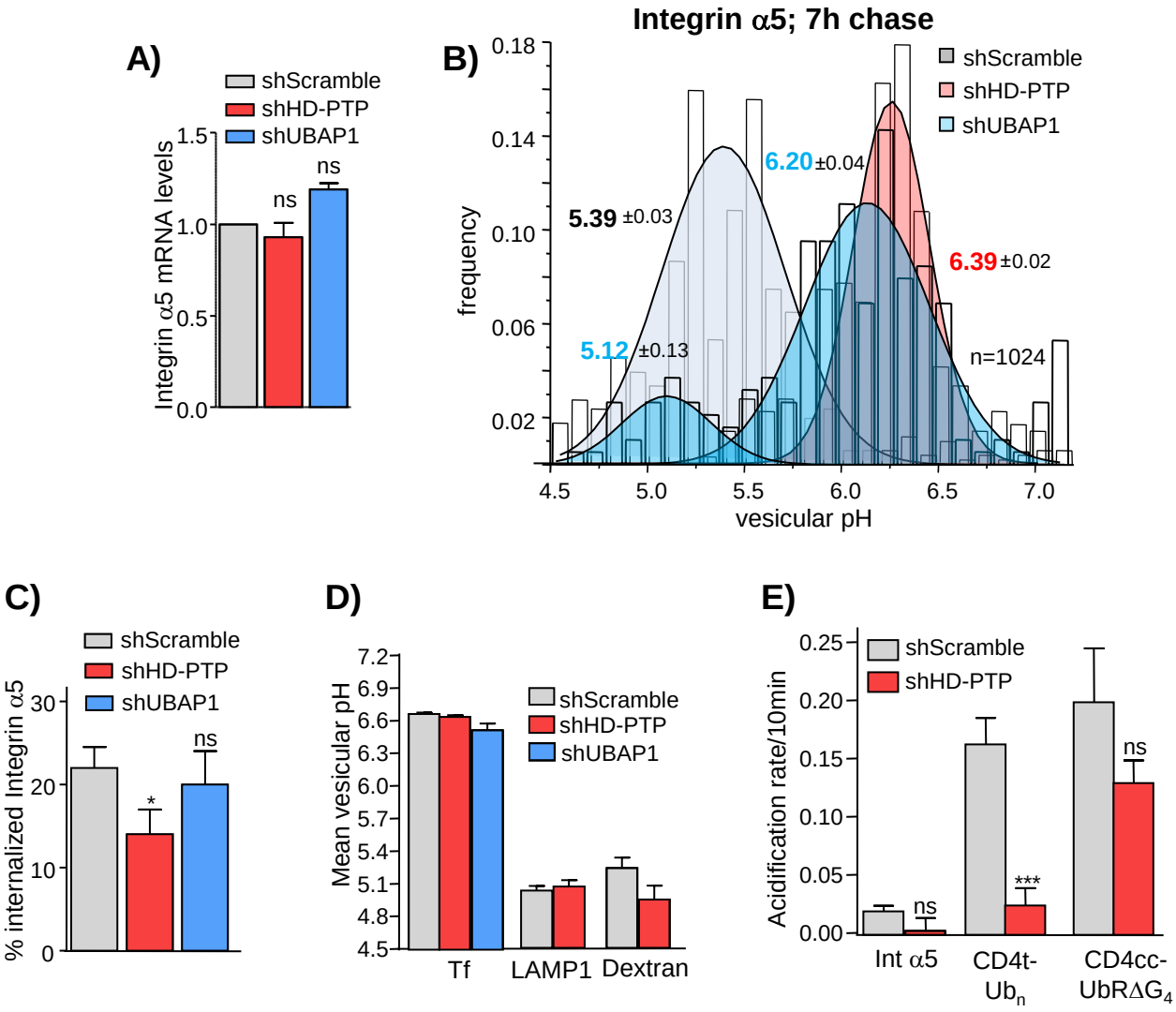
A)
shScramble
shHD-PTP
shUBAP1
Integrin α5 mRNA levels
1.5
1.0
0.5
0.0
ns
ns
B)
Integrin α5; 7h chase
shScramble
shHD-PTP
shUBAP1
frequency
0.18
0.14
0.10
0.06
0.02
5.39 ±0.03
6.20 ±0.04
6.39 ±0.02
5.12 ±0.13
n=1024
4.5
5.0
5.5
6.0
6.5
7.0
vesicular pH
C)
shScramble
shHD-PTP
shUBAP1
% internalized Integrin α5
30
20
10
0
*
ns
D)
shScramble
shHD-PTP
shUBAP1
Mean vesicular pH
7.2
6.9
6.6
6.3
6.0
5.7
5.4
5.1
4.8
4.5
Tf
LAMP1
Dextran
E)
shScramble
shHD-PTP
Acidification rate/10min
0.25
0.20
0.15
0.10
0.05
0.00
ns
***
ns
Int α5
CD4t-Ub$_n$
CD4cc-UbRΔG$_4$

Figure S2.5

Figure S2.6: Ubiquitin binding to HDPTP and UBAP1 and fractionation assay of ESCRT0-I.

(A) HD-PTP and UBAP1 interact with ESCRT-0/I components (Stam11, Hrs and TSG101). Endogenous co-IP was performed in HeLa cells using HD-PTP and UBAP1 antibodies.

(B) Recombinant GST-tagged linear mono- or poly-Ub constructs were purified and incubated with HeLa cell lysate for two hours. Protein complexes were pulled down by glutathione agarose beads, washed and analysed by immunoblotting for ESCRT components. The GST-Ub constructs, containing at least 2 Ub moieties, were able to pull-down components of ESCRT machinery, Stam1, Hrs, TSG101 and HD-PTP.

(C) Reduction in poly-Ub recognition by Hrs and Stam11 ESCRT components was observed upon depletion of HD-PTP and UBAP1. GST-4Ub pulldown was performed as in panel B. Quantification of the indicated ESCRT binding was quantified from immunoblots using ImageJ software (lower panel). The binding capacity was normalized for the respective protein expression in the lysate.

(D) Subcellular fractionation of ESCRT in HD-PTP depleted cell by size-exclusion chromatography. Cytosol was isolated by ultracentrifugation from HeLa cell lysates and fractionated on Superdex 200 column. The molecular mass average of each fraction is indicated. HD-PTP depletion results in destabilization of ESCRT-0/I machinery.

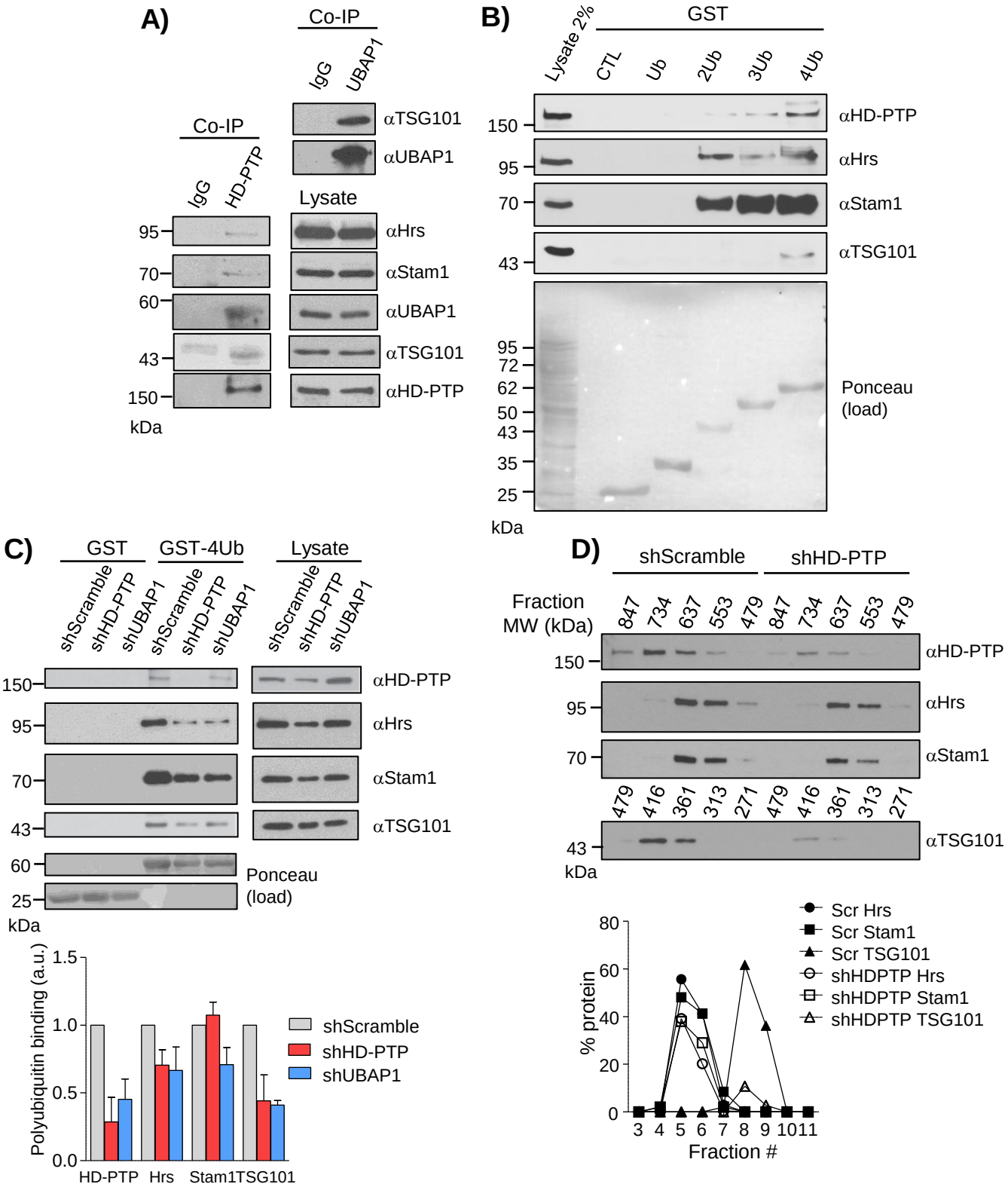
A)
Co-IP
IgG
UBAP1
αTSG101
αUBAP1
Co-IP
IgG
HD-PTP
Lysate
95
70
60
43
150
kDa
αHrs
αStam1
αUBAP1
αTSG101
αHD-PTP
B)
Lysate 2%
GST
CTL
Ub
2Ub
3Ub
4Ub
150
95
70
43
αHD-PTP
αHrs
αStam1
αTSG101
95
72
62
50
43
35
25
kDa
Ponceau
(load)
C)
GST
GST-4Ub
Lysate
shScramble
shHD-PTP
shUBAP1
150
95
70
43
60
25
kDa
αHD-PTP
αHrs
αStam1
αTSG101
Ponceau
(load)
Polyubiquitin binding (a.u.)
1.5
1.0
0.5
0.0
HD-PTP
Hrs
Stam1
TSG101
shScramble
shHD-PTP
shUBAP1
D)
shScramble
shHD-PTP
Fraction
MW (kDa)
847
734
637
553
479
150
95
70
43
kDa
αHD-PTP
αHrs
αStam1
αTSG101
479
416
361
313
271
% protein
80
60
40
20
0
3
4
5
6
7
8
9
10
11
Fraction #
Scr Hrs
Scr Stam1
Scr TSG101
shHDPTP Hrs
shHDPTP Stam1
shHDPTP TSG101

Figure S2.6

Figure S2.7: HD-PTP and UBAP1 regulation of cell migration and cell spreading.

(A) Quantification of phosphorylation of the indicated signalling molecules from Western blots in Figure 2.7A.

(B-D) Wound healing assay of HeLa cells, monitored by live-cell microscopy on FN as described in the Experimental procedures. Depletion of HD-PTP or UBAP1 increased the cellular migratory distance (B), velocity (C) and decreased the motion persistence (D) as quantified by single cell tracking using Metamorph software (30-40 cells were tracked in each experiment). Means ±SEM, n=3; *$p<0.05$.

(E) HeLa cells were subjected to xCELLigence invasion assay as described in Figure 7B on FN or Collagen I matrix. Cells depleted of HD-PTP preferentially invaded through FN matrix.

(F-G) Cells depleted of HD-PTP or UBAP1 are spreading faster than control cells. Cells were plated on FN or Collagen I coated plates and adhered for 15min. Unattached cells were washed off and spreading was monitored for 45min. Then cells were fixed, stained with Alexa-594 phalloidin, and visualised by fluorescence microscopy. The cell areas were quantified by ImageJ software and expressed in relative units (G). *$p<0.025$; n=120-160cells/condition.

(H) Western blot analysis of serum starved HD-PTP depleted cell lysates, following stimulation with EGF (10ng/ml) or FN (10µg/ml) for 7h in presence or absence of EGFR inhibition (Gefitinib, 2nM). EGFR signalling only partially enhanced integrin pro-migratory (pFAK, pSrc) and proliferative (pErk1/2) signalling upon HD-PTP depletion.

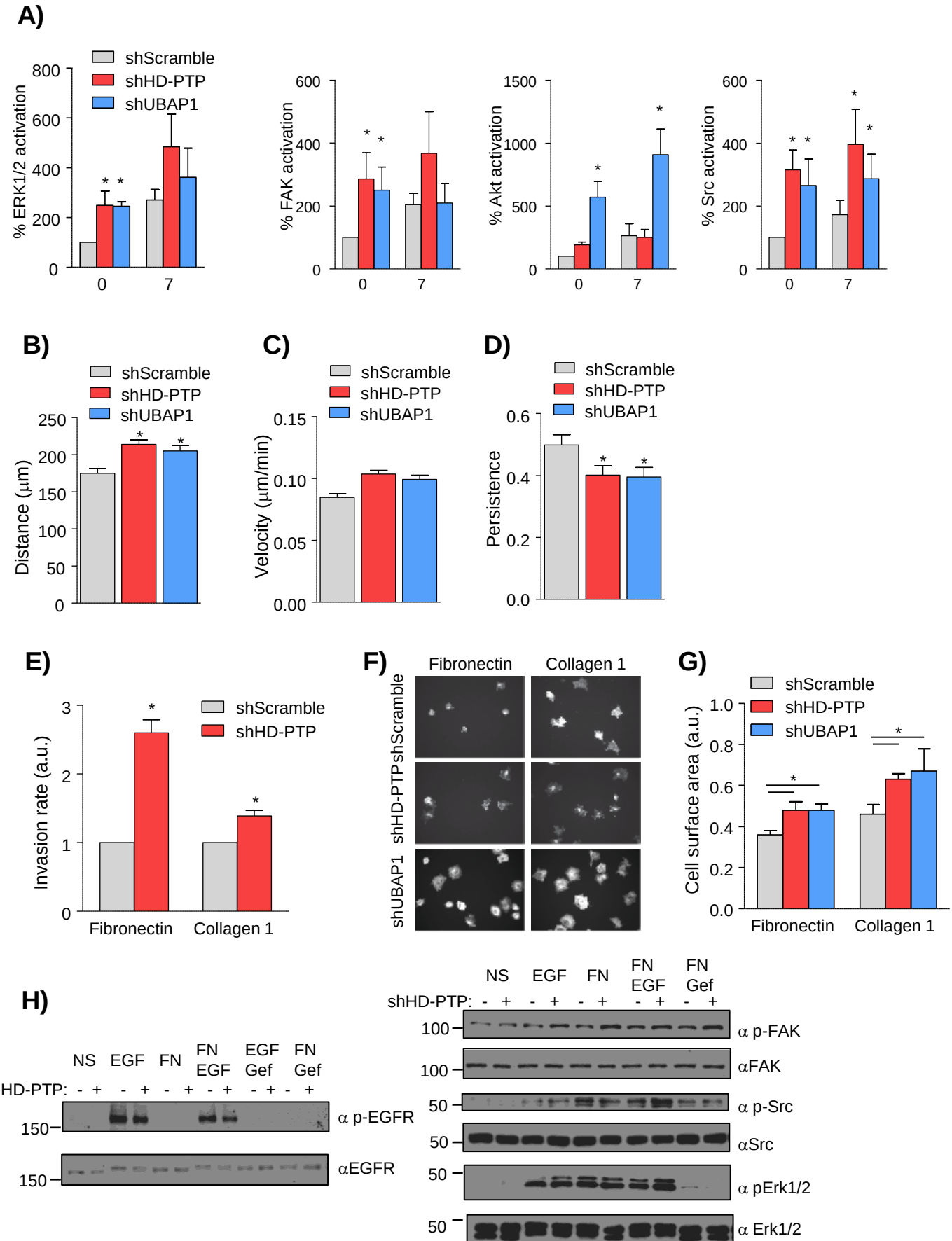
A)
shScramble
shHD-PTP
shUBAP1
% ERK1/2 activation
% FAK activation
% Akt activation
% Src activation
B)
Distance (µm)
C)
Velocity (µm/min)
D)
Persistence
E)
Invasion rate (a.u.)
Fibronectin
Collagen 1
F)
shScramble
shHD-PTP
shUBAP1
G)
Cell surface area (a.u.)
H)
NS
EGF
FN
FN EGF
EGF Gef
FN Gef
shHD-PTP:
α p-EGFR
αEGFR
α p-FAK
αFAK
α p-Src
αSrc
α pErk1/2
α Erk1/2

Figure S2.7

CHAPTER 3:

3. HD-PTP role in Downstream Signalling of Tumor Necrosis Factor Receptor 1

Dmitri Kharitidi*, Sanaz Manteghi*, Maya Poffenberger, Eric Ma and Arnim Pause

* equal author contribution

3.1 Preface

In the previous chapter we have outlined our findings in integrin receptor sorting through dynamic ubiquitination and the profound implication of these on integrin receptor turnover and downstream signalling. Here, we build on our expertise in endosomal sorting of receptors and cell signalling to study Tumor Necrosis Factor Receptor 1 (TNFR1), a cell surface receptor known to undergo polyubiquitination upon ligand engagement. NF-κB signalling downstream of TNFR1 is a key signalling pathway regulating inflammation and cell survival. Despite the extensive knowledge on NF-κB signalling regulation, little is known about the TNFR1 regulation by endocytic sorting. In the previous chapter, we outlined the role of the ESCRT component HD-PTP in the degradative sorting of cell surface receptors. Here, we demonstrate the inhibitory role of HD-PTP in NF-κB signalling downstream of TNFR1. Therefore, the endocytic sorting contributes to signalling termination of the activated TNFR1, an event that is crucial during inflammatory response and tumorigenesis.

3.2. Abstract

Tumor Necrosis Factor alpha is a key activator of NF-κB pathway downstream of Tumor Necrosis Factor Receptor 1 (TNFR1), leading to the pro-inflammatory, pro-survival signalling, as well as to the apoptosis induction. TNFR1 induces NF-κB signalling at the cell surface, while the pro-apoptotic signalling occurs after receptor endocytosis, demonstrating a spatiotemporal regulation of TNFR1 activity. However, the events regulating endocytosis and sorting of TNFR1 are largely unknown. Here, we provide evidence that the ESCRT component HD-PTP plays a key function in the regulation of TNFR1-driven canonical NF-κB signalling. Upon HD-PTP depletion, TNFα treatment accelerates NF-κB disinhibition and nuclear translocation, leading to a potentiated target gene transcription. These effects are due to an elevated presence of TNFR1 at the cell surface in the context of HD-PTP depletion, leading to the increased TNFR1 signalling complex scaffolding. Altogether, these effects are likely due to the function of HD-PTP in the ESCRT pathway, suggesting a regulatory role by endocytic sorting in TNFR1 signalling.

3.3. Introduction:

Tumor Necrosis Factor signalling is largely responsible for the regulation of pro-inflammatory response, cell survival, proliferation, as well as apoptosis (reviewed in (Israel, 2010; Napetschnig and Wu, 2013; Ofengeim and Yuan, 2013)). Typically, TNFα engagement with its receptor, TNFR1, leads to the activation of the canonical NF-κB pathway and its downstream transcription program (Hsu et al., 1996a; Hsu et al., 1995). The canonical NF-κB pathway is executed by the p65/p50 transcription factor heterodimer (Oeckinghaus et al., 2011), which is rapidly activated following TNFα stimulation and is responsible for the transcription of target genes driving the execution of the aforementioned cellular processes. Due to its primordial importance, the canonical NF-κB pathway is under tight regulation in resting cells by inhibitory action of IκB, which associates with and retains the p65/p50 transcription factor in the cytosol (Pahl, 1999).

TNFα is a well-known inducer of canonical NF-κB signalling via its activation of TNFR1 and TNFR2 (MacEwan, 2002). Upon TNFα binding to the receptor, the latter undergoes trimerization, recruiting the adaptor protein TRADD via receptors death domains (DD) located within its cytoplasmic domain (Hsu et al., 1996a; Hsu et al., 1996b; Hsu et al., 1995). Following TRADD binding, the receptor complex recruits additional factors such as TRAF2, RIP1 and cIAP1/2 (Hsu et al., 1996a; Liu et al., 1996). Altogether, these proteins constitute the "TNFR1 Signalling Complex I" (TNFR1-SCI) a signalling entity responsible for the initiation of pro-inflammatory and pro-survival NF-κB signalling (Micheau and Tschopp, 2003). The polyubiquitination of RIP1 by TRAF2 and cIAP1/2 represents a key scaffolding step for recruitment and phosphorylation of TAK1 kinase and IKKα/β complex (Ea et al., 2006; Li et al., 2006; Yin et al., 2009). IKKα/β, once activated by TAK1-mediated phosphorylation, phosphorylates the Inhibitor of κB (IκB) (Wang et al., 2001). The phosphorylated form of IκB is rapidly polyubiquitinated and is targeted to the proteasomal degradation (Hoffmann et al., 2002), releasing the p65/p50 NF-κB transcription factor from inhibition, leading to its nuclear translocation and target gene transcription (Blackwell et al., 2013).

Following activation of NF-κB signalling, TNFR1 complex undergoes internalization and a shift in signalling scaffold occurs (Schutze et al., 2008). The receptor maintains its association with TRADD, yet the NF-κB signalling activators TRAF2 and RIP1 are disengaged (Micheau et al., 2001). Instead, TRADD recruits the pro-apoptotic factors FADD and Caspase-8, leading to

activation of the pro-apoptotic signalling via the caspase cascade (Micheau and Tschopp, 2003). The formation of this pro-apoptotic TNFR1 complex is termed "TNFR1 Signalling Complex II" (TNFR1-SCII), and it occurs in the endosomal compartment (Schutze et al., 2008). Moreover, the spatiotemporal control of TNFR1 endocytosis and signalling is regulated by the ubiquitination of the receptor (Fritsch et al., 2014). Upon TNFα binding, TNFR1 was reported to undergo K63-polyubiquitination by RNF8 E3-ubiquitin ligase leading to TNFR1 clathrin-dependent internalization (Fritsch et al., 2014). Once localised to endosomes, the ubiquitinated form of the receptor is capable of recruiting the pro-apoptotic complex containing FADD and caspase-8. Thus ubiquitination event is a determinant event of TNF receptor signalling compartmentalization, where the non-ubiquitinated receptor signals from cell surface through NF-κB signaling axis, whereas the K63-ubiquitinated receptors are internalized and promote apoptosis induction via caspase signalling from endosomes (Schutze and Schneider-Brachert, 2009; Schutze et al., 2008).

The regulation of NF-κB response occurs at multiple levels, including feedback mechanisms, crosstalk with other signalling pathways and signalling complexes composition. However, the regulation of TNFR1 downstream signalling by the endocytic machinery is poorly understood. Previous report suggests that NF-κB signalling may be under control of Endosomal Sorting Complex Required for Transport (ESCRT) machinery, since cellular depletion of the ESCRT-0/I components led to a transcriptional upregulation of several NF-κB target genes (Brankatschk et al., 2012). The ESCRT machinery is responsible for the degradative sorting of K63-polyubiquitinated receptors to lysosomes (Katzmann et al., 2001; Lauwers et al., 2009; Piper et al., 2014). During this process, the polyubiquitinated receptors are recognized by the ubiquitin binding domains of the ESCRT components and are sequestered within the Multivesicular Bodies (MVBs), leading to signalling termination and eventual degradation of receptors upon lysosomal fusion with MVBs (Teis et al., 2008; Wollert and Hurley, 2010). In the absence of ESCRTs, the polyubiquitinated receptors cannot be packaged inside MVBs and do not undergo degradation, often leading to receptor persistent signalling from endosomes and/or increased resensitization of receptors due to cell surface return (recycling) (Rodahl et al., 2009; Wegner et al., 2011). Therefore, it is likely that the ESCRT pathway regulates TNFR1 endocytic sorting and the tight balance of its pro-survival and pro-apoptotic signalling.

One of the components of the ESCRT machinery is an endosomal pseudophosphatase HD-PTP (Histidine Domain containing Protein Tyrosine Phosphatase) (Ali et al., 2013; Ichioka et al., 2007). HD-PTP has been described as a key player in ESCRT function of ubiquitinated cargo degradation (Doyotte et al., 2008), MVB morphogenesis and signalling of several cell surface receptors (Doyotte et al., 2008), including EGFR and Toll-like receptor in *Drosophila* (Huang et al., 2010; Miura et al., 2008). HD-PTP bears an ability of K63-polyubiquitin recognition, and its depletion results in the ubiquitinated cargo retention/accumulation in the early and recycling endosomes, increasing the receptors' degradation half-life ((Ali et al., 2013; Doyotte et al., 2008; Pashkova et al., 2013) and Chapter 2).

Here, we demonstrate a key negative role of HD-PTP in regulation of TNFR1 NF-κB signalling. HD-PTP plays an inhibitory function in TNFα induction of NF-κB pathway, illustrated by the accelerated IκB degradation, p65 nuclear translocation and target gene transcription upon HD-PTP depletion. These events are due to increased cell surface presence of TNFR1, resulting in the increased scaffold of TNFR1 Complex I and its downstream signalling. Furthermore, increased TNFα induced apoptosis was observed upon HD-PTP depletion. Altogether, these results suggest that the HD-PTP function in ubiquitinated receptor sorting translates into a dual effect on TNFα signalling, spatiotemporally affecting TNFα-dependent NF-κB and apoptotic pathways.

3.4. Results

3.4.1. HD-PTP inhibits canonical Nf-κB pathway activation

Previously, the negative function of the ESCRT components in NF-κB signalling was suggested in a nanostring gene expression screen (Brankatschk et al., 2012). However, the exact regulatory mechanism of this signalling pathway by the ESCRT machinery remains unsolved. We have used HD-PTP as a model ESCRT component to investigate the potential role of degradative endosomal machinery in NF-κB pathway activation. For this purpose, we employed several cellular systems, such as HD-PTP-deficient mouse embryonic fibroblasts (MEFs), as well as NIH3T3 and HeLa cells depleted of HD-PTP by stable shRNA expression (Figure 3.1A).

Canonical NF-κB pathway activation is exemplified by an accelerated degradation of IκBα following TNFα treatment (Israel, 2010). To test whether HD-PTP affects IκBα degradation, cells deficient of HD-PTP were stimulated with TNFα (10ng/ml) for periods up to 30min. In the context of HD-PTP deficiency, IkBα degradation occurred significantly more rapidly, indicating that HD-PTP plays an inhibitory role in NF-κB signalling activation (Figure 3.1B). TNFα-induced activation of NF-κB cross-talk is known to activate several other signalling pathways, including MAPK cascade (Oeckinghaus et al., 2011). However, in the context of HD-PTP depletion, acute TNFα treatment did not upregulate activation of MAPK pathway more than in control cells, illustrated by similar levels of Erk1/2 phosphorylation in control and HD-PTP-deficient cells (Figure 3.1C).

To further investigate the downstream effect of the accelerated IκBα degradation in HD-PTP depleted cells, we probed for the extent of p65 transcription factor nuclear translocation following TNFα treatment. Indeed, after TNFα stimulation, p65 nuclear localization was increased approximatively two-fold in HD-PTP depleted cells as demonstrated by immunofluorescence experiments and subcellular fractionations (Figure 3.1D and 3.1E). Altogether, these results suggest that HD-PTP plays a negative role in the canonical NF-κB pathway activation.

Figure 3.1: HD-PTP inhibits canonical NF-κB signalling.

(A) HD-PTP protein levels were measured in WT and heterozygous MEFs, and stable shHD-PTP RNA expressing NIH3T3 and HeLa cells. HD-PTP was efficiently depleted at the levels indicated.

(B) TNFα response in HD-PTP depleted cells. MEFs, NIH3T3 and HeLa cells were treated with TNFα (10ng/ml) and the levels of IκBα were measured by western blot at indicated timepoints. HD-PTP deficiency results in accelerated degradation of IκBα.

(C) HD-PTP deficient cells were serum deprived and then stimulated with TNFα (10ng/ml) for indicated timepoints. The activation of ERK1/2 was analysed by western blot, indicative that HD-PTP deficiency leads to potentiated ERK1/2 activity downstream of TNFα.

(D) The extent of p65 nuclear translocation was assessed by immunofluorescence in HeLa cells. Control and HD-PTP depleted cells were treated for 10min with TNFα (10ng/ml), fixed and stained with anti-p65 antibody and DAPI. The images were acquired by confical microscopy and the extent of p65 nuclear translocation was quantified using Metamorph software. Quantification in lower panel. Means ±SEM, $n \geq 3$; *$p < 0.05$.

(E) Cellular fractionation was done to analyse p65 nuclear translocation. Control and shHD-PTP cells were stimulated with TNFα (10ng/ml), lysed in fractionation buffer, the nuclear fraction was isolated by sequential centrifugation and the extent of p65 nuclear translocation was analysed by SDS-PAGE and immunoblot. ImageJ quantification in lower panels. Means ±SEM, $n=3$; *$p < 0.05$

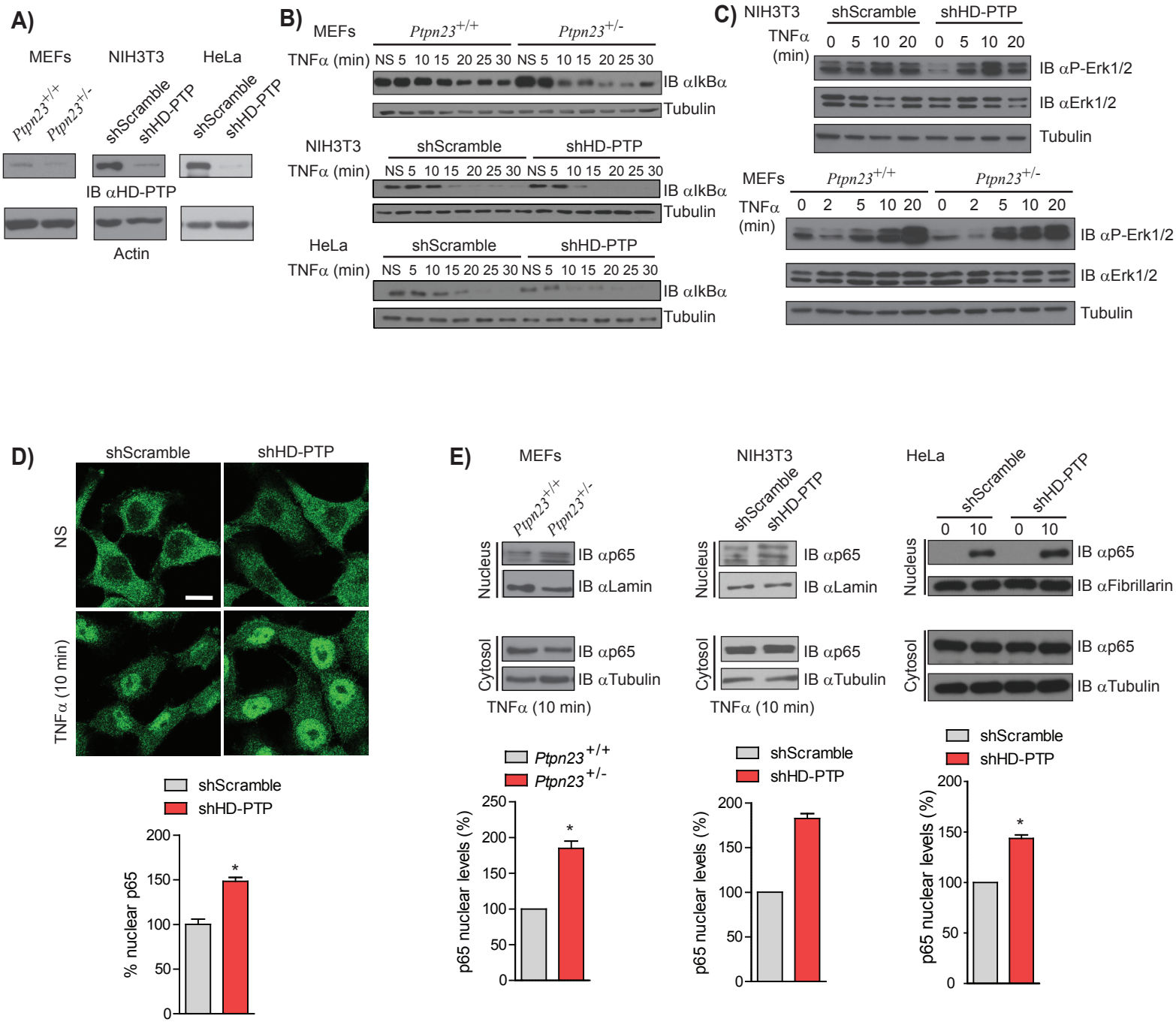
A)
MEFs
NIH3T3
HeLa
Ptpn23+/+
Ptpn23+/-
shScramble
shHD-PTP
shScramble
shHD-PTP
IB αHD-PTP
Actin
B)
MEFs
Ptpn23+/+
Ptpn23+/-
TNFα (min) NS 5 10 15 20 25 30 NS 5 10 15 20 25 30
IB αIkBα
Tubulin
NIH3T3
shScramble
shHD-PTP
TNFα (min) NS 5 10 15 20 25 30 NS 5 10 15 20 25 30
IB αIkBα
Tubulin
HeLa
shScramble
shHD-PTP
TNFα (min) NS 5 10 15 20 25 30 NS 5 10 15 20 25 30
IB αIkBα
Tubulin
C)
NIH3T3
shScramble
shHD-PTP
TNFα (min) 0 5 10 20 0 5 10 20
IB αP-Erk1/2
IB αErk1/2
Tubulin
MEFs
Ptpn23+/+
Ptpn23+/-
TNFα (min) 0 2 5 10 20 0 2 5 10 20
IB αP-Erk1/2
IB αErk1/2
Tubulin
D)
shScramble
shHD-PTP
NS
TNFα (10 min)
shScramble
shHD-PTP
% nuclear p65
200
150
100
50
0
*
E)
MEFs
Ptpn23+/+
Ptpn23+/-
Nucleus
IB αp65
IB αLamin
Cytosol
IB αp65
IB αTubulin
TNFα (10 min)
NIH3T3
shScramble
shHD-PTP
Nucleus
IB αp65
IB αLamin
Cytosol
IB αp65
IB αTubulin
TNFα (10 min)
HeLa
shScramble
shHD-PTP
0 10 0 10
Nucleus
IB αp65
IB αFibrillarin
Cytosol
IB αp65
IB αTubulin
Ptpn23+/+
Ptpn23+/-
p65 nuclear levels (%)
250
200
150
100
50
0
*
shScramble
shHD-PTP
p65 nuclear levels (%)
200
150
100
50
0
shScramble
shHD-PTP
p65 nuclear levels (%)
200
150
100
50
0
*

Figure 3.1

3.4.2. HD-PTP inhibits transcriptional activity of NF-κB transcription factor and transcription of NF-κB target genes

The end goal of the canonical NF-κB pathway activation is p65 nuclear translocation and induction of NF-κB target gene expression (Pahl, 1999). To test whether the increased p65 nuclear translocation in the context of HD-PTP depletion leads to a potentiated NF-κB transcriptional activity, we have performed luciferase assays using NF-κB response promoter dual-luciferase assay. Indeed, upon TNFα treatment, NF-κB promoter activity was upregulated two-fold in MEFs and NIH3T3 cells deficient of HD-PTP expression (Figure 3.2A).

To further confirm the inhibitory effect of HD-PTP in NF-κB signalling, we have examined the extent of transcription of NF-κB target genes in the context of HD-PTP depletion by qPCR. Indeed, following TNFα stimulation, the transcription of mRNA of several NF-κB target genes (IL6, I-κB, COX2 and c-FLIP) was upregulated to various extent in HD-PTP deficient cell lines (Figure 3.2B-D). These results are consistent with the accelerated p65 nuclear translocation and NF-κB promoter activation in HD-PTP deficient context, suggesting that HD-PTP plays a negative regulatory role in NF-κB pathway activation by TNFα.

3.4.3. HD-PTP regulates cytokine production and secretion

Our results and previous reports strongly indicate that HD-PTP and related ESCRT components negatively regulate NF-κB transcription program and cytokine/chemokine transcription (Ofengeim and Yuan, 2013). To determine if the effect of HD-PTP downregulation translates into an upregulation of the chemokine production and secretion, the expression of IL6 and TNFα was determined in conditioned media after 24 hours TNFα stimulation by ELISA. As expected, cells depleted of HD-PTP secrete up to 10-fold more IL6 and a display a higher secretion trend of TNFα, although not statistically significant (Figure 3.2F, G and H). Moreover, a high-throughput analysis of the cytokine secretion upon TNFα stimulation in control and HD-PTP depleted cells revealed an upregulation of secretion of several cytokines, other than IL6 and TNFα (Figure S3.1) Collectively, these results indicate that HD-PTP plays an inhibitory role in TNFα-induced canonical NF-κB signalling, target gene expression and chemokine secretion.

Figure 3.2: HD-PTP inhibits NF-κB target gene transcription and cytokine secretion.

(A) NF-κB promoter activity was determined by luciferase assays. Control and HD-PTP depleted cells were transfected with vector bearing luciferase gene under the control of NF-κB promoter, treated for 8h with TNFα (10ng/ml), and the luciferase bioluminescence was measured. The NF-κB promoter activity was increased twofold in the context of HD-PTP deficiency. Means ±SEM, n=3; *p<0.05.

(B-D) NF-κB target gene expression. The expression of NF-κB target genes was determined by qPCR after TNFα (10ng/ml) stimulation for indicated timepoints in MEFs (B), NIH3T3 (C) and HeLa cells (D). Means ±SEM, n=3; *p<0.05.

(E) Relative IL6 mRNA levels quantified by qRT-PCR in *Ptpn23*$^{+/+}$ and *Ptpn23*$^{+/-}$ MEFs. Cells were treated or not with BAY 11-7082 (10μM) for 3hrs before treatment with TNF (10 ng/ml) for 1hrs. Representative data is shown from three independent experiments, Means±SEM; *p<0.05.

(F-H) Cytokine secretion was analysed by ELISA. Control and HD-PTP deficient cells were treated with TNFα (10ng/ml) for 24hrs, and the conditioned media was collected and probed for cytokine levels by ELISA. Means ±SEM, n=3; *p<0.05.

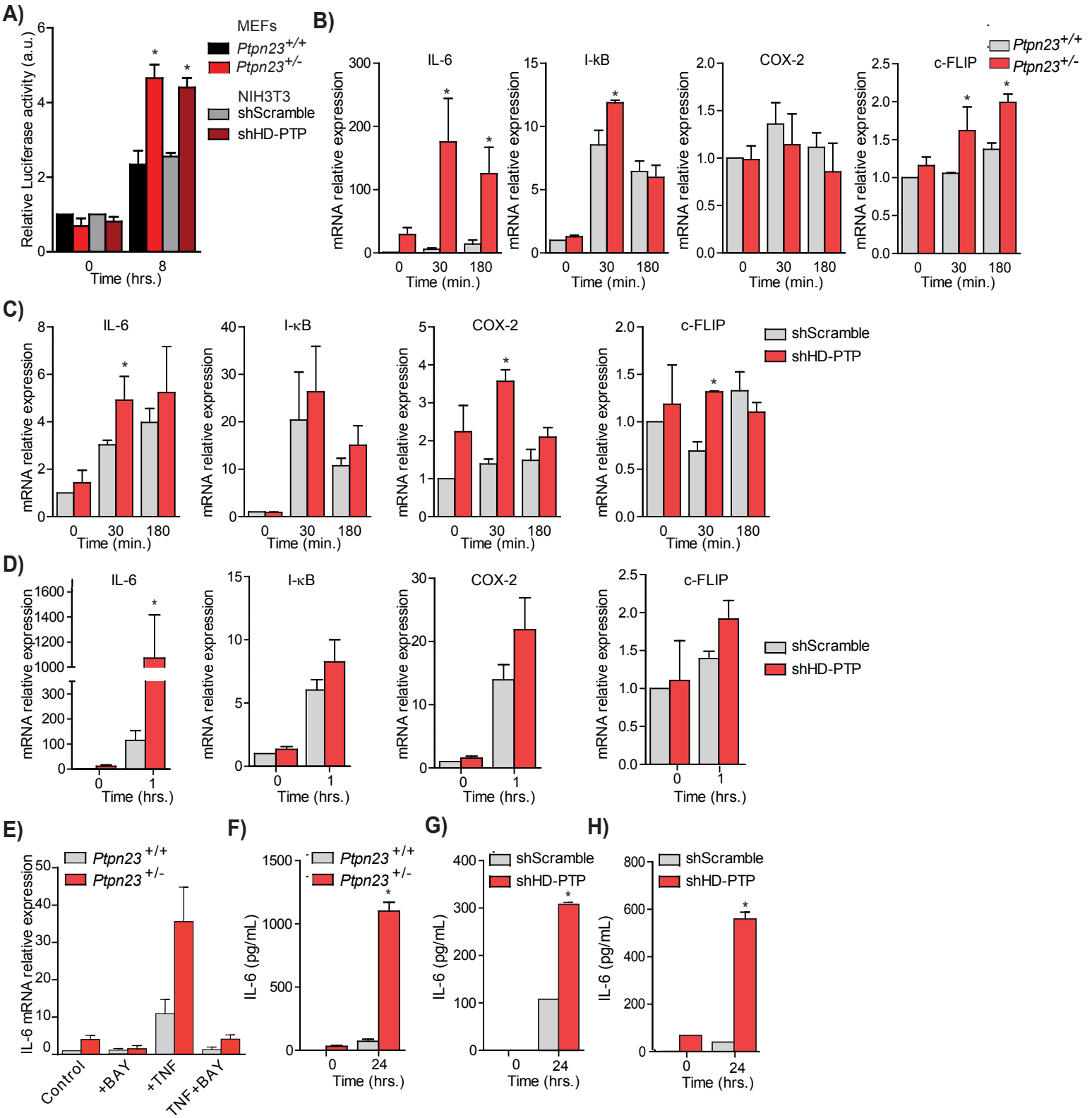
A)
Relative Luciferase activity (a.u.)
MEFs
Ptpn23+/+
Ptpn23+/-
NIH3T3
shScramble
shHD-PTP
Time (hrs.)
B)
IL-6
I-kB
COX-2
c-FLIP
mRNA relative expression
Time (min.)
C)
I-κB
shScramble
shHD-PTP
D)
Time (hrs.)
E)
IL-6 mRNA relative expression
Control
+BAY
+TNF
TNF+BAY
F)
IL-6 (pg/mL)
G)
H)

Figure 3.2

3.4.4. HD-PTP specifically regulates TNFR1-mediated signalling

TNFα is known to be capable of engaging and inducing activation of both TNRF1 and TNFR2. In order to discriminate the TNF receptor responsible for potentiated NF-κB signalling in HD-PTP depleted cells, human TNFα was used as a stimulus on NIH3T3 cells, since only the mTNFR1, and not the mTNFR2, is responsive to hTNFα in mouse cells. Upon NIH3T3 cells treatment with hTNFα, a profile of enhanced TNFR1 signalling was observed, such as accelerated IkBα degradation, as well as increased and rapid IKKα/β phosphorylation (Figure 3.3A). These observations confirm that TNFR1 is responsible for accelerated NF-κB signalling in HD-PTP depleted cells and the signalling potentiation occurs early in the NF-κB signalling cascade, likely at the level of the TNFR1 signalling complex scaffolding.

HD-PTP has been described as a component of ESCRT machinery responsible for the cell surface receptors sorting towards degradation. For instance, HD-PTP plays a key role in plasma membrane and total receptor stability of EGFR, integrin receptors and Toll-like receptor in Drosophila ((Ali et al., 2013; Doyotte et al., 2008; Miura et al., 2008) and Chapter 2). The critical function of HD-PTP in receptor degradation suggests that TNFR1 levels may be affected by depletion of HD-PTP. Therefore, we measured the cell surface levels of TNRF1 by FACS and cs-ELISA in cells deficient of HD-PTP. Indeed, TNFR1 plasma membrane levels were upregulated by ~20% in cells deficient of HD-PTP (Figure 3.3B), suggesting that HD-PTP may regulate its cell surface turnover via endocytic function. The increased cell surface presence and resensitization of TNRF1 might be responsible for the potentiated signalling induced by TNFα stimulation.

Figure 3.3: Potentiated NF-κB signalling in HD-PTP deficiency context is due to increased cell surface TNFR1 levels.

(A) Control and HD-PTP depleted NIH3T3 cells were treated with human TNFα (10ng/ml) for indicated timepoints. The TNFR1 downstream signalling was analysed by western blot. The accelerated IKKα/β phosphorylation and IκBα degradation indicate that the signalling occurs indeed downstream of TNFR1.

(B) FACS analysis of cell surface TNFR1 levels in MEFs and NIH 3T3 cells. Deficiency in HD-PTP leads to increase in TNFR1 levels at plasma membrane. Means ±SEM, n=3; *p<0.05.

(C) Cell surface TNFR1 in HeLa cells. Flag-TNF was used to detect the levels of TNFR1 at plasma membrane of HeLa cells. Means ±SEM, n=3; *p<0.05.

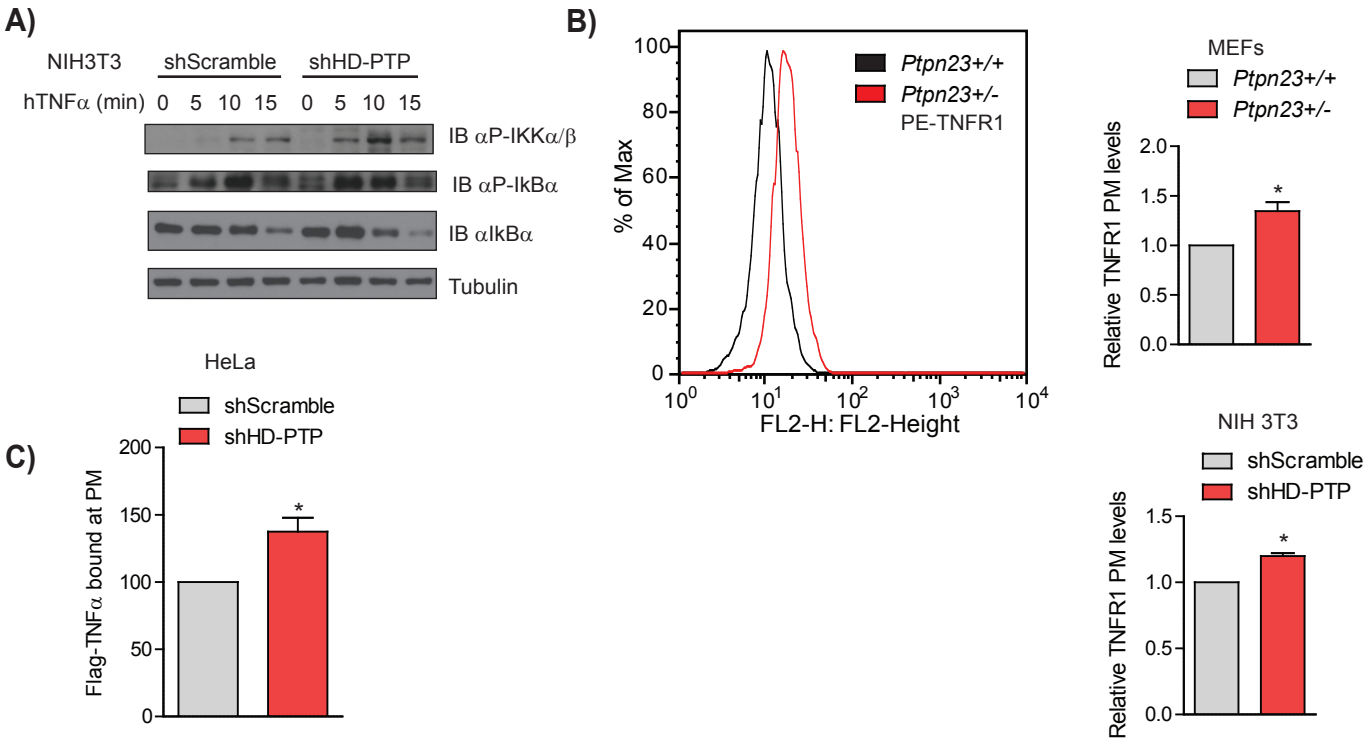
A)
NIH3T3
shScramble
shHD-PTP
hTNFα (min) 0 5 10 15 0 5 10 15
IB αP-IKKα/β
IB αP-IkBα
IB αIkBα
Tubulin
B)
Ptpn23+/+
Ptpn23+/-
PE-TNFR1
% of Max
FL2-H: FL2-Height
MEFs
Ptpn23+/+
Ptpn23+/-
Relative TNFR1 PM levels
C)
HeLa
shScramble
shHD-PTP
Flag-TNFα bound at PM
NIH 3T3
shScramble
shHD-PTP
Relative TNFR1 PM levels

Figure 3.3

3.4.5. TNFR1 signalling complex scaffolding is increased in absence of HD-PTP

Increased TNFR1 cell surface levels in cells deficient of HD-PTP suggest that there could be a larger number of TNFR1 signalling complexes forming upon TNFα treatment. To evaluate the scaffolding rate and the abundance of TNFR1-SCI, cells were treated with a recombinant Flag-tagged human TNFα and the resulting molecular complexes were immunoprecipitated and their contents were analysed by western blotting (as described in (Ramakrishnan and Baltimore, 2011)). Importantly, in cells depleted of HD-PTP, TNFR1 complexes contained 2-fold higher levels of key NF-κB signalling players, such as TRAF2, TRADD and RIP1 (Figure 3.4A and B). Importantly, the RIP1 ubiquitination, a key event leading to the NF-κB signalling activation, was also potentiated in HD-PTP depleted cells (Figure 3.4B). The exacerbated presence of signalling scaffold likely is responsible for the accelerated NF-κB downstream signalling in HD-PTP deficient cells and represents the first event in the cascade of downstream signal amplification.

Figure 3.4: TNFR1 signalling complex scaffolding is increased in absence of HD-PTP.

(A-B) TNFR1-SCI scaffold assembly. Control and shHD-PTP cells MEFs (A) and HeLa cells (B) were treated with Flag-tagged recombinant hTNFα (1ug/ml). At indicated timepoints cells were collected, lysed and Flag-hTNFα containing complexes were immunoprecipitated with anti-Flag antibody as described (Ramakrishnan and Baltimore, 2011). The TNFR1 complexes were resolved by SDS-PAGE and probed for TNFR1-SCI scaffold signalling constituents by western blot. Relative TNFR1 complexes scaffolding components levels were quantified by ImageJ software (lower panel). Means ±SEM, n=3; *$p<0.05$

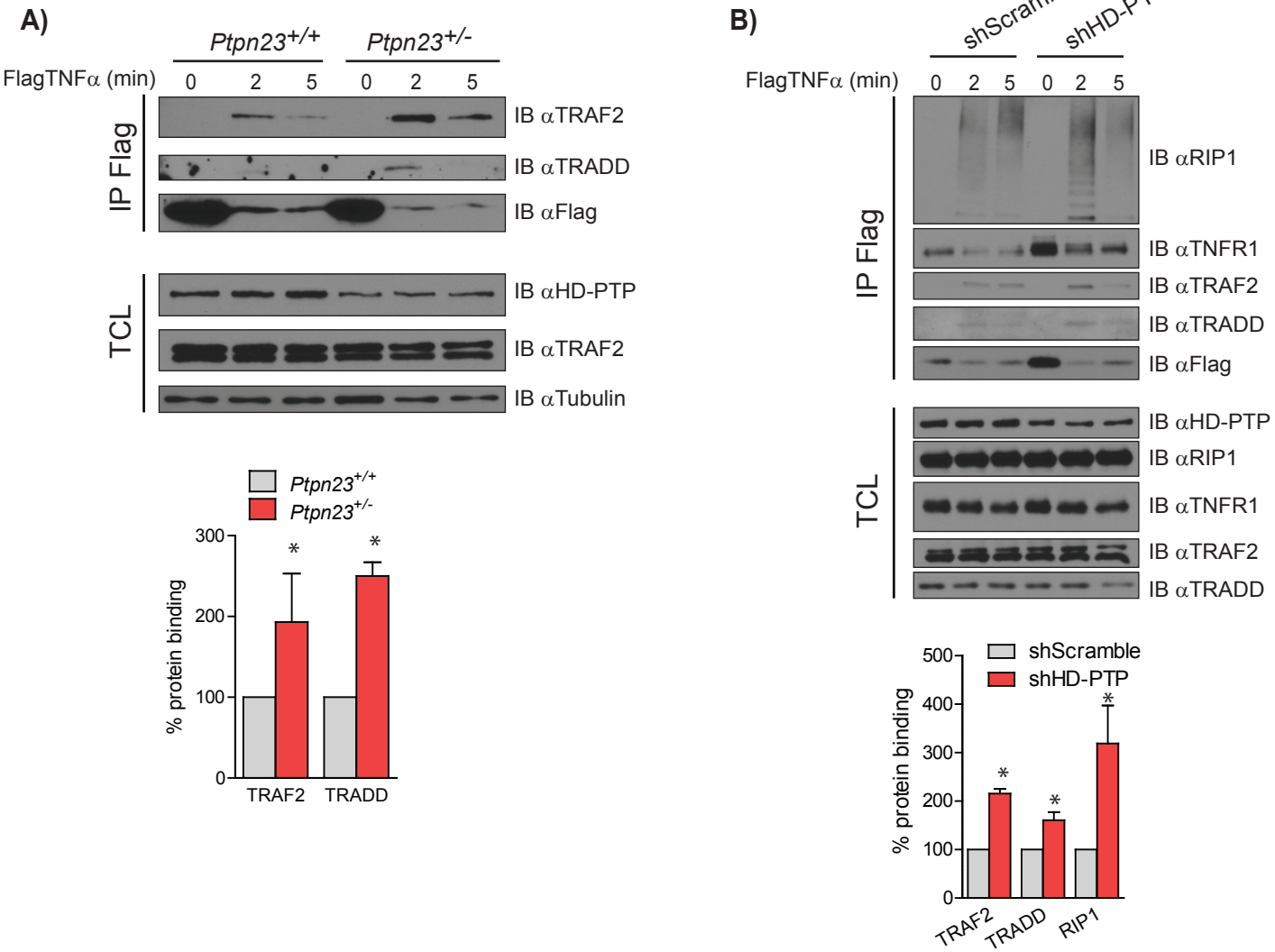
A)
Ptpn23+/+
Ptpn23+/-
FlagTNFα (min)
0 2 5 0 2 5
IP Flag
IB αTRAF2
IB αTRADD
IB αFlag
TCL
IB αHD-PTP
IB αTRAF2
IB αTubulin
Ptpn23+/+
Ptpn23+/-
% protein binding
300
200
100
0
*
*
TRAF2
TRADD
B)
shScramble
shHD-PTP
FlagTNFα (min)
0 2 5 0 2 5
IP Flag
IB αRIP1
IB αTNFR1
IB αTRAF2
IB αTRADD
IB αFlag
TCL
IB αHD-PTP
IB αRIP1
IB αTNFR1
IB αTRAF2
IB αTRADD
shScramble
shHD-PTP
% protein binding
500
400
300
200
100
0
*
*
*
TRAF2
TRADD
RIP1

Figure 3.4

3.4.6. TNFR1 pro-apoptotic signalling is potentiated in absence of HD-PTP

HD-PTP plays a key role in K63-polyubiquitinated cell surface receptors degradation. TNFR1 was reported to be polyubiquitinated with K63-Ub (Fritsch et al., 2014), a modification that acts as a requirement for theformation of endosomal TNFR1-SCII and its pro-apoptotic signalling. To evaluate a potential role of HD-PTP sorting function in TNFR1 pro-apoptotic effect, cells depleted of HD-PTP were treated with TNFα and cycloheximide (10ng/ml and 10μg/ml, respectively) for 6 hours and their viability was assessed. As expected, cells deficient of HD-PTP displayed lower viability, which could be partially reverted by caspase inhibitor zVAD treatment (Figure 3.5A and data not shown). Moreover, the enhanced execution of the apoptotic program was exemplified by an accelerated cleavage of PARP and Caspase-3 in HD-PTP depletion context (Figure 3.5B). These effects are likely due to retention of ubiquitinated TNFR1 in endosomes in the absence of HD-PTP degradative function, resulting in the prolonged TNFR1-SCII pro-apoptotic signalling.

Figure 3.5: Potentiated TNFα induced apoptosis in HD-PTP depleted cells

(A) Viability analysis upon TNFα and CHX treatment. Control and HD-PTP depleted HeLa cells were treated with human TNFα (10ng/ml) and cycloheximide (10µg/ml) for indicated timepoints. Dead cells were washed out, while the remaining cells were counted and expressed in percentage numbers relative to the untreated condition. Means ±SEM, n=3; *$p<0.05$.

(B) Apoptosis induction upon TNFα and CHX treatment. Control and HD-PTP depleted HeLa cells were treated with human TNFα (10ng/ml) and cycloheximide (10µg/ml) for indicated timepoints. The cells were collected and analysed by SDS-PAGE followed by western blot for cleavage of PARP and Caspase-3.

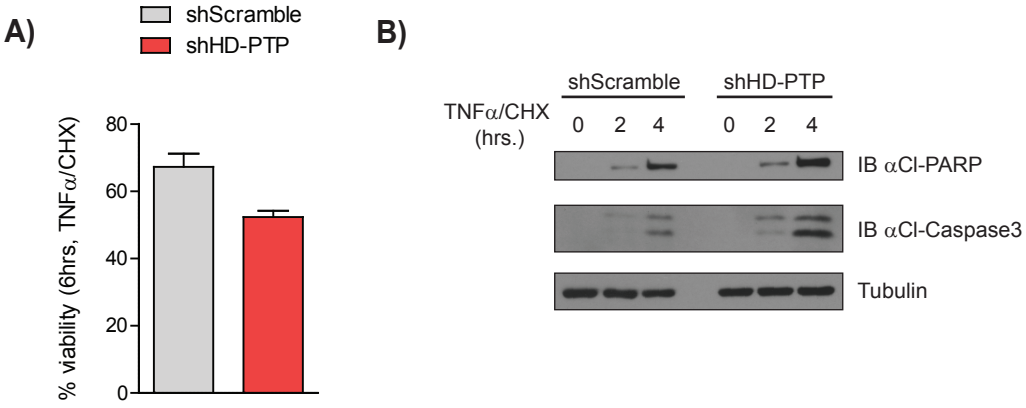
A)
shScramble
shHD-PTP
% viability (6hrs, TNFα/CHX)
80
60
40
20
0
B)
shScramble
shHD-PTP
TNFα/CHX
(hrs.)
0 2 4 0 2 4
IB αCl-PARP
IB αCl-Caspase3
Tubulin

Figure 3.5

3.5. Discussion

In the light of emerging evidence of the spatiotemporal regulation of TNFR1 signalling by endocytic mechanism, we have investigated the role of ESCRT component HD-PTP in this process. Similarly to the previously published effect of the other ESCRT components depletion on NF-κB signalling (Brankatschk et al., 2012), deficiency in HD-PTP has resulted in an accelerated induction of NF-κB pathway following TNFα stimulation. Interestingly enough, the previous study used knockdown of other ESCRT components, notably Hrs and TSG101, and the NF-κB gene analysis was performed after EGF stimulation. While the NF-κB target gene expression is upregulated in HD-PTP depleted cells after TNFα stimulation, it is likely that the disruption of endocytic sorting by the ESCRT depletion affects signalling of several receptors. Such, EGFR was demonstrated to be required for the canonical NF-κB signalling activation and gene expression (De et al., 2014). Depletion of the ESCRT machinery results in prolonged EGFR signalling (Eden et al., 2009), likely driving NF-κB transcriptional response due to the defect in receptor sorting. Since endosomes serve as signalling platforms for many cell surface receptors (reviewed in (Rodahl et al., 2009; Stuffers et al., 2009; Tu et al., 2011)), it is possible that the general disruption of degradative sorting by the ESCRT depletion may affect the crosstalk and the downstream signalling of many receptors, perhaps also contributing to the variability of NF-κB transcriptional response observed here.

The downstream signalling by TNFR1 is largely regulated by scaffolding of a molecular complex at its intracellular domain, and the composition of the complex (i.e. Complex I vs. Complex II) dictates the signalling pathway (i.e. inflammatory/survival vs. apoptotic signalling). As aforementioned, the cellular localization of TNFR1 and its ubiquitination status are crucial for its signalling regulation, since the TNFR1-SCI forms at the plasma membrane while the TNFR1-SCII forms and signals on the endosomes. ESCRT machinery is responsible for cell surface receptor degradation, and, in its absence, the ubiquitinated receptors are not degraded, favoring their cell surface return. Given the ubiquitination dynamics of TNFR1 and HD-PTP role in the ubiquitinated cargo trafficking, it is expected to find increased TNFR1 cell surface levels upon HD-PTP depletion. Higher levels of TNFR1 on cell surface of HD-PTP deficient cells are indicative of the increased receptor resensitization and availability for ligand engagement. Indeed, higher presence of TNFR1 on the cell surface resulted in a more abundant TNFR1 Complex I formation upon TNFα stimulation. Unlike several studies that demonstrate a change

in TNFR1-SCI formation due to a shift in binding or recruitment of its constituents (Ramakrishnan and Baltimore, 2011), this is not the case upon HD-PTP depletion. Likely, the increased TNFR1 complex I formation is a direct result of the abundant TNFR1 cell surface presence, resulting in more TNFR1 molecules available for the ligand engagement and consequent scaffolding of the signalling complex. Altogether, the increase in TNFR1-SCI abundance drives the accelerated NF-κB downstream signalling cascade.

The spatiotemporal control of TNFR1 signalling shift is further exemplified by the molecular switch in TNFR1 signalling complex composition. Upon TNFR1 ubiquitination and internalization, it recruits the pro-apoptotic TNFR1-SCII, responsible for the caspase dependent apoptosis. Since HD-PTP and ESCRT function is essential for K63-polybiquitinated receptors degradation, in their absence, polyubiquitinated cargo is retained at the early endosomal level, and eventually is deubiquitinated and recycled to the cell surface. Therefore, depletion of HD-PTP has a profound implication not only on the the TNFR1 signalling at the plasma membrane, but also on its pro-apoptotic signalling function at the endosomal compartment. HD-PTP deficiency resulted in a potentiated apoptosis upon TNFα treatment. These events are likely driven by the increased retention of ubiquitinated TNFR1 at endosomes and accompanied signalling via TNFR1-SCII, in the absence of the ESCRT machinery function. Interestingly, the involvement of ESCRT machinery in TNFR1-dependent apoptosis was previously suggested by findings of Alix/ALG2 complex (ESCRT associated proteins) role in recruitment of caspase-8 to the activated TNFR1 at endosomes (Mahul-Mellier et al., 2008). Since the integrity of Alix/ALG2 interaction relies on calcium ions, it is likely that this pro-apoptotic mechanism will be dependent on a calcium release in certain types of apoptotic pathway. Therefore, the ESCRT machinery is likely to play a dual counteractive role in TNFα-induced apoptosis, first by preventing the extensive apoptotic signalling via TNFR1 signalling termination inside MVBs, and secondly by recruiting the caspase-8 to TNFR1-SCII to induce apoptosis, perhaps in a subpopulation of extensively damaged cells.

Herein, we have observed a robust NF-κB dependent upregulation of cytokine transcription and secretion in cells deficient of HD-PTP. The increased secretion of pro-inflammatory molecules is a hallmark of cancer development and progression (reviewed in (Landskron et al., 2014)). HD-PTP was previously suggested to play a tumor suppressive function, and we have observed

accelerated lymphoma development in HD-PTP deficient mice (Manteghi et al, submitted manuscript). Although deficiency of HD-PTP in tumor cells can promote their tumorigenicity, it is likely that a whole animal deficiency of HD-PTP may result in a pro-inflammatory environment favorable for the tumor initiation and growth. Therefore, it would be important to understand whether the pro-inflammatory environment of HD-PTP deficient mice can lead to accelerated tumor formation.

3.6. Experimental procedures

Cell Culture and shRNA lentiviral knockdowns

HeLa and NIH3T3 cells were cultured in DMEM, 10% FBS (Wisent). MEFs were generated from embryos at 12.5 or 13.5 days postcoitum as described previously (Gingras et al., 2009a). After removal of head and red organs, embryos were homogenized using a razor blade in a trypsin solution (Gibco; no. 25300-054). The smashed embryo was incubated in trypsin for 15 min at 37°C followed by dilution in 25 ml DMEM by pipetting. The MEFs were centrifuged and plated in 100-mm culture dishes (passage 0). MEFs were cultured in DMEM, supplemented with 10% FCS (Wysent) and 1% penicillin-streptomycin.

Constitutive Mission shRNA TRC2 Lentiviral plasmids pLKO1-puro for human HDPTP (clone ID: NM_015466.x-1004s1c1; NM_015466.x-167s1c1), mouse HD-PTP (clone ID: NM_001081043.1-1648s21c1; NM_001081043.1-1387s21c1) and scramble control (clone ID: SHC002) were purchased from Sigma. The knockdown was generated by expression of shRNA carrying lentivirus in 293T cells, and infection of subconfluent HeLa or NIH3T3 cells for 48hrs. Afterwards, the viral media was removed, infected cells trypsinized and replated for puromycin (1µg/ml) selection and maintain in presence of puromycin in culture.

NF-κB signalling analysis and western blot

Cells were plated to achieve 70% confluence on the day of experiment. TNFα was added at indicated concentration for indicated time points, cells were washed with ice-cold PBS and lysed on ice. The cell extracts were quantified and analysed by SDS-PAGE followed by western blot.

Nuclear fractionation

Cells were treated with TNFα for indicated timepoints. Afterwards, cells were washed and scraped in ice-cold PBS, and progressively lysed in nuclear fractionation buffer (20mM Tris HCl pH7.5; 150mM NaCl; 0.1% NP-40; 1mM DTT and protease inhibitor cocktail) by gentle vortex and incubation on ice for 10min. An aliquot of total lysate was kept and the remaining lysate was spun at 400g for 5min. The cytosolic supernatant was separated from nuclear pellet and both

were diluted in Laemli buffer to equivalent volumes. The fractions were analysed by SDS-PAGE and western blot of indicated proteins.

Immunofluorescence

HeLa cells were stimulated for indicated timepoints with TNFα (10ng/ml), fixed with 4% paraformaldehyde and permeabilized for labelling with primary antibodies (as indicated in figure legend). Following primary staining, cells were washed and labelled with fluorescent secondary Ab and mounted for imaging. Sequential image acquisition was done on LSM710 microscope (Carl Zeiss MicroImaging, Inc), using the Plan-Apochromat 63x/NA 1.4 objective. The extent of nuclear localization of p65 was quantified using Metamorph software.

Luciferase reporter assays

WT and *Ptpn23*$^{+/-}$ MEFs were transfected in 24-well plates with 5 μg of NF-κB reporter vectors using Lipofectamine 2000 reagent according to the manufacturer's instructions (Life Technologies). The cells were analysed 72 h post-transfection and Luciferase was measured with the Dual-Glo® Luciferase Assay System (Promega).

qPCR and gene expression analysis

Cells were stimulated for indicated timepoints with TNFα, washed twice with ice-cold PBS and scraped. RNA was extracted with RNAeasy mini kit (Qiagen) and the cDNA was prepared by iScript reverse transcript mix (Bio-Rad). The qPCR was performed using specific primers for genes of interest (listed in Table S2), SYBR Green Universal mix (Bio-Rad) on Mx3000P cycler (Roche). Relative gene expression was quantified ΔCt method and normalised against housekeeping gene (RPL0).

ELISA-based cytokine excretion analysis

Cells were plated and stimulate for indicated timepoints with TNFα, the cell media was collected, centrifuged (15000g) to eliminate cells debris and used in previously prepared ELISA plates (eBiosciences). For ELISA, 96-well plates were coated with capture antibodies against the cytokines of interest, the excess of antibody washed out, and the cells' conditioned media incubated in antibody coated wells (O/N, 4ºC). A serial dilution of standard cytokine was used as

control. The samples were removed, wells washed five times with PBS tween-20 (0.05%), incubated with detection antibody (1h, RT), washed and revealed using HRP-avidin. The absorbance was read at 450nm in plate reader. The cytokine standard curve was used to quantitate the sample cytokine concentrations.

Immunoprecipitations

Cells were plated in 150mm dishes and stimulated with Flag-tagged TNFα (1µg/ml) for indicated timepoints. The excess of TNFα was washed out with cold PBS, cells scraped and lysed in IP buffer (50mM Hepes pH 7.5; 150mM NaCl; 1mM EDTA; 0.2% NP-40; 5% Glycerol; 4mM DTT; protease inhibitors), the lysates were precleared with protein-A/G beads and incubated with Flag-Ab conjugated beads. The immunocomplexes were precipitated, washed with lysis buffer and the protein complexes were eluted with 3xFlag peptide (150ng/ml), three times. The eluted fractions were analysed by SDS-PAGE and western blot for presence of TNFR1 complex components.

3.7. Acknowledgments

D.K. holds Fonds de la recherche en santé du Quebec doctoral award. S.M. holds McGill Biochemistry Merit Fellowship and MICRTP scholarship. A.P. was a recipient of the Canada Research Chair in Molecular Oncology. This work was supported by Canadian Cancer Society Research Institute grant 2010-700525 and Cancer Research Society grant (to A.P.).

3.9. Supplemental Figures

Figure S3.1

Control and HD-PTP depleted HeLa cells were stimulated with TNFα (10ng/ml) for 24h, the conditioned media was collected, centrifuged to avoid cell debris and subjected to Human Cytokine 41-Plex Discovery Assay by Eve Technologies.

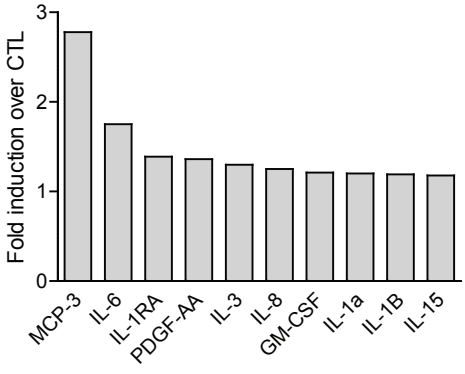
Fold induction over CTL
3
2
1
0
MCP-3
IL-6
IL-1RA
PDGF-AA
IL-3
IL-8
GM-CSF
IL-1a
IL-1B
IL-15

Figure S3.1

CHAPTER 4:

4. Characterization of an Alternative ESCRT-0 Complex and its role in Endocytic Sorting

Dmitri Kharitidi, Pirjo M. Apaja, Sanaz Manteghi, Marie-Claude Gingras, Elena Malitskaya,

Anne-Claude Gingras, Gergely L. Lukacs and Arnim Pause

4.1. Preface

In the second chapter we have outlined the profound implication of the ESCRT machinery on ubiquitinated cargo sorting to degradation, notably integrin receptors. While the ESCRT machinery is required for the lysosomal degradation of receptors, there is emerging evidence that ESCRT complexes are diverse in their nature and may have variable specificity for cargoes. To better understand the evolution and roles of the individual ESCRT components, we perform an analysis of HD-PTP interactome and identify Endofin as a new player in the ESCRT pathway. In complex with TOM1, it acts as an alternative ESCRT-0 complex, which is involved in ubiquitinated cargo recognition and degradation. Furthermore, we outline its link to the classic ECSRT pathway and present it as an evolutionary conserved alternative ESCRT-0 complex, with a partially redundant function of classic ESCRT-0.

4.2. Abstract

Endosomal sorting to degradation is a key process for the downregulation of cell surface receptors and for the termination of their signalling. This process relies on the function of Endosomal Sorting Complex Required for Transport (ESCRT), four sequential protein complexes (ESCRT-0,-I,-II and III) that recognise the ubiquitinated receptors and sequester them within Multivesicular Bodies (MVB) for lysosomal degradation. Despite being evolutionary conserved, the mammalian ESCRT core machinery requires activity of several accessory proteins. Here, we show that Histidine Domain containing Protein Tyrosine Phosphatase, previously identified as an accessory module of ESCRT-I, interacts with Endosomal FYVE-domain Protein, Endofin. The latter acts as an early ESCRT-0 component, involved in the ubiquitinated cargo recognition and its sorting to degradation. These findings suggest that HD-PTP plays a key function linking the alternative ESCRT-0 complex Endofin/TOM1 to the core ESCRT-I machinery and allows for the efficient cargo sorting through the ESCRT pathway.

4.3. Introduction

Endocytic sorting is a key cellular process regulating a plethora of signalling pathways by cell surface receptor turnover and resensitization (reviewed in (Miaczynska, 2013; Sorkin and von Zastrow, 2009; Wegner et al., 2011)). Following receptor endocytosis, internalised cargo is likely to follow two distinct routes: lysosomal degradation or cell surface recycling. The lysosomal targeting of receptors is typically defined by a post-translational modifications, such as K63 polyubiquitination (Erpapazoglou et al., 2012; Lauwers et al., 2009). Endosomal Sorting Complex Required for Transport (ESCRT) is responsible for ubiquitinated cargo recognition and its subsequent packaging within Multivesicular Bodies (MVB), necessary steps for the receptors' signalling termination and their proteolytic degradation upon MVB fusion with lysosome (Katzmann et al., 2001; Shields et al., 2009; Woodman, 2009).

ESCRT is an evolutionary conserved cellular machinery composed of four complexes (ESCRT-0, I, II, and -III) acting in concert to drive MVB biogenesis and ubiquitinated cargo degradation (Henne et al., 2011; Henne et al., 2013; Teis et al., 2008). The ESCRT-0 complex is composed of Hrs/Stam1 and is targeted to the early endosomes via PIP3-binding module (FYVE domain) of Hrs (Kojima et al., 2014; Mayers et al., 2011; Ren and Hurley, 2010; Ren et al., 2009). ESCRT-0 bears polyubiquitin recognition capacity via the action of UIM and VHS domains, whose collaborative ubiquitin binding enhances affinity to the ubiquitinated cargo (Ren and Hurley, 2010), thus engaging polyubiquitinated cargo and playing the first key step in ESCRT pathway. Afterwards, the ubiquitinated cargo is transferred to the ESCRT-I complex, conventionally composed of Tsg101, Vps28, Vps37 and MVB12a/b (Ren and Hurley, 2011b). ESCRT-I maintains interaction with ubiquitinated cargo (Oestreich et al., 2007; Pornillos et al., 2002; Tsunematsu et al., 2010), and ensures its transfer to the ESCRT-II complex, which is responsible for cargo clustering on the endosomal membrane, as well as for the recruitment and nucleation of ESCRT-III (Im et al., 2009; Teis et al., 2010). ESCRT-III drives the scission of the vesicle inside the endosomal lumen (intraluminal vesicles, ILVs) by oligomerization of CHMP4b filaments, thus contributing to the MVB biogenesis and cargo sequestration within ILVs (reviewed in (Henne et al., 2011; Shields and Piper, 2011; Teis et al., 2010)).

Recently, the classical model of ESCRT-dependent cargo sorting was improved by the identification of ESCRT-0/I associated factors playing a crucial role in receptor degradation,

such as Histidine Domain containing Protein Tyrosine Phosphatase (HD-PTP) and Ubiquitin Associated Protein 1 (UBAP1) (Ali et al., 2013; Stefani et al., 2011; Wunderley et al., 2014). HD-PTP is an inactive phosphatase, interacting with core ESCRT-0/I and III components (Stam1, Hrs, Tsg101, UBAP1 and CHMP4b) and capable of ubiquitin recognition (Doyotte et al., 2008; Gingras et al., 2009b; Pashkova et al., 2013). Together with UBAP1, HD-PTP was proposed to act as a specific endosomal ESCRT-I complex responsible for polyubiquitinated cargo degradation (Stefani et al., 2011; Wunderley et al., 2014), since their depletion results in ubiquitinated cargo accumulation and defects in the MVB biogenesis.

The emergence of such specific ESCRT-I complexes may serve as accommodation mechanism for an alternative ESCRT-0 complex, carrying the ubiquitinated cargo recognition function. Other than the classic Hrs/Stam1 ESCRT-0 complex, several other protein modules were proposed to carry out the same function in cargo recognition at the endosomes (Wang et al., 2010). One of the alternatives ESCRT-0 is proposed to be Endofin/TOM1 complex (Blanc et al., 2009). This module contains the key characteristics of ESCRT-0 i.e. PIP3 binding and endosomal recruitment via Endofin FYVE-domain (Seet et al., 2004), ubiquitin recognition via TOM1 VHS/GAT domains (Akutsu et al., 2005; Andersen et al., 2005; Shiba et al., 2004; Yamakami et al., 2003) and an interaction with clathrin (Seet and Hong, 2005). However, the function of Endofin/TOM1 complex in the ESCRT pathway and cargo recognition/degradation has never been demonstrated.

Here, we validate the alternative ESCRT-0 function of Endofin/TOM1 complex by defining their interaction with the ESCRT-I machinery (via binding to HD-PTP, UBAP1, Tsg101 and Vps28). The Endofin/TOM1 complex is localised and acts on the separate endosomal population than classical ESCRT-0, Hrs/Stam1. In addition, we demonstrate the requirement of Endofin for ubiquitinated cargo sorting through the endolysosomal pathway towards degradation, further supporting Endofin/TOM1 function in the ESCRT-dependent ubiquitinated cargo sorting.

4.4. Results

4.4.1. Mass-spectrometry analysis of HD-PTP interactions

HD-PTP was previously reported to interact with several ESCRT-0, I and -III components, including Hrs, Stam1, UBAP1, TSG101 and CHMP4B. In an attempt to identify additional and novel binding partners of HD-PTP, we performed an affinity purification coupled to mass-spectrometry (AP-MS) analysis of the HD-PTP interacting molecules. 3X-FLAG-HD-PTP was inserted into embryonic kidney (HEK) 293T cells using the Flp-In TREx system, immunoprecipitated using FLAG antibody and the pulled-down protein complexes were digested with trypsin. The resulting peptides were analysed by mass spectrometry and the interaction probability scores were assigned via SAINTexpress approach (Significance Analysis of INTeractome), using 3X-FLAG-GFP as negative control for possible non-specific binding.

MS identified HD-PTP interactors included some of the previously described molecules (i.e. CHMP4B) (Ichioka et al., 2007), but also novel interactors, such as Endofin (ZFYVE16), an endosomal FYVE-domain protein, and the clathrin heavy chain (CLTC) (Table 1). To complement these results, we have performed a similar AP-MS analysis of Endofin interactome. Indeed, among Endofin binding partners were several ESCRT-I/III machinery proteins (TSG101, UBAP1, VPS28, VPS 37a and CHMP4b), as well as HD-PTP (Table 1). These results pinpoint that Endofin may form a molecular complex with the key ESCRT machinery components and execute similar function in the endolysosomal sorting of ubiquitinated cargo.

4.4.2. HD-PTP interacts with Endofin

To confirm the interactions observed by our AP-MS analysis of the HD-PTP and Endofin binding partners, their binding was tested by co-immunoprecipitation. Following transient overexpression of Flag-HD-PTP and Myc-tagged Endofin in 293T cells and respective co-immunoprecipitations, an interaction between HD-PTP and Endofin was observed (Figure 4.1A). Furthermore, the interactions of HD-PTP with Endofin and Clathrin were confirmed at endogenous level by co-IP using HD-PTP antibody (Figure 4.1B). To map the region of HD-PTP responsible for Endofin binding, Flag-tagged HD-PTP truncation constructs were used in co-IP experiments. The BRO domain of HD-PTP was sufficient and required for Endofin interaction, since the ΔBRO construct was incapable of Endofin binding (Figure 4.1C and D). Previous studies have identified the critical cysteine residue (C753) within Endofin FYVE-domain,

responsible for PI3P binding and the endosomal localisation of Endofin (Seet et al., 2004). Notably, the C753S mutation in Endofin FYVE-domain does not disrupt Endofin interaction with HD-PTP (Figure S4.1A), but the overexpression of the Endofin C753S mutant leads to a redistribution of HD-PTP protein in the cell, likely due to an effect of mutant overexpression on the endosomal morphogenesis and/or homotypic fusion (Figure S4.2A).

To further understand the HD-PTP/Endofin complex formation, a size-exclusion chromatography (HPLC) analysis of the complex was performed. Endofin/HD-PTP appeared to be primarily located in the high-molecular weight fractions, however other ESCRT components (Hrs, Stam1, Tsg101) were eluted in the lower molecular weight fractions (Figure 4.1E), suggesting an existence of Endofin in a separate ESCRT-0 complex.

Figure 4.1: Endofin interacts with ESCRT-0/I associated protein HD-PTP

A) Co-IP experiments of HD-PTP and Endofin. HEK293T cells were transfected with Flag-HD-PTP and Myc-Endofin and the immunoprecipitations were performed using Flag or Myc antibodies respectively, immunocomplexes were analysed by SDS-PAGE and western blot.

B) Endogenous co-IPs of HD-PTP with Endofin (left panel) and Clathrin (right panel) in 293T cells demonstrates HD-PTP ability to endogenously interact with these proteins.

C) Domain mapping of HD-PTP/Endofin interaction. Flag-tagged HD-PTP deletion constructs were co-transfected in 293T cells with Myc-Endofin construct. The deletion constructs and full-length Endofin were immunoprecipitated with Flag and Myc antibodies respectively and the immunocoplexes were analysed by SDS-PAGE and immunoblot.

D) Schematic representation of HD-PTP deletion constructs (used in C) and their capacity of interaction with Endofin.

E) Subcellular fractionation of ESCRT components using size-exclusion chromatography. HeLa cells were lysed in mild buffer and the cytosolic fraction was isolated by ultracentrifugation. The cytosolic fraction was resolved on Supedex 200 column and collected fractions were analysed by SDS-PAGE and immunoblot. The calculated molecular weight of every fraction is indicated.

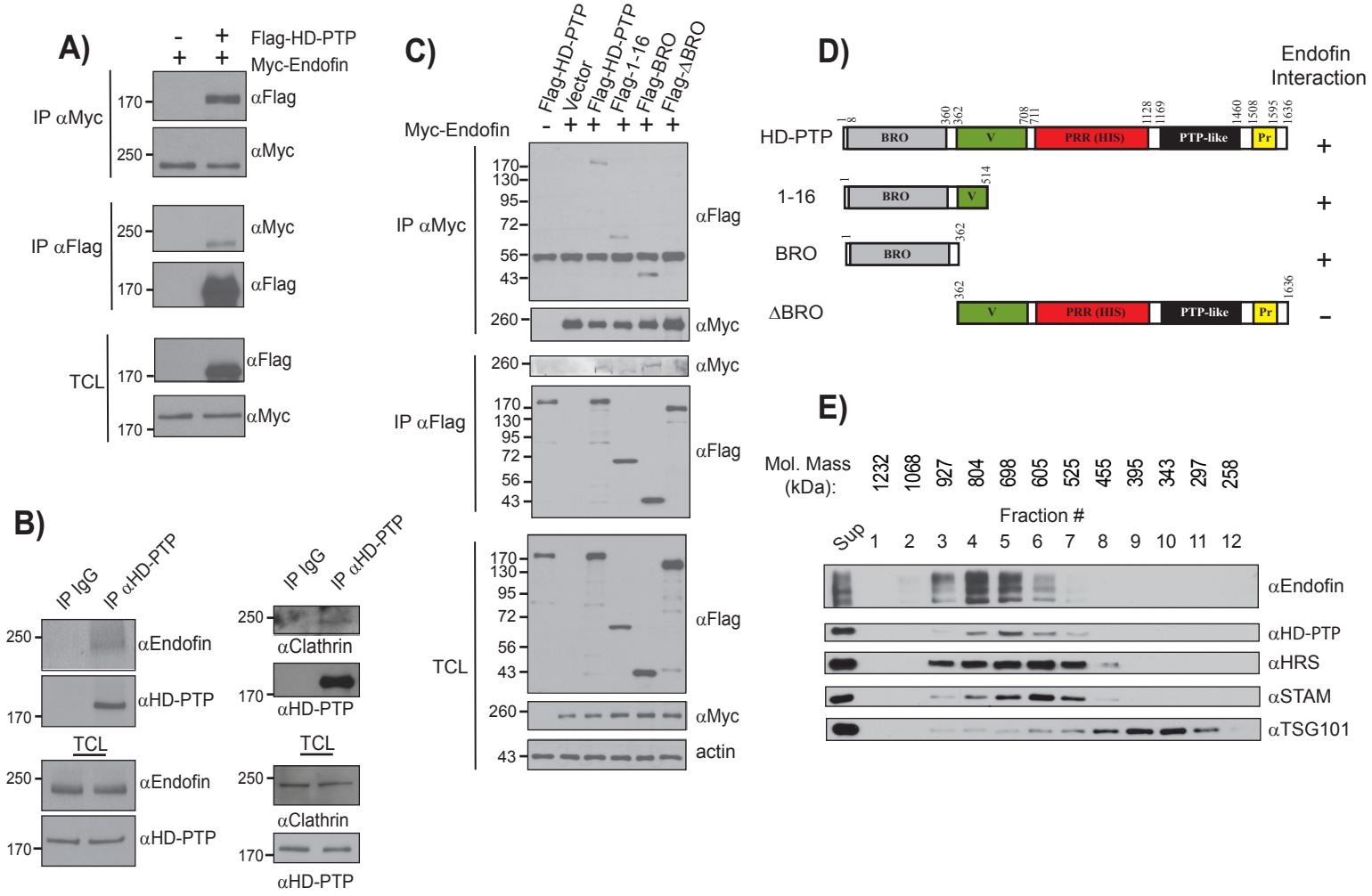
A)
Flag-HD-PTP
Myc-Endofin
IP αMyc
IP αFlag
TCL
αFlag
αMyc
B)
IP IgG
IP αHD-PTP
αEndofin
αHD-PTP
αClathrin
TCL
C)
Flag-HD-PTP
Vector
Flag-HD-PTP
Flag-1-16
Flag-BRO
Flag-ΔBRO
Myc-Endofin
IP αMyc
IP αFlag
TCL
αFlag
αMyc
actin
D)
Endofin Interaction
HD-PTP
1-16
BRO
ΔBRO
BRO
V
PRR (HIS)
PTP-like
Pr
E)
Mol. Mass (kDa):
Fraction #
Sup
αEndofin
αHD-PTP
αHRS
αSTAM
αTSG101

Figure 4.1

4.4.3. Endofin colocalized with ESCRT-I but not ESCRT-0 subunits

Endofin bears a PI3P binding FYVE-domain and was reported to localise to early endosomes (Seet and Hong, 2001). Indeed, co-localization with the early endosomal marker EEA1 confirms these results (Figure 4.2B) and is further supported by the isopycnic sucrose gradient cell fractionation, where Endofin distribution overlaps with the light membrane fraction (EEA1 marker), alongside with HD-PTP and other ESCRT components, TSG101, Hrs and UBAP1 (Figure 4.2A).

To identify whether Endofin and the "classic" ESCRT-0 complex (Hrs/Stam1) localization is mutually exclusive, co-immunofluorescence experiment was performed. Endofin appeared to partially co-localize with Stam1 and HD-PTP (Figure 4.2C), but not with the other ESCRT-0 component Hrs. This suggests that Endofin localization is confined to a distinct endosomal population, than the "classic" ESCRT-0 complex Hrs/Stam1.

4.4.4. Endofin shares polyubiquitin binding capacity

Endofin was reported to interact with TOM1 and recruit it to the early endosomes (Seet and Hong, 2005; Seet et al., 2004). TOM1 contains VHS and GAT domains, bearing ubiquitin binding capacity (Shiba et al., 2004). Together, this protein complex was proposed to play a role of an alternative ESCRT-0 complex, involved in the ubiquitinated receptor recognition, similarly to Hrs/Stam1 (Mayers et al., 2011). Endofin does not contain any known domains capable of a direct ubiquitin interaction, yet it is likely to interact with polyubiquitin via its association with TOM1. To demonstrate Endofin/TOM1 complex polyubiquitin recognition capacity, pulldowns using recombinant GST-mono- and poly-Ub were performed on HeLa cells lysates (Barriere et al., 2007a; Barriere et al., 2006b). In accordance with the previously described TOM1 ubiquitin binding, Endofin and TOM1 were precipitated with polyubiquitin chains mimicking K63 polyubiquitin conformation, but not the mono-Ub (Figure 4.2D). Altogether, these findings indicate that Endofin/TOM1 complex has the main characteristics of ESCRT-0 complex, such as localisation at the early endosomes, interaction with the later ESCRT complexes (i.e. ESCRT-I,-III) and ability to recognize the polyubiquitinated proteins.

Figure 4.2: Endofin containing vesicles are distinct of ESCRT-0 compartments

A) Cellular fractionation was performed by isopycnic sucrose gradient centrifugation. Cells were homogenized, the post nuclear supernatant was applied on sucrose gradient (10-40%) and subjected to ultracentrifugation. The fractions were collected and analysed by SDS-PAGE followed by immunoblot. The light and heavy density fractions are identified by EEA1 and LAMP1 immunoblots. The heavier membrane compartments had a distinct fractionation pattern (LAMP1– lysosomes, Tom20– mitochondria).

B) Endofin cellular localization by immunofluorescence. HeLa cells were fixed and co-stained with Endofin Ab and early endosomal marker (EEA1) or lysosomal marker (LAMP1) Abs. The staining was revealed by secondary Alexa-488 and -594 conjugated secondary antibodies and visualised by confocal microscopy. Scale bar (10μm).

C) Endofin colocalization with ESCRT subunits Hrs, Stam1 and HD-PTP. HeLa cells were fixed and co-stained with Endofin Ab and ESCRT Abs. The staining was revealed by secondary Alexa-488 and -594 conjugated secondary antibodies and visualised by confocal microscopy.

D) Endofin polyubiquitin recognition. Recombinant GST-tagged linear mono- or poly-Ub constructs were purified and incubated with HeLa cell lysate for two hours. Protein complexes were pulled down by glutathione agarose beads, washed and analysed by immunoblotting for Endofin and TOM1. GST-Ub constructs, containing at least 2 Ub moieties, were able to pull-down Endofin and TOM1.

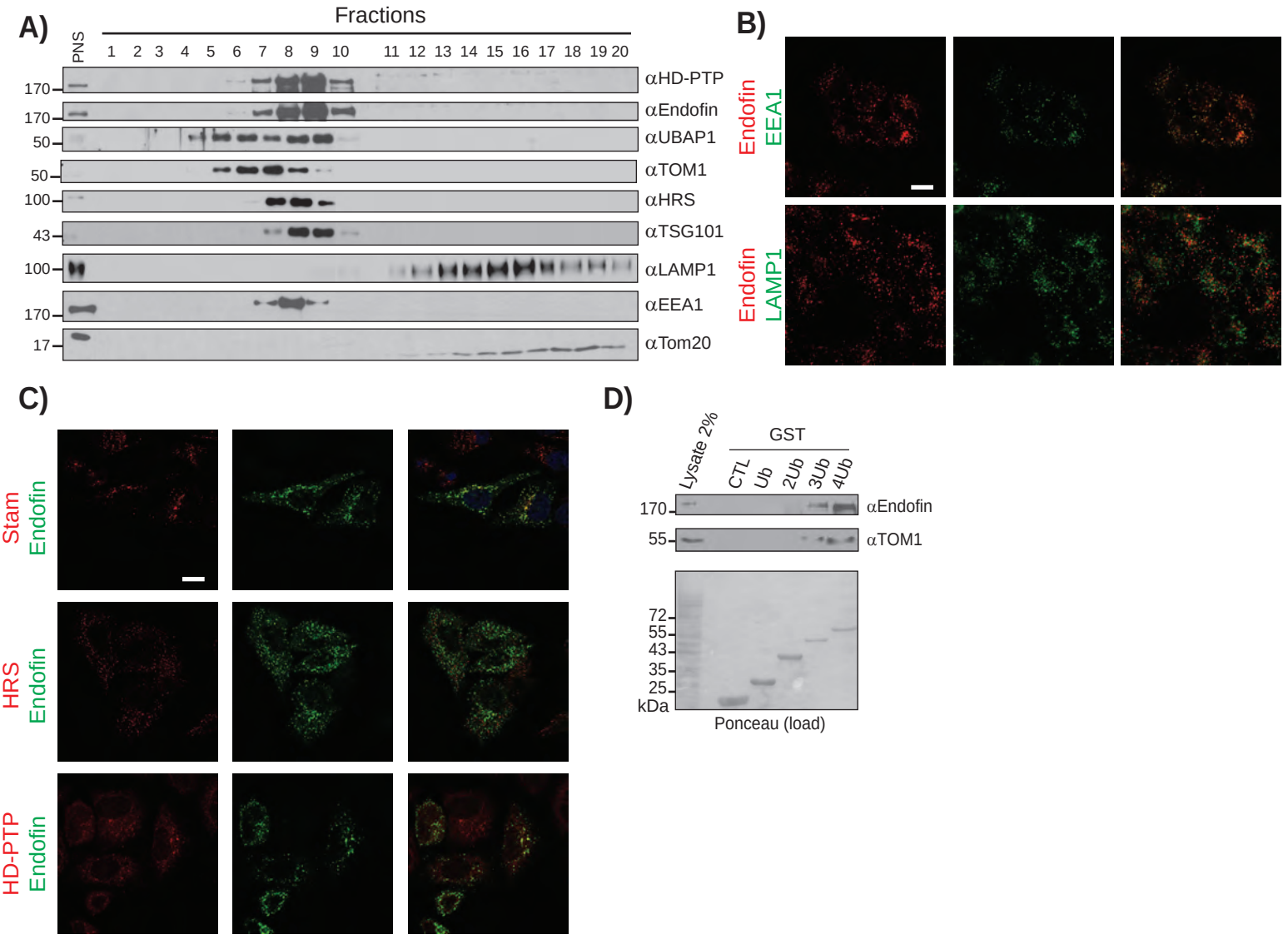
A)
Fractions
PNS
1 2 3 4 5 6 7 8 9 10 11 12 13 14 15 16 17 18 19 20
170
170
50
50
100
43
100
170
17
αHD-PTP
αEndofin
αUBAP1
αTOM1
αHRS
αTSG101
αLAMP1
αEEA1
αTom20
B)
Endofin
EEA1
Endofin
LAMP1
C)
Stam
Endofin
HRS
Endofin
HD-PTP
Endofin
D)
Lysate 2%
GST
CTL
Ub
2Ub
3Ub
4Ub
170
55
αEndofin
αTOM1
72
55
43
35
25
kDa
Ponceau (load)

Figure 4.2

4.4.5. Endofin is required for lysosomal delivery of polyubiquitinated cargo

Although Endofin/TOM1 complex has been proposed to play a role of an alternative ESCRT-0 complex, its role in ubiquitinated cargo sorting has never been demonstrated. To study the function of Endofin in the endolysosomal transfer of polyubiquitinated receptors, we used HeLa cells stably depleted of Endofin expression using shRNA (Figure 4.3A). The role of Endofin in the polyubiquitinated cargo lysosomal delivery was assessed using two model cargo molecules, CD4t-Ub_n chimera, which undergoes constitutive polyubiquitination and the CD4cc-UbRΔG_4 chimera that contains a tetrameric mono-Ub sorting signal. The endolysosomal transfer kinetics of the model cargoes was determined by monitoring the luminal pH of the cargo containing endocytic vesicles (pH_v), with fluorescent ratiometric image analysis (FRIA). This method allows precise measurement of the cargo localization by the quantitative endosomal pH measurement.

As expected in the case of depletion of a ESCRT component, the endolysosomal transfer of polyubiquitinated CD4t-Ub_n cargo was significantly delayed upon Endofin depletion, as the cargo was retained at the early/recycling endosomes (pH~6.3-6.5) after 2h chase, relative to control cells, where the cargo reached the late endosomal/lysosomal compartments (pH~5) (Figure 4.3B). However, no delay in the lysosomal delivery of the CD4cc-UbRΔG_4 chimera was observed, suggesting that the Endofin-dependent sorting is selective to the polyubiquitinated cargoes (Figure 4.3C). Interestingly, a mild, but significant defect in transferrin trafficking was observed in Endofin depleted cells, but no effects on Lamp1/CD63 lysosomal marker or fluid phase marker FITC-Dextran were noted (Figure 4.3E). In accordance with the integrin α5β1 ubiquitination and lysosomal delivery (Chapter 2), Endofin depletion delays its endolysosomal transfer as measured by FRIA (Figure 4.3D). This quantitative measurement was also supported by a immunofluorescence analysis of integrin α5 colocalization with early, but not the late endosomal markers (Figure S4.3A). Overall, these data strongly suggests that Endofin plays a key role in the ESCRT-dependent degradation of polyubiquitinated cargo, due to its polyubiquitin recognition capacity and activity in concert with ESCRT-I,-III.

Figure 4.3: Endofin is required for lysosomal delivery of polyubiquitinated cargo

A) HeLa cells were stably depleted of Endofin expression by lentiviral shRNA infection.

B) FRIA analysis of endolysosomal transfer of model CD4-receptor chimeric model cargo, modified by polyubiquitination in the context of Endofin depletion. Briefly, anti-CD4 Ab and FITC-Fab were bound on ice, chased and FRIA was performed at 37ºC for indicated timepoints. Endofin is required for poly-Ub CD4t-Ub_n lysosomal delivery. The graph shows the mean pH_v at each chase point. Means ±SEM, n=3; *$p<0.05$.

C) FRIA analysis of endolysosomal transfer of tetra-monoubiquitinated Ub CD4cc-UbRΔG_4 lysosomal delivery in the context of Endofin depletion, performed as in (B).

D) FRIA analysis of endolysosomal transfer of integrin α5β1 following fibronectin stimulation (as in Chapter 2). Endofin is required for lysosomal transfer of integrin α5β1. Means ±SEM, n=3; *$p<0.05$.

E) FRIA analysis of endocytic sorting of control cargoes (transferrin, LAMP1 and fluid-phase marker dextran) in cells depleted of Endofin. Means ±SEM, n=3.

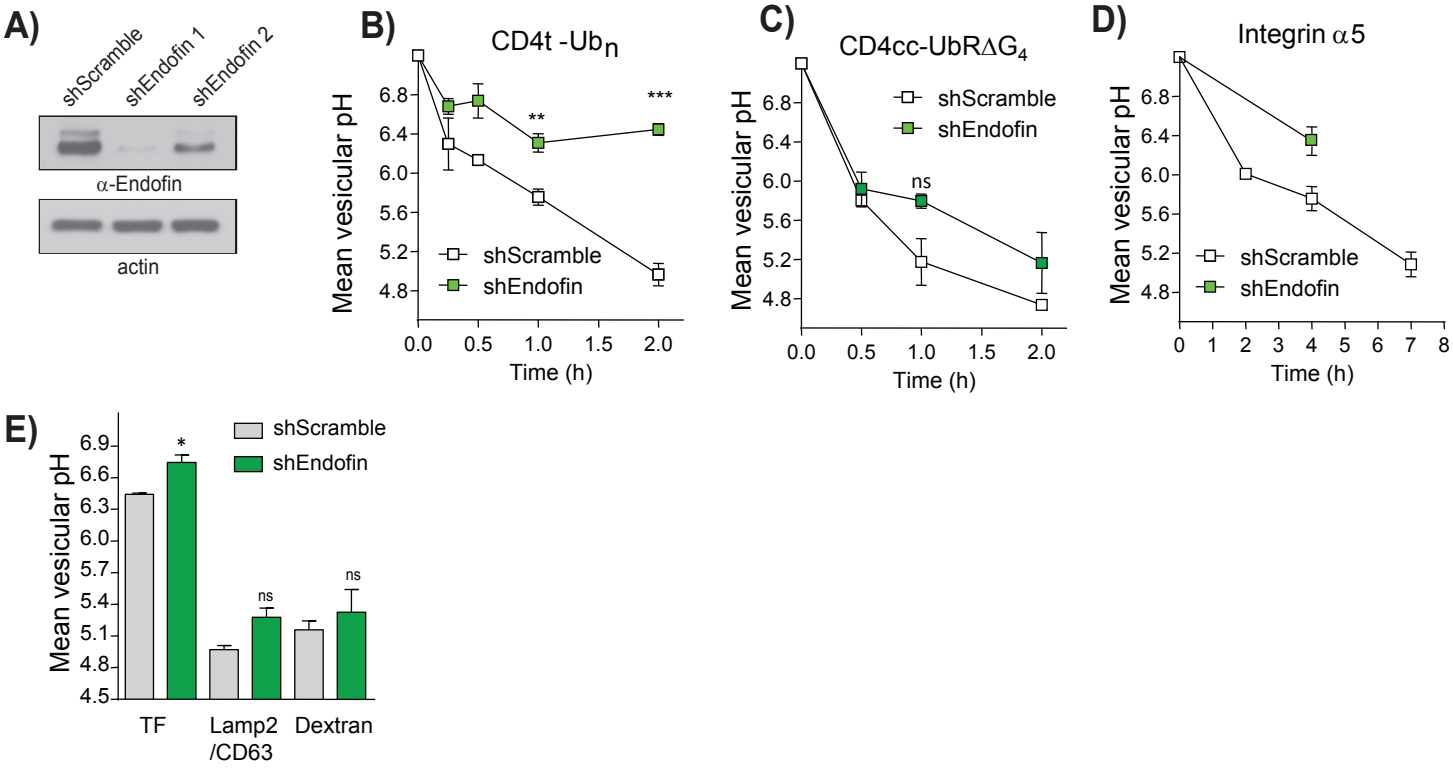
A)
shScramble
shEndofin 1
shEndofin 2
α-Endofin
actin
B)
CD4t -Ubn
Mean vesicular pH
6.8
6.4
6.0
5.6
5.2
4.8
**
***
shScramble
shEndofin
0.0
0.5
1.0
1.5
2.0
Time (h)
C)
CD4cc-UbRΔG4
Mean vesicular pH
6.8
6.4
6.0
5.6
5.2
4.8
shScramble
shEndofin
ns
0.0
0.5
1.0
1.5
2.0
Time (h)
D)
Integrin α5
Mean vesicular pH
6.8
6.4
6.0
5.6
5.2
4.8
shScramble
shEndofin
0
1
2
3
4
5
6
7
8
Time (h)
E)
Mean vesicular pH
6.9
6.6
6.3
6.0
5.7
5.4
5.1
4.8
4.5
shScramble
shEndofin
*
ns
ns
TF
Lamp2
/CD63
Dextran

Figure 4.3

4.4.6. Endofin depletion confers promigratory phenotype

Previous reports have indicated a role for Endofin in the MAPK signalling cascade, as well as TGF-beta signalling (Chen et al., 2007; Shi et al., 2007; Toy et al., 2010). Since Endofin mediates regulation of these signalling pathways, and its role in integrin α5β1 sorting may contribute to promigratory signalling, the effect of Endofin in cellular migration and matrigel invasion was determined by real-time cell migration analysis. Depletion of Endofin upregulated cellular migration and invasion two-fold (Figure 4.4A) and had a minor (non-significant) effect on the rate of cell spreading on fibronectin and collagen I matrices (Figure 4.4B).

Recent studies have proposed a tumor suppressive role for ESCRT machinery during carcinogenesis (reviewed in (Jiang et al., 2013; Mattissek and Teis, 2014)). Therefore, the effect of Endofin depletion on the cellular proliferation and xenograft outgrowth was determined. Endofin downregulation had no effect on the cellular proliferation (data not shown). Also, there was no difference observed in xenograph tumor outgrowth using lung cancer (A549) and breast cancer cells (MDA1833) (Figure 4.4C and D). These results suggest that Endofin plays a specific role in endocytic sorting of polyubiquitinated cargo with little implication in tumor growth.

Figure 4.4: Endofin depletion enhances cell migration

A) Cell migration and invasion assays using RTCA xCelligence system. HeLa cells depleted of Endofin were subjected to transwell migration and matrigel invasion assays towards serum gradient, over period of 6 and 12 hours respectively. Means ±SEM, n=3; *p<0.05.

B) Cell spreading assays on fibronectin and Collagen I matrices. Control and Endofin depleted cells were plated in matrix precoated plates, after 15min the unattached cells were washed out. Seeded cells were allowed to spread for 45min, fixed, stained with phalloidin and visualised by fluorescence microscopy. Relative cell spreading was quantified using ImageJ software (left panel), representative images are shown. Scale bar 100μm.

C) A549 xenograft tumor outgrowth in nude mice. A549 cells were depleted of Endofin by stable shRNA and subcutaneously injected in flank of nude mice. The tumor growth was monitored weekly for the period of 7 weeks.

D) MDA1833 breast xenograft tumor outgrowth in SCID mice. MDA1833 cells were stably depleted of Endofin by shRNA and injected into mammary fat pad of SCID mice. The xenograft outgrowth was monitored weekly.

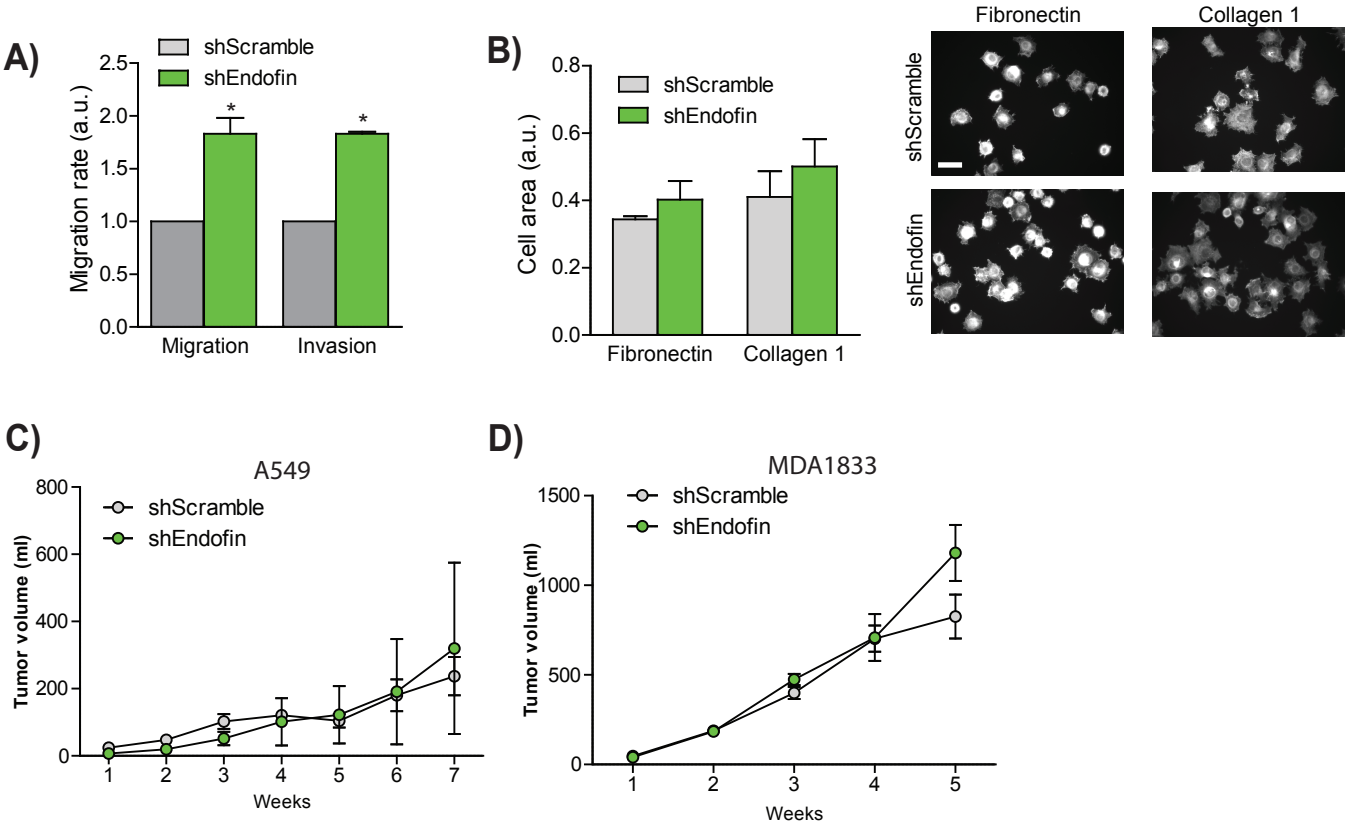
A)
shScramble
shEndofin
Migration rate (a.u.)
2.5
2.0
1.5
1.0
0.5
0.0
*
*
Migration
Invasion
B)
shScramble
shEndofin
Cell area (a.u.)
0.8
0.6
0.4
0.2
0.0
Fibronectin
Collagen 1
Fibronectin
Collagen 1
shScramble
shEndofin
C)
A549
shScramble
shEndofin
Tumor volume (ml)
800
600
400
200
0
1
2
3
4
5
6
7
Weeks
D)
MDA1833
shScramble
shEndofin
Tumor volume (ml)
1500
1000
500
0
1
2
3
4
5
Weeks

Figure 4.4

4.5. Discussion

Here we demonstrate the interaction of an "alternative" ESCRT-0 subunit Endofin with HD-PTP and other components of the ESCRT-I machinery. In addition, Endofin carries out a polyubiquitin binding ability, does not interact with or colocalize with the "classic" ESCRT-0 components, such as Stam1 or Hrs, and is required for the endocytic sorting of polyubiquitinated cargoes. These findings confirm the role of Endofin as an alternative ESCRT-0 and its function in the sorting of ubiquitinated receptors.

Endofin role as an alternative ESCRT-0 was proposed following identification of its interaction with TOM1, an evolutionary conserved protein bearing ubiquitin and clathrin binding capacity (Seet and Hong, 2005; Yamakami et al., 2003). TOM1 was proposed to be the primordial ESCRT-0 complex, that originated early in the evolution in lower organisms such as in amoeba *D. Discoideum* (Blanc et al., 2009). Upon emergence of the "classic" ESCRT-0 components Stam1/Hrs later in the metazoan evolution, TOM1 may have maintained its sorting function in a cooperation with Endofin (Leung et al., 2008). However, the evidence for the Endofin/TOM1 role in ESCRT pathway is lacking. The interactions of Endofin with the ESCRT-I subunits HD-PTP, TSG101 and Vps28 and Vps37a are described here, providing a missing link between the ESCRT machinery and the ancestral ESCRT-0 complex. Therefore, the ESCRT-I machinery can accommodate both ESCRT-0 complexes (i.e. Hrs/Stam1 and Endofin/TOM1) and accept polyubiquitinated cargo from either of the two.

While carrying out the function in ubiquitinated cargo recognition and sorting, Endofin appears to have a distinct cellular distribution than the classic ESCRT-0 complex Hrs/Stam1. These results indicate that the sorting function of ESCRT-0 complexes may be spatially regulated and that there may be a distinct endosomal population characterized by the presence of either the classic ESCRT-0 or the alternative ESCRT-0 complex. Later in the endocytic process, the homotypic fusion of endosomes may lead to a formation of an endosome unifying cargo from both ESCRT-0 complexes, thus becoming the compartment where the sequestration of cargo inside ILVs occurs via the action of ESCRTs-I,II, and –III. However, the exact function of a distinct endosome population defined by a specific ESCRT-0 complex is not clear. It is likely that these distinct endosomes may arise from a different endocytosis routes or are designed for a

specific cargo sorting, possibly defined by the specificity of polyubiquitin chain recognition by the ESCRTs-0 complexes.

Although, Hrs/Stam1 UBA and UIM domains are known to cooperatively recognise and bind K63-polyubiquitin chains (Bache et al., 2003; Mizuno et al., 2003; Takahashi et al., 2015), the specificity of Endofin/TOM1 ubiquitin binding domains is unknown. TOM1 is capable of binding to polyubiquitin via its GAT and VHS domains (Shiba et al., 2004; Yamakami et al., 2003), while Endofin does not contain any domains known for ubiquitin binding capacity. Despite the lack of ubiquitin-interacting domains, Endofin was efficiently precipitated from the cell lysate using recombinant polyubiquitin. It is possible that Endofin indirect interaction with polyubiquitin occurs through TOM1 or another ESCRT component, bearing polyubiquitin recognition motifs (i.e. UBAP1, HD-PTP or TSG101). Polyubiquitin binding domains are diverse in nature (reviewed in (Erpapazoglou et al., 2014; Piper et al., 2014; Randles and Walters, 2012)) and the structural studies of Endofin have not been performed, it is possible that this protein contains some non-identified ubiquitin binding domain responsible for its engagement with polyubiquitinated cargo. Also, it is conceivable that Endofin structure in the complex with TOM1 assists the cooperative polyubiquitin interaction of TOM1's GAT and VHS domains, thus increasing the overall avidity to polyubiquitinated molecules.

Endocytic sorting by the ESCRT machinery is known to affect a number of cell surface receptors and downstream signalling pathways and thus has profound implication on some processes regulating tumor initiation and progression. Endofin was reported to play a role in EGFR, TNFRβ and BMP receptor signalling (Chen et al., 2007; Shi et al., 2007; Toy et al., 2010). The signalling downstream of these receptors is crucial for tumor survival, proliferation, epithelial-mesenchymal transition (EMT) and invasion/metastasis (reviewed in (Corallino et al., 2015; Papageorgis, 2015)). We have not observed notable effects of Endofin depletion on cellular proliferation or outgrowth of the xenograft tumors. However, a significant increase in cell migration and invasion was observed in Endofin depleted cells, suggesting that Endofin can play a role in integrin-dependent cell migration and invasion, similarly to HD-PTP and UBAP1 (described in Chapter 2). However, Endofin role in TNFβ and BMP signalling suggests that its cellular expression may be required for TGFβRII and BMPR1 activation and downstream signalling leading to EMT initiation (Chen et al., 2007; Shi et al., 2007). Therefore, Endofin may

play a dual role in the tumor invasion process, at early stages it may promote EMT, permitting tumor cells to acquire migratory properties, while after the migration initiation, Endofin might be downregulated by an unknown mechanism to allow for the faster invasion rate via reduced integrin degradation in favor of their recycling. Therefore, it will be important to understand whether Endofin expression is differentially regulated in the early and late stage tumors and whether it can become a target of regulation of promigratory signalling in tumor cells.

In conclusion, we identify the Endofin/TOM1 complex function as an evolutionary conserved ESCRT-0 complex, mediating ubiquitinated cargo degradation via recognition of ubiquitinated receptors and their subsequent transfer to the later stages of the ESCRT pathway.

4.6. Experimental Procedures:

Plasmid constructs, reagents and cell culture

Flag-tagged HD-PTP and Endofin constructs were generated by was introduced into the Gateway entry vector pDONR223 (Life Technologies), and recombined into pDEST-pcDNA5-FRT-TO for AP-MS procedures (described below). Flag-tagged HD-PTP in pcDNA3.1 was described previously (Gingras et al., 2009b), the deletion constructs were generated by subcloning HD-PTP fragments into Flag-tagged pcDNA3.1. Myc-tagged Endofin was a kind gift from Dr. H. Wang (Seet and Hong, 2001), and mutated to C753S by point-mutagenesis. Ubiquitin GST-Ub/2Ub/3Ub/4Ub were in pGEX-4T1, and pcDNA3-CD4 c-tail was replaced either with WT Ub (CD4t-Ub_n) or CC tetramerization domain with mutant Ub (all K to R and deletion of 76GG (CD4cc-UbRΔG_4) as described (Barriere et al., 2007b). GFP-Integrin α5 was purchased from Addgene. Complete list of antibodies, reagents and primers is included in Table S4.1.

HeLa, H1299, MDA1833TR and HEK293T cells were cultured in DMEM, 10% FBS (Wisent). Constitutive Mission shRNA TRC2 Lentiviral plasmids pLKO1-puro for human Endofin (clone ID: NM_014733.2-4263s1c1; NM_014733.2-929s1c1) and Scramble control (clone ID: SHC002) were purchased from Sigma.

AP-MS Cloning and Stable Cell Line Generation

The ORFs were transferred via Gateway cloning into N-terminal 3XFLAG mammalian expression vector for isogenic stable cell line generation and tetracycline-inducible expression. Flip-In T-REx 293T cells were transfected in a 6 well format with 0.2µg of tagged DNA [pcDNA5-FLAG-protein] and 2µg pOG44 (OpenFreezer V4134), using lipofectamine PLUS (Invitrogen), according to the manufacturer's instructions. On day 2, cells were trypsinized, and passaged into 10 cm plates. On day 3, the medium is replaced by DMEM 5% Fetal bovine serum 5% calf serum 100 units/ml pen/strep 200 ug/ml hygromycin. Medium was replaced every 2- 4 days until non-transfected cells died and isolated clones were ~1-2 mm in diameter (13-15 days). Pools of cells were generated by trypsinization of the entire plate and replating in fresh selection medium (the size of the plate was dictated by the number and size of initial colonies). Cells at

~60-70% confluence were induced with 1ug/ml tetracycline for 24 hours. Subconfluent cells (~85-95% confluent) were harvested for AP-MS analysis.

Affinity Purification

Cells were lysed by passive lysis assisted by freeze-thaw. Briefly, to the frozen cell pellet, 1:4 pellet weight:volume ratio of ice-cold lysis buffer was added and the frozen pellet was resuspended by pipetting up and down. Lysis buffer was 50 mM Hepes-NaOH pH 8.0, 100 mM KCl, 2 mM EDTA, 0.1% NP40, 10% glycerol, 1 mM PMSF, 1 mM DTT and Sigma protease inhibitor cocktail, P8340, 1:500. Tubes were frozen and thawed once by putting on dry ice ~5-10min, then transferring in a 37°C water bath with agitation until only a small amount of ice remained. The 2 ml tubes were centrifuged at 14000 rpm for 20 min at 4°C, and the supernatant transferred to fresh 15 ml conical tubes. During centrifugation, anti-FLAG M2 magnetic beads (SIGMA) were prepared, the equivalent of 12.5ul packed FLAG M2 magnetic beads was added, and the mixture incubated 2 hours at 4°C with gentle agitation (nutator). Beads were pelleted by centrifugation (1000 rpm for 1 min) and a 15ul aliquot of the lysate post-IP was taken for analysis. Two washes with 1ml lysis buffer and two washes with 20mM Tris-HCl (pH 8.0) 2mM CaCl2 were performed.

Tryptic Digestion

The beads were resuspended in 5ul of 20mM Tris-HCl (pH 8.0). 500ng of trypsin (Sigma Trypsin Singles, T7575; resuspended at 200ng/µl in Tris buffer) was added, and the mixture was incubated at 37 C with agitation for 4 hours. After this first incubation, the sample was magnetized and the supernatant transferred to a fresh tube. Another 500ng of trypsin was added, and the resulting sample was incubated at 37ºC overnight (no agitation required). The next morning, formic acid was added to the sample to a final concentration of 2% (from 50% stock solution).

Mass Spectrometry

Half the sample was used per analysis. A spray tip was formed on fused silica capillary column (0.75 um ID, 350 um OD) using a laser puller (program = 4; heat = 280, FIL = 0, VEL = 18, DEL = 200). 10 cm (/- 1 cm) of C18 reversed-phase material (Reprosil-Pur 120 C18-AQ, 3 um)

was packed in the column by pressure bomb (in MeOH). The column was then pre-equilibrated in buffer A (6 ul) before being connected in-line to a NanoLC-Ultra 2D plus HPLC system (Eksigent, Dublin, USA) coupled to a LTQ-Orbitrap Velos (Thermo Electron, Bremen, Germany) equipped with a nanoelectrospray ion source (Proxeon Biosystems, Odense, Denmark). The LTQ-Orbitrap Velos instrument under Xcalibur 2.0 was operated in the data dependent mode to automatically switch between MS and up to 10 subsequent MS/MS acquisition. Buffer A is 100% H2O, 0.1% formic acid; buffer B is 100 ACN, 0.1% formic acid. The HPLC gradient program delivered an acetonitrile gradient over 125 minutes. For the first twenty minutes, the flow rate was of 400uL/min at 2%B. The flow rate was then reduced to 200uL/min and the fraction of solvent B increase in a linear fashion to 35% until the 95.5 minutes. Solvent B was then increased to 80% over 5 minutes and maintained at that level until 107 minutes. The mobile phase was then reduced 2% B until the end of the run (125min). The parameters for data dependent acquisition on the mass spectrometer were: 1 centroid MS (mass range 400-2000) followed by MS/MS on the 10 most abundant ions. General parameters were: activation type = CID, isolation width = 1 m/z, normalized collision energy = 35, activation Q = 0.25, activation time = 10 msec. For data dependent acquisition, minimum threshold was 500, the repeat count = 1, repeat duration = 30 sec, exclusion size list = 500, exclusion duration = 30 sec, exclusion mass width (by mass) = low 0.03, high 0.03.

Data analysis and SAINT

Files were searched using Mascot (within ProHits) using the following parameters:

Mascot Database: Human_RefseqV53; Taxonomy: All entries; Fixed Mod: Variable Mod: Deamidated (NQ):Oxidation (M):Phospho (ST):Phospho (Y); Missed Cleavages: 1; Peptide tol: 12 ppm; MS/MS tol: 0.6 Da; MASS: Monoisotopic; Peptide charge: 2+, 3+ and 4+; Enzyme: Trypsin.

SAINT analysis was performed using 16 biological replicates of FLAG-GFP (all from asynchronous HEK293 T-Rex cells, all run on the Orbitrap Velos) as negative controls, including two samples run in tandem with the two biological replacates. SAINT was run using default parameters (detailed below) with the sixteen control runs grouped into four compressed

controls. Version:mrf-Dec22; has_control:16; nControl:4; nburn:2000; niter:5000; lowMode:0; minFold:1; normalize:1; old_version:0.

Immunoprecipitations

HEK293T cells were transiently transfected with indicated plasmids using Lipofectamine2000 reagent (Invitrogen). After 24hrs expression, cells were lysed (50mM Hepes pH 7.5; 150mM NaCl; 1mM EDTA; 0.5% Triton; 5% Glycerol; 4mM DTT; protease inhibitors), the lysates were precleared with protein-A/G beads and incubated with respective antibodies. The immunocomplexes were precipitated with protein-G beads, washed with lysis buffer and analysed by western blot.

Immunofluorescence

HeLa cells were fixed with 4% paraformaldehyde and permeabilized for labelling with primary antibodies (as indicated in figure legend). Following primary staining, cells were washed and labelled with fluorescent secondary Ab and mounted for imaging. Sequential image acquisition was done on LSM710 microscope (Carl Zeiss MicroImaging, Inc), using the Plan-Apochromat 63x/NA 1.4 objective.

Size-Exclusion Chromatography fractionation:

Cells were lysed in buffer (150mM NaCl, 0.1% NP40, 6.25mM TrisHCl ph8, 2mM EDTA, 0.1mM MgCl2, 1mM EGTA, +Protease inhibitor cocktail) on ice. The lysate was centrifuged first at 16000g for 10min, and then the resulting supernatant was centrifuged at 100,000g for 1h. The supernatant was loaded on Superdex200 HPLC column and 0.3ml fractions were collected. Protein analysis was performed on collected fraction by SDS-PAGE followed by western blot.

Isopycnic sucrose gradient cellular fractionation

HEK293T cells were washed with PBS on ice, scraped in low volume of ice cold PBS and scraped on ice. The cell pellet was resuspended in isotonic buffer (20mM Hepes pH7.5; 150mM NaCl; 1mM DTT and protease inhibitors) and the cells were progressively broken down by needle strokes (10 strokes with 25-gauge needle, followed by 20 strokes with 27-gauge needle). The lysate was spun at 400g to eliminate nuclei, and the cytosolic supernatant

was loaded on 10-40% sucrose gradient, centrifuged 16hrs at 100000g in Beckman Ti-55 rotor. The fractions were collected (0.25ml) and analysed by western blot using the indicated markers.

Recombinant protein production and pull-down assay

The recombinant Ub-constructs expression, purification and GST pull-down were done as described (Barriere et al., 2006a). Briefly, their expression was induced with 0.1mM IPTG for 4 h at 22 °C and bacteria was lysed in (100mM Tris HCl pH 7.5; 150mM NaCl; 5mM EDTA; 0.75% Triton; 5% Glycerol; 4mM DTT; protease inhibitors, 1mM PMSF), and affinity purified on glutathione-Sepharose beads (Pierce). HeLa cell lysate (2mg) was used to detect protein interactions.

Vesicular cargo tracking using FRIA

Methodology for cargo labelled vesicular pH determination in live cells by using FRIA has been described in detail before (Apaja et al., 2013; Apaja et al., 2010; Barriere and Lukacs, 2008b). Integrin α5β1 receptor was labelled with anti-α5 (CD49e) and fluorescein isothiocyanate (FITC)-conjugated goat anti-mouse secondary Fab (Jackson ImmunoResearch, USA) on ice and chased for indicated times. Transiently expressed CD4-Ub or CD4tCCUb were used as before (Apaja et al., 2010). Concentrated ascites fluid against CD63/LAMP2 1:1 mixture and the fluid phase marker, FITC-dextran (10 kDa, 50 μg/ml, Molecular Probes) were used as controls for lysosomal delivery. Dextran was endocytosed for 1h and chased for 2 h at 37 °C. Zeiss Observer Z1 (Carl Zeiss MicroImaging) equipped with X-Cite 120Q system (Lumen Dynamics Group Inc.) and MetaFluor software (Molecular Devices) were used to measure fluorescence intensities.

HeLa cell migration/invasion and spreading assays

Migration/invasion assays were performed using xCELLingence system (Roche). 60,000 HeLa cells in serum free media were allowed to migrate for 6h towards 10% FBS medium. In invasion assays, the chamber separating membrane was coated with Matrigel. Invasion was scored after 18h.

Cell spreading: 250,000 cells were plated on FN (20μg/ml) or collagen I for 15min, non-attached cells were removed. The attached cells spread for 45min at 37°C, were fixed, stained with Alexa

549 Phalloidin (Life Technologies inc.), and visualized on a Zeiss Axiovert200 microscope. The relative cell surface area was quantified using ImageJ software (NIH).

Xenograft assays

H1299 and MDA1833 cells were infected with lentivirus carrying shRNA against Endofin. Following puromycin selection and knockdown verification by western blot, 50000 H1299 cells were resuspended in PBS/matrigel and injected subcutaneously in nude mice (Charles River) or 50000 MDA1833 cells were injected into the mammary fatpad of female SCID mice (Charles River). The tumor growth was monitored weekly by measurements of tumor with caliper. Upon reaching critical stage the mice were sacrificed and the tumors collected, weighted and re-verified for presence of Endofin knockdown.

Statistical analysis:

Data were analysed by Student's unpaired t-test or one-way Anova (where applicable). P-values at $p<0.05$ were considered significant and are described in the figure legends.

4.7. Acknowledgements

We thank Dr. Wajin Hong for sharing the Myc-Endofin construct and Drs. Anders Dydensborg and Anna Mourskaya for assistance with xenograft assays. D.K. holds Fonds de la recherche en santé du Quebec doctoral award. S.M. holds McGill Biochemistry Merit Fellowship. A.P. was a recipient of the Canada Research Chair in Molecular Oncology. This work was supported by Canadian Cancer Society Research Institute grant 2010-700525 and Cancer Research Society grant (to A.P.). G.L. is the holder of a Canada Research Chair.

4.9 Supplemental Figures and Figure Legends:

Figure S4.1

HEK293T cells were transfected with Flag-HD-PTP and Myc-Endofin C753S constructs and the immunoprecipitations were performed using Flag antibody as in Figure 4.1A.

Figure S4.2

Co-immunofluorescence experiment of Myc-tagged WT and C753S mutant Endofin with HD-PTP in HeLa cells as in Figure 4.2C. The overexpression of Endofin C753S leads to a disruption in endosomal morphology and distinct HD-PTP localization. Scale bar 10µm.

Figure S4.3

Control or Endofin depleted HeLa cells were transfected with GFP-Integrin α5, serum starved and stimulated with FN for 7 hours. Co-immunofluorescence was performed by staining with early endosomal (EEA1), recycling (transferrin) and lysosomal (LAMP1) markers. Integrin was retained in early and recycling endosomal compartment upon Endofin depletion. Scale bar 10µm.

Figure S4.1

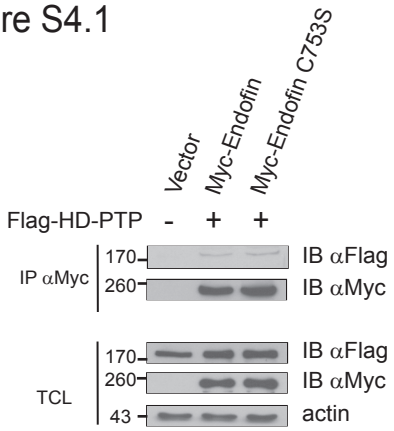

Figure S4.2

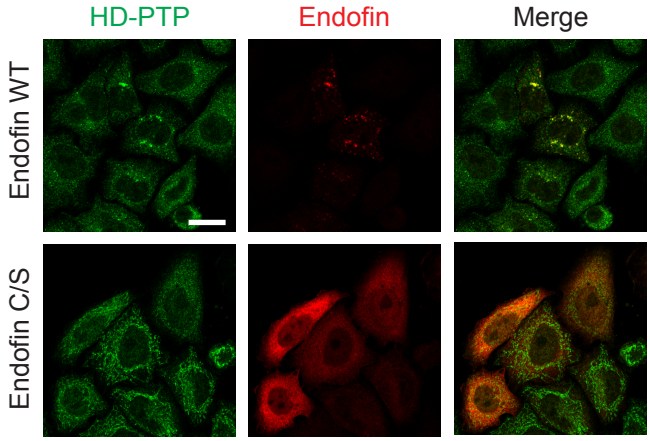

Figure S4.3

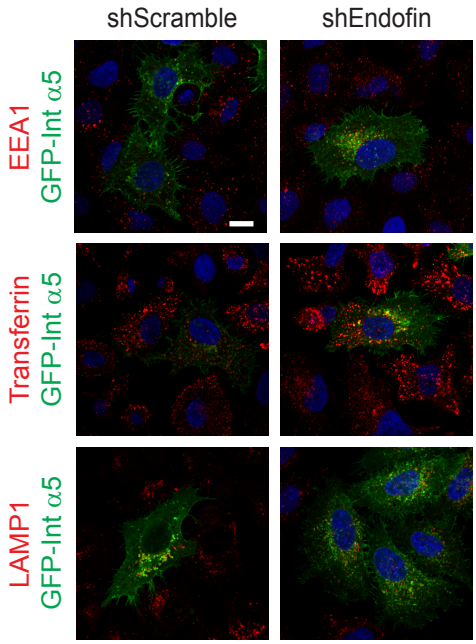

Table 4.1: MS-AP Saint analysis of HD-PTP and Endofin interactions.

Bait Symbol	Prey Accession	Prey Symbol	Spectra	Sum Spectra	Spectral counts in negative controls	SAINT Score
PTPN23	4758012	CLTC	236|160	396	11|0|5|0|8|13|0|0|0|3|11|5|16|15|13|49|13|53|36|27|23|15|12|22	1
PTPN23	157426864	ZFYVE16	23|23	46	0|0|0|0|0|4|0|0|0|0|0|0|0|0|0|0|0|0|0|0|0|0|0	0.96
PTPN23	186928835	LEPRE1	10|6	16	0|0|0|0|0|0|0|0|0|0|0|0|0|0|0|0|0|0|0|0|1|0|0	0.99
PTPN23	4502901	CLTB	4|5	9	0|0|0|0|0|0|0|0|0|0|0|0|0|0|0|0|0|0|0|0|0|0|0	0.97
PTPN23	28827795	CHMP4B	4|3	7	0|0|0|0|0|0|0|0|0|0|0|0|0|0|0|0|0|0|0|0|0|0|0	0.87
ZFYVE16	8394499	UBAP1	64|80	144	0|0|0|0|0|0|0|0|0|0|0|0|0|0|0|0|0|0|0|0|0|0|0	1
ZFYVE16	96974985	CC2D1A	43|43	86	0|0|0|0|1|0|0|0|0|0|0|0|0|0|0|0|0|0|0|1|0|0	1
ZFYVE16	24308073	PTPN23	20|23	43	0|0|0|0|0|0|0|0|0|0|0|0|0|0|0|0|0|0|0|0|0|0|0	1
ZFYVE16	5454140	TSG101	16|15	31	0|0|0|0|0|0|0|0|0|0|0|0|0|0|0|0|0|0|0|0|0|0|0	1
ZFYVE16	223555919	VPS37A	14|14	28	0|0|0|0|0|0|0|0|0|0|0|0|0|0|0|0|0|0|0|0|0|0|0	1
ZFYVE16	15011880	MST4	11|9	20	1|0|0|0|0|0|0|0|0|0|1|0|0|0|2|1|1|0|0|0|1|1|0	0.96
ZFYVE16	20070158	STK24	12|7	19	0|0|0|0|0|0|0|0|0|0|0|0|0|0|2|0|0|0|0|0|0|0	0.81
ZFYVE16	7705885	VPS28	7|6	13	0|0|0|0|0|0|0|0|0|0|0|0|0|0|0|0|0|0|0|0|0|0|0	1
ZFYVE16	28827795	CHMP4B	3|3	6	0|0|0|0|0|0|0|0|0|0|0|0|0|0|0|0|0|0|0|0|0|0|0	0.79

CHAPTER 5:
5. GENERAL DISCUSSION

5.1. Insights on integrin α5β1 sorting mechanism and its physiological impact

In Chapter 2 of this thesis, we have provided a new understanding of the endocytic sorting of integrin α5β1, with an implication into its downstream signalling and cell migration and invasion. While reconciling an important controversy in the mechanism of integrin sorting, we brought up additional questions regarding this process. Which subunit of integrin α5β1 complex is ubiquitinated? How is ubiquitination and consequent sorting of integrin receptor regulated by other receptor crosstalk? What are the clinical relevance of integrin α5β1 ubiquitination and the impact of its sorting in the disease, such as cancer? The relevance of these topics and their potential as research avenues are discussed here.

5.1.1. The impact of ubiquitination on integrin α5β1 endosomal sorting

The ubiquitination of α5β1 complex and its role in receptor downregulation has been now demonstrated extensively. We have provided additional evidence for the high-resolution timecourse of ubiquitination and its dynamic nature, suggesting that USP9x is responsible for the deubiquitination of integrin α5β1 leading to the receptor resensitization and recycling.

However, it remains to be elucidated which subunit of integrin α5β1 complex is directly ubiquitinated and which E3-ligase is responsible for this process. Indeed, the identification of ubiquitination sites in the integrin receptor or the associated components of adhesion complex represents a major challenge. Previous studies suggest that both α5 and β1 subunits can be ubiquitinated, since the mutagenesis of lysine residues in their cytoplasmic tails resulted in decrease in ubiquitination (when only α5 was K/R mutated) or stabilization of α5β1 K/R integrin (Bottcher et al., 2012; Lobert et al., 2010). The K/R mutagenesis of α5β1 subunits was extensive, since all cytoplasmic tail lysines were removed (4K on α5; 7K on β1), including the one in the transmembrane topological sequence. Such mutations might have compromised the receptor function, interaction with adhesion components or alter its endocytic dynamics, thus yielding misleading results regarding the endocytic sorting of non-ubiquitinatable integrin α5β1. Therefore, to locate the ubiquitinated lysine of receptor an individual lysine residue mutagenesis approach is recommended.

It is likely that β1 subunit cytoplasmic tail is not able to accommodate polyubiquitin modification (preliminary data not-shown), because of the scaffolding events of adhesion

complex at this region. Both Kindlin and Talin are bulky molecules, interact in close vicinity on β1 cytoplasmic tail and accommodate additional adhesion scaffold factors upon integrin activation. The buildup of these components might result in sterical hindrance at the cytoplasmic tail of β1 subunit, preventing its modification with polyubiquitin chains. However, α5 subunit cytoplasmic tail is not involved in interaction with the adhesion complex components, it is separated from β1 cytoplasmic tail in the activated integrin heterodimer and therefore may be an attractive target for ubiquitination by a E3-ligase (Takagi and Springer, 2002; Takagi et al., 2003). This hypothesis is further supported by a described decrease in α5 ubiquitination upon K/R mutagenesis of its cytoplasmic tail (Lobert and Stenmark, 2010).

Interestingly, proteomic mass-spectrometry analysis of the cellular factors undergoing ubiquitination has revealed that some integrin adhesion complex components may be ubiquitinated. These include Talin, Vinculin, Paxillin and Src kinase. While their ubiquitination was never demonstrated directly, they might contribute to the ubiquitination status of the α5β1 complex and also may act as factors recruiting the E3-ligase or the DUB to integrin complex (Danielsen et al., 2011).

The E3-ligase is possibly recruited upon the formation of the focal adhesion, immediately prior to the internalization of integrin α5β1 and focal complex recycling. Although, Cbl was proposed to act as the E3-ligase for integrin α5β1 (Kaabeche et al., 2005), the evidence for this mechanism is weak and we were unable to confirm these results (data not shown). To identify the E3-ligase for integrin α5β1, a siRNA library screen can be used, scoring for the integrin plasma membrane stability or the rate of internalization. The efficiency of this screening approach has been demonstrated in Chapter 2 by identification of α5β1 DUB USP9x. Notably, the screen has identified several candidate DUBs, but these were eliminated during the validation of screen results using multiple individual siRNAs.

The recruitment mechanism of USP9x DUB to integrin α5β1 complex is not fully understood. SNX17 binding to integrin α5β1 was described as a protective mechanism for the receptor, rerouting it away from the lysosomal degradation. Therefore, it is possible that SNX17 recruits USP9x to the β1 cytoplasmic tail upon displacement of kindlin-2 by SNX17. This event may

play a dual function: deubiquitinating the receptor complex and sorting of the receptor to tubules at the early endosomes, thus resulting in an efficient recycling of integrins. Moreover, the displacement of kindlin by SNX17 may also be influenced by the pH-dependent ligand dissociation, which is likely to affect the active state of integrins and the conformation of α5β1 cytoplasmic tails.

5.1.2. Sorting implications of integrin α5β1 crosstalk with other integrins and receptors

Integrin α5β1 extensively crosstalks with other cell surface receptors, including RTKs (EGFR, Met, PDGFR and VEGFR), other integrins and GPCRs (Caswell et al., 2008; Muller et al., 2013; White et al., 2007; Xu et al., 1996). The crosstalk can originate through a concomitant activation of signalling pathways, a collaborative signalling between the receptors complexes, direct activation of the receptor by the active integrin in absence of ligand and induction of integrin expression by receptor signalling. The sorting of integrin α5β1 may have several implications on receptor signalling and may be the subject of regulation by other receptors.

Indeed, integrin α5β1 recycling is negatively regulated by αvβ3 (White et al., 2007). In addition, we describe profound effects of αvβ3 integrin inhibition on integrin α5β1 endocytosis, turnover and recycling. While the inhibition of αvβ3 integrin with Cilengitide typically results in an accelerated α5β1 recycling due to the potentiated recruitment of RCP to α5β1 (Caswell et al., 2007; Mai et al., 2011; Reynolds et al., 2009), little is known about the regulation of endocytosis of these integrins by their crosstalk. We show that the endocytosis rate of α5β1 is decreased upon concomitant inactivation of αvβ3 integrin and E1-Ub-activating enzyme. This suggests an existence of an allosteric regulation of fibronectin receptors endocytosis, in addition to the signalling crosstalk regulating their cell surface recycling.

The signalling cooperation between α5β1 integrin and several RTKs, such as EGFR and Met is well described (Caswell et al., 2008; Mitra et al., 2011; Muller et al., 2013). The signalling downstream of EGFR and Met can be stimulated upon α5β1 activation by the fibronectin matrix engagement. Furthermore, the recycling of EGFR is tightly linked with α5β1 PM return (Caswell et al., 2008). In our studies of EGFR and α5β1 crosstalk, we have identified EGFR kinase activity as a requirement for integrin α5β1 PM stability and internalization. Inhibition of EGFR

signalling with kinase inhibitor Gefitinib, resulted in a rapid internalization and destabilization of α5β1 from plasma membrane, with its subsequent lysosomal delivery (data not shown). Although, the exact molecular mechanism of these events remains to be elucidated, it is possible that the downstream EGFR signalling promotes activity of the integrin recycling machinery and is responsible for its cell surface return (Caswell et al., 2008). These events occur in absence of EGF, suggesting that the signalling from EGFR in these conditions may be due to cross activation of EGFR by active α5β1 or by other HER family receptors.

Integrin α5β1 induced activation of RTKs may be a key signalling event promoting cell proliferative and pro-survival signalling. In certain conditions, such in the context of HD-PTP depletion, the stabilization of α5β1 on cell surface may drive RTKs activation and their downstream signalling. However, dissection of these pathways is challenging due to a broad endosomal function of HD-PTP and of the other ESCRT components, which affects turnover and plasma membrane stability of several cell surface receptors (Ali et al., 2013). Therefore, upon HD-PTP depletion, signalling downstream of cell surface receptors may represent a combinational effect of several signalling cascades with an extensive crosstalk.

5.1.3. Physiological and clinical relevance of endocytic sorting of integrins

A variety of integrin inhibitors (synthetic peptides, antibodies) are tested in the clinical setting as antitumor agents. The inhibition of αvβ3 integrin by Cilengitide (cyclic RGD peptide) is under investigation for treatment of lung, prostate and glioblastoma cancers (Yamada et al., 2006). The compound is well tolerated by patients in the clinical phase I trials, and several ongoing trials are investigating its efficacy in phase II studies (Scaringi et al., 2012). The estimated completion of the key glioblastoma studies that assess Cilengitide efficacy in disease treatment are expected to be completed in 2016. Yet, Cilengitide failed to demonstrate higher efficacy in combinational use with chemotherapeutic agent docetaxel (vs. docetaxel alone) in non-small cell lung cancer (Manegold et al., 2013). Similarly, a non-RGD antagonist of α5β1 (ATN-161) is in clinical trials for breast cancer (Cianfrocca et al., 2006; Khalili et al., 2006). Some monoclonal antibodies against β1 integrin can prevent tumor resistance to therapy and will be entering the clinical trials (Park et al., 2006). Yet, the endocytic sorting of integrins has not been the target of therapeutic applications.

Chloroquine is a lysosomotropic agent, which has a well-known history of usage to treat malaria. Recent discovery of autophagy's protumorigenic function has spiked the clinical interest in chloroquine as an inhibitor of autophagy for tumor treatment (Duffy et al., 2015). Also, chloroquine was demonstrated to play an inhibitory role on breast metastasis formation in mice (Jiang et al., 2010). Here we provide evidence for the chloroquine effect on integrin α5β1 ubiquitination maintenance and its endocytic sorting, with a negative impact on α5β1 recycling and the cell migration. Thus, chloroquine becomes an attractive agent for inhibition of tumor cell invasiveness via its negative effect on integrin recycling in primary tumor. However, the tumor acidic environment represents a potential roadblock for this attractive therapeutic strategy. Typically, tumors are well-known to have a more acidic extracellular environment than normal tissues, partially due to a shift in tumor metabolism towards Warburg metabolism and high lactic acid secretion (Peppicelli et al., 2014). Such acidic environment may abrogate the basic properties of chloroquine before its delivery inside the tumor cells, therefore making the chloroquine treatment of tumor inefficient (Pellegrini et al., 2014).

The intrinsic sensitivity of integrin α5β1 to the acidic environment of endosomes can also be exploited for design of drug delivery nanosystems. Some of the pH-sensitive nanoparticles are in use for the targeted delivery of chemotherapeutic agents via RGD peptide receptors, such as integrins αvβ3 and α5β1 (Danhier et al., 2012). The design of nanoparticles capable of mimicking the FN-α5β1 pH-sensitive dissociation dynamics may allow for a targeted delivery of therapeutic agents to the integrin α5β1 expressing tumors and spatiotemporal regulation of their release in the endolysosomal system (Wang et al., 2009). Moreover, similar nanoparticles could be used in diagnostic and theranostic procedures, aiming to quantify vesicular pH, to control for the particle release or to track intracellular radioactive tracers (Danhier et al., 2012).

In addition to modulating integrin receptor function via direct inhibition, targeting of the machinery involved in integrin sorting should be investigated. As described in Chapter 2, USP9x is the DUB responsible for deubiquitination of α5β1 complex and its cell surface return, thus promoting migration. Thus, inhibition of USP9x becomes an attractive target for modulation of integrin stability and cell migration. However, the existing pharmacological inhibitor (WP1130) of USP9x is not sufficiently specific and the engineered ubiquitin protein constructs inhibitors

cannot be used in vivo, yet (Ernst et al., 2013; Kapuria et al., 2010). In addition, USP9x plays a broad cellular function and affects several pathways, thus it will be crucial to confine the inhibition of USP9x to a specific function of this enzyme. Intriguingly, both USP9x and integrin α5β1 are essential for mediating cancer chemo- and radio-resistance (Kapuria et al., 2010; Schaffner et al., 2013). While the therapy resistance mechanism by USP9x was attributed to its role in MCL1 stabilization and apoptosis inhibition (Peddaboina et al., 2012; Schwickart et al., 2010), it becomes evident that USP9x can also contribute to the integrin mediated therapy resistance by promoting the receptor stabilization. Such dual impact of USP9x on chemo- and radio- resistance in tumors is indicative of a central role that this DUB plays in cancer (Peng et al., 2013).

Altogether, the findings on integrin α5β1 sorting mechanism outlined in this thesis open a number of new avenues for the cancer therapy and metastasis control.

5.2. Death receptor sorting in inflammation, survival and apoptosis

In addition to studying the mechanism of integrin sorting, we have investigated the impact of the ESCRT pathway on signalling of TNFR1. Tumor necrosis factor receptor's signalling is well studied, but the role of the endocytic machinery in this process is unknown. We have identified ESCRT component HD-PTP as a key modulator of TNFR1 signalling and TNFR1 induced apoptosis. Here we discuss the implication of defects of the ESCRT machinery on TNFR1 signalling, from physiological and disease relevant perspective.

5.2.1. Spatiotemporal regulation of TNFR1 signalling

Signalling downstream of TNFR1 is tightly regulated by multiple events of phosphorylation, ubiquitination and transcription feedback loops. In addition, TNFR1 signalling complexes are segregated spatiotemporally: the TNFR1-SCI signals from PM to activate NF-κB pathway, while the apoptosis-inducing TNFR1-SCII is localised to endosomes (Micheau and Tschopp, 2003; Schutze et al., 2008). Strikingly, the depletion of the ESCRT component HD-PTP resulted in upregulation of the signalling downstream of both complexes.

TNFR1 was reported to be K63 polyubiquitinated, therefore its postendocytic sorting and degradation are very likely to be orchestrated by the ESCRT machinery (Fritsch et al., 2014).

Indeed, we observed a notable increase in the cell surface levels of TNFR1 upon depletion of HD-PTP, consistent with HD-PTP role in ubiquitinated receptor downregulation. Increased plasma membrane presence of TNFR1 led to a higher abundance of the TNFR1-SCI and accelerated activation of the NF-κB pathway. This phenotype is not unique to the depletion of HD-PTP, since UBAP1 downregulation resulted in similar effect, suggesting that depletion of the ESCRT machinery promotes TNFα induced NF-κB activation.

ESCRT depletion mediated effect on cell surface receptors stability can be explained by the lack of receptor degradation through the MVB pathway in absence of ESCRTs. In addition, the ESCRT depletion may lead to an accumulation of the ubiquitinated receptors at the early endosomes and potentiate their signalling from this compartment. TNFR1-SCII is formed upon TNFR1 ubiquitination, internalization and endosomal delivery. From this location, the TNFR1-SCII activates the caspase cascade and apoptosis (Micheau and Tschopp, 2003; Ramakrishnan and Baltimore, 2011). The increased residency time of the TNFR1-SCII on the endosomes in HD-PTP depleted cells resulted in a higher caspase-3 cleavage and apoptosis induction. However, these phenotypes could only be observed upon a translational inhibition of NF-κB survival program induced downstream of the TNFR1-SCI (Dillon et al., 2012; Pop et al., 2011). Therefore, HD-PTP (and other ESCRTs) plays a dual role in the attenuation of both TNFR1 signalling complexes by regulating the receptor cell surface levels and the residency time at the early endosomes. Such dual function in TNFR1 signalling may be a common regulatory mechanism, since adaptor protein Sam68 was previously described to be required for the formation and signalling of both TNFR1 signalling complexes (Ramakrishnan and Baltimore, 2011).

Despite of the recent advances in understanding of the TNFR1 trafficking and signalling regulation by compartmentalization, several aspects of the regulation of TNFR1 sorting are incompletely understood. Does TNFR1 undergo a pH-dependent ligand dissociation and resensitization similar to other receptors? How is the recycling of TNFR1 coordinated?

TNFR1 is activated following ligand binding and receptor trimerization, which recruits the signalling scaffold (TRADD, TRAF2, RIP1, etc.) (Li et al., 2006; Ofengeim and Yuan, 2013).

This complex and TNFR1 ubiquitination are preserved upon TNFR1 localization to endosomes, suggesting that the trimeric receptor conformation, accommodating the binding of TRADD, is maintained in this compartment (Fritsch et al., 2014). Thus, even if TNFα ligand dissociates from the receptor in the lumen of an acidic endosome, this event does not impact the conformation of the cytoplasmic domain of the receptor and the binding of TRADD and RIP1, allowing for the efficient recruitment of DISC factors FADD and Caspase-8 (Dillon et al., 2012; Fritsch et al., 2014; Pop et al., 2011).

5.2.2. TNFR1 sorting in inflammation and cancer

Chronic inflammation is a well-established hallmark of cancer, promoting cancer aggressiveness and tumor immune invasion. Signalling downstream of TNFR1-SCI leads to a proinflammatory NF-κB signalling and transcriptional induction of several interleukins (IL-6, IL8) and chemokines (Landskron et al., 2014; Ofengeim and Yuan, 2013). TNFα induced NF-κB transcriptional program and IL-6 secretion are stimulated upon HD-PTP depletion, resulting in an environment rich in pro-inflammatory factors. Similar effect on IL-6 secretion was observed upon downregulation of the other ESCRTs (UBAP1 and TSG101, data not shown), suggesting that TNFα-induced proinflammatory factors secretion is a common event in the ESCRT deficient cells. Upregulated IL-6 secretion can act in autocrine and paracrine fashion to promote proliferation, survival and the metastatic progression of tumors, as well as assist in the recruitment of macrophages to tumor surroundings and dendritic cells differentiation (Cho et al., 2009; Gerlach et al., 2011; Landskron et al., 2014).

Loss of expression of HD-PTP and other ESCRTs is common in several cancers (Manteghi et al., submitted manuscript). Moreover, the loss of HD-PTP expression is correlated with increased expression of pro-inflammatory cytokines in tumors, including IL-6. This suggests that the ESCRT deficiency in tumors may promote the inflammation and drive tumor progression via the inflammatory signalling and immune cells response. Also, the deficiency of ESCRTs in tumor stroma may result in a similar effect on pro-inflammatory factor secretion in the tumor vicinity and/or macrophages recruitment to tumor, thus further contributing to tumor aggressiveness (De Plaen et al., 2006; Phillips et al., 2001). Preliminary evidence of ESCRT deficiency contribution

to the tumor promoting microenvironment comes from HD-PTP deficient mouse model, where the systemic heterozygous deletion of HD-PTP results in accelerated ectopic Eμ-Myc lymphoma development and growth (Manteghi et al., submitted manuscript). This phenotype may be partially attributed to increased levels of certain pro-inflammatory cytokines in serum of the HD-PTP deficient mice, likely contributing to the lymphoma growth.

Altogether, these findings suggest that HD-PTP and other ESCRTs attenuate TNFR1 pro-inflammatory signalling and the loss of their expression may be an indicator of inflammatory response in the tumor tissue or in the tumor surrounding microenvironment.

5.3. Novel insights in ESCRT pathway and its cellular function

The ESCRT pathway has long been established as a key mechanism for the ubiquitinated cell surface receptors downregulation via lysosomal targeting. The new players in ESCRT machinery and their novel functions continue to emerge. Here, we describe our contribution to the understanding of the ESCRT associated protein HD-PTP and its interacting partners, as well as their contribution to the cell biology and physiological processes.

5.3.1. HD-PTP as a central regulator of ESCRT efficiency

Originally, HD-PTP was described as an ESCRT-associated protein, assisting the MVB formation and ubiquitinated cargo degradation. More recent studies position HD-PTP as a central coordinator of ESCRT-0 to –III exchange and as a recruiting factor for the deubiquitinating enzyme UBPY/USP8, required for cargo deubiquitination, prior to cargo packaging within MVB (Ali et al., 2013). Interestingly, the yeast orthologue of HD-PTP, Bro1, also contributes to Doa4-mediated (UBPY/USP8 yeast orthologue) cargo deubiquitination by promoting its catalytic activity (Richter et al., 2013). It is unknown whether HD-PTP can exert a similar effect on UPBY/USP8 in mammalian cells and the investigation of this paradigm may be challenging due to a lack of in vitro expression tool for both proteins.

While involved in the polyubiquitin-dependent cargo sorting, HD-PTP does not contain any classic ubiquitin binding domains, such as UBD, UIM or VHS. However, the V-domain of HD-PTP was reported to interact with the K63 polyubiquitin, similarly to the other V-domains of related proteins (Bro1 and Alix). The structural analysis of HD-PTP V-domain has suggested a

few residues in the α-helix of V-domain (SLYSKEE motif) potentially responsible for the Ub recognition (Rob Piper, personal communications). However, the functional essays of such HD-PTP V-domain mutant have not revealed a significant impact on the sorting of the ubiquitinated cargo (i.e. integrin α5β1), indicating that the V-domain Ub-binding might be dispensable for ESCRT function or it may be compensated by the ubiquitin recognition function of other ESCRT components.

Importantly, HD-PTP is required for the overall stability of the ESCRT machinery. We observed a drastic destabilization of the ESCRT-0 and –I constituents upon HD-PTP depletion, without a significant perturbation of the ESCRT complex formation. This suggests that the formation of stable and functional ESCRT complexes is dependent on HD-PTP expression levels. In addition, HD-PTP mediated recruitment of UBPY/USP8 may contribute to the ESCRT stability, since this DUB was described to be responsible for the protection of ESCRT-0 from degradation (Zhang et al., 2014). Therefore, loss-of-expression of HD-PTP in tumors might compromise the integrity and function of the ESCRT machinery as a whole, further supporting the tumor suppressive potetnial of HD-PTP and of the ESCRT pathway.

5.3.2. Novel constituents of ESCRT machinery and their function

While studying the cellular function of HD-PTP, we have identified several interacting partners of HD-PTP by mass-spectrometry. One of them is Endofin, an endosomal protein responsible for recruitment of TOM1 and clathrin to the early endosomes (Seet and Hong, 2001, 2005; Seet et al., 2004). Analysis of the cellular function of Endofin/TOM1 molecular complex has suggested a significant involvement of Endofin in polyubiquitinated cargo recognition and its subsequent delivery to the lysosomal degradation. Previously, Endofin/TOM1 has been proposed to act as an alternative ESCRT-0 complex, which has evolved before the classical Hrs/Stam1 containing ESCRT-0 (Clague et al., 2012; Wang et al., 2010).

Strikingly, Endofin and Hrs/Stam1 share the same binding site on HD-PTP in the Bro-domain, indicating that HD-PTP can act as a universal adaptor for both ESCRT-0 complexes in a mutually exclusive manner. This property of HD-PTP may allow a funneling of ubiquitinated cargo bound to either of the ESCRT-0 complexes to the later stages of ESCRT pathway. Moreover, both HD-PTP and Endofin were found to interact with clathrin heavy chain, an

important feature that assists ESCRT-0 function of cargo clustering on the endosomal membrane (Seet and Hong, 2005).

So why would a mammalian cell require two separate ESCRT-0 complexes performing the same function? A tempting hypothesis is that the two complexes are distributed differentially across endosomes and recognize different types of polyubiquitinated cargoes. Endofin has no reported ubiquitin binding domains, but interacts with TOM1 that contains GGA and VHS domains (Kawasaki et al., 2005; Shiba et al., 2004). So far, no thorough analysis of Endofin/TOM1 polyubiquitin chain preferences was performed, but both were efficient in pulling down recombinant polyubiquitin chains mimicking the K63-linken polyubiquitin conformation. Also, Hrs/Stam1 containing endosomes and Endofin/TOM1 containing endosomes may receive cargo from the different endocytosis routes (i.e. CME and non-CME endocytosis).

A function in the endosomal motility may be an additional role for Endofin/TOM1 complex. TOM1 was reported to interact with myosin VI, a microtubule motor protein responsible for the autophagosome delivery to the lysosome (Tumbarello et al., 2012). This interaction also allows TOM1 to act as an autophagosomal cargo adaptor, as well as to deliver the endosomal vesicles for fusion with autophagosome/lysosome (Tumbarello et al., 2012). Such a dual role of TOM1 in both endosomal and autophagic vesicle trafficking may be a result of its primordial ESCRT function in primitive organisms, where the same adaptor molecules were employed for the endosomal and for the autophagic pathways. However, TOM1 may be involved in the autophagosome delivery and transport independently of Endofin. The latter has not been reported to be involved in autophagy processing or endosome motility. Likely, TOM1 pool can be distributed between the different complexes, each executing a specific function that requires TOM1 as an adaptor protein.

5.3.3. ESCRT in disease

As outlined in Chapter 1, ESCRT proteins may act as tumor suppressor genes. Our studies of HD-PTP function *in vivo* (not part of this thesis) have confirmed the tumor suppressive potential of HD-PTP in several tumor models (Manteghi et al., submitted manuscript). Moreover, HD-PTP deficiency conferred a more invasive tumor phenotype, consistent with its inhibitory role in integrin-dependent cell migration. These observations, and the reported downregulation of HD-

PTP expression in tumors, suggest that HD-PTP status in tumors can be used as a relevant biomarker for evaluation of the tumor progression or aggressiveness. A similar use may be proposed for another ESCRT component, Vps37a, which appears to significantly downregulated in cancers (Wittinger et al., 2011).

In addition to their potential use as cancer-relevant biomarkers, some ESCRT proteins may be considered as therapy targets. These include ESCRT components involved in other cellular processes, such as cytokinesis and viral budding. TSG101, Alix and CHMP4b are required for cytokinesis (Dukes et al., 2008; Morita et al., 2007), thus inhibition of CHMP4b oligomerization or Alix dimerization at midbody could be an avenue for inhibition of cell proliferation. Due to their broad role in membrane sculpting and fission, these proteins are also essential for HIV viral release (Im et al., 2010; Ren and Hurley, 2011a; Sette et al., 2012). Antiviral compound mediated inhibition of HIV Gag protein interaction with TSG101 UEV domain or Alix Gag interaction results in efficient decrease of viral release, without affecting their endosomal sorting functions (Im et al., 2010). Therefore, targeting ESCRT machinery may become an attractive approach to control viral replication in humans.

Altogether, these notions outline a potential clinical role of ESCRT pathway in the fields of cancer prognosis, therapy and anti-viral therapies development.

6. BIBLIOGRAPHY

Agromayor, M., Soler, N., Caballe, A., Kueck, T., Freund, S.M., Allen, M.D., Bycroft, M., Perisic, O., Ye, Y., McDonald, B., *et al.* (2012). The UBAP1 subunit of ESCRT-I interacts with ubiquitin via a SOUBA domain. Structure *20*, 414-428.

Akutsu, M., Kawasaki, M., Katoh, Y., Shiba, T., Yamaguchi, Y., Kato, R., Kato, K., Nakayama, K., and Wakatsuki, S. (2005). Structural basis for recognition of ubiquitinated cargo by Tom1-GAT domain. FEBS letters *579*, 5385-5391.

Ali, N., Zhang, L., Taylor, S., Mironov, A., Urbe, S., and Woodman, P. (2013). Recruitment of UBPY and ESCRT exchange drive HD-PTP-dependent sorting of EGFR to the MVB. Current biology : CB *23*, 453-461.

Allaire, P.D., Seyed Sadr, M., Chaineau, M., Seyed Sadr, E., Konefal, S., Fotouhi, M., Maret, D., Ritter, B., Del Maestro, R.F., and McPherson, P.S. (2013). Interplay between Rab35 and Arf6 controls cargo recycling to coordinate cell adhesion and migration. Journal of cell science *126*, 722-731.

Andersen, K.M., Hofmann, K., and Hartmann-Petersen, R. (2005). Ubiquitin-binding proteins: similar, but different. Essays in biochemistry *41*, 49-67.

Angers, A., Ramjaun, A.R., and McPherson, P.S. (2004). The HECT domain ligase itch ubiquitinates endophilin and localizes to the trans-Golgi network and endosomal system. The Journal of biological chemistry *279*, 11471-11479.

Apaja, P.M., Foo, B., Okiyoneda, T., Valinsky, W.C., Barriere, H., Atanasiu, R., Ficker, E., Lukacs, G.L., and Shrier, A. (2013). Ubiquitination-dependent quality control of hERG K+ channel with acquired and inherited conformational defect at the plasma membrane. Molecular biology of the cell *24*, 3787-3804.

Apaja, P.M., Xu, H., and Lukacs, G.L. (2010). Quality control for unfolded proteins at the plasma membrane. The Journal of cell biology *191*, 553-570.

Arjonen, A., Alanko, J., Veltel, S., and Ivaska, J. (2012). Distinct recycling of active and inactive beta1 integrins. Traffic *13*, 610-625.

Asao, H., Sasaki, Y., Arita, T., Tanaka, N., Endo, K., Kasai, H., Takeshita, T., Endo, Y., Fujita, T., and Sugamura, K. (1997). Hrs is associated with STAM, a signal-transducing adaptor molecule. Its suppressive effect on cytokine-induced cell growth. The Journal of biological chemistry *272*, 32785-32791.

Azakir, B.A., and Angers, A. (2009). Reciprocal regulation of the ubiquitin ligase Itch and the epidermal growth factor receptor signaling. Cellular signalling *21*, 1326-1336.

Babst, M. (2005). A protein's final ESCRT. Traffic *6*, 2-9.

Babst, M., Katzmann, D.J., Estepa-Sabal, E.J., Meerloo, T., and Emr, S.D. (2002a). Escrt-III: an endosome-associated heterooligomeric protein complex required for mvb sorting. Developmental cell *3*, 271-282.

Babst, M., Katzmann, D.J., Snyder, W.B., Wendland, B., and Emr, S.D. (2002b). Endosome-associated complex, ESCRT-II, recruits transport machinery for protein sorting at the multivesicular body. Developmental cell *3*, 283-289.

Bache, K.G., Raiborg, C., Mehlum, A., and Stenmark, H. (2003). STAM and Hrs are subunits of a multivalent ubiquitin-binding complex on early endosomes. The Journal of biological chemistry *278*, 12513-12521.
Bache, K.G., Slagsvold, T., Cabezas, A., Rosendal, K.R., Raiborg, C., and Stenmark, H. (2004). The growth-regulatory protein HCRP1/hVps37A is a subunit of mammalian ESCRT-I and mediates receptor down-regulation. Molecular biology of the cell *15*, 4337-4346.
Bache, K.G., Stuffers, S., Malerod, L., Slagsvold, T., Raiborg, C., Lechardeur, D., Walchli, S., Lukacs, G.L., Brech, A., and Stenmark, H. (2006). The ESCRT-III subunit hVps24 is required for degradation but not silencing of the epidermal growth factor receptor. Molecular biology of the cell *17*, 2513-2523.
Barczyk, M., Carracedo, S., and Gullberg, D. (2010). Integrins. Cell and tissue research *339*, 269-280.
Barriere, H., and Lukacs, G.L. (2008a). Analysis of endocytic trafficking by single-cell fluorescence ratio imaging. Current protocols in cell biology / editorial board, Juan S Bonifacino [et al] *Chapter 15*, Unit 15.13.
Barriere, H., and Lukacs, G.L. (2008b). Analysis of endocytic trafficking by single-cell fluorescence ratio imaging. Current protocols in cell biology / editorial board, Juan S Bonifacino [et al] *Chapter 15*, Unit 15 13.
Barriere, H., Nemes, C., Du, K., and Lukacs, G.L. (2007a). Plasticity of polyubiquitin recognition as lysosomal targeting signals by the endosomal sorting machinery. Molecular biology of the cell *18*, 3952-3965.
Barriere, H., Nemes, C., Du, K., and Lukacs, G.L. (2007b). Plasticity of Polyubiquitin Recognition as Lysosomal Targeting Signals by the Endosomal Sorting Machinery. Molecular biology of the cell *18*, 3952-3965.
Barriere, H., Nemes, C., Lechardeur, D., Khan-Mohammad, M., Fruh, K., and Lukacs, G.L. (2006a). Molecular Basis of Oligoubiquitin-Dependent Internalization of Membrane Proteins in Mammalian Cells. Traffic *7*, 282-297.
Barriere, H., Nemes, C., Lechardeur, D., Khan-Mohammad, M., Fruh, K., and Lukacs, G.L. (2006b). Molecular basis of oligoubiquitin-dependent internalization of membrane proteins in Mammalian cells. Traffic (Copenhagen, Denmark) *7*, 282-297.
Bashkirov, P.V., Akimov, S.A., Evseev, A.I., Schmid, S.L., Zimmerberg, J., and Frolov, V.A. (2008). GTPase cycle of dynamin is coupled to membrane squeeze and release, leading to spontaneous fission. Cell *135*, 1276-1286.
Beglova, N., Blacklow, S.C., Takagi, J., and Springer, T.A. (2002). Cysteine-rich module structure reveals a fulcrum for integrin rearrangement upon activation. Nature structural biology *9*, 282-287.
Bhandari, D., Trejo, J., Benovic, J.L., and Marchese, A. (2007). Arrestin-2 interacts with the ubiquitin-protein isopeptide ligase atrophin-interacting protein 4 and mediates endosomal sorting of the chemokine receptor CXCR4. The Journal of biological chemistry *282*, 36971-36979.
Bilodeau, P.S., Urbanowski, J.L., Winistorfer, S.C., and Piper, R.C. (2002). The Vps27p Hse1p complex binds ubiquitin and mediates endosomal protein sorting. Nature cell biology *4*, 534-539.
Blackwell, K., Zhang, L., Workman, L.M., Ting, A.T., Iwai, K., and Habelhah, H. (2013). Two coordinated mechanisms underlie tumor necrosis factor alpha-induced immediate and delayed IkappaB kinase activation. Molecular and cellular biology *33*, 1901-1915.

Blanc, C., Charette, S.J., Mattei, S., Aubry, L., Smith, E.W., Cosson, P., and Letourneur, F. (2009). Dictyostelium Tom1 participates to an ancestral ESCRT-0 complex. Traffic (Copenhagen, Denmark) *10*, 161-171.
Bocking, T., Aguet, F., Harrison, S.C., and Kirchhausen, T. (2011). Single-molecule analysis of a molecular disassemblase reveals the mechanism of Hsc70-driven clathrin uncoating. Nature structural & molecular biology *18*, 295-301.
Bottcher, R.T., Stremmel, C., Meves, A., Meyer, H., Widmaier, M., Tseng, H.Y., and Fassler, R. (2012). Sorting nexin 17 prevents lysosomal degradation of beta1 integrins by binding to the beta1-integrin tail. Nature cell biology *14*, 584-592.
Bowers, K., Piper, S.C., Edeling, M.A., Gray, S.R., Owen, D.J., Lehner, P.J., and Luzio, J.P. (2006). Degradation of endocytosed epidermal growth factor and virally ubiquitinated major histocompatibility complex class I is independent of mammalian ESCRTII. The Journal of biological chemistry *281*, 5094-5105.
Brankatschk, B., Wichert, S.P., Johnson, S.D., Schaad, O., Rossner, M.J., and Gruenberg, J. (2012). Regulation of the EGF transcriptional response by endocytic sorting. Science signaling *5*, ra21.
Broussard, J.A., Webb, D.J., and Kaverina, I. (2008). Asymmetric focal adhesion disassembly in motile cells. Current opinion in cell biology *20*, 85-90.
Brummelkamp, T.R., Nijman, S.M., Dirac, A.M., and Bernards, R. (2003). Loss of the cylindromatosis tumour suppressor inhibits apoptosis by activating NF-kappaB. Nature *424*, 797-801.
Bryant, D.M., Kerr, M.C., Hammond, L.A., Joseph, S.R., Mostov, K.E., Teasdale, R.D., and Stow, J.L. (2007). EGF induces macropinocytosis and SNX1-modulated recycling of E-cadherin. Journal of cell science *120*, 1818-1828.
Budhidarmo, R., Nakatani, Y., and Day, C.L. (2012). RINGs hold the key to ubiquitin transfer. Trends in biochemical sciences *37*, 58-65.
Byron, A., Morgan, M.R., and Humphries, M.J. (2010). Adhesion signalling complexes. Current biology : CB *20*, R1063-1067.
Cai, C., Zhang, D., Lu, P., Gao, Y., and Chang, J. (2008). [Expression and its significance of TSG101 in lung cancer tissue and lung cancer cell lines.]. Zhongguo fei ai za zhi = Chinese journal of lung cancer *11*, 172-177.
Castiglioni, S., Maier, J.A., and Mariotti, M. (2007). The tyrosine phosphatase HD-PTP: A novel player in endothelial migration. Biochemical and biophysical research communications *364*, 534-539.
Caswell, P.T., Chan, M., Lindsay, A.J., McCaffrey, M.W., Boettiger, D., and Norman, J.C. (2008). Rab-coupling protein coordinates recycling of alpha5beta1 integrin and EGFR1 to promote cell migration in 3D microenvironments. The Journal of cell biology *183*, 143-155.
Caswell, P.T., and Norman, J.C. (2006). Integrin trafficking and the control of cell migration. Traffic *7*, 14-21.
Caswell, P.T., Spence, H.J., Parsons, M., White, D.P., Clark, K., Cheng, K.W., Mills, G.B., Humphries, M.J., Messent, A.J., Anderson, K.I., *et al.* (2007). Rab25 associates with alpha5beta1 integrin to promote invasive migration in 3D microenvironments. Developmental cell *13*, 496-510.

Chao, W.T., and Kunz, J. (2009). Focal adhesion disassembly requires clathrin-dependent endocytosis of integrins. FEBS letters *583*, 1337-1343.
Chen, D.Y., Li, M.Y., Wu, S.Y., Lin, Y.L., Tsai, S.P., Lai, P.L., Lin, Y.T., Kuo, J.C., Meng, T.C., and Chen, G.C. (2012). The Bro1-domain-containing protein Myopic/HDPTP coordinates with Rab4 to regulate cell adhesion and migration. Journal of cell science *125*, 4841-4852.
Chen, N.J., Chio, II, Lin, W.J., Duncan, G., Chau, H., Katz, D., Huang, H.L., Pike, K.A., Hao, Z., Su, Y.W., *et al.* (2008). Beyond tumor necrosis factor receptor: TRADD signaling in toll-like receptors. Proceedings of the National Academy of Sciences of the United States of America *105*, 12429-12434.
Chen, Y.G., Wang, Z., Ma, J., Zhang, L., and Lu, Z. (2007). Endofin, a FYVE domain protein, interacts with Smad4 and facilitates transforming growth factor-beta signaling. The Journal of biological chemistry *282*, 9688-9695.
Chen, Z.J., and Sun, L.J. (2009). Nonproteolytic functions of ubiquitin in cell signaling. Molecular cell *33*, 275-286.
Cho, Y.S., Challa, S., Moquin, D., Genga, R., Ray, T.D., Guildford, M., and Chan, F.K. (2009). Phosphorylation-driven assembly of the RIP1-RIP3 complex regulates programmed necrosis and virus-induced inflammation. Cell *137*, 1112-1123.
Choi, C.K., Vicente-Manzanares, M., Zareno, J., Whitmore, L.A., Mogilner, A., and Horwitz, A.R. (2008). Actin and alpha-actinin orchestrate the assembly and maturation of nascent adhesions in a myosin II motor-independent manner. Nature cell biology *10*, 1039-1050.
Christofferson, D.E., Li, Y., Hitomi, J., Zhou, W., Upperman, C., Zhu, H., Gerber, S.A., Gygi, S., and Yuan, J. (2012). A novel role for RIP1 kinase in mediating TNFalpha production. Cell death & disease *3*, e320.
Cianfrocca, M.E., Kimmel, K.A., Gallo, J., Cardoso, T., Brown, M.M., Hudes, G., Lewis, N., Weiner, L., Lam, G.N., Brown, S.C., *et al.* (2006). Phase 1 trial of the antiangiogenic peptide ATN-161 (Ac-PHSCN-NH(2)), a beta integrin antagonist, in patients with solid tumours. British journal of cancer *94*, 1621-1626.
Clague, M.J., Barsukov, I., Coulson, J.M., Liu, H., Rigden, D.J., and Urbe, S. (2013). Deubiquitylases from genes to organism. Physiological reviews *93*, 1289-1315.
Clague, M.J., Liu, H., and Urbe, S. (2012). Governance of endocytic trafficking and signaling by reversible ubiquitylation. Developmental cell *23*, 457-467.
Clague, M.J., Urbe, S., Aniento, F., and Gruenberg, J. (1994). Vacuolar ATPase activity is required for endosomal carrier vesicle formation. The Journal of biological chemistry *269*, 21-24.
Cocucci, E., Aguet, F., Boulant, S., and Kirchhausen, T. (2012). The first five seconds in the life of a clathrin-coated pit. Cell *150*, 495-507.
Cohen, P., and Frame, S. (2001). The renaissance of GSK3. Nature reviews Molecular cell biology *2*, 769-776.
Corallino, S., Malabarba, M.G., Zobel, M., Di Fiore, P.P., and Scita, G. (2015). Epithelial-to-Mesenchymal Plasticity Harnesses Endocytic Circuitries. Frontiers in oncology *5*, 45.
Courbard, J.R., Fiore, F., Adelaide, J., Borg, J.P., Birnbaum, D., and Ollendorff, V. (2002). Interaction between two ubiquitin-protein isopeptide ligases of different classes, CBLC and AIP4/ITCH. The Journal of biological chemistry *277*, 45267-45275.

Curtiss, M., Jones, C., and Babst, M. (2007). Efficient cargo sorting by ESCRT-I and the subsequent release of ESCRT-I from multivesicular bodies requires the subunit Mvb12. Molecular biology of the cell *18*, 636-645.
Dai, J., Li, J., Bos, E., Porcionatto, M., Premont, R.T., Bourgoin, S., Peters, P.J., and Hsu, V.W. (2004). ACAP1 promotes endocytic recycling by recognizing recycling sorting signals. Developmental cell *7*, 771-776.
Dai, Y., Liu, Y., Huang, D., Yu, C., Cai, G., Pi, L., Ren, C., Chen, G.Z., Tian, Y., and Zhang, X. (2012). Increased expression of Rab coupling protein in squamous cell carcinoma of the head and neck and its clinical significance. Oncology letters *3*, 1231-1236.
Danhier, F., Le Breton, A., and Preat, V. (2012). RGD-based strategies to target alpha(v) beta(3) integrin in cancer therapy and diagnosis. Molecular pharmaceutics *9*, 2961-2973.
Danielsen, J.M., Sylvestersen, K.B., Bekker-Jensen, S., Szklarczyk, D., Poulsen, J.W., Horn, H., Jensen, L.J., Mailand, N., and Nielsen, M.L. (2011). Mass spectrometric analysis of lysine ubiquitylation reveals promiscuity at site level. Molecular & cellular proteomics : MCP *10*, M110 003590.
Dannhauser, P.N., and Ungewickell, E.J. (2012). Reconstitution of clathrin-coated bud and vesicle formation with minimal components. Nature cell biology *14*, 634-639.
Davies, B.A., Azmi, I.F., Payne, J., Shestakova, A., Horazdovsky, B.F., Babst, M., and Katzmann, D.J. (2010). Coordination of substrate binding and ATP hydrolysis in Vps4-mediated ESCRT-III disassembly. Molecular biology of the cell *21*, 3396-3408.
Davis, C.G., Goldstein, J.L., Sudhof, T.C., Anderson, R.G., Russell, D.W., and Brown, M.S. (1987). Acid-dependent ligand dissociation and recycling of LDL receptor mediated by growth factor homology region. Nature *326*, 760-765.
De Plaen, I.G., Han, X.B., Liu, X., Hsueh, W., Ghosh, S., and May, M.J. (2006). Lipopolysaccharide induces CXCL2/macrophage inflammatory protein-2 gene expression in enterocytes via NF-kappaB activation: independence from endogenous TNF-alpha and platelet-activating factor. Immunology *118*, 153-163.
De, S., Dermawan, J.K., and Stark, G.R. (2014). EGF receptor uses SOS1 to drive constitutive activation of NFkappaB in cancer cells. Proceedings of the National Academy of Sciences of the United States of America *111*, 11721-11726.
Degterev, A., Hitomi, J., Germscheid, M., Ch'en, I.L., Korkina, O., Teng, X., Abbott, D., Cuny, G.D., Yuan, C., Wagner, G.*, et al.* (2008). Identification of RIP1 kinase as a specific cellular target of necrostatins. Nature chemical biology *4*, 313-321.
del Rio, A., Perez-Jimenez, R., Liu, R., Roca-Cusachs, P., Fernandez, J.M., and Sheetz, M.P. (2009). Stretching single talin rod molecules activates vinculin binding. Science *323*, 638-641.
Digman, M.A., Brown, C.M., Horwitz, A.R., Mantulin, W.W., and Gratton, E. (2008). Paxillin dynamics measured during adhesion assembly and disassembly by correlation spectroscopy. Biophysical journal *94*, 2819-2831.
Dillon, C.P., Oberst, A., Weinlich, R., Janke, L.J., Kang, T.B., Ben-Moshe, T., Mak, T.W., Wallach, D., and Green, D.R. (2012). Survival function of the FADD-CASPASE-8-cFLIP(L) complex. Cell reports *1*, 401-407.
Doherty, G.J., Ahlund, M.K., Howes, M.T., Moren, B., Parton, R.G., McMahon, H.T., and Lundmark, R. (2011). The endocytic protein GRAF1 is directed to cell-matrix adhesion sites and regulates cell spreading. Molecular biology of the cell *22*, 4380-4389.

Dowlatshahi, D.P., Sandrin, V., Vivona, S., Shaler, T.A., Kaiser, S.E., Melandri, F., Sundquist, W.I., and Kopito, R.R. (2012). ALIX is a Lys63-specific polyubiquitin binding protein that functions in retrovirus budding. Developmental cell *23*, 1247-1254.
Doyotte, A., Mironov, A., McKenzie, E., and Woodman, P. (2008). The Bro1-related protein HD-PTP/PTPN23 is required for endosomal cargo sorting and multivesicular body morphogenesis. Proceedings of the National Academy of Sciences of the United States of America *105*, 6308-6313.
Dozynkiewicz, M.A., Jamieson, N.B., Macpherson, I., Grindlay, J., van den Berghe, P.V., von Thun, A., Morton, J.P., Gourley, C., Timpson, P., Nixon, C.*, et al.* (2012). Rab25 and CLIC3 collaborate to promote integrin recycling from late endosomes/lysosomes and drive cancer progression. Developmental cell *22*, 131-145.
Duffy, A., Le, J., Sausville, E., and Emadi, A. (2015). Autophagy modulation: a target for cancer treatment development. Cancer chemotherapy and pharmacology *75*, 439-447.
Dukes, J.D., Richardson, J.D., Simmons, R., and Whitley, P. (2008). A dominant-negative ESCRT-III protein perturbs cytokinesis and trafficking to lysosomes. The Biochemical journal *411*, 233-239.
Duval, M., Bedard-Goulet, S., Delisle, C., and Gratton, J.P. (2003). Vascular endothelial growth factor-dependent down-regulation of Flk-1/KDR involves Cbl-mediated ubiquitination. Consequences on nitric oxide production from endothelial cells. The Journal of biological chemistry *278*, 20091-20097.
Ea, C.K., Deng, L., Xia, Z.P., Pineda, G., and Chen, Z.J. (2006). Activation of IKK by TNFalpha requires site-specific ubiquitination of RIP1 and polyubiquitin binding by NEMO. Molecular cell *22*, 245-257.
Ebisawa, T., Fukuchi, M., Murakami, G., Chiba, T., Tanaka, K., Imamura, T., and Miyazono, K. (2001). Smurf1 interacts with transforming growth factor-beta type I receptor through Smad7 and induces receptor degradation. The Journal of biological chemistry *276*, 12477-12480.
Eden, E.R., White, I.J., and Futter, C.E. (2009). Down-regulation of epidermal growth factor receptor signalling within multivesicular bodies. Biochemical Society transactions *37*, 173-177.
Eichhorn, P.J., Rodon, L., Gonzalez-Junca, A., Dirac, A., Gili, M., Martinez-Saez, E., Aura, C., Barba, I., Peg, V., Prat, A.*, et al.* (2012). USP15 stabilizes TGF-beta receptor I and promotes oncogenesis through the activation of TGF-beta signaling in glioblastoma. Nature medicine *18*, 429-435.
Elia, N., Sougrat, R., Spurlin, T.A., Hurley, J.H., and Lippincott-Schwartz, J. (2011). Dynamics of endosomal sorting complex required for transport (ESCRT) machinery during cytokinesis and its role in abscission. Proceedings of the National Academy of Sciences of the United States of America *108*, 4846-4851.
Emmerich, C.H., Ordureau, A., Strickson, S., Arthur, J.S., Pedrioli, P.G., Komander, D., and Cohen, P. (2013). Activation of the canonical IKK complex by K63/M1-linked hybrid ubiquitin chains. Proceedings of the National Academy of Sciences of the United States of America *110*, 15247-15252.
Emmerich, C.H., Schmukle, A.C., Haas, T.L., Gerlach, B., Cordier, S.M., Rieser, E., and Walczak, H. (2011). The linear ubiquitin chain assembly complex forms part of the TNF-R1 signalling complex and is required for effective TNF-induced gene induction and prevents TNF-induced apoptosis. Advances in experimental medicine and biology *691*, 115-126.

Enesa, K., Zakkar, M., Chaudhury, H., Luong le, A., Rawlinson, L., Mason, J.C., Haskard, D.O., Dean, J.L., and Evans, P.C. (2008). NF-kappaB suppression by the deubiquitinating enzyme Cezanne: a novel negative feedback loop in pro-inflammatory signaling. The Journal of biological chemistry *283*, 7036-7045.
Ernst, A., Avvakumov, G., Tong, J., Fan, Y., Zhao, Y., Alberts, P., Persaud, A., Walker, J.R., Neculai, A.M., Neculai, D., *et al.* (2013). A strategy for modulation of enzymes in the ubiquitin system. Science *339*, 590-595.
Erpapazoglou, Z., Dhaoui, M., Pantazopoulou, M., Giordano, F., Mari, M., Leon, S., Raposo, G., Reggiori, F., and Haguenauer-Tsapis, R. (2012). A dual role for K63-linked ubiquitin chains in multivesicular body biogenesis and cargo sorting. Molecular biology of the cell *23*, 2170-2183.
Erpapazoglou, Z., Walker, O., and Haguenauer-Tsapis, R. (2014). Versatile roles of k63-linked ubiquitin chains in trafficking. Cells *3*, 1027-1088.
Ezratty, E.J., Bertaux, C., Marcantonio, E.E., and Gundersen, G.G. (2009). Clathrin mediates integrin endocytosis for focal adhesion disassembly in migrating cells. The Journal of cell biology *187*, 733-747.
Felder, S., Miller, K., Moehren, G., Ullrich, A., Schlessinger, J., and Hopkins, C.R. (1990). Kinase activity controls the sorting of the epidermal growth factor receptor within the multivesicular body. Cell *61*, 623-634.
Filimonenko, M., Stuffers, S., Raiborg, C., Yamamoto, A., Malerod, L., Fisher, E.M., Isaacs, A., Brech, A., Stenmark, H., and Simonsen, A. (2007). Functional multivesicular bodies are required for autophagic clearance of protein aggregates associated with neurodegenerative disease. The Journal of cell biology *179*, 485-500.
Flannagan, R.S., Jaumouille, V., and Grinstein, S. (2012). The cell biology of phagocytosis. Annual review of pathology *7*, 61-98.
Fritsch, J., Stephan, M., Tchikov, V., Winoto-Morbach, S., Gubkina, S., Kabelitz, D., and Schutze, S. (2014). Cell fate decisions regulated by K63 ubiquitination of tumor necrosis factor receptor 1. Molecular and cellular biology *34*, 3214-3228.
Fujita, Y., Krause, G., Scheffner, M., Zechner, D., Leddy, H.E., Behrens, J., Sommer, T., and Birchmeier, W. (2002). Hakai, a c-Cbl-like protein, ubiquitinates and induces endocytosis of the E-cadherin complex. Nature cell biology *4*, 222-231.
Fushman, D., and Walker, O. (2010). Exploring the linkage dependence of polyubiquitin conformations using molecular modeling. Journal of molecular biology *395*, 803-814.
Gerlach, B., Cordier, S.M., Schmukle, A.C., Emmerich, C.H., Rieser, E., Haas, T.L., Webb, A.I., Rickard, J.A., Anderton, H., Wong, W.W., *et al.* (2011). Linear ubiquitination prevents inflammation and regulates immune signalling. Nature *471*, 591-596.
Giancotti, F.G., and Ruoslahti, E. (1999). Integrin signaling. Science *285*, 1028-1032.
Gilbert, M.M., Tipping, M., Veraksa, A., and Moberg, K.H. (2011). A screen for conditional growth suppressor genes identifies the Drosophila homolog of HD-PTP as a regulator of the oncoprotein Yorkie. Developmental cell *20*, 700-712.
Gill, D.J., Teo, H., Sun, J., Perisic, O., Veprintsev, D.B., Emr, S.D., and Williams, R.L. (2007). Structural insight into the ESCRT-I/-II link and its role in MVB trafficking. The EMBO journal *26*, 600-612.
Gingras, M.C., Kharitidi, D., Chenard, V., Uetani, N., Bouchard, M., Tremblay, M.L., and Pause, A. (2009a). Expression analysis and essential role of the putative tyrosine phosphatase His-

domain-containing protein tyrosine phosphatase (HD-PTP). The International journal of developmental biology *53*, 1069-1074.
Gingras, M.C., Zhang, Y.L., Kharitidi, D., Barr, A.J., Knapp, S., Tremblay, M.L., and Pause, A. (2009b). HD-PTP is a catalytically inactive tyrosine phosphatase due to a conserved divergence in its phosphatase domain. PloS one *4*, e5105.
Glaser, S.P., Lee, E.F., Trounson, E., Bouillet, P., Wei, A., Fairlie, W.D., Izon, D.J., Zuber, J., Rappaport, A.R., Herold, M.J., *et al.* (2012). Anti-apoptotic Mcl-1 is essential for the development and sustained growth of acute myeloid leukemia. Genes & development *26*, 120-125.
Goodman, O.B., Jr., Krupnick, J.G., Gurevich, V.V., Benovic, J.L., and Keen, J.H. (1997). Arrestin/clathrin interaction. Localization of the arrestin binding locus to the clathrin terminal domain. The Journal of biological chemistry *272*, 15017-15022.
Grashoff, C., Hoffman, B.D., Brenner, M.D., Zhou, R., Parsons, M., Yang, M.T., McLean, M.A., Sligar, S.G., Chen, C.S., Ha, T., *et al.* (2010). Measuring mechanical tension across vinculin reveals regulation of focal adhesion dynamics. Nature *466*, 263-266.
Gross, S., Blanchetot, C., Schepens, J., Albet, S., Lammers, R., den Hertog, J., and Hendriks, W. (2002). Multimerization of the protein-tyrosine phosphatase (PTP)-like insulin-dependent diabetes mellitus autoantigens IA-2 and IA-2beta with receptor PTPs (RPTPs). Inhibition of RPTPalpha enzymatic activity. The Journal of biological chemistry *277*, 48139-48145.
Gruenberg, J., Griffiths, G., and Howell, K.E. (1989). Characterization of the early endosome and putative endocytic carrier vesicles in vivo and with an assay of vesicle fusion in vitro. The Journal of cell biology *108*, 1301-1316.
Gu, Z., Noss, E.H., Hsu, V.W., and Brenner, M.B. (2011). Integrins traffic rapidly via circular dorsal ruffles and macropinocytosis during stimulated cell migration. The Journal of cell biology *193*, 61-70.
Haglund, K., Sigismund, S., Polo, S., Szymkiewicz, I., Di Fiore, P.P., and Dikic, I. (2003). Multiple monoubiquitination of RTKs is sufficient for their endocytosis and degradation. Nature cell biology *5*, 461-466.
Hansen, C.G., Howard, G., and Nichols, B.J. (2011). Pacsin 2 is recruited to caveolae and functions in caveolar biogenesis. Journal of cell science *124*, 2777-2785.
Hansen, C.G., and Nichols, B.J. (2010). Exploring the caves: cavins, caveolins and caveolae. Trends in cell biology *20*, 177-186.
Hanson, P.I., Roth, R., Lin, Y., and Heuser, J.E. (2008). Plasma membrane deformation by circular arrays of ESCRT-III protein filaments. The Journal of cell biology *180*, 389-402.
Harburger, D.S., Bouaouina, M., and Calderwood, D.A. (2009). Kindlin-1 and -2 directly bind the C-terminal region of beta integrin cytoplasmic tails and exert integrin-specific activation effects. The Journal of biological chemistry *284*, 11485-11497.
Harford, J., Bridges, K., Ashwell, G., and Klausner, R.D. (1983). Intracellular dissociation of receptor-bound asialoglycoproteins in cultured hepatocytes. A pH-mediated nonlysosomal event. The Journal of biological chemistry *258*, 3191-3197.
Harhaj, E.W., and Dixit, V.M. (2011). Deubiquitinases in the regulation of NF-kappaB signaling. Cell research *21*, 22-39.

Hawryluk, M.J., Keyel, P.A., Mishra, S.K., Watkins, S.C., Heuser, J.E., and Traub, L.M. (2006). Epsin 1 is a polyubiquitin-selective clathrin-associated sorting protein. Traffic (Copenhagen, Denmark) *7*, 262-281.
Heideker, J., and Wertz, I.E. (2015). DUBs, the regulation of cell identity and disease. The Biochemical journal *467*, 191.
Henley, J.R., Krueger, E.W., Oswald, B.J., and McNiven, M.A. (1998). Dynamin-mediated internalization of caveolae. The Journal of cell biology *141*, 85-99.
Henne, W.M., Buchkovich, N.J., and Emr, S.D. (2011). The ESCRT pathway. Developmental cell *21*, 77-91.
Henne, W.M., Stenmark, H., and Emr, S.D. (2013). Molecular mechanisms of the membrane sculpting ESCRT pathway. Cold Spring Harbor perspectives in biology *5*.
Herman, E.K., Walker, G., van der Giezen, M., and Dacks, J.B. (2011). Multivesicular bodies in the enigmatic amoeboflagellate Breviata anathema and the evolution of ESCRT 0. Journal of cell science *124*, 613-621.
Hicke, L. (1999). Gettin' down with ubiquitin: turning off cell-surface receptors, transporters and channels. Trends in cell biology *9*, 107-112.
Hicke, L., and Dunn, R. (2003). Regulation of membrane protein transport by ubiquitin and ubiquitin-binding proteins. Annual review of cell and developmental biology *19*, 141-172.
Hirano, S., Kawasaki, M., Ura, H., Kato, R., Raiborg, C., Stenmark, H., and Wakatsuki, S. (2006). Double-sided ubiquitin binding of Hrs-UIM in endosomal protein sorting. Nature structural & molecular biology *13*, 272-277.
Hoffmann, A., Levchenko, A., Scott, M.L., and Baltimore, D. (2002). The IkappaB-NF-kappaB signaling module: temporal control and selective gene activation. Science *298*, 1241-1245.
Homan, Claire C., Kumar, R., Nguyen, Lam S., Haan, E., Raymond, F.L., Abidi, F., Raynaud, M., Schwartz, C.E., Wood, Stephen A., Gecz, J., *et al.* (2014). Mutations in USP9X Are Associated with X-Linked Intellectual Disability and Disrupt Neuronal Cell Migration and Growth. The American Journal of Human Genetics *94*, 470-478.
Howes, M.T., Kirkham, M., Riches, J., Cortese, K., Walser, P.J., Simpson, F., Hill, M.M., Jones, A., Lundmark, R., Lindsay, M.R., *et al.* (2010). Clathrin-independent carriers form a high capacity endocytic sorting system at the leading edge of migrating cells. The Journal of cell biology *190*, 675-691.
Hsu, H., Huang, J., Shu, H.B., Baichwal, V., and Goeddel, D.V. (1996a). TNF-dependent recruitment of the protein kinase RIP to the TNF receptor-1 signaling complex. Immunity *4*, 387-396.
Hsu, H., Shu, H.B., Pan, M.G., and Goeddel, D.V. (1996b). TRADD-TRAF2 and TRADD-FADD interactions define two distinct TNF receptor 1 signal transduction pathways. Cell *84*, 299-308.
Hsu, H., Xiong, J., and Goeddel, D.V. (1995). The TNF receptor 1-associated protein TRADD signals cell death and NF-kappa B activation. Cell *81*, 495-504.
Huang, F., Kirkpatrick, D., Jiang, X., Gygi, S., and Sorkin, A. (2006). Differential regulation of EGF receptor internalization and degradation by multiubiquitination within the kinase domain. Molecular cell *21*, 737-748.

Huang, H.R., Chen, Z.J., Kunes, S., Chang, G.D., and Maniatis, T. (2010). Endocytic pathway is required for Drosophila Toll innate immune signaling. Proceedings of the National Academy of Sciences of the United States of America *107*, 8322-8327.
Humphries, M.J., Symonds, E.J., and Mould, A.P. (2003). Mapping functional residues onto integrin crystal structures. Current opinion in structural biology *13*, 236-243.
Husedzinovic, A., Neumann, B., Reymann, J., Draeger-Meurer, S., Chari, A., Erfle, H., Fischer, U., and Gruss, O.J. (2015). The catalytically inactive tyrosine phosphatase HD-PTP/PTPN23 is a novel regulator of SMN complex localization. Molecular biology of the cell *26*, 161-171.
Hynes, R.O. (2002). Integrins: bidirectional, allosteric signaling machines. Cell *110*, 673-687.
Ichioka, F., Takaya, E., Suzuki, H., Kajigaya, S., Buchman, V.L., Shibata, H., and Maki, M. (2007). HD-PTP and Alix share some membrane-traffic related proteins that interact with their Bro1 domains or proline-rich regions. Archives of biochemistry and biophysics *457*, 142-149.
Idriss, H.T., and Naismith, J.H. (2000). TNF alpha and the TNF receptor superfamily: structure-function relationship(s). Microscopy research and technique *50*, 184-195.
Im, Y.J., Kuo, L., Ren, X., Burgos, P.V., Zhao, X.Z., Liu, F., Burke, T.R., Jr., Bonifacino, J.S., Freed, E.O., and Hurley, J.H. (2010). Crystallographic and functional analysis of the ESCRT-I /HIV-1 Gag PTAP interaction. Structure *18*, 1536-1547.
Im, Y.J., Wollert, T., Boura, E., and Hurley, J.H. (2009). Structure and function of the ESCRT-II-III interface in multivesicular body biogenesis. Developmental cell *17*, 234-243.
Israel, A. (2000). The IKK complex: an integrator of all signals that activate NF-kappaB? Trends in cell biology *10*, 129-133.
Israel, A. (2010). The IKK complex, a central regulator of NF-kappaB activation. Cold Spring Harbor perspectives in biology *2*, a000158.
Ivaska, J., and Heino, J. (2011). Cooperation between integrins and growth factor receptors in signaling and endocytosis. Annual review of cell and developmental biology *27*, 291-320.
Jiang, P.D., Zhao, Y.L., Deng, X.Q., Mao, Y.Q., Shi, W., Tang, Q.Q., Li, Z.G., Zheng, Y.Z., Yang, S.Y., and Wei, Y.Q. (2010). Antitumor and antimetastatic activities of chloroquine diphosphate in a murine model of breast cancer. Biomedicine & pharmacotherapy = Biomedecine & pharmacotherapie *64*, 609-614.
Jiang, Y., Ou, Y., and Cheng, X. (2013). Role of TSG101 in cancer. Frontiers in bioscience (Landmark edition) *18*, 279-288.
Jones, M.C., Caswell, P.T., and Norman, J.C. (2006). Endocytic recycling pathways: emerging regulators of cell migration. Current opinion in cell biology *18*, 549-557.
Kaabeche, K., Guenou, H., Bouvard, D., Didelot, N., Listrat, A., and Marie, P.J. (2005). Cbl-mediated ubiquitination of alpha5 integrin subunit mediates fibronectin-dependent osteoblast detachment and apoptosis induced by FGFR2 activation. Journal of cell science *118*, 1223-1232.
Kamata, T., and Takada, Y. (1994). Direct binding of collagen to the I domain of integrin alpha 2 beta 1 (VLA-2, CD49b/CD29) in a divalent cation-independent manner. The Journal of biological chemistry *269*, 26006-26010.
Kapuria, V., Peterson, L.F., Fang, D., Bornmann, W.G., Talpaz, M., and Donato, N.J. (2010). Deubiquitinase inhibition by small-molecule WP1130 triggers aggresome formation and tumor cell apoptosis. Cancer research *70*, 9265-9276.

Katoh, Y., Shiba, Y., Mitsuhashi, H., Yanagida, Y., Takatsu, H., and Nakayama, K. (2004). Tollip and Tom1 form a complex and recruit ubiquitin-conjugated proteins onto early endosomes. The Journal of biological chemistry *279*, 24435-24443.
Katzmann, D.J., Babst, M., and Emr, S.D. (2001). Ubiquitin-dependent sorting into the multivesicular body pathway requires the function of a conserved endosomal protein sorting complex, ESCRT-I. Cell *106*, 145-155.
Katzmann, D.J., Stefan, C.J., Babst, M., and Emr, S.D. (2003). Vps27 recruits ESCRT machinery to endosomes during MVB sorting. The Journal of cell biology *162*, 413-423.
Kavsak, P., Rasmussen, R.K., Causing, C.G., Bonni, S., Zhu, H., Thomsen, G.H., and Wrana, J.L. (2000). Smad7 binds to Smurf2 to form an E3 ubiquitin ligase that targets the TGF beta receptor for degradation. Molecular cell *6*, 1365-1375.
Kawasaki, M., Shiba, T., Shiba, Y., Yamaguchi, Y., Matsugaki, N., Igarashi, N., Suzuki, M., Kato, R., Kato, K., Nakayama, K.*, et al.* (2005). Molecular mechanism of ubiquitin recognition by GGA3 GAT domain. Genes to cells : devoted to molecular & cellular mechanisms *10*, 639-654.
Kelly, B.T., McCoy, A.J., Spate, K., Miller, S.E., Evans, P.R., Honing, S., and Owen, D.J. (2008). A structural explanation for the binding of endocytic dileucine motifs by the AP2 complex. Nature *456*, 976-979.
Kelly, B.T., and Owen, D.J. (2011). Endocytic sorting of transmembrane protein cargo. Current opinion in cell biology *23*, 404-412.
Khalili, P., Arakelian, A., Chen, G., Plunkett, M.L., Beck, I., Parry, G.C., Donate, F., Shaw, D.E., Mazar, A.P., and Rabbani, S.A. (2006). A non-RGD-based integrin binding peptide (ATN-161) blocks breast cancer growth and metastasis in vivo. Molecular cancer therapeutics *5*, 2271-2280.
Kirchhausen, T., and Harrison, S.C. (1981). Protein organization in clathrin trimers. Cell *23*, 755-761.
Kirchhausen, T., Owen, D., and Harrison, S.C. (2014). Molecular structure, function, and dynamics of clathrin-mediated membrane traffic. Cold Spring Harbor perspectives in biology *6*, a016725.
Kojima, K., Amano, Y., Yoshino, K., Tanaka, N., Sugamura, K., and Takeshita, T. (2014). ESCRT-0 protein hepatocyte growth factor-regulated tyrosine kinase substrate (Hrs) is targeted to endosomes independently of signal-transducing adaptor molecule (STAM) and the complex formation with STAM promotes its endosomal dissociation. The Journal of biological chemistry *289*, 33296-33310.
Koo, B.K., Spit, M., Jordens, I., Low, T.Y., Stange, D.E., van de Wetering, M., van Es, J.H., Mohammed, S., Heck, A.J., Maurice, M.M.*, et al.* (2012). Tumour suppressor RNF43 is a stem-cell E3 ligase that induces endocytosis of Wnt receptors. Nature *488*, 665-669.
Kovalenko, A., Chable-Bessia, C., Cantarella, G., Israel, A., Wallach, D., and Courtois, G. (2003). The tumour suppressor CYLD negatively regulates NF-kappaB signalling by deubiquitination. Nature *424*, 801-805.
Krupnick, J.G., Goodman, O.B., Jr., Keen, J.H., and Benovic, J.L. (1997). Arrestin/clathrin interaction. Localization of the clathrin binding domain of nonvisual arrestins to the carboxy terminus. The Journal of biological chemistry *272*, 15011-15016.

Kulka, R.G., Raboy, B., Schuster, R., Parag, H.A., Diamond, G., Ciechanover, A., and Marcus, M. (1988). A Chinese hamster cell cycle mutant arrested at G2 phase has a temperature-sensitive ubiquitin-activating enzyme, E1. The Journal of biological chemistry *263*, 15726-15731.
Kuratomi, G., Komuro, A., Goto, K., Shinozaki, M., Miyazawa, K., Miyazono, K., and Imamura, T. (2005). NEDD4-2 (neural precursor cell expressed, developmentally down-regulated 4-2) negatively regulates TGF-beta (transforming growth factor-beta) signalling by inducing ubiquitin-mediated degradation of Smad2 and TGF-beta type I receptor. The Biochemical journal *386*, 461-470.
Kurban, G., Duplan, E., Ramlal, N., Hudon, V., Sado, Y., Ninomiya, Y., and Pause, A. (2008). Collagen matrix assembly is driven by the interaction of von Hippel-Lindau tumor suppressor protein with hydroxylated collagen IV alpha 2. Oncogene *27*, 1004-1012.
Kurban, G., Hudon, V., Duplan, E., Ohh, M., and Pause, A. (2006). Characterization of a von Hippel Lindau pathway involved in extracellular matrix remodeling, cell invasion, and angiogenesis. Cancer research *66*, 1313-1319.
Landskron, G., De la Fuente, M., Thuwajit, P., Thuwajit, C., and Hermoso, M.A. (2014). Chronic inflammation and cytokines in the tumor microenvironment. Journal of immunology research *2014*, 149185.
Larson, R.S., Corbi, A.L., Berman, L., and Springer, T. (1989). Primary structure of the leukocyte function-associated molecule-1 alpha subunit: an integrin with an embedded domain defining a protein superfamily. The Journal of cell biology *108*, 703-712.
Lata, S., Schoehn, G., Jain, A., Pires, R., Piehler, J., Gottlinger, H.G., and Weissenhorn, W. (2008). Helical structures of ESCRT-III are disassembled by VPS4. Science *321*, 1354-1357.
Lauwers, E., Jacob, C., and Andre, B. (2009). K63-linked ubiquitin chains as a specific signal for protein sorting into the multivesicular body pathway. The Journal of cell biology *185*, 493-502.
Lee, J.A., Beigneux, A., Ahmad, S.T., Young, S.G., and Gao, F.B. (2007). ESCRT-III dysfunction causes autophagosome accumulation and neurodegeneration. Current biology : CB *17*, 1561-1567.
Lee, J.O., Rieu, P., Arnaout, M.A., and Liddington, R. (1995). Crystal structure of the A domain from the alpha subunit of integrin CR3 (CD11b/CD18). Cell *80*, 631-638.
Lee, T.H., Shank, J., Cusson, N., and Kelliher, M.A. (2004). The kinase activity of Rip1 is not required for tumor necrosis factor-alpha-induced IkappaB kinase or p38 MAP kinase activation or for the ubiquitination of Rip1 by Traf2. The Journal of biological chemistry *279*, 33185-33191.
Lenz, M., Crow, D.J., and Joanny, J.F. (2009a). Membrane buckling induced by curved filaments. Physical review letters *103*, 038101.
Lenz, M., Morlot, S., and Roux, A. (2009b). Mechanical requirements for membrane fission: common facts from various examples. FEBS letters *583*, 3839-3846.
Leung, K.F., Dacks, J.B., and Field, M.C. (2008). Evolution of the multivesicular body ESCRT machinery; retention across the eukaryotic lineage. Traffic (Copenhagen, Denmark) *9*, 1698-1716.
Levkowitz, G., Waterman, H., Ettenberg, S.A., Katz, M., Tsygankov, A.Y., Alroy, I., Lavi, S., Iwai, K., Reiss, Y., Ciechanover, A.*, et al.* (1999). Ubiquitin ligase activity and tyrosine phosphorylation underlie suppression of growth factor signaling by c-Cbl/Sli-1. Molecular cell *4*, 1029-1040.

Li, H., Kobayashi, M., Blonska, M., You, Y., and Lin, X. (2006). Ubiquitination of RIP is required for tumor necrosis factor alpha-induced NF-kappaB activation. The Journal of biological chemistry *281*, 13636-13643.
Li, J., Ballif, B.A., Powelka, A.M., Dai, J., Gygi, S.P., and Hsu, V.W. (2005). Phosphorylation of ACAP1 by Akt regulates the stimulation-dependent recycling of integrin beta1 to control cell migration. Developmental cell *9*, 663-673.
Li, J., Belogortseva, N., Porter, D., and Park, M. (2008). Chmp1A functions as a novel tumor suppressor gene in human embryonic kidney and ductal pancreatic tumor cells. Cell cycle *7*, 2886-2893.
Li, L., and Cohen, S.N. (1996). Tsg101: a novel tumor susceptibility gene isolated by controlled homozygous functional knockout of allelic loci in mammalian cells. Cell *85*, 319-329.
Li, M., Chen, D., Shiloh, A., Luo, J., Nikolaev, A.Y., Qin, J., and Gu, W. (2002). Deubiquitination of p53 by HAUSP is an important pathway for p53 stabilization. Nature *416*, 648-653.
Lin, G., Aranda, V., Muthuswamy, S.K., and Tonks, N.K. (2011). Identification of PTPN23 as a novel regulator of cell invasion in mammary epithelial cells from a loss-of-function screen of the 'PTP-ome'. Genes & development *25*, 1412-1425.
Lin, H.H., Li, X., Chen, J.L., Sun, X., Cooper, F.N., Chen, Y.R., Zhang, W., Chung, Y., Li, A., Cheng, C.T., *et al.* (2012). Identification of an AAA ATPase VPS4B-dependent pathway that modulates epidermal growth factor receptor abundance and signaling during hypoxia. Molecular and cellular biology *32*, 1124-1138.
Liu, Z.G., Hsu, H., Goeddel, D.V., and Karin, M. (1996). Dissection of TNF receptor 1 effector functions: JNK activation is not linked to apoptosis while NF-kappaB activation prevents cell death. Cell *87*, 565-576.
Lloyd, T.E., Atkinson, R., Wu, M.N., Zhou, Y., Pennetta, G., and Bellen, H.J. (2002). Hrs regulates endosome membrane invagination and tyrosine kinase receptor signaling in Drosophila. Cell *108*, 261-269.
Lobert, V.H., Brech, A., Pedersen, N.M., Wesche, J., Oppelt, A., Malerod, L., and Stenmark, H. (2010). Ubiquitination of alpha 5 beta 1 integrin controls fibroblast migration through lysosomal degradation of fibronectin-integrin complexes. Developmental cell *19*, 148-159.
Lobert, V.H., and Stenmark, H. (2010). Ubiquitination of alpha-integrin cytoplasmic tails. Communicative & integrative biology *3*, 583-585.
Lobert, V.H., and Stenmark, H. (2011). Cell polarity and migration: emerging role for the endosomal sorting machinery. Physiology *26*, 171-180.
Lobert, V.H., and Stenmark, H. (2012). The ESCRT machinery mediates polarization of fibroblasts through regulation of myosin light chain. Journal of cell science *125*, 29-36.
Locksley, R.M., Killeen, N., and Lenardo, M.J. (2001). The TNF and TNF receptor superfamilies: integrating mammalian biology. Cell *104*, 487-501.
Loncle, N., Agromayor, M., Martin-Serrano, J., and Williams, D.W. (2015). An ESCRT module is required for neuron pruning. Scientific reports *5*, 8461.
Lu, A., Tebar, F., Alvarez-Moya, B., Lopez-Alcala, C., Calvo, M., Enrich, C., Agell, N., Nakamura, T., Matsuda, M., and Bachs, O. (2009). A clathrin-dependent pathway leads to KRas signaling on late endosomes en route to lysosomes. The Journal of cell biology *184*, 863-879.

Lu, Q., Hope, L.W., Brasch, M., Reinhard, C., and Cohen, S.N. (2003). TSG101 interaction with HRS mediates endosomal trafficking and receptor down-regulation. Proceedings of the National Academy of Sciences of the United States of America *100*, 7626-7631.
Luhtala, N., and Odorizzi, G. (2004). Bro1 coordinates deubiquitination in the multivesicular body pathway by recruiting Doa4 to endosomes. The Journal of cell biology *166*, 717-729.
Luo, B.H., and Springer, T.A. (2006). Integrin structures and conformational signaling. Current opinion in cell biology *18*, 579-586.
Luo, B.H., Springer, T.A., and Takagi, J. (2004). A specific interface between integrin transmembrane helices and affinity for ligand. PLoS biology *2*, e153.
Luzio, J.P., Piper, S.C., Bowers, K., Parkinson, M.D., Lehner, P.J., and Bright, N.A. (2009). ESCRT proteins and the regulation of endocytic delivery to lysosomes. Biochemical Society transactions *37*, 178-180.
Luzio, J.P., Pryor, P.R., and Bright, N.A. (2007). Lysosomes: fusion and function. Nature reviews Molecular cell biology *8*, 622-632.
Ma, Y.Q., Qin, J., Wu, C., and Plow, E.F. (2008). Kindlin-2 (Mig-2): a co-activator of beta3 integrins. The Journal of cell biology *181*, 439-446.
MacEwan, D.J. (2002). TNF ligands and receptors--a matter of life and death. British journal of pharmacology *135*, 855-875.
Macia, E., Ehrlich, M., Massol, R., Boucrot, E., Brunner, C., and Kirchhausen, T. (2006). Dynasore, a cell-permeable inhibitor of dynamin. Developmental cell *10*, 839-850.
Macpherson, I.R., Rainero, E., Mitchell, L.E., van den Berghe, P.V., Speirs, C., Dozynkiewicz, M.A., Chaudhary, S., Kalna, G., Edwards, J., Timpson, P., *et al.* (2014). CLIC3 controls recycling of late endosomal MT1-MMP and dictates invasion and metastasis in breast cancer. Journal of cell science *127*, 3893-3901.
Magnifico, A., Ettenberg, S., Yang, C., Mariano, J., Tiwari, S., Fang, S., Lipkowitz, S., and Weissman, A.M. (2003). WW domain HECT E3s target Cbl RING finger E3s for proteasomal degradation. The Journal of biological chemistry *278*, 43169-43177.
Mahul-Mellier, A.L., Strappazzon, F., Petiot, A., Chatellard-Causse, C., Torch, S., Blot, B., Freeman, K., Kuhn, L., Garin, J., Verna, J.M., *et al.* (2008). Alix and ALG-2 are involved in tumor necrosis factor receptor 1-induced cell death. The Journal of biological chemistry *283*, 34954-34965.
Mai, A., Veltel, S., Pellinen, T., Padzik, A., Coffey, E., Marjomaki, V., and Ivaska, J. (2011). Competitive binding of Rab21 and p120RasGAP to integrins regulates receptor traffic and migration. The Journal of cell biology *194*, 291-306.
Maiorano, E., Favia, G., Pece, S., Resta, L., Maisonneuve, P., Di Fiore, P.P., Capodiferro, S., Urbani, U., and Viale, G. (2007). Prognostic implications of NUMB immunoreactivity in salivary gland carcinomas. International journal of immunopathology and pharmacology *20*, 779-789.
Malerod, L., Stuffers, S., Brech, A., and Stenmark, H. (2007). Vps22/EAP30 in ESCRT-II mediates endosomal sorting of growth factor and chemokine receptors destined for lysosomal degradation. Traffic *8*, 1617-1629.
Mao, Y., Nickitenko, A., Duan, X., Lloyd, T.E., Wu, M.N., Bellen, H., and Quiocho, F.A. (2000). Crystal structure of the VHS and FYVE tandem domains of Hrs, a protein involved in membrane trafficking and signal transduction. Cell *100*, 447-456.

Margadant, C., Kreft, M., de Groot, D.J., Norman, J.C., and Sonnenberg, A. (2012). Distinct roles of talin and kindlin in regulating integrin alpha5beta1 function and trafficking. Current biology : CB *22*, 1554-1563.
Margadant, C., Monsuur, H.N., Norman, J.C., and Sonnenberg, A. (2011). Mechanisms of integrin activation and trafficking. Current opinion in cell biology *23*, 607-614.
Mariotti, M., Castiglioni, S., Garcia-Manteiga, J.M., Beguinot, L., and Maier, J.A. (2009). HD-PTP inhibits endothelial migration through its interaction with Src. The international journal of biochemistry & cell biology *41*, 687-693.
Marshansky, V., and Futai, M. (2008). The V-type H+-ATPase in vesicular trafficking: targeting, regulation and function. Current opinion in cell biology *20*, 415-426.
Martin-Serrano, J., Zang, T., and Bieniasz, P.D. (2001). HIV-1 and Ebola virus encode small peptide motifs that recruit Tsg101 to sites of particle assembly to facilitate egress. Nature medicine *7*, 1313-1319.
Marx, C., Held, J.M., Gibson, B.W., and Benz, C.C. (2010). ErbB2 trafficking and degradation associated with K48 and K63 polyubiquitination. Cancer research *70*, 3709-3717.
Matsumoto, M.L., Wickliffe, K.E., Dong, K.C., Yu, C., Bosanac, I., Bustos, D., Phu, L., Kirkpatrick, D.S., Hymowitz, S.G., Rape, M.*, et al.* (2010). K11-linked polyubiquitination in cell cycle control revealed by a K11 linkage-specific antibody. Molecular cell *39*, 477-484.
Mattissek, C., and Teis, D. (2014). The role of the endosomal sorting complexes required for transport (ESCRT) in tumorigenesis. Molecular membrane biology *31*, 111-119.
Maxfield, F.R., and McGraw, T.E. (2004). Endocytic recycling. Nature reviews Molecular cell biology *5*, 121-132.
Maxfield, F.R., and Yamashiro, D.J. (1987). Endosome acidification and the pathways of receptor-mediated endocytosis. Advances in experimental medicine and biology *225*, 189-198.
Mayers, J.R., Fyfe, I., Schuh, A.L., Chapman, E.R., Edwardson, J.M., and Audhya, A. (2011). ESCRT-0 assembles as a heterotetrameric complex on membranes and binds multiple ubiquitinylated cargoes simultaneously. The Journal of biological chemistry *286*, 9636-9645.
Mayor, S., Parton, R.G., and Donaldson, J.G. (2014). Clathrin-independent pathways of endocytosis. Cold Spring Harbor perspectives in biology *6*.
McCullough, J., Clague, M.J., and Urbe, S. (2004). AMSH is an endosome-associated ubiquitin isopeptidase. The Journal of cell biology *166*, 487-492.
McMahon, H.T., and Boucrot, E. (2011). Molecular mechanism and physiological functions of clathrin-mediated endocytosis. Nature reviews Molecular cell biology *12*, 517-533.
Merrifield, C.J., Perrais, D., and Zenisek, D. (2005). Coupling between clathrin-coated-pit invagination, cortactin recruitment, and membrane scission observed in live cells. Cell *121*, 593-606.
Miaczynska, M. (2013). Effects of membrane trafficking on signaling by receptor tyrosine kinases. Cold Spring Harbor perspectives in biology *5*, a009035.
Micheau, O., Lens, S., Gaide, O., Alevizopoulos, K., and Tschopp, J. (2001). NF-kappaB signals induce the expression of c-FLIP. Molecular and cellular biology *21*, 5299-5305.
Micheau, O., and Tschopp, J. (2003). Induction of TNF receptor I-mediated apoptosis via two sequential signaling complexes. Cell *114*, 181-190.

Michelet, X., Djeddi, A., and Legouis, R. (2010). Developmental and cellular functions of the ESCRT machinery in pluricellular organisms. Biology of the cell / under the auspices of the European Cell Biology Organization *102*, 191-202.
Michishita, M., Videm, V., and Arnaout, M.A. (1993). A novel divalent cation-binding site in the A domain of the beta 2 integrin CR3 (CD11b/CD18) is essential for ligand binding. Cell *72*, 857-867.
Mills, G.B., Jurisica, I., Yarden, Y., and Norman, J.C. (2009). Genomic amplicons target vesicle recycling in breast cancer. The Journal of clinical investigation *119*, 2123-2127.
Misra, S., Beach, B.M., and Hurley, J.H. (2000). Structure of the VHS domain of human Tom1 (target of myb 1): insights into interactions with proteins and membranes. Biochemistry *39*, 11282-11290.
Mitra, A.K., Sawada, K., Tiwari, P., Mui, K., Gwin, K., and Lengyel, E. (2011). Ligand-independent activation of c-Met by fibronectin and alpha(5)beta(1)-integrin regulates ovarian cancer invasion and metastasis. Oncogene *30*, 1566-1576.
Miura, G.I., Roignant, J.Y., Wassef, M., and Treisman, J.E. (2008). Myopic acts in the endocytic pathway to enhance signaling by the Drosophila EGF receptor. Development (Cambridge, England) *135*, 1913-1922.
Miyake, S., Lupher, M.L., Jr., Druker, B., and Band, H. (1998). The tyrosine kinase regulator Cbl enhances the ubiquitination and degradation of the platelet-derived growth factor receptor alpha. Proceedings of the National Academy of Sciences of the United States of America *95*, 7927-7932.
Mizuno, E., Kawahata, K., Kato, M., Kitamura, N., and Komada, M. (2003). STAM proteins bind ubiquitinated proteins on the early endosome via the VHS domain and ubiquitin-interacting motif. Molecular biology of the cell *14*, 3675-3689.
Moberg, K.H., Schelble, S., Burdick, S.K., and Hariharan, I.K. (2005). Mutations in erupted, the Drosophila ortholog of mammalian tumor susceptibility gene 101, elicit non-cell-autonomous overgrowth. Developmental cell *9*, 699-710.
Morita, E., Sandrin, V., Chung, H.Y., Morham, S.G., Gygi, S.P., Rodesch, C.K., and Sundquist, W.I. (2007). Human ESCRT and ALIX proteins interact with proteins of the midbody and function in cytokinesis. The EMBO journal *26*, 4215-4227.
Moser, M., Nieswandt, B., Ussar, S., Pozgajova, M., and Fassler, R. (2008). Kindlin-3 is essential for integrin activation and platelet aggregation. Nature medicine *14*, 325-330.
Mouchantaf, R., Azakir, B.A., McPherson, P.S., Millard, S.M., Wood, S.A., and Angers, A. (2006). The ubiquitin ligase itch is auto-ubiquitylated in vivo and in vitro but is protected from degradation by interacting with the deubiquitylating enzyme FAM/USP9X. The Journal of biological chemistry *281*, 38738-38747.
Mukai, A., Yamamoto-Hino, M., Awano, W., Watanabe, W., Komada, M., and Goto, S. (2010). Balanced ubiquitylation and deubiquitylation of Frizzled regulate cellular responsiveness to Wg/Wnt. The EMBO journal *29*, 2114-2125.
Muller, P.A., Caswell, P.T., Doyle, B., Iwanicki, M.P., Tan, E.H., Karim, S., Lukashchuk, N., Gillespie, D.A., Ludwig, R.L., Gosselin, P., *et al.* (2009). Mutant p53 drives invasion by promoting integrin recycling. Cell *139*, 1327-1341.

Muller, P.A., Trinidad, A.G., Timpson, P., Morton, J.P., Zanivan, S., van den Berghe, P.V., Nixon, C., Karim, S.A., Caswell, P.T., Noll, J.E., *et al.* (2013). Mutant p53 enhances MET trafficking and signalling to drive cell scattering and invasion. Oncogene *32*, 1252-1265.
Mullershausen, F., Zecri, F., Cetin, C., Billich, A., Guerini, D., and Seuwen, K. (2009). Persistent signaling induced by FTY720-phosphate is mediated by internalized S1P1 receptors. Nature chemical biology *5*, 428-434.
Murray, R.Z., Jolly, L.A., and Wood, S.A. (2004). The FAM deubiquitylating enzyme localizes to multiple points of protein trafficking in epithelia, where it associates with E-cadherin and beta-catenin. Molecular biology of the cell *15*, 1591-1599.
Murtaza, M., Jolly, L.A., Gecz, J., and Wood, S.A. (2015). La FAM fatale: USP9X in development and disease. Cellular and molecular life sciences : CMLS.
Nagae, M., Re, S., Mihara, E., Nogi, T., Sugita, Y., and Takagi, J. (2012). Crystal structure of alpha5beta1 integrin ectodomain: atomic details of the fibronectin receptor. The Journal of cell biology *197*, 131-140.
Napetschnig, J., and Wu, H. (2013). Molecular basis of NF-kappaB signaling. Annual review of biophysics *42*, 443-468.
Nishida, N., Xie, C., Shimaoka, M., Cheng, Y., Walz, T., and Springer, T.A. (2006). Activation of leukocyte beta2 integrins by conversion from bent to extended conformations. Immunity *25*, 583-594.
Oberst, A., Dillon, C.P., Weinlich, R., McCormick, L.L., Fitzgerald, P., Pop, C., Hakem, R., Salvesen, G.S., and Green, D.R. (2011). Catalytic activity of the caspase-8-FLIP(L) complex inhibits RIPK3-dependent necrosis. Nature *471*, 363-367.
Odorizzi, G., Katzmann, D.J., Babst, M., Audhya, A., and Emr, S.D. (2003). Bro1 is an endosome-associated protein that functions in the MVB pathway in Saccharomyces cerevisiae. Journal of cell science *116*, 1893-1903.
Oeckinghaus, A., Hayden, M.S., and Ghosh, S. (2011). Crosstalk in NF-kappaB signaling pathways. Nature immunology *12*, 695-708.
Oestreich, A.J., Davies, B.A., Payne, J.A., and Katzmann, D.J. (2007). Mvb12 is a novel member of ESCRT-I involved in cargo selection by the multivesicular body pathway. Molecular biology of the cell *18*, 646-657.
Ofengeim, D., and Yuan, J. (2013). Regulation of RIP1 kinase signalling at the crossroads of inflammation and cell death. Nature reviews Molecular cell biology *14*, 727-736.
Ohno, H., Stewart, J., Fournier, M.C., Bosshart, H., Rhee, I., Miyatake, S., Saito, T., Gallusser, A., Kirchhausen, T., and Bonifacino, J.S. (1995). Interaction of tyrosine-based sorting signals with clathrin-associated proteins. Science *269*, 1872-1875.
Pahl, H.L. (1999). Activators and target genes of Rel/NF-kappaB transcription factors. Oncogene *18*, 6853-6866.
Palacios, F., Tushir, J.S., Fujita, Y., and D'Souza-Schorey, C. (2005). Lysosomal targeting of E-cadherin: a unique mechanism for the down-regulation of cell-cell adhesion during epithelial to mesenchymal transitions. Molecular and cellular biology *25*, 389-402.
Palecek, S.P., Huttenlocher, A., Horwitz, A.F., and Lauffenburger, D.A. (1998). Physical and biochemical regulation of integrin release during rear detachment of migrating cells. Journal of cell science *111 (Pt 7)*, 929-940.

Papageorgis, P. (2015). TGFbeta Signaling in Tumor Initiation, Epithelial-to-Mesenchymal Transition, and Metastasis. Journal of oncology *2015*, 587193.
Parachoniak, C.A., Luo, Y., Abella, J.V., Keen, J.H., and Park, M. (2011). GGA3 functions as a switch to promote Met receptor recycling, essential for sustained ERK and cell migration. Developmental cell *20*, 751-763.
Park, C.C., Zhang, H., Pallavicini, M., Gray, J.W., Baehner, F., Park, C.J., and Bissell, M.J. (2006). Beta1 integrin inhibitory antibody induces apoptosis of breast cancer cells, inhibits growth, and distinguishes malignant from normal phenotype in three dimensional cultures and in vivo. Cancer research *66*, 1526-1535.
Parsons, J.T., Horwitz, A.R., and Schwartz, M.A. (2010). Cell adhesion: integrating cytoskeletal dynamics and cellular tension. Nature reviews Molecular cell biology *11*, 633-643.
Parton, R.G., and del Pozo, M.A. (2013). Caveolae as plasma membrane sensors, protectors and organizers. Nature reviews Molecular cell biology *14*, 98-112.
Pashkova, N., Gakhar, L., Winistorfer, S.C., Sunshine, A.B., Rich, M., Dunham, M.J., Yu, L., and Piper, R.C. (2013). The yeast Alix homolog Bro1 functions as a ubiquitin receptor for protein sorting into multivesicular endosomes. Developmental cell *25*, 520-533.
Peddaboina, C., Jupiter, D., Fletcher, S., Yap, J.L., Rai, A., Tobin, R.P., Jiang, W., Rascoe, P., Rogers, M.K., Smythe, W.R., *et al.* (2012). The downregulation of Mcl-1 via USP9X inhibition sensitizes solid tumors to Bcl-xl inhibition. BMC cancer *12*, 541.
Pellegrini, P., Strambi, A., Zipoli, C., Hagg-Olofsson, M., Buoncervello, M., Linder, S., and De Milito, A. (2014). Acidic extracellular pH neutralizes the autophagy-inhibiting activity of chloroquine: implications for cancer therapies. Autophagy *10*, 562-571.
Pellinen, T., Tuomi, S., Arjonen, A., Wolf, M., Edgren, H., Meyer, H., Grosse, R., Kitzing, T., Rantala, J.K., Kallioniemi, O., *et al.* (2008). Integrin trafficking regulated by Rab21 is necessary for cytokinesis. Developmental cell *15*, 371-385.
Peng, J., Hu, Q., Liu, W., He, X., Cui, L., Chen, X., Yang, M., Liu, H., Wei, W., Liu, S., *et al.* (2013). USP9X expression correlates with tumor progression and poor prognosis in esophageal squamous cell carcinoma. Diagnostic pathology *8*, 177.
Peppicelli, S., Bianchini, F., and Calorini, L. (2014). Extracellular acidity, a "reappreciated" trait of tumor environment driving malignancy: perspectives in diagnosis and therapy. Cancer metastasis reviews *33*, 823-832.
Perez-Mancera, P.A., Rust, A.G., van der Weyden, L., Kristiansen, G., Li, A., Sarver, A.L., Silverstein, K.A., Grutzmann, R., Aust, D., Rummele, P., *et al.* (2012). The deubiquitinase USP9X suppresses pancreatic ductal adenocarcinoma. Nature *486*, 266-270.
Peschard, P., Fournier, T.M., Lamorte, L., Naujokas, M.A., Band, H., Langdon, W.Y., and Park, M. (2001). Mutation of the c-Cbl TKB domain binding site on the Met receptor tyrosine kinase converts it into a transforming protein. Molecular cell *8*, 995-1004.
Peter, M.E., and Krammer, P.H. (2003). The CD95(APO-1/Fas) DISC and beyond. Cell death and differentiation *10*, 26-35.
Phillips, T.A., Ni, J., and Hunt, J.S. (2001). Death-inducing tumour necrosis factor (TNF) superfamily ligands and receptors are transcribed in human placentae, cytotrophoblasts, placental macrophages and placental cell lines. Placenta *22*, 663-672.
Piper, R.C., Dikic, I., and Lukacs, G.L. (2014). Ubiquitin-dependent sorting in endocytosis. Cold Spring Harbor perspectives in biology *6*.

Piper, R.C., and Katzmann, D.J. (2007). Biogenesis and function of multivesicular bodies. Annual review of cell and developmental biology *23*, 519-547.
Pop, C., Oberst, A., Drag, M., Van Raam, B.J., Riedl, S.J., Green, D.R., and Salvesen, G.S. (2011). FLIP(L) induces caspase 8 activity in the absence of interdomain caspase 8 cleavage and alters substrate specificity. The Biochemical journal *433*, 447-457.
Popov, N., Wanzel, M., Madiredjo, M., Zhang, D., Beijersbergen, R., Bernards, R., Moll, R., Elledge, S.J., and Eilers, M. (2007). The ubiquitin-specific protease USP28 is required for MYC stability. Nature cell biology *9*, 765-774.
Pornillos, O., Alam, S.L., Rich, R.L., Myszka, D.G., Davis, D.R., and Sundquist, W.I. (2002). Structure and functional interactions of the Tsg101 UEV domain. The EMBO journal *21*, 2397-2406.
Powelka, A.M., Sun, J., Li, J., Gao, M., Shaw, L.M., Sonnenberg, A., and Hsu, V.W. (2004). Stimulation-dependent recycling of integrin beta1 regulated by ARF6 and Rab11. Traffic *5*, 20-36.
Pradhan-Sundd, T., and Verheyen, E.M. (2014). The role of Bro1- domain-containing protein Myopic in endosomal trafficking of Wnt/Wingless. Developmental biology *392*, 93-107.
Qiu, L., Joazeiro, C., Fang, N., Wang, H.Y., Elly, C., Altman, Y., Fang, D., Hunter, T., and Liu, Y.C. (2000). Recognition and ubiquitination of Notch by Itch, a hect-type E3 ubiquitin ligase. The Journal of biological chemistry *275*, 35734-35737.
Rahighi, S., Ikeda, F., Kawasaki, M., Akutsu, M., Suzuki, N., Kato, R., Kensche, T., Uejima, T., Bloor, S., Komander, D.*, et al.* (2009). Specific recognition of linear ubiquitin chains by NEMO is important for NF-kappaB activation. Cell *136*, 1098-1109.
Raiborg, C., Bache, K.G., Gillooly, D.J., Madshus, I.H., Stang, E., and Stenmark, H. (2002). Hrs sorts ubiquitinated proteins into clathrin-coated microdomains of early endosomes. Nature cell biology *4*, 394-398.
Raiborg, C., Bache, K.G., Mehlum, A., Stang, E., and Stenmark, H. (2001a). Hrs recruits clathrin to early endosomes. The EMBO journal *20*, 5008-5021.
Raiborg, C., Bache, K.G., Mehlum, A., and Stenmark, H. (2001b). Function of Hrs in endocytic trafficking and signalling. Biochemical Society transactions *29*, 472-475.
Raiborg, C., Malerod, L., Pedersen, N.M., and Stenmark, H. (2008). Differential functions of Hrs and ESCRT proteins in endocytic membrane trafficking. Experimental cell research *314*, 801-813.
Rainero, E., and Norman, J.C. (2013). Late endosomal and lysosomal trafficking during integrin-mediated cell migration and invasion: cell matrix receptors are trafficked through the late endosomal pathway in a way that dictates how cells migrate. BioEssays : news and reviews in molecular, cellular and developmental biology *35*, 523-532.
Rajan, V.P., and Menon, K.M. (1985). Evidence that dissociation, not intracellular degradation, is the major pathway for removal of receptor-bound 125I-human chorionic gonadotropin in cultured rat luteal cells. Biology of reproduction *33*, 60-66.
Ramakrishnan, P., and Baltimore, D. (2011). Sam68 is required for both NF-kappaB activation and apoptosis signaling by the TNF receptor. Molecular cell *43*, 167-179.
Randles, L., and Walters, K.J. (2012). Ubiquitin and its binding domains. Frontiers in bioscience (Landmark edition) *17*, 2140-2157.

Ren, X., and Hurley, J.H. (2010). VHS domains of ESCRT-0 cooperate in high-avidity binding to polyubiquitinated cargo. The EMBO journal *29*, 1045-1054.
Ren, X., and Hurley, J.H. (2011a). Proline-rich regions and motifs in trafficking: from ESCRT interaction to viral exploitation. Traffic *12*, 1282-1290.
Ren, X., and Hurley, J.H. (2011b). Structural basis for endosomal recruitment of ESCRT-I by ESCRT-0 in yeast. The EMBO journal *30*, 2130-2139.
Ren, X., Kloer, D.P., Kim, Y.C., Ghirlando, R., Saidi, L.F., Hummer, G., and Hurley, J.H. (2009). Hybrid structural model of the complete human ESCRT-0 complex. Structure (London, England : 1993) *17*, 406-416.
Reynolds, A.R., Hart, I.R., Watson, A.R., Welti, J.C., Silva, R.G., Robinson, S.D., Da Violante, G., Gourlaouen, M., Salih, M., Jones, M.C., *et al.* (2009). Stimulation of tumor growth and angiogenesis by low concentrations of RGD-mimetic integrin inhibitors. Nature medicine *15*, 392-400.
Reynolds, L.E., Wyder, L., Lively, J.C., Taverna, D., Robinson, S.D., Huang, X., Sheppard, D., Hynes, R.O., and Hodivala-Dilke, K.M. (2002). Enhanced pathological angiogenesis in mice lacking beta3 integrin or beta3 and beta5 integrins. Nature medicine *8*, 27-34.
Richter, C.M., West, M., and Odorizzi, G. (2013). Doa4 function in ILV budding is restricted through its interaction with the Vps20 subunit of ESCRT-III. Journal of cell science *126*, 1881-1890.
Ridley, A.J., Schwartz, M.A., Burridge, K., Firtel, R.A., Ginsberg, M.H., Borisy, G., Parsons, J.T., and Horwitz, A.R. (2003). Cell migration: integrating signals from front to back. Science *302*, 1704-1709.
Rives, A.F., Rochlin, K.M., Wehrli, M., Schwartz, S.L., and DiNardo, S. (2006). Endocytic trafficking of Wingless and its receptors, Arrow and DFrizzled-2, in the Drosophila wing. Developmental biology *293*, 268-283.
Rodahl, L.M., Stuffers, S., Lobert, V.H., and Stenmark, H. (2009). The role of ESCRT proteins in attenuation of cell signalling. Biochemical Society transactions *37*, 137-142.
Saksena, S., Wahlman, J., Teis, D., Johnson, A.E., and Emr, S.D. (2009). Functional reconstitution of ESCRT-III assembly and disassembly. Cell *136*, 97-109.
Schaffner, F., Ray, A.M., and Dontenwill, M. (2013). Integrin alpha5beta1, the Fibronectin Receptor, as a Pertinent Therapeutic Target in Solid Tumors. Cancers *5*, 27-47.
Schneider-Brachert, W., Tchikov, V., Neumeyer, J., Jakob, M., Winoto-Morbach, S., Held-Feindt, J., Heinrich, M., Merkel, O., Ehrenschwender, M., Adam, D., *et al.* (2004). Compartmentalization of TNF receptor 1 signaling: internalized TNF receptosomes as death signaling vesicles. Immunity *21*, 415-428.
Schulman, B.A. (2011). Twists and turns in ubiquitin-like protein conjugation cascades. Protein science : a publication of the Protein Society *20*, 1941-1954.
Schutze, S., and Schneider-Brachert, W. (2009). Impact of TNF-R1 and CD95 internalization on apoptotic and antiapoptotic signaling. Results and problems in cell differentiation *49*, 63-85.
Schutze, S., Tchikov, V., and Schneider-Brachert, W. (2008). Regulation of TNFR1 and CD95 signalling by receptor compartmentalization. Nature reviews Molecular cell biology *9*, 655-662.
Schwickart, M., Huang, X., Lill, J.R., Liu, J., Ferrando, R., French, D.M., Maecker, H., O'Rourke, K., Bazan, F., Eastham-Anderson, J., *et al.* (2010). Deubiquitinase USP9X stabilizes MCL1 and promotes tumour cell survival. Nature *463*, 103-107.

Scott, A., Chung, H.Y., Gonciarz-Swiatek, M., Hill, G.C., Whitby, F.G., Gaspar, J., Holton, J.M., Viswanathan, R., Ghaffarian, S., Hill, C.P., *et al.* (2005a). Structural and mechanistic studies of VPS4 proteins. The EMBO journal *24*, 3658-3669.
Scott, A., Gaspar, J., Stuchell-Brereton, M.D., Alam, S.L., Skalicky, J.J., and Sundquist, W.I. (2005b). Structure and ESCRT-III protein interactions of the MIT domain of human VPS4A. Proceedings of the National Academy of Sciences of the United States of America *102*, 13813-13818.
Seet, L.F., and Hong, W. (2001). Endofin, an endosomal FYVE domain protein. The Journal of biological chemistry *276*, 42445-42454.
Seet, L.F., and Hong, W. (2005). Endofin recruits clathrin to early endosomes via TOM1. Journal of cell science *118*, 575-587.
Seet, L.F., Liu, N., Hanson, B.J., and Hong, W. (2004). Endofin recruits TOM1 to endosomes. The Journal of biological chemistry *279*, 4670-4679.
Sen, A., Madhivanan, K., Mukherjee, D., and Aguilar, R.C. (2012). The epsin protein family: coordinators of endocytosis and signaling. Biomolecular concepts *3*, 117-126.
Sette, P., Dussupt, V., and Bouamr, F. (2012). Identification of the HIV-1 NC binding interface in Alix Bro1 reveals a role for RNA. Journal of virology *86*, 11608-11615.
Sheff, D.R., Daro, E.A., Hull, M., and Mellman, I. (1999). The receptor recycling pathway contains two distinct populations of early endosomes with different sorting functions. The Journal of cell biology *145*, 123-139.
Shestakova, A., Hanono, A., Drosner, S., Curtiss, M., Davies, B.A., Katzmann, D.J., and Babst, M. (2010). Assembly of the AAA ATPase Vps4 on ESCRT-III. Molecular biology of the cell *21*, 1059-1071.
Shi, F., and Sottile, J. (2008). Caveolin-1-dependent beta1 integrin endocytosis is a critical regulator of fibronectin turnover. Journal of cell science *121*, 2360-2371.
Shi, F., and Sottile, J. (2011). MT1-MMP regulates the turnover and endocytosis of extracellular matrix fibronectin. Journal of cell science *124*, 4039-4050.
Shi, W., Chang, C., Nie, S., Xie, S., Wan, M., and Cao, X. (2007). Endofin acts as a Smad anchor for receptor activation in BMP signaling. Journal of cell science *120*, 1216-1224.
Shiba, Y., Katoh, Y., Shiba, T., Yoshino, K., Takatsu, H., Kobayashi, H., Shin, H.W., Wakatsuki, S., and Nakayama, K. (2004). GAT (GGA and Tom1) domain responsible for ubiquitin binding and ubiquitination. The Journal of biological chemistry *279*, 7105-7111.
Shields, S.B., Oestreich, A.J., Winistorfer, S., Nguyen, D., Payne, J.A., Katzmann, D.J., and Piper, R. (2009). ESCRT ubiquitin-binding domains function cooperatively during MVB cargo sorting. The Journal of cell biology *185*, 213-224.
Shields, S.B., and Piper, R.C. (2011). How ubiquitin functions with ESCRTs. Traffic (Copenhagen, Denmark) *12*, 1306-1317.
Shim, S., Kimpler, L.A., and Hanson, P.I. (2007). Structure/function analysis of four core ESCRT-III proteins reveals common regulatory role for extreme C-terminal domain. Traffic *8*, 1068-1079.
Shimaoka, M., Takagi, J., and Springer, T.A. (2002). Conformational regulation of integrin structure and function. Annual review of biophysics and biomolecular structure *31*, 485-516.
Sierra, M.I., Wright, M.H., and Nash, P.D. (2010). AMSH interacts with ESCRT-0 to regulate the stability and trafficking of CXCR4. The Journal of biological chemistry *285*, 13990-14004.

Sigismund, S., Algisi, V., Nappo, G., Conte, A., Pascolutti, R., Cuomo, A., Bonaldi, T., Argenzio, E., Verhoef, L.G., Maspero, E.*, et al.* (2013). Threshold-controlled ubiquitination of the EGFR directs receptor fate. The EMBO journal *32*, 2140-2157.
Sigismund, S., Argenzio, E., Tosoni, D., Cavallaro, E., Polo, S., and Di Fiore, P.P. (2008). Clathrin-mediated internalization is essential for sustained EGFR signaling but dispensable for degradation. Developmental cell *15*, 209-219.
Sigismund, S., Woelk, T., Puri, C., Maspero, E., Tacchetti, C., Transidico, P., Di Fiore, P.P., and Polo, S. (2005). Clathrin-independent endocytosis of ubiquitinated cargos. Proceedings of the National Academy of Sciences of the United States of America *102*, 2760-2765.
Song, M.S., Salmena, L., Carracedo, A., Egia, A., Lo-Coco, F., Teruya-Feldstein, J., and Pandolfi, P.P. (2008). The deubiquitinylation and localization of PTEN are regulated by a HAUSP-PML network. Nature *455*, 813-817.
Sonnichsen, B., De Renzis, S., Nielsen, E., Rietdorf, J., and Zerial, M. (2000). Distinct membrane domains on endosomes in the recycling pathway visualized by multicolor imaging of Rab4, Rab5, and Rab11. The Journal of cell biology *149*, 901-914.
Sorkin, A., and von Zastrow, M. (2009). Endocytosis and signalling: intertwining molecular networks. Nature reviews Molecular cell biology *10*, 609-622.
Sottile, J., and Chandler, J. (2005). Fibronectin matrix turnover occurs through a caveolin-1-dependent process. Molecular biology of the cell *16*, 757-768.
Stachowiak, J.C., Brodsky, F.M., and Miller, E.A. (2013). A cost-benefit analysis of the physical mechanisms of membrane curvature. Nature cell biology *15*, 1019-1027.
Stachowiak, J.C., Schmid, E.M., Ryan, C.J., Ann, H.S., Sasaki, D.Y., Sherman, M.B., Geissler, P.L., Fletcher, D.A., and Hayden, C.C. (2012). Membrane bending by protein-protein crowding. Nature cell biology *14*, 944-949.
Stang, E., Blystad, F.D., Kazazic, M., Bertelsen, V., Brodahl, T., Raiborg, C., Stenmark, H., and Madshus, I.H. (2004). Cbl-dependent ubiquitination is required for progression of EGF receptors into clathrin-coated pits. Molecular biology of the cell *15*, 3591-3604.
Stefani, F., Zhang, L., Taylor, S., Donovan, J., Rollinson, S., Doyotte, A., Brownhill, K., Bennion, J., Pickering-Brown, S., and Woodman, P. (2011). UBAP1 is a component of an endosome-specific ESCRT-I complex that is essential for MVB sorting. Current biology : CB *21*, 1245-1250.
Steinberg, F., Heesom, K.J., Bass, M.D., and Cullen, P.J. (2012). SNX17 protects integrins from degradation by sorting between lysosomal and recycling pathways. The Journal of cell biology *197*, 219-230.
Stevenson, L.F., Sparks, A., Allende-Vega, N., Xirodimas, D.P., Lane, D.P., and Saville, M.K. (2007). The deubiquitinating enzyme USP2a regulates the p53 pathway by targeting Mdm2. The EMBO journal *26*, 976-986.
Stuffers, S., Brech, A., and Stenmark, H. (2009). ESCRT proteins in physiology and disease. Experimental cell research *315*, 1619-1626.
Sundvall, M., Korhonen, A., Paatero, I., Gaudio, E., Melino, G., Croce, C.M., Aqeilan, R.I., and Elenius, K. (2008). Isoform-specific monoubiquitination, endocytosis, and degradation of alternatively spliced ErbB4 isoforms. Proceedings of the National Academy of Sciences of the United States of America *105*, 4162-4167.

Swanson, J.A. (2008). Shaping cups into phagosomes and macropinosomes. Nature reviews Molecular cell biology *9*, 639-649.
Takagi, J., DeBottis, D.P., Erickson, H.P., and Springer, T.A. (2002). The role of the specificity-determining loop of the integrin beta subunit I-like domain in autonomous expression, association with the alpha subunit, and ligand binding. Biochemistry *41*, 4339-4347.
Takagi, J., and Springer, T.A. (2002). Integrin activation and structural rearrangement. Immunological reviews *186*, 141-163.
Takagi, J., Strokovich, K., Springer, T.A., and Walz, T. (2003). Structure of integrin alpha5beta1 in complex with fibronectin. The EMBO journal *22*, 4607-4615.
Takahashi, H., Mayers, J.R., Wang, L., Edwardson, J.M., and Audhya, A. (2015). Hrs and STAM function synergistically to bind ubiquitin-modified cargoes in vitro. Biophysical journal *108*, 76-84.
Tartaglia, L.A., Ayres, T.M., Wong, G.H., and Goeddel, D.V. (1993a). A novel domain within the 55 kd TNF receptor signals cell death. Cell *74*, 845-853.
Tartaglia, L.A., Rothe, M., Hu, Y.F., and Goeddel, D.V. (1993b). Tumor necrosis factor's cytotoxic activity is signaled by the p55 TNF receptor. Cell *73*, 213-216.
Teckchandani, A., Mulkearns, E.E., Randolph, T.W., Toida, N., and Cooper, J.A. (2012). The clathrin adaptor Dab2 recruits EH domain scaffold proteins to regulate integrin beta1 endocytosis. Molecular biology of the cell *23*, 2905-2916.
Teckchandani, A., Toida, N., Goodchild, J., Henderson, C., Watts, J., Wollscheid, B., and Cooper, J.A. (2009). Quantitative proteomics identifies a Dab2/integrin module regulating cell migration. The Journal of cell biology *186*, 99-111.
Teis, D., Saksena, S., and Emr, S.D. (2008). Ordered assembly of the ESCRT-III complex on endosomes is required to sequester cargo during MVB formation. Developmental cell *15*, 578-589.
Teis, D., Saksena, S., Judson, B.L., and Emr, S.D. (2010). ESCRT-II coordinates the assembly of ESCRT-III filaments for cargo sorting and multivesicular body vesicle formation. The EMBO journal *29*, 871-883.
Temkin, P., Lauffer, B., Jager, S., Cimermancic, P., Krogan, N.J., and von Zastrow, M. (2011). SNX27 mediates retromer tubule entry and endosome-to-plasma membrane trafficking of signalling receptors. Nature cell biology *13*, 715-721.
Teo, H., Gill, D.J., Sun, J., Perisic, O., Veprintsev, D.B., Vallis, Y., Emr, S.D., and Williams, R.L. (2006). ESCRT-I core and ESCRT-II GLUE domain structures reveal role for GLUE in linking to ESCRT-I and membranes. Cell *125*, 99-111.
Teo, H., Perisic, O., Gonzalez, B., and Williams, R.L. (2004). ESCRT-II, an endosome-associated complex required for protein sorting: crystal structure and interactions with ESCRT-III and membranes. Developmental cell *7*, 559-569.
Theard, D., Labarrade, F., Partisani, M., Milanini, J., Sakagami, H., Fon, E.A., Wood, S.A., Franco, M., and Luton, F. (2010). USP9x-mediated deubiquitination of EFA6 regulates de novo tight junction assembly. The EMBO journal *29*, 1499-1509.
Thelen, K., Georg, T., Bertuch, S., Zelina, P., and Pollerberg, G.E. (2008). Ubiquitination and endocytosis of cell adhesion molecule DM-GRASP regulate its cell surface presence and affect its role for axon navigation. The Journal of biological chemistry *283*, 32792-32801.

Tiwari, A., Jung, J.J., Inamdar, S.M., Brown, C.O., Goel, A., and Choudhury, A. (2011). Endothelial cell migration on fibronectin is regulated by syntaxin 6-mediated alpha5beta1 integrin recycling. The Journal of biological chemistry *286*, 36749-36761.
Tong, J.H., Ng, D.C., Chau, S.L., So, K.K., Leung, P.P., Lee, T.L., Lung, R.W., Chan, M.W., Chan, A.W., Lo, K.W., *et al.* (2010). Putative tumour-suppressor gene DAB2 is frequently down regulated by promoter hypermethylation in nasopharyngeal carcinoma. BMC cancer *10*, 253.
Tonks, N.K. (2006). Protein tyrosine phosphatases: from genes, to function, to disease. Nature reviews Molecular cell biology *7*, 833-846.
Tonks, N.K. (2013). Protein tyrosine phosphatases--from housekeeping enzymes to master regulators of signal transduction. The FEBS journal *280*, 346-378.
Toy, W., Lim, S.K., Loh, M.C., and Lim, Y.P. (2010). EGF-induced tyrosine phosphorylation of Endofin is dependent on PI3K activity and proper localization to endosomes. Cellular signalling *22*, 437-446.
Toyoshima, M., Tanaka, N., Aoki, J., Tanaka, Y., Murata, K., Kyuuma, M., Kobayashi, H., Ishii, N., Yaegashi, N., and Sugamura, K. (2007). Inhibition of tumor growth and metastasis by depletion of vesicular sorting protein Hrs: its regulatory role on E-cadherin and beta-catenin. Cancer research *67*, 5162-5171.
Trebinska, A., Rembiszewska, A., Ciosek, K., Ptaszynski, K., Rowinski, S., Kupryjanczyk, J., Siedlecki, J.A., and Grzybowska, E.A. (2010). HAX-1 overexpression, splicing and cellular localization in tumors. BMC cancer *10*, 76.
Trempe, J.F. (2011). Reading the ubiquitin postal code. Current opinion in structural biology *21*, 792-801.
Trivigno, D., Essmann, F., Huber, S.M., and Rudner, J. (2012). Deubiquitinase USP9x confers radioresistance through stabilization of Mcl-1. Neoplasia *14*, 893-904.
Trompouki, E., Hatzivassiliou, E., Tsichritzis, T., Farmer, H., Ashworth, A., and Mosialos, G. (2003). CYLD is a deubiquitinating enzyme that negatively regulates NF-kappaB activation by TNFR family members. Nature *424*, 793-796.
Tsunematsu, T., Yamauchi, E., Shibata, H., Maki, M., Ohta, T., and Konishi, H. (2010). Distinct functions of human MVB12A and MVB12B in the ESCRT-I dependent on their posttranslational modifications. Biochemical and biophysical research communications *399*, 232-237.
Tu, C., Ahmad, G., Mohapatra, B., Bhattacharyya, S., Ortega-Cava, C.F., Chung, B.M., Wagner, K.U., Raja, S.M., Naramura, M., Band, V., *et al.* (2011). ESCRT proteins: Double-edged regulators of cellular signaling. Bioarchitecture *1*, 45-48.
Tu, C., Ortega-Cava, C.F., Winograd, P., Stanton, M.J., Reddi, A.L., Dodge, I., Arya, R., Dimri, M., Clubb, R.J., Naramura, M., *et al.* (2010). Endosomal-sorting complexes required for transport (ESCRT) pathway-dependent endosomal traffic regulates the localization of active Src at focal adhesions. Proceedings of the National Academy of Sciences of the United States of America *107*, 16107-16112.
Tumbarello, D.A., Waxse, B.J., Arden, S.D., Bright, N.A., Kendrick-Jones, J., and Buss, F. (2012). Autophagy receptors link myosin VI to autophagosomes to mediate Tom1-dependent autophagosome maturation and fusion with the lysosome. Nature cell biology *14*, 1024-1035.
Umasankar, P.K., Sanker, S., Thieman, J.R., Chakraborty, S., Wendland, B., Tsang, M., and Traub, L.M. (2012). Distinct and separable activities of the endocytic clathrin-coat components Fcho1/2 and AP-2 in developmental patterning. Nature cell biology *14*, 488-501.

Vaccari, T., Lu, H., Kanwar, R., Fortini, M.E., and Bilder, D. (2008). Endosomal entry regulates Notch receptor activation in Drosophila melanogaster. The Journal of cell biology *180*, 755-762.
Valdembri, D., and Serini, G. (2012). Regulation of adhesion site dynamics by integrin traffic. Current opinion in cell biology *24*, 582-591.
van der Sluijs, P., Hull, M., Webster, P., Male, P., Goud, B., and Mellman, I. (1992). The small GTP-binding protein rab4 controls an early sorting event on the endocytic pathway. Cell *70*, 729-740.
Varshavsky, A. (2012). The ubiquitin system, an immense realm. Annual review of biochemistry *81*, 167-176.
Vinogradova, O., Velyvis, A., Velyviene, A., Hu, B., Haas, T., Plow, E., and Qin, J. (2002). A structural mechanism of integrin alpha(IIb)beta(3) "inside-out" activation as regulated by its cytoplasmic face. Cell *110*, 587-597.
Wang, C., Deng, L., Hong, M., Akkaraju, G.R., Inoue, J., and Chen, Z.J. (2001). TAK1 is a ubiquitin-dependent kinase of MKK and IKK. Nature *412*, 346-351.
Wang, S., Kollipara, R.K., Srivastava, N., Li, R., Ravindranathan, P., Hernandez, E., Freeman, E., Humphries, C.G., Kapur, P., Lotan, Y., *et al.* (2014). Ablation of the oncogenic transcription factor ERG by deubiquitinase inhibition in prostate cancer. Proceedings of the National Academy of Sciences of the United States of America *111*, 4251-4256.
Wang, T., Liu, N.S., Seet, L.F., and Hong, W. (2010). The emerging role of VHS domain-containing Tom1, Tom1L1 and Tom1L2 in membrane trafficking. Traffic (Copenhagen, Denmark) *11*, 1119-1128.
Wang, X.L., Xu, R., Wu, X., Gillespie, D., Jensen, R., and Lu, Z.R. (2009). Targeted systemic delivery of a therapeutic siRNA with a multifunctional carrier controls tumor proliferation in mice. Molecular pharmaceutics *6*, 738-746.
Waterman, H., Levkowitz, G., Alroy, I., and Yarden, Y. (1999). The RING finger of c-Cbl mediates desensitization of the epidermal growth factor receptor. The Journal of biological chemistry *274*, 22151-22154.
Wegener, K.L., and Campbell, I.D. (2008). Transmembrane and cytoplasmic domains in integrin activation and protein-protein interactions (review). Molecular membrane biology *25*, 376-387.
Wegner, C.S., Rodahl, L.M., and Stenmark, H. (2011). ESCRT proteins and cell signalling. Traffic (Copenhagen, Denmark) *12*, 1291-1297.
Weller, M., Reardon, D., Nabors, B., and Stupp, R. (2009). Will integrin inhibitors have proangiogenic effects in the clinic? Nature medicine *15*, 726; author reply 727.
Wemmer, M., Azmi, I., West, M., Davies, B., Katzmann, D., and Odorizzi, G. (2011). Bro1 binding to Snf7 regulates ESCRT-III membrane scission activity in yeast. The Journal of cell biology *192*, 295-306.
Wertz, I.E., O'Rourke, K.M., Zhou, H., Eby, M., Aravind, L., Seshagiri, S., Wu, P., Wiesmann, C., Baker, R., Boone, D.L., *et al.* (2004). De-ubiquitination and ubiquitin ligase domains of A20 downregulate NF-kappaB signalling. Nature *430*, 694-699.
Westhoff, B., Colaluca, I.N., D'Ario, G., Donzelli, M., Tosoni, D., Volorio, S., Pelosi, G., Spaggiari, L., Mazzarol, G., Viale, G., *et al.* (2009). Alterations of the Notch pathway in lung cancer. Proceedings of the National Academy of Sciences of the United States of America *106*, 22293-22298.

White, D.P., Caswell, P.T., and Norman, J.C. (2007). alpha v beta3 and alpha5beta1 integrin recycling pathways dictate downstream Rho kinase signaling to regulate persistent cell migration. The Journal of cell biology *177*, 515-525.
Windler, S.L., and Bilder, D. (2010). Endocytic internalization routes required for delta/notch signaling. Current biology : CB *20*, 538-543.
Wittinger, M., Vanhara, P., El-Gazzar, A., Savarese-Brenner, B., Pils, D., Anees, M., Grunt, T.W., Sibilia, M., Holcmann, M., Horvat, R., *et al.* (2011). hVps37A Status affects prognosis and cetuximab sensitivity in ovarian cancer. Clinical cancer research : an official journal of the American Association for Cancer Research *17*, 7816-7827.
Wobst, H., Forster, S., Laurini, C., Sekulla, A., Dreiseidler, M., Hohfeld, J., Schmitz, B., and Diestel, S. (2012). UCHL1 regulates ubiquitination and recycling of the neural cell adhesion molecule NCAM. The FEBS journal *279*, 4398-4409.
Wolfe, B.L., and Trejo, J. (2007). Clathrin-dependent mechanisms of G protein-coupled receptor endocytosis. Traffic (Copenhagen, Denmark) *8*, 462-470.
Wollert, T., and Hurley, J.H. (2010). Molecular mechanism of multivesicular body biogenesis by ESCRT complexes. Nature *464*, 864-869.
Wollert, T., Wunder, C., Lippincott-Schwartz, J., and Hurley, J.H. (2009). Membrane scission by the ESCRT-III complex. Nature *458*, 172-177.
Woodman, P. (2009). ESCRT proteins, endosome organization and mitogenic receptor down-regulation. Biochemical Society transactions *37*, 146-150.
Wright, M.H., Berlin, I., and Nash, P.D. (2011). Regulation of endocytic sorting by ESCRT-DUB-mediated deubiquitination. Cell biochemistry and biophysics *60*, 39-46.
Wunderley, L., Brownhill, K., Stefani, F., Tabernero, L., and Woodman, P. (2014). The molecular basis for selective assembly of the UBAP1-containing endosome-specific ESCRT-I complex. Journal of cell science *127*, 663-672.
Xiao, B., Fan, S., Zeng, Z., Xiong, W., Cao, L., Yang, Y., Li, W., Wang, R., Tang, K., Qian, J., *et al.* (2006). Purification of novel UBAP1 protein and its decreased expression on nasopharyngeal carcinoma tissue microarray. Protein expression and purification *47*, 60-67.
Xie, C., Zhu, J., Chen, X., Mi, L., Nishida, N., and Springer, T.A. (2010). Structure of an integrin with an alphaI domain, complement receptor type 4. The EMBO journal *29*, 666-679.
Xie, Y., Avello, M., Schirle, M., McWhinnie, E., Feng, Y., Bric-Furlong, E., Wilson, C., Nathans, R., Zhang, J., Kirschner, M.W., *et al.* (2013). Deubiquitinase FAM/USP9X interacts with the E3 ubiquitin ligase SMURF1 protein and protects it from ligase activity-dependent self-degradation. The Journal of biological chemistry *288*, 2976-2985.
Xiong, J.P., Stehle, T., Diefenbach, B., Zhang, R., Dunker, R., Scott, D.L., Joachimiak, A., Goodman, S.L., and Arnaout, M.A. (2001). Crystal structure of the extracellular segment of integrin alpha Vbeta3. Science *294*, 339-345.
Xiong, J.P., Stehle, T., Goodman, S.L., and Arnaout, M.A. (2004). A novel adaptation of the integrin PSI domain revealed from its crystal structure. The Journal of biological chemistry *279*, 40252-40254.
Xu, J., Zutter, M.M., Santoro, S.A., and Clark, R.A. (1996). PDGF induction of alpha 2 integrin gene expression is mediated by protein kinase C-zeta. The Journal of cell biology *134*, 1301-1311.

Xu, S., Zhu, J., and Wu, Z. (2014). Loss of Dab2 expression in breast cancer cells impairs their ability to deplete TGF-beta and induce Tregs development via TGF-beta. PloS one *9*, e91709.
Yamada, S., Bu, X.Y., Khankaldyyan, V., Gonzales-Gomez, I., McComb, J.G., and Laug, W.E. (2006). Effect of the angiogenesis inhibitor Cilengitide (EMD 121974) on glioblastoma growth in nude mice. Neurosurgery *59*, 1304-1312; discussion 1312.
Yamakami, M., Yoshimori, T., and Yokosawa, H. (2003). Tom1, a VHS domain-containing protein, interacts with tollip, ubiquitin, and clathrin. The Journal of biological chemistry *278*, 52865-52872.
Yamakawa, K., Takahashi, T., Horio, Y., Murata, Y., Takahashi, E., Hibi, K., Yokoyama, S., Ueda, R., Takahashi, T., and Nakamura, Y. (1993). Frequent homozygous deletions in lung cancer cell lines detected by a DNA marker located at 3p21.3-p22. Oncogene *8*, 327-330.
Yamashiro, D.J., and Maxfield, F.R. (1987). Kinetics of endosome acidification in mutant and wild-type Chinese hamster ovary cells. The Journal of cell biology *105*, 2713-2721.
Yau, W.L., Lung, H.L., Zabarovsky, E.R., Lerman, M.I., Sham, J.S., Chua, D.T., Tsao, S.W., Stanbridge, E.J., and Lung, M.L. (2006). Functional studies of the chromosome 3p21.3 candidate tumor suppressor gene BLU/ZMYND10 in nasopharyngeal carcinoma. International journal of cancer Journal international du cancer *119*, 2821-2826.
Yin, Q., Lamothe, B., Darnay, B.G., and Wu, H. (2009). Structural basis for the lack of E2 interaction in the RING domain of TRAF2. Biochemistry *48*, 10558-10567.
Yoshida, H., Jono, H., Kai, H., and Li, J.D. (2005). The tumor suppressor cylindromatosis (CYLD) acts as a negative regulator for toll-like receptor 2 signaling via negative cross-talk with TRAF6 AND TRAF7. The Journal of biological chemistry *280*, 41111-41121.
Zaidel-Bar, R., Itzkovitz, S., Ma'ayan, A., Iyengar, R., and Geiger, B. (2007a). Functional atlas of the integrin adhesome. Nature cell biology *9*, 858-867.
Zaidel-Bar, R., Milo, R., Kam, Z., and Geiger, B. (2007b). A paxillin tyrosine phosphorylation switch regulates the assembly and form of cell-matrix adhesions. Journal of cell science *120*, 137-148.
Zhang, J., Du, J., Lei, C., Liu, M., and Zhu, A.J. (2014). Ubpy controls the stability of the ESCRT-0 subunit Hrs in development. Development *141*, 1473-1479.
Zhang, J., Liu, X., Datta, A., Govindarajan, K., Tam, W.L., Han, J., George, J., Wong, C., Ramnarayanan, K., Phua, T.Y., *et al.* (2009). RCP is a human breast cancer-promoting gene with Ras-activating function. The Journal of clinical investigation *119*, 2171-2183.
Zhang, L., Zhou, F., Drabsch, Y., Gao, R., Snaar-Jagalska, B.E., Mickanin, C., Huang, H., Sheppard, K.A., Porter, J.A., Lu, C.X., *et al.* (2012). USP4 is regulated by AKT phosphorylation and directly deubiquitylates TGF-beta type I receptor. Nature cell biology *14*, 717-726.

7. APPENDIX

7.1 Supplemental reagents and primer sequences associated with Chapter 2

Table S2.1: Antibodies and reagents		
Primary Antibodies:		
Antigen	Host, clone #	Manufacturer
HD-PTP	Rabbit	Homemade (Gingras et al., 2009)
Actin	Mouse, AC-75	Sigma
pAkt (T308)	Rabbit	Cell Signalling
Akt	Rabbit	Cell Signalling
CD49e (Int α5), IP, IF	Mouse, VC5	BD Pharmigen
CD49e (Int α5), WB	Rabbit	Santa Cruz
Int α5β1, block	Mouse, JBS5	Millipore
CD29 (Int β1), WB	Mouse, 18/CD29	BD Pharmigen
CD29 (Int β1), IP	Mouse, TS2/16	Santa Cruz
CD (Int αV), block	Mouse	BD Pharmigen
CD4	Mouse, RTA-T4	BD Pharmigen
CD63	Mouse, H5C6-c	Developmental Studies Hybridoma bank, University of Iowa
EEA1	Rabbit	Cell Signalling
pErk1/2 (T202/Y204)	Mouse	Cell Signalling
Erk1/2	Rabbit	Cell Signalling
FAK pY397	Mouse	Millipore
FAK	Rabbit	Millipore
Hrs	Mouse, C-7	Santa Cruz
LAMP1	Rabbit	Cell Signalling
LAMP2	Mouse, H4B4-s	Developmental Studies Hybridoma bank, University of Iowa
pSrc (Y416)	Rabbit	Cell Signalling
Src	Rabbit	Cell Signalling
Stam	Mouse, N-17	Santa Cruz
TSG101	Mouse, Y16J	Santa Cruz
UBAP1	Rabbit	ProteinTech
Ubiquitin	Mouse, P4D1	Santa Cruz
Ubiquitin K-63	mRabbit, Apu3	Millipore
USP9x	Rabbit	Bethyl
Secondary Antibodies:		
Anti-Mouse Alexa 488	Goat	Life Technologies Inc. Molecular Probes
Anti-Rabbit Alexa 594	Goat	Life Technologies Inc. Molecular Probes
Anti-Mouse HRP	Donkey	Amersham Biosciences
Anti-Rabbit HRP	Donkey	Jackson Immunoresearch
anti-mouse, $F(ab')_2$ specific	Goat	Jackson Immunoresearch
Reagents:		

Fibronectin	Sigma
Fibronectin-biotin	Cytoskeleton Inc.
Collagen 1	BD Biosciences
Matrigel, serum-free	BD Biosciences
Neutravidin-HRP, -FITC	Pierce, Life Technologies Inc. Molecular Probes
Transferrin-Alexa 594, -FITC	Life Technologies Inc. Molecular Probes, Jackson Immunoresearch
Phalloidin-Alexa 594	Life Technologies Inc. Molecular Probes
Mono-Ubiquitin	Boston Biochem
Poly-Ubiquitin K48	Boston Biochem
Poly-Ubiquitin K63	Boston Biochem
Chloroquine	Sigma
Cilengitide	Selleckchem

Nystatin	Sigma
Amplex ® Red	Life Technologies Inc. Molecular Probes
Dextran-FITC	Life Technologies Inc. Molecular Probes
EZ link NHS-SS-Biotin	Pierce
MG132	Sigma
WP1130	Life Sensors

Table S2.2: Primer sequences	
Primer name	Sequence
Int α5 qPCR FRD	GACAGGGTTACTGCCAAGGA
Int α5 qPCR RVS	CTGCAATCTGCTCCTGAGTG
UBAP1 pGEX2 cloning FRD	CGCGGATCCATGGCTTCTAAGAAGTTGGGTG
UBAP1 pGEX2 cloning RVS	TCC CCC CGG GTC AGC TGG CTC CTG CCC

7.2 Supplemental reagents and primer sequences associated with Chapter 4

Table S4.1: Antibodies and reagents		
Primary Antibodies:		
Antigen	Host, clone #	Manufacturer
HD-PTP	Rabbit	Homemade (Gingras et al., 2009)
Actin	Mouse, AC-75	Sigma
CD49e (Int α5), IP, IF	Mouse, VC5	BD Pharmigen
CD4	Mouse, RTA-T4	BD Pharmigen
CD63	Mouse, H5C6-c	Developmental Studies Hybridoma bank, University of Iowa
EEA1	Rabbit	Cell Signalling
Endofin	Rabbit	ProteinTech
Hrs	Mouse, C-7	Santa Cruz
LAMP1	Rabbit	Cell Signalling
LAMP2	Mouse, H4B4-s	Developmental Studies Hybridoma bank, University of Iowa
Stam1	Mouse, N-17	Santa Cruz
TSG101	Mouse, Y16J	Santa Cruz
UBAP1	Rabbit	ProteinTech
Ubiquitin	Mouse, P4D1	Santa Cruz
Secondary Antibodies:		
Anti-Mouse Alexa 488	Goat	Life Technologies Inc. Molecular Probes
Anti-Rabbit Alexa 594	Goat	Life Technologies Inc. Molecular Probes
Anti-Mouse HRP	Donkey	Amersham Biosciences
Anti-Rabbit HRP	Donkey	Jackson Immunoresearch
Reagents:		
Fibronectin	Sigma	
Collagen 1	BD Biosciences	
Matrigel, serum-free	BD Biosciences	
Transferrin-Alexa 594	Life Technologies Inc. Molecular Probes	
Phalloidin-Alexa 594	Life Technologies Inc. Molecular Probes	
Amplex ® Red	Life Technologies Inc. Molecular Probes	
Dextran-FITC	Life Technologies Inc. Molecular Probes	

Table S4.2: Primer sequences	
Primer name	Sequence

Endofin C753S FRD	GATTCAGAAGCTCCAAACT**C**TATGAAC
Endofin C753S RVS	GACTTGGCAGTTCATA**G**AGTTTGG
BRO-domain cloning FRD	CG GA ATT CTG ATG GAG GCC GTG CCC C
BRO-domain cloning RVS	CCG CTCGAG GGG TAC CAG TTT GGC AAA G
ΔBRO-domain cloning FRD	CG GA ATT CCC ATG GCT GCC CAC GAG
ΔBRO-domain cloning RVS	CG GA ATT CCC ATG CCC ATG GCT GCC CAC GAG GC